



Investigación de las interacciones de los microorganismos con el uranio en aguas contaminadas de origen antropogénico como base para el desarrollo de una tecnología de biorremediación

Investigation of the interactions of microorganisms with uranium in anthropogenic contaminated waters as basis for the development of a bioremediation technology

Tesis Doctoral

Antonio Martín Newman Portela
Granada, 2024



**UNIVERSIDAD
DE GRANADA**

HZDR
HELMHOLTZ ZENTRUM
DRESDEN ROSENDOF

**INVESTIGACIÓN DE LAS INTERACCIONES DE LOS
MICROORGANISMOS CON EL URANIO EN AGUAS
CONTAMINADAS DE ORIGEN ANTROPOGÉNICO COMO
BASE PARA EL DESARROLLO DE UNA TECNOLOGÍA DE
BIORREMEDIACIÓN**



**UNIVERSIDAD
DE GRANADA**

Universidad de Granada
Facultad de Ciencias
Departamento de Microbiología

*Investigation of the interactions of microorganisms with uranium in
anthropogenic contaminated waters as basis for the development of a
bioremediation technology*

TESIS DOCTORAL
Antonio Martín Newman Portela
Granada, 2024

Programa de Doctorado en Biología Fundamental y de Sistemas

Editor: Universidad de Granada. Tesis Doctorales
Autor: Antonio Martín Newman Portela
ISBN: 978-84-1195-428-0
URI: <https://hdl.handle.net/10481/94827>

**INVESTIGACIÓN DE LAS INTERACCIONES DE LOS
MICROORGANISMOS CON EL URANIO EN AGUAS
CONTAMINADAS DE ORIGEN ANTROPOGÉNICO COMO
BASE PARA EL DESARROLLO DE UNA TECNOLOGÍA DE
BIORREMEDIACIÓN**

TESIS DOCTORAL

Programa de Doctorado en Biología Fundamental y de Sistemas

Departamento de Microbiología, Facultad de Ciencias

Universidad de Granada

Granada, 2024

Memoria presentada por el graduado en Biología D. Antonio Martín Newman Portela para aspirar al Grado de Doctor por la Universidad de Granada con Mención Internacional. Esta Tesis Doctoral ha sido dirigida por D. Mohamed Larbi Merroun, Catedrático de la Universidad de Granada, y D. Johannes Raff, Director de Departamento de Biogeoquímica del Instituto de Investigación Helmholtz Zentrum Dresden-Rossendorf (Alemania)

Doctorando [Doctoral Candidate]

Antonio Martín Newman Portela

Directores de la Tesis Doctoral [Doctoral Thesis Supervisors]

Mohamed Larbi Merroun

Catedrático de Universidad

Universidad de Granada

Johannes Raff

Leader of the Department of Biogeo-
chemistry

Helmholtz-Zentrum

Dresden-Rossendorf e.V.

Vº Bº del Director

Vº Bº del Director



**UNIVERSIDAD
DE GRANADA**



Esta tesis doctoral ha sido realizada en el Departamento de Microbiología (Grupo de investigación mixobacterias (BIO103)) de la Facultad de Ciencias de la Universidad de Granada y en el *Department of Biogeochemistry (FWOB) del Institute of Resource Ecology del Helmholtz-Zentrum Dresden-Rossendorf (HZDR)* durante los años 2020-2024. Asimismo, esta tesis doctoral ha contado con una estrecha colaboración con la empresa Wismut GmbH, encargada de la remediación de ambas minas las cuales han sido objeto de estudio durante el trabajo realizado.

Esta tesis doctoral se ha realizado en el marco del Programa Conjunto UGR-HZDR, coordinado por el Propio de Investigación y Transferencia de la Universidad de Granada, bajo el título “*Investigation of the interactions of microorganisms with uranium in anthropogenic contaminated waters as basis for the development of a bioremediation technology*“. Este contrato se enmarca dentro de las Ayudas Predoctorales para la realización de tesis en colaboración con empresas (HZDR, Alemania). Esta ayuda ha sido financiada tanto por el *Helmholtz-Zentrum Dresden-Rossendorf*, como la Universidad de Granada (*ref. 4345*), y abarca el período comprendido entre el 15 de junio de 2020 hasta el 14 de enero de 2024. Además, esta tesis doctoral ha sido realizada en el marco del Proyecto Europeo “*Towards effective radiation protection based on improved scientific evidence and social considerations - focus on radon and NORM (RADONORM)*” con *ref. 900009*, financiado por el EU- EURATOM-NFRP-2019-2020. La duración del proyecto abarca desde el 1 de septiembre de 2020 hasta el 31 de agosto de 2025.

Además, el doctorando disfruto de varias becas de movilidad, incluyendo tres veces el programa Erasmus Prácticas (ERASMUS+) del Vicerrectorado de Estudiantes de la Universidad de Granada, dos veces el programa de ayudas de movilidad del proyecto Europeo RADONORM, una ayuda de movilidad de la Alianza Europea de Radioecología (ALLIANCE), una ayuda de movilidad para estancias en centros de investigación nacionales y extranjeros del Plan Propio de Investigación y Transferencia de la

Universidad de Granada, financiando la realización de tres estancias de investigación de seis meses cada una en el centro de investigación *Helmholtz-Zentrum Dresden-Rossendorf* (Alemania) y dos estancias breves en el *European Synchrotron Research Facility* (ESRF) (Grenoble, Francia) bajo la supervisión de la Dra. Evelyn Krawczyk-Bärsch. Además, el doctorado fue beneficiario de dos becas para la participación en conferencias: una para la asistencia a congresos y reuniones científicas del Plan Propio de Investigación y Transferencia de la Universidad de Granada, y otra para la participación en congresos nacionales e internacionales de la Escuela Internacional de Postgrado de la Universidad de Granada.



UNIVERSIDAD
DE GRANADA

HZDR
HELMHOLTZ ZENTRUM
DRESDEN ROSENDORF



RadoNorm
Managing risks from radon and NORM



EUROPEAN RADIOECOLOGY ALLIANCE


WISMUT

This PhD thesis was conducted at the Department of Microbiology (*Mixobacterias* research group (BIO103)) of the Faculty of Sciences at the University of Granada (UGR, Spain) and the Department of Biogeochemistry (FWOB) of the Institute of Resource Ecology at the Helmholtz-Zentrum Dresden-Rossendorf (HZDR, Germany) during the years 2020-2024. Additionally, this PhD thesis has benefited from close collaboration with Wismut GmbH (Germany), responsible for the remediation of both mines which have been the subject of study during the research conducted.

This PhD thesis was carried out within a Joint UGR-HZDR Program coordinated by the University of Granada through the “*Plan Propio de Investigación y Transferencia*”, under the title “*Investigation of the interactions of microorganisms with uranium in anthropogenic contaminated waters as basis for the development of a bioremediation technology*”. This joint PhD position is part of this Pre-doctoral Grants program for the realization of PhD studies in collaboration with abroad institutions and was funded by both, the HZDR and the UGR (*ref. 4345*) It covers the period from June 15th, 2020 to January 14th, 2024. Additionally, this PhD thesis was carried out within the framework of the European Project “*Towards effective radiation protection based on improved scientific evidence and social considerations - focus on radon and NORM (RADONORM)*” with *ref. 900009*, funded by the EU-EURATOM-NFRP-2019-2020. The duration of the project spans from September 1st, 2020, to August 31st, 2025.

Additionally, the doctoral candidate benefited from several mobility grants, including three times the Erasmus Traineeship program (ERASMUS+) from the “*Vicerrectorado de Estudiantes*” of the University of Granada, two times the mobility grant program of the European project RADONORM, a mobility grant from the European Radioecology Alliance (ALLIANCE), a mobility grant for research visits in national and foreign research institutes, from the “*Plan Propio de Investigación y Transferencia*” of the University of Granada, funding the realization of three research stays of six months, each at the HZDR (Germany) and two short stays at the European Synchrotron

Research Facility (ESRF) in Grenoble (France) under the supervision of Dr. Evelyn Krawczyk-Bärsch. Additionally, the doctoral candidate was the beneficiary of two conference attendance grants: one for attending congresses and scientific meetings from the “*Plan Propio de Investigación y Transferencia*” of the University of Granada, and another for participating in national and international conferences from the “*Escuela Internacional de Postgrado*” of the University of Granada.



UNIVERSIDAD
DE GRANADA

HZDR
HELMHOLTZ ZENTRUM
DRESDEN ROSENDORF



Los resultados alcanzados durante la elaboración de esta Tesis Doctoral han sido divulgados o están en proceso de preparación para su difusión en revistas científicas de renombre y en congresos a nivel nacional e internacional.

I. Artículos científicos que han sido publicados con los resultados obtenidos en el transcurso de esta Tesis Doctoral:

- **Newman-Portela, A.M.**, Krawczyk-Bärsch, E., Lopez-Fernandez, M., Bok, F., Kassahun, A., Drobot, B., Steudtner, R., Stumpf, T., Raff, J., Merroun, M.L. (2024) Biostimulation of indigenous microbes for uranium bioremediation in former U mine water: multidisciplinary approach assessment. *Environmental Science and Pollution Research*. 31(5):7227-7245. <https://doi.org/10.1007/s11356-023-31530-4>. **IF: 5.8, Q1**.

II. Conferencias y seminarios nacionales e internacionales donde se ha participado con los resultados obtenidos en el transcurso de esta Tesis Doctoral:

- **Newman-Portela, A.M.***, Krawczyk-Bärsch, E., Lopez-Fernandez, M., Bok, F., Kassahun, A., Kvashnina, K., Bazarkina, E., Roßberg, A., Raff, J., Merroun, M.L. (October 10th, 2023) *Exploring the Influence of Water Chemistry and Microbial Interactions on U Speciation in Former U Mine Water - Implications for Bioremediation Strategies*. **[Oral communication]**. Sustainable Remediation of Radionuclide Impacts (SURRI) Workshop. Granada (España).
- **Newman-Portela, A.M.***, Krawczyk-Bärsch, E., Lopez-Fernandez, M., Bok, F., Kassahun, A., Kvashnina, K., Bazarkina, E., Roßberg, A., Raff, J., Merroun, M.L. (June 6th, 2023 to June 7th, 2023) *Investigation of the interactions of microorganisms with uranium in anthropogenic contaminated waters as basis for the development of a bioremediation technology*. **[Oral communication]**. 3rd Workshop of the ALLIANCE Topical Roadmap WG NORM. Granada (España).

- **Newman-Portela, A.M.***, Krawczyk-Bärsch, E., Lopez-Fernandez, M., Bok, F., Kassahun, A., Kvashnina, K., Bazarkina, E., Roßberg, A., Raff, J., Merroun, M.L. (October 28th to October 29th, 2022) *Microbially induced reduction of Uranium in contaminated mine water for bioremediation purposes: A multidisciplinary approach study*. [Oral communication]. 20th Jena Remediation Colloquium. Jena (Alemania).
- **Newman-Portela, A.M.***, Krawczyk-Bärsch, E., Lopez-Fernandez, M., Bok, F., Kassahun, A., Kvashnina, K., Bazarkina, E., Roßberg, A., Raff, J., Merroun, M.L. (October 9th to October 15th, 2022) *Microbially induced reduction of soluble uranium in mine water*. [Oral communication]. Helmholtz-Zentrum Dresden-Rossendorf - PhD Seminar 2022. Scheffau (Austria).
- **Newman-Portela, A.M.***, Krawczyk-Bärsch, E., Lopez-Fernandez, M., Bok, F., Kassahun, A., Raff, J., Merroun, M.L. (July 10th to July 15th, 2022) *Biostimulation of uranium reducing bacteria in contaminated mine water for bioremediation purposes: multidisciplinary approach study*. [Oral communication]. Goldschmidt'22 Conference. Honolulu, Hawaii (Estados Unidos).
- **Newman-Portela, A.M.***, Krawczyk-Bärsch, E., Lopez-Fernandez, M., Bok, F., Kassahun, A., Raff, J., Merroun, M.L. (December 2nd to December 3rd, 2021) *Multidisciplinary Characterization of Uranium Mine Waters: A Bioremediation Perspective*. [Poster]. New Topics in Mineralogy 2: The mineral-microbe interface through time and space. Online.
- **Newman-Portela, A.M.***, Krawczyk-Bärsch, E., Lopez-Fernandez, M., Bok, F., Kassahun, A., Raff, J., Merroun, M.L. (October 3th to October 9th, 2021) *Design of U mine water bioremediation strategy through U(VI) bioreduction process: Multidisciplinary characterization*. [Oral communication]. Helmholtz-Zentrum Dresden-Rossendorf - PhD Seminar 2021. Scheffau (Austria)

- **Newman-Portela, A.M.***, Krawczyk-Bärsch, E., Lopez-Fernandez, M., Bok, F., Kassahun, A., Raff, J., Merroun, M.L. (July 4th to July 9th, 2021) *Design of U mine water bioremediation strategy through U(VI) bioreduction process: multidisciplinary characterization*. [Oral communication]. Goldschmidt'21 Conference. Online.
- **Newman-Portela, A.M.***, Krawczyk-Bärsch, E., Lopez-Fernandez, M., Bok, F., Kassahun, A., Raff, J., Merroun, M.L. (June 14th, 2021) *Microbially induced reduction of uranium in mine water*. [Oral communication]. European Radioecology ALLIANCE - PhD Webinars. Online.
- **Newman-Portela, A.M.***, Krawczyk-Bärsch, E., Lopez-Fernandez, M., Bok, F., Kassahun, A., Raff, J., Merroun, M.L. (June 28th to July 2nd, 2021). *Biorremediación de aguas contaminadas: estudio multidisciplinar de la reducción microbiana de uranio (U) en aguas de mina*. [Oral communication]. XXVIII Congreso de la Sociedad Española de Microbiología. Online.
- **Newman-Portela, A.M.***, Krawczyk-Bärsch, E., Lopez-Fernandez, M., Bok, F., Kassahun, A., Raff, J., Merroun, M.L. (June 7th to June 10th, 2021). *Design of U mine water bioremediation strategy through U(VI) bioreduction process: multidisciplinary characterization*. [Oral communication]. Biomining '21 Conference. Online.
- **Newman-Portela, A.M.***, Krawczyk-Bärsch, E., Lopez-Fernandez, M., Bok, F., Kassahun, A., Raff, J., Merroun, M.L. (April 15th, 2021) *Multidisciplinary Characterization of Mine Water from a Former Uranium Mine for Bioremediation Purposes*. [Oral communication]. 1st RadoNorm PhD Day 2021. Online.
- **Newman-Portela, A.M.***, Krawczyk-Bärsch, E., Lopez-Fernandez, M., Bok, F., Kassahun, A., Raff, J., Merroun, M.L. (October 5th to October 7th, 2020) *Investigation of the interactions of microorganisms with uranium in anthropogenic contaminated*

waters as basis for the development of a bioremediation technology.
[**Oral communication**]. Helmholtz-Zentrum Dresden-Rossendorf -
PhD Seminar 2020. Dresden (Alemania).

The results achieved during the PhD thesis have been disseminated or are in the process of being prepared for dissemination in scientific journals and conferences both nationally and internationally.

- I. Scientific publications that have been published with the results obtained during the course of this PhD thesis:
 - **Newman-Portela, A.M.**, Krawczyk-Bärsch, E., Lopez-Fernandez, M., Bok, F., Kassahun, A., Drobot, B., Steudtner, R., Stumpf, T., Raff J., Merroun, M.L. (2024) Biostimulation of indigenous microbes for uranium bioremediation in former U mine water: multidisciplinary approach assessment. *Environmental Science and Pollution Research*. 31(5):7227-7245. <https://doi.org/10.1007/s11356-023-31530-4>. **IF: 5.8, Q1**.
- II. National and international conferences and seminars where the results obtained during the course of this PhD thesis have been presented:
 - **Newman-Portela, A.M.***, Krawczyk-Bärsch, E., Lopez-Fernandez, M., Bok, F., Kassahun, A., Kvashnina, K., Bazarkina, E., Roßberg, A., Raff, J., Merroun, M.L. (October 10th, 2023) *Exploring the Influence of Water Chemistry and Microbial Interactions on U Speciation in Former U Mine Water - Implications for Bioremediation Strategies*. [**Oral communication**]. Sustainable Remediation of Radionuclide Impacts (SURRI) Workshop. Granada (España).
 - **Newman-Portela, A.M.***, Krawczyk-Bärsch, E., Lopez-Fernandez, M., Bok, F., Kassahun, A., Kvashnina, K., Bazarkina, E., Roßberg, A., Raff, J., Merroun, M.L. (June 6th, 2023 to June 7th, 2023) *Investigation of the interactions of microorganisms with uranium in anthropogenic contaminated waters as basis for the development of a bioremediation technology*. [**Oral communication**]. 3rd Workshop of the ALLIANCE Topical Roadmap WG NORM. Granada (España).

- **Newman-Portela, A.M.***, Krawczyk-Bärsch, E., Lopez-Fernandez, M., Bok, F., Kassahun, A., Kvashnina, K., Bazarkina, E., Roßberg, A., Raff, J., Merroun, M.L. (October 28th to October 29th, 2022) *Microbially induced reduction of Uranium in contaminated mine water for bioremediation purposes: A multidisciplinary approach study*. [Oral communication]. 20th Jena Remediation Colloquium. Jena (Alemania).
- **Newman-Portela, A.M.***, Krawczyk-Bärsch, E., Lopez-Fernandez, M., Bok, F., Kassahun, A., Kvashnina, K., Bazarkina, E., Roßberg, A., Raff, J., Merroun, M.L. (October 9th to October 15th, 2022) *Microbially induced reduction of soluble uranium in mine water*. [Oral communication]. Helmholtz-Zentrum Dresden-Rossendorf - PhD Seminar 2022. Scheffau (Austria).
- **Newman-Portela, A.M.***, Krawczyk-Bärsch, E., Lopez-Fernandez, M., Bok, F., Kassahun, A., Raff, J., Merroun, M.L. (July 10th to July 15th, 2022) *Bio-stimulation of uranium reducing bacteria in contaminated mine water for bioremediation purposes: multidisciplinary approach study*. [Oral communication]. Goldschmidt'22 Conference. Honolulu, Hawaii (Estados Unidos).
- **Newman-Portela, A.M.***, Krawczyk-Bärsch, E., Lopez-Fernandez, M., Bok, F., Kassahun, A., Raff, J., Merroun, M.L. (December 2nd to December 3rd, 2021) *Multidisciplinary Characterization of Uranium Mine Waters: A Bioremediation Perspective*. [Poster]. New Topics in Mineralogy 2: The mineral-microbe interface through time and space. Online.
- **Newman-Portela, A.M.***, Krawczyk-Bärsch, E., Lopez-Fernandez, M., Bok, F., Kassahun, A., Raff, J., Merroun, M.L. (October 3th to October 9th, 2021) *Design of U mine water bioremediation strategy through U(VI) bioreduction process: Multidisciplinary characterization*. [Oral communication]. Helmholtz-Zentrum Dresden-Rossendorf - PhD Seminar 2021. Scheffau (Austria)

- **Newman-Portela, A.M.***, Krawczyk-Bärsch, E., Lopez-Fernandez, M., Bok, F., Kassahun, A., Raff, J., Merroun, M.L. (July 4th to July 9th, 2021) *Design of U mine water bioremediation strategy through U(VI) bioreduction process: multidisciplinary characterization*. [Oral communication]. Goldschmidt'21 Conference. Online.
- **Newman-Portela, A.M.***, Krawczyk-Bärsch, E., Lopez-Fernandez, M., Bok, F., Kassahun, A., Raff, J., Merroun, M.L. (June 14th, 2021) *Microbially induced reduction of uranium in mine water*. [Oral communication]. European Radioecology ALLIANCE - PhD Webinars. Online.
- **Newman-Portela, A.M.***, Krawczyk-Bärsch, E., Lopez-Fernandez, M., Bok, F., Kassahun, A., Raff, J., Merroun, M.L. (June 28th to July 2nd, 2021). *Biorremediación de aguas contaminadas: estudio multidisciplinar de la reducción microbiana de uranio (U) en aguas de mina*. [Oral communication]. XXVIII Congreso de la Sociedad Española de Microbiología. Online.
- **Newman-Portela, A.M.***, Krawczyk-Bärsch, E., Lopez-Fernandez, M., Bok, F., Kassahun, A., Raff, J., Merroun, M.L. (June 7th to June 10th, 2021). *Design of U mine water bioremediation strategy through U(VI) bioreduction process: multidisciplinary characterization*. [Oral communication]. Biomining '21 Conference. Online.
- **Newman-Portela, A.M.***, Krawczyk-Bärsch, E., Lopez-Fernandez, M., Bok, F., Kassahun, A., Raff, J., Merroun, M.L. (April 15th, 2021) *Multidisciplinary Characterization of Mine Water from a Former Uranium Mine for Bioremediation Purposes*. [Oral communication]. 1st RadoNorm PhD Day 2021. Online.
- **Newman-Portela, A.M.***, Krawczyk-Bärsch, E., Lopez-Fernandez, M., Bok, F., Kassahun, A., Raff, J., Merroun, M.L. (October 5th to October 7th, 2020) *Investigation of the interactions of microorganisms with uranium in anthropogenic contaminated waters as basis*

for the development of a bioremediation technology. [Oral communication]. Helmholtz-Zentrum Dresden-Rossendorf - PhD Seminar 2020. Dresden (Alemania).

ACKNOWLEDGEMENTS

Through this section, I wish to express my sincere gratitude to all the people and institutions who have played a fundamental role in this PhD thesis. I want to extend my sincere thanks to my thesis supervisors, Prof. Dr. Mohamed L. Merroun and Dr. Johannes Raff, as well as to my supervisor, Dr. Evelyn Krawczyk-Bärsch, who entrusted me with the task of carrying out this amazing project and PhD thesis. I appreciate Professor Mohamed for providing me with the opportunity to fully immerse myself in the realm of research, an experience that has significantly contributed to my academic and personal growth. His constant help, understanding, and support have been invaluable throughout the process, teaching me that every detail enriches our knowledge and strength. To Dr. Evelyn, my gratitude for her warm welcome from the outset in a country unfamiliar to me and for helping me in every possible way. Additionally, I sincerely thank her for all the support provided during the thesis, her constant commitment to our work, and for the experiences shared both inside and outside the laboratory. To Dr. Johannes for his constant support and understanding throughout the thesis. His support and trust have allowed us to achieve great results. I am very grateful to have been part of this team.

Furthermore, I would like to express my sincere gratitude to Prof. Dr. Thorsten Stumpf for his valuable support and interest during the course of my PhD thesis. I especially appreciate his generosity in allowing me to use the facilities at the Institute of Resource Ecology of the Helmholtz-Zentrum Dresden-Rossendorf (HZDR, Germany), as well as for providing me with the opportunity to participate in enriching PhD seminars organized in Scheffau (Austria). Likewise, I want to express my gratitude to WISMUT GmbH (Germany), especially Mr. Ulf Barnekow and Ms. Andrea Kassahun for facilitating the case study, sharing relevant information about the recovery site, and providing technical support during the sampling campaigns. I particularly want to highlight Ms. Andrea Kassahun for her firm dedication and continued interest in the project, facilitating data,

organisation of sampling campaigns and for her dedicated reading of the text and suggestions for improvement.

Additionally, I wish to express my profound gratitude to the Department of Molecular Structures of the Institute of Resource Ecology (HZDR, Germany) for providing me with the opportunity to conduct measurements at the BM20 beamline facilities (ROBL) at the European Synchrotron Radiation Facility (ESRF) in Grenoble (France). I especially want to highlight the invaluable collaboration of Prof. Dr. Kristina Kvashnina, Dr. Elena Bazarkina, and Dr. André Roßberg, who dedicated their time, patience, and expertise both during the measurement sessions and in the interpretation of the data.

I would like to express my sincere thanks to Dr. María del Mar Abad and Mrs. Cecilia de la Prada Sánchez from the *Centro de Instrumentación Científica* (CIC, Granada), for their valuable collaboration during the microscopy sessions. We especially acknowledge the excellent work done by Mr. Daniel García Muñoz from the Biological Sample Preparation Laboratory (CIC, Granada), in the meticulous preparation of biological samples. Likewise, I appreciate the contribution of Mr. Andreas Worbs from the Institute of Ion Beam Physics and Materials Research (HZDR, Germany) in the microscopy sessions, as well as the assistance of my colleagues from the Institute of Resource Ecology (HZDR, Germany): Salim Shams (HZDR, Germany) in the preparation and analysis of samples using Powder X-ray diffraction. Furthermore, my thanks to Dr. Björn Drobot and Dr. Robin Steudtner for their advice and support in the use of techniques such as cryo-TRLFS, UV/vis, and data analysis using PARAFAC. Additionally, I thank Dr. Frank Book for his invaluable assistance and ongoing dedication. Likewise, I wish to extend my sincere gratitude to Dr. Susanne Sachs, Dr. Thuro Arnold, Dr. Andrea Cherkouk and Ms. Katrin Flemming for their wise advice and support. Also, appreciation goes to Dr. Ting-Shyang Wei for assistance by evaluating the metatranscriptomic analysis. Moreover, I want to express my gratitude to other colleagues whose support was

essential, to Ms. Sabrina Beutner and Ms. Sylvia Schöne for their assistance in analytical measurements. To Stephan Weiß, Ms. Sindy Kluge, and Ms. Rahel Bertheau for their willingness and assistance in the development of experiments. To Ms. Susana Jiménez for her great help in the radioactive control laboratories.

Además, este camino ha sido mucho más sencillo gracias al apoyo de todos mis compañeros, como dice el refrán “las penas compartidas pesan menos”. A mis compañeros de departamento, A Marcos “marquiños”, Mar “maremoto”, mi Sancho Panza y Dulcinea, gracias por soportarme. Al Dr. Seleneda, gran persona y mejor “*gym-bro*”. A Jaime, mi “*crypto-bro*”, algún día acertaremos con el “All-Time High”. A Chacho, que nunca pierda esa sonrisa y por esos deliciosos dulces canarios. A Esther, primera de España y próxima promesa en la micología, gracias por todas esas tardes de laboratorio. A Cristina y Fadwa, muchas gracias por toda la ayuda, consejos y apoyo. A Margarita, por los momentos compartidos en el Departamento y en las prácticas. A Sonia, por ser Sonia (mucha grandeza). A Guillermo por esa solución de safranina que aún deja marcas. A Alejandro, gracias por todo lo compartido en Dresden, por esa habilidad para hacer pino al final de la noche y las quedadas en el “Irish Fiddler”. A Raulito, por esa alegría diaria, bailes y los cafés en el “Oswaldz”. A Miguel Rabelo por todas esas tardes en el laboratorio y por tu paciencia en mis inicios. A Juanma, por ser un gran compañero y estar siempre presente, que calidad tiene el ser gaditano. También deseo expresar mi agradecimiento a la Profesora Inés Martín por el entusiasmo transmitido por la Micología, y a la Profesora María Teresa González por su ayuda en la revisión de varias secciones de esta tesis doctoral. A Don Manolo por su compañía los fines de semana en el departamento y sus consejos. Asimismo, a mis compañeros, Pablo, Iván, Ylenia, Jesús, Yon, Adam, Lidia, Victoria, Francesca, Sonia, Mónica, Tamara, Conchi Millán, Ana España y a los profesores Manuel y Platero, gracias por acompañarme en esta gran etapa.

Igualmente, a mis grandes amigos Marco, Laura, Irene, Luís, Violeta,

Gabriela, María Luque, María Espejo, María Augusta, Isa y Carmen, muchas gracias por todos los momentos vividos. En especial a ustedes, Marco, Laura e Irene por comprenderme, apoyarme y siempre estar presentes. También a mis amigos Gabi, Miguel, Israel, Julián, Juan Ramón, Juan Carlos, Ismael, Chemi y Don Juan Cotano. Del mismo modo, a Ángela por su ayuda en la maquetación de este trabajo.

A mis “tutores legales” en Dresden, Susana, Aurelio y Natalia. Os estaré eternamente agradecidos por acogermme, ayudarme y apoyarme durante todo este tiempo.

In addition, I would like to express my sincere gratitude to all the colleagues at the HZDR: Stephan, Rodrigo, Victor, Claudia, Jessica, Thomas, Irene, Tamara, Boseok, Chris, Katrin, Luíza, Janis, Klemen, Warren, Jenny, Isi, Max, Isabelle, Sebastian, and Vlad.

Moreover, I would like to express my gratitude to the Institute of Resource Ecology (HZDR, Germany), the University of Granada (Spain), the European Radioecology Alliance (ALLIANCE), and RadoNorm project for their financial support. This has enabled me to undertake research stays at the Helmholtz-Zentrum Dresden-Rossendorf (Germany) and at the ESRF in Grenoble (France), as well as to participate in international conferences.

Finally, I would like to thank my parents, Esther and Antonio, and my brother Juan, for their support during this process, sharing with me both the frustrating and the happy moments along the way. Their constant presence and support were essential. Also, to my aunt Ana María and my cousins Juan and Jimena.

*A mis padres, hermano, familia y a todos aquellos
que siempre supieron hacerme sonreír.*

“Think globally, act locally”

David Brower

LIST OF ABBREVIATIONS

Å: Angstrom

AA: Amino Acid

ABTS: 2,2'-azino-bis(3-ethylbenzothiazoline-6-sulphonic acid)

ASR: Assimilatory Sulphate Reduction

ASVs: Amplicon Sequence Variants

BLAST: Basic Local Alignment Search Tool

BSE: Backscattered Electrons

CBB: Calvin-Benson-Bassham

CMC: Carboxymethylcellulose

Cryo-TRLFS: Cryo-Time-Resolved Laser Fluorescence Spectroscopy

DADA2: Divisive Amplicon Denoising Algorithm 2

DGE: Differential Gene Expression

DNA: Deoxyribonucleic Acid

DNase: Deoxyribonuclease

DOC: Dissolved Organic Carbon

DSR: Dissimilatory Sulphate Reduction

EC: Electrical Conductivity

EDXS: Energy-Dispersive X-Ray Spectroscopy

E_H: Redox potential

eV: Electronvolt

EXAFS: Extended X-Ray

Absorption Fine Structure

FDR: False-Discovery-Rate

FeOB: Fe-Oxidizing Bacteria

FeRB: Fe-Reducing Bacteria

FESEM: Field Emission Scanning Electron Microscopy

FFT: Fast Fourier Transform

FT: Fourier Transforms

G2P: Glycerol-2-Phosphate

HAADF: High-Angle Annular Dark-Field

HERFD-XANES: High-Energy-Resolution Fluorescence-Detected X-ray Absorption Near-Edge Structure

HPIC: High Performance Ionic Chromatography

HRTEM: High-Resolution Transmission Electron Microscope

ICP-MS: Inductively Coupled Plasma Mass Spectrometry

IPBLN: Instituto de Parasitología y Biomedicina López Neyra

ITFA: Iterative Transformation Factor Analysis

ITS: Internal Transcribed Spacer

LiP: Lignin Peroxidase

m-Se: Monoclinical Selenium

MIC: Minimum Inhibitory Concentration

mRNA: messenger RNA

NCBI: National Center for Biotechnology Information

NCBI: National Centre for Biotechnology Information
NGS: Next Generation Sequencing
NMDS: Non-metric Multidimensional Scaling
NPs: Nanoparticles
NRB: Nitrate-Reducing Bacteria
PARAFAC: Parallel Factor Analysis
PCA: Perform Principal Component Analysis
PCR: Polymerase Chain Reaction
PDA: Potato Dextrose Agar
PDB: Potato Dextrose Broth
PERMANOVA: Permutational Analysis of Variance
PXRD: Powder X-Ray Diffraction
QIIME: Quantitative Insights into Microbial Ecology
RIN: RNA Integrity Number
RNA: Ribonucleic Acid
rRNA: Ribosomal Ribonucleic Acid
rTCA: Reverse Tricarboxylic Acid
RuBisCo: Ribulose-1,5-bisphosphate carboxylase/oxygenase
SAED: Selected Area Electron Diffraction
Se(-II): Selenide
Se(0): Elemental selenium
Se(IV): Selenite
Se(VI): Selenate
SEM: Scanning Electron Microscopy
SeNPs: Selenium nanoparticles
SOB: Sulphur-Oxidizing Bacteria
SRA Sequence Reads Archive
SRB: Sulphate-Reducing Bacteria
STEM: Scanning Transmission Electron Microscopy
t-Se: Trigonal selenium
TCA: Tricarboxylic acid
TEM: Transmission Electron Microscopy
TFA: Target Factor Analysis
TI: Tolerance Index
TIC: Total Inorganic Carbon
TN: Total Nitrogen
TOC: Total Organic Carbon
U(IV): Uranium tetravalent
U(V): Uranium pentavalent
U(VI): Uranium hexavalent
UNPs: Uranium nanoparticles
UV/Vis: Ultraviolet-Visible Spectroscopy
WHO: World Health Organization
XRD: X-Ray Diffraction
θ: Theta
CIC: Centro de Instrumentación Científica.



Índice

Open-pit mine. Photo by C.
Photography

RESUMEN	33
SUMMARY	41
INTRODUCTION	47
1. Uranium: A Historical Perspective	48
2. Physicochemical Properties of U	48
3. Natural Occurrence of U Minerals	52
4. U Extraction Methods	54
5. Utilities and production of U	59
6. U Contamination and potential health risks	64
7. Environmental remediation of U: technologies	65
8. U bioremediation	66
OBJECTIVES	91
MATERIALS AND METHODS	95
1. Sampling campaigns	96
2. Characterization of the microbial community in the mine water	96
3. Metatranscriptomic study	97
4. Molecular and biochemical characterization of isolated fungi	97
5. Geochemical characterization of the mine waters	99
6. Prediction and determination of soluble U species	99
7. Experimental design of microcosms	101
8. Characterization of reduced U products in the microcosms	102
CHAPTER I: Biostimulation of indigenous microbes for uranium bioremediation in former U mine water: Multidisciplinary approach assessment	114
CHAPTER II: Metatranscriptomics studies decipher key microbial metabolic pathways and their contribution to U(VI) reduction in mine waters	171
CHAPTER III: New insight into U(IV) and U(V) formation by glycerol-based stimulation of indigenous U reducing bacteria in U mine water: multidisciplinary approach characterization	232
CHAPTER IV: Exploring the fungal community in U-contaminated mine waters: a strategic approach for the mycoremediation of metalloids and radionuclide-contaminated environments	290
GENERAL DISCUSSION	344
CONCLUSIONES	364
CONCLUSIONS	368



Photo from Unsplash



Resumen

RESUMEN

La presencia de uranio (U), y otros metales pesados, representan una amenaza potencial tanto para el medio ambiente como para la salud humana debido a la contaminación del suelo y del agua. Esta contaminación se debe, principalmente, a la minería. No obstante, está bien documentado que también pueden contribuir a esta contaminación otras actividades humanas, tales como las prácticas agronómicas y los conflictos militares. De todos estos contaminantes el U se ha convertido en uno de los elementos más importantes del mundo en los últimos 60 años, debido a su uso potencial en la producción de energía nuclear. Por lo tanto, es esencial desarrollar programas de rehabilitación ambiental en las áreas afectadas, junto con la adopción de estrategias de gestión de residuos. Dentro de este contexto, la minería de uranio (U) ha dejado un legado de contaminación ambiental en los Estados Federales de Sajonia y Turingia (Alemania) al que sería preciso prestar atención.

Para la remediación de ambientes contaminados con U se han utilizado, de forma tradicional, tecnologías convencionales basadas en procesos fisicoquímicos. Sin embargo, estas tecnologías, tienden a ser costosas, complejas de aplicar e ineficaces para tratar bajas concentraciones de U. Por lo tanto, una alternativa prometedora, menos costosa, fácil de implementar y efectiva para bajas concentraciones de U es la biorremediación, basada en los mecanismos de interacción de los sistemas biológicos con el U.

Según la extensa literatura disponible, las principales estrategias recomendadas para la biorremediación de U, incluyen dos enfoques: biomineralización de fosfatos de U(VI) en condiciones óxicas y reducción enzimática en condiciones anóxicas de U(VI) soluble, altamente móvil y biodisponible, a U(IV) insoluble, menos móvil y, por lo tanto, menos biodisponible.

El objetivo de esta tesis doctoral fue caracterizar, a través de un enfoque multidisciplinar, aguas procedentes de dos minas de U de Sajonia: Schlema-Alberoda y Pöhla (Wismut GmbH), con el fin de diseñar una futura estrategia de biorremediación de U basada en la bioestimulación de la comunidad microbiana autóctona reductora de U.

En primer lugar, se caracterizaron las propiedades fisicoquímicas de ambas aguas de mina utilizando técnicas analíticas como *Inductively Coupled Plasma Mass Spectrometry* y *High-Performance Ion Chromatography*. Estas técnicas, junto con cálculos termodinámicos y estudios espectroscópicos utilizando *cryo-Time-Resolved Laser Fluorescence Spectroscopy* y Análisis de Factores Paralelos, permitieron predecir y confirmar la especiación de U en las aguas mineras en condiciones ambientales y experimentales. El agua procedente de Schlema-Alberoda presentó concentraciones más altas de U y SO_4^{2-} (U: 1 mg/l; SO_4^{2-} : 335 mg/l) que la de Pöhla (U: 0.01 mg/l; SO_4^{2-} : 0.5 mg/l). Estos datos indican que, en contraste con Pöhla, el agua de la mina de Schlema-Alberoda supera la concentración máxima permitida de U, según la Organización Mundial de la Salud, tanto en agua potable (0.03 mg/l), como en agua de descarga a masas de agua (0.5 mg/l). Por lo tanto, se seleccionó el agua de la mina de Schlema-Alberoda en estudios posteriores, con el objetivo de reducir las concentraciones de U a niveles permitidos mediante el diseño de una estrategia eficiente de biorremediación. Además, se identificaron dos especies de U solubles en el agua de mina de Schlema-Alberoda: $\text{Ca}_2\text{UO}_2(\text{CO}_3)_3(\text{aq})$ y $\text{UO}_2(\text{CO}_3)_3^{4-}$. Debido a las concentraciones extremadamente bajas de U en el agua de la mina de Pöhla, no se pudo determinar la especiación de U.

En segundo lugar, mediante secuenciación del gen 16S del ARN ribosomal y el espaciador transcrito interno fúngico, caracterizamos una comunidad bacteriana dominada por los filos Campylobacterota, Proteobacteria y Patescibacteria, con alta tolerancia a metales pesados y radionucleidos. Asimismo, se identificó una comunidad fúngica involucrada en la degradación de la madera (por ejemplo, filo Basidiomycetes). Cabe destacar que estas comunidades microbianas identificadas podrían afectar los ciclos biogeoquímicos de elementos como S, C, Fe y N, relevantes para la eliminación de U a través de procesos de biomineralización y reducción enzimática.

Posteriormente, estudios de metatranscriptómica basados en la secuenciación del ARN, mostraron una comunidad microbiana activa con rutas metabólicas relacionadas con los ciclos biogeoquímicos de C, N y S

en las aguas de mina, tanto de Schlema-Alberoda como de Pöhla. Estos estudios han permitido identificar bacterias (*Sulfurimonas* y *Sulfuricurvum*) capaces de oxidar compuestos reducidos de S utilizando nitrato como aceptor terminal de electrones, promoviendo así el crecimiento de bacterias reductoras de sulfato como *Desulfobacca*. Además, con una mayor expresión en Pöhla que en Schlema-Alberoda, se identificó la reducción disimilatoria de sulfato como la posible vía principal para reducción de sulfato por bacterias reductoras de sulfato. Por otra parte, y solo en las muestras de Pöhla, se puso de manifiesto la expresión de dos genes (*OmcS* (547981_1 y 237412_1)) para la reducción de hierro por bacterias reductoras de hierro. Estos resultados sugieren que la presencia de una comunidad microbiana activa podría ser clave en la reducción de SO_4^{2-} , Fe y también U en aguas mineras, procesos de gran relevancia para la biorremediación de U.

Finalmente, para evaluar el potencial de biorremediación de la comunidad microbiana nativa en el agua de la mina, se elaboró un conjunto de microcosmos anóxicos utilizando agua de la mina de Schlema-Alberoda y se enriqueció con glicerol (10 mM) como donador de electrones. El glicerol se eligió con esta finalidad al mostrar mejores tasas de reducción de U(VI) soluble que otros donadores de electrones, como el ácido glucónico o el ácido vanílico.

A través de un enfoque multidisciplinario, que combina técnicas analíticas (*Inductively Coupled Plasma Mass Spectrometry* y *High-Performance Ion Chromatography*) y espectroscópicas (*High-Energy-Resolution Fluorescence-Detection X-Ray Absorption Near-Edge Structure Spectroscopy*, *Extended X-ray Absorption Fine Structure* y *Ultraviolet-Visible spectroscopy*), se confirmó claramente la reducción de U(VI) a especies de U(V) y U(IV) en los microcosmos enriquecidos con glicerol.

La coordinación local de U en la muestra estudiada es similar a la de uraninita y carbonatos de U(V)/U(VI). Mediante *High-Angle Annular Dark-Field Scanning Transmission Electron Microscopy* y *Energy-Dispersive X-Ray Spectroscopy* se confirmó la formación de nanopartículas (NPs) de U(IV) y U(V). Por lo tanto, los resultados indican que el glicerol es un donador de electrones efectivo para promover la reducción enzimática de U(VI)

soluble a U(IV) en forma de NPs de uraninita y U(V) como NPs de FeUO_4 biogénicas, descritas por primera vez en este trabajo. Además, estas NPs de U(V) mostraron estabilidad química en presencia de oxígeno durante 4 semanas, lo que no se había descrito hasta el momento en ningún otro trabajo científico.

Por otro lado, la comunidad fúngica, previamente identificada en las dos aguas mineras, podría tener un gran potencial en la biorremediación de U ya que los hongos muestran una mayor tolerancia frente a metales pesados que las bacterias. La biorremediación basada en el uso de hongos tolerantes a los metales se considera una estrategia prometedora y rentable. Por este motivo, en este trabajo se aislaron hongos autóctonos del agua de las minas de Schlemma-Alberoda y Pöhla utilizando técnicas dependientes de cultivo y se procedió a su caracterización bioquímica e identificación molecular mediante secuenciación de Sanger. Además, se evaluó su potencial para la biorremediación de U y selenio (Se). En concreto, las cepas fúngicas aisladas fueron catorce, pertenecientes a varios géneros, la mayoría de las cuales mostraron una alta actividad enzimática lignocelulolítica y fosfatasa. El potencial de biorremediación de estas cepas fúngicas se evaluó utilizando aislados de los géneros *Cadophora*, *Aspergillus* y *Penicillium* expuestos a U, y de *Schizophyllum*, *Trichoderma*, *Cladosporium* y *Acremonium* expuestos a Se. Mediante *Field Emission Scanning Electron Microscopy* se observó la capacidad de algunas de estas cepas para formar acúmulos de fosfato de U, probablemente debido a la actividad fosfatasa fúngica. Además, *High-Resolution Transmission Electron Microscope* y *High-Angle Annular Dark-Field Detector* acoplado a *Energy-Dispersive X-Ray Spectroscopy* revelaron la reducción de Se(IV) y la formación de nanoestructuras de Se(0).

De todo lo dicho cabe deducir que la biorremediación de aguas contaminadas con bajas concentraciones de U presenta un desafío significativo, que puede abordarse estimulando la actividad de bacterias reductoras de U, como se describe en esta tesis doctoral. Además, este estudio no solo proporciona nuevos conocimientos sobre la reducción de U(VI) a U(IV), sino que también enfatiza que el U(V), como estado de oxidación intermedio, es

más estable en forma de NPs de FeUO_4 biogénicas que la uraninita, lo que aumenta el potencial de esta estrategia, considerando el riesgo de re-oxidación del U.



Photo from Unsplash



Summary

SUMMARY

Uranium (U) mining has left a legacy of environmental contamination in the Federal States of Saxony and Thuringia (Germany). Concentrations of U and other heavy metals pose a potential threat to both the environment and human health through contamination of soil and water. Additionally, it is well documented that other human activities, such as agronomic practices and military conflicts, have contributed to the contamination of the environment. However, U has become one of the world's most important elements in the last 60 years due to its potential use in nuclear energy production. Therefore, it is essential to develop environmental rehabilitation programs in affected areas, along with adopting waste management practices.

Traditionally, physicochemical based conventional technologies have been used to remediate environments contaminated with U. However, these approaches tend to be costly, complex to apply, and ineffective for low concentrations of U. Hence, a promising alternative, less expensive, easy to implement, and effective for low U concentrations is bioremediation, based on the interaction mechanisms of biological systems with U. Based on extensive available literature, the main suggested strategies for U bioremediation include two approaches: biomineralization of U(VI) phosphates under oxic conditions and enzymatic reduction under anoxic conditions from soluble, highly mobile, and bioavailable U(VI) to insoluble, less mobile, and thus less bioavailable U(IV) by biostimulation.

The aim of this PhD thesis was to characterize, through a multidisciplinary approach, two former German mine waters contaminated with U, Schlemma-Alberoda and Pöhla (Wismut GmbH), in order to design a future U bioremediation strategy based on biostimulation of the native U-reducing microbial community.

Initially, the chemistry of both mine waters was characterized using analytical techniques such as Inductively Coupled Plasma Mass Spectrometry and High-Performance Ion Chromatography. These techniques, along with thermodynamic calculations and spectroscopic studies using cryo-Time-Resolved Laser Fluorescence Spectroscopy and Parallel Factor Analysis,

allowed the prediction and confirmation of U speciation in the mine waters under environmental and experimental conditions. Schlema-Alberoda showed higher concentrations of U, and SO_4^{2-} (U: 1 mg/l; SO_4^{2-} : 335 mg/l) in mine water compared to Pöhla (U: 0.01 mg/l; SO_4^{2-} : 0.5 mg/l). These data indicate that, in contrast to Pöhla, Schlema-Alberoda mine water exceeds the maximum allowed U concentration in drinking water according to WHO (0.03 mg/l) and in water discharge (0.5 mg/l). Therefore, Schlema-Alberoda mine water was selected in further studies, with aim to decrease of U concentrations to permitted levels through the design of an efficient bioremediation strategy. Additionally, two soluble U species were identified in Schlema-Alberoda: $\text{Ca}_2\text{UO}_2(\text{CO}_3)_3(\text{aq})$ and $\text{UO}_2(\text{CO}_3)_3^{4-}$. Due to the extremely low U concentrations in the mine water of Pöhla, U speciation could not be determined. Through next-generation sequencing of the 16S ribosomal RNA gene and fungal internal transcribed spacer, we characterized a bacterial community dominated by the phyla Campylobacterota, Proteobacteria, and Patescibacteria, with high tolerance to heavy metals and radionuclides. Likewise, a fungal community involved in wood degradation (e.g., Basidiomycetes phylum) was identified. The identified microbial communities could affect the biogeochemical cycles of elements like S, C, Fe and N relevant for removal of U through biomineralization and reduction processes.

Subsequently, metatranscriptomic studies based on RNA sequencing showed an active microbial community with key metabolic pathways and activities related to the biogeochemical cycles of C, N, and S in the mine waters of Schlema-Alberoda and Pöhla. We identified bacteria (*Sulfurimonas* and *Sulfuricurvum*) capable of oxidizing reduced S compounds and utilizing nitrate as a terminal electron acceptor, thus promoting the growth of sulphate-reducing bacteria (SRB) such as *Desulfobacca*. Additionally, with higher expression in Pöhla than in Schlema-Alberoda, dissimilatory sulphate reduction was identified as the possible main pathway for SRB to reduce sulphate. Moreover, exclusively in Pöhla, the expression of two genes (*OmcS* (547981_1 and 237412_1)) for iron reduction by iron-reducing bacteria (FeRB) was identified. These results suggest that the presence

of an active microbial community could be key in reducing SO_4^{2-} , Fe, and also U in mine waters, thus offering opportunities for U bioremediation.

Finally, to assess the bioremediation potential of the native microbial community in mine water, a set of anoxic microcosms was elaborated using Schlema-Alberoda mine water and amended with glycerol (10 mM) as an electron donor. Glycerol exhibited better rates of soluble U(VI) reduction compared to other electron donors such as gluconic acid or vanillic acid. Through a multidisciplinary approach combining analytical (Inductively Coupled Plasma Mass Spectrometry and High-Performance Ion Chromatography) and spectroscopic techniques (High-Energy-Resolution Fluorescence-Detection X-Ray Absorption Near-Edge Structure, Extended X-Ray Absorption Fine Structure, and Ultraviolet–Visible spectroscopy), the reduction of U(VI) to U(V) and U(IV) species in the microcosms amended with glycerol was clearly confirmed. The local coordination of U in the studied sample is similar to that of uraninite and U(V)/U(VI)-carbonates. High-Angle Annular Dark-Field Scanning Transmission Electron Microscopy and Energy-Dispersive X-Ray Spectroscopy confirmed the formation of U(IV) and U(V) nanoparticles (NPs). Therefore, the results indicate that glycerol is an effective electron donor for promoting enzymatic reduction of soluble U(VI) to U(IV) in the form of uraninite NPs and U(V) as biogenic FeUO_4 NPs reported in the present work for the first time. Additionally, these U(V) NPs exhibited a 4-week stability under oxic conditions, what has not been reported so far.

On the other hand, the previously identified fungal community in the two mine waters could have a great potential in U bioremediation as fungi exhibit higher tolerance than bacteria. Bioremediation using metal-tolerant fungi is considered a promising and cost-effective strategy. Therefore, in this work we isolated indigenous fungi from Schlema-Alberoda and Pöhla mine water using culture-dependent techniques and proceeded to their biochemical characterization and molecular identification through Sanger sequencing. Additionally, we evaluated their potential for U and selenium (Se) bioremediation. Fourteen fungal strains belonging to various genera were isolated, most of which showed high lignocellulolytic enzyme and

phosphatase activity. The bioremediation potential was evaluated using isolates from the genera *Cadophora*, *Aspergillus*, and *Penicillium* exposed to U, and from *Schizophyllum*, *Trichoderma*, *Cladosporium*, and *Acremonium* exposed to Se. Field Emission Scanning Electron Microscopy showed the ability of some strains to form U-phosphate associations, probably due to fungal phosphatase activity. Additionally, High-Resolution Transmission Electron Microscope and the High-Angle Annular Dark-Field detector coupled with Energy-Dispersive X-Ray Spectroscopy revealed the reduction of Se(IV) and the formation of Se(0) nanostructures.

The bioremediation of contaminated waters with low U concentrations shows a significant challenge, which can be addressed by stimulating U-reducing bacterial activity, as described in this PhD thesis. Moreover, this study not only provides new insights on the reduction of U(VI) to U(IV) but also emphasizes that U(V) as intermediate oxidation state is more stable in form of biogenic FeUO_4 NPs than uraninite, thus increasing the potential of this strategy, considering the risk of U reoxidation.



Photo by Ivan Bandura



Introduction

INTRODUCTION

1. Uranium: A Historical Perspective

Uranium (U) is the 49th most abundant element in the Earth's crust, with an abundance similar to that of beryllium (Be), tin (Sn), and arsenic (As) (Smedley and Kinniburgh 2023). Its origins trace back over 6 billion years, originating during the formation of supernovae, although recent research challenges these theories by suggesting that some U is generated during the merger of two neutron stars (WNA 2021). In 1789, the German chemist Martin Heinrich Klaproth discovered U while studying "pitchblende" from the Joachimsthal (Jáchymov) mines located in the Bohemian Ore Mountains, near the current German-Czech border (Marshall and Marshall 2008). M.H. Klaproth named it in honour of the planet Uranus, discovered in 1781 by the English astronomer William Herschel. Subsequently, in 1896, Antoine Henri Becquerel attributed radioactive properties to U, referring to them as "active radiations," thus laying the groundwork for the term later established by Maria Salomea Skłodowska-Curie as radioactivity (Carvalho 2011).

2. Physicochemical Properties of U

U is the heaviest natural occurring element on the periodic table of elements ($Z = 92$), with a relative atomic mass of 238.03 g/mol and a specific density of approximately 19.07 g/cm³, making it 1.67 times denser than lead (11.4 g/cm³) (Smedley and Kinniburgh 2023). Pure U is a silver-white metal and can be characterized as a heavy, ductile, and slightly paramagnetic metal (Gavrilescu et al. 2009). Its boiling and melting points are 3818°C and 1132°C, respectively (Bem and Bou-Rabee 2004). U belongs to the actinides, a series of chemical elements that belong to the group 3 of the periodic table of elements, and along with thorium (Th), they are the only natural actinides in the periodic table of elements (Fig. 1). Actinides are heavy metals and radioactive that share chemical similarities due to their electronic configuration. The actinide series includes all elements from actinium (Ac, $Z = 89$) to lawrencium (Lr, $Z = 103$).

U has many isotopes, all of which are radioactive in nature, including ²²⁷U, ²³⁰U, ²³¹U, ²³²U, ²³³U, ²³⁴U, ²³⁵U, ²³⁶U, ²³⁷U, and ²³⁸U (Taylor and Taylor

1997; Khani 2011). However, natural U, predominantly composed of three isotopes (^{234}U , ^{235}U , and ^{238}U), is weakly radioactive. The isotopic composition of natural U is composed by ^{238}U (99.27%), with a less significant presence of ^{235}U (0.72%) and ^{234}U (0.006%) (Lakaniemi et al. 2019). The half-life of these U isotopes ranges from 2.5×10^5 to 4.5×10^9 years (Mettler and Upton 2008). The most abundant isotope, ^{238}U , has the longest half-life, about 4.5×10^9 years. In contrast, ^{235}U and ^{234}U have shorter half-lives, 7.1×10^8 years and 2.5×10^5 years, respectively (Mettler and Upton 2008). The decay chain of these isotopes includes radioactive elements that decay into lead (Pb) (Fig. 2) (Elafia et al. 2024). Most of the U present in nature is the isotope ^{238}U , which undergoes radioactive decay along an extended series of 13 distinct radionuclides before reaching a stable state in ^{206}Pb (Gavrilescu et al. 2009; Elafia et al. 2024). These radionuclides emit *alpha* or *beta* radiation, and some also emit *gamma* radiation with varying energies (Gavrilescu et al. 2009).

92 238.03

U

Uranium

[Rn]5f⁶6d¹7s² Actinide

Boiling point: 3818 °C

Melting point: 1132 °C

Density: 19.07 g/cm³



Uraninite

1	2											18	19	20	21	22	23	24	25	26	27	28	29	30	31	32	33	34	35	36	37	38	39	40	41	42	43	44	45	46	47	48	49	50	51	52	53	54	55	56	57	58	59	60	61	62	63	64	65	66	67	68	69	70	71	72	73	74	75	76	77	78	79	80	81	82	83	84	85	86	87	88	89	90	91	92	93	94	95	96	97	98	99	100																																																											
H	He																	Li	Be	B	C	N	O	F	Ne											Na	Mg	Al	Si	P	S	Cl	Ar											K	Ca	Sc	Ti	V	Cr	Mn	Fe	Co	Ni	Cu	Zn	Ga	Ge	As	Se	Br	Kr											Rb	Sr	Y	Zr	Nb	Mo	Tc	Ru	Rh	Pd	Ag	Cd	In	Sn	Sb	Te	I	Xe											Cs	Ba	Hf	Ta	W	Re	Os	Ir	Pt	Au	Hg	Tl	Pb	Bi	Po	At	Rn											Fr	Ra	Rf	Db	Sg	Bh	Hs	Mt	Ds	Rg	Cn	Nh	Fl	Mc	Lv	Ts	Og
		La		Ce	Pr	Nd	Pm	Sm	Eu	Gd	Tb	Dy	Ho	Er	Tm	Yb	Lu											Ac	Th	Pa	U	Np	Pu	Am	Cm	Bk	Cf	Es	Fm	Md	No	Lr																																																																																																															

Figure 1. Overview of the physicochemical characteristics of the element U. Image of the mineral uraninite obtained from King (2024).

U exhibits four oxidation states: trivalent (U(III)), tetravalent (U(IV)), pentavalent (U(V)), and hexavalent (U(VI)), with U(IV) and U(VI) being the most common, stable, and predominant oxidation states in nature (Smedley and Kinniburgh 2023). U(III) in aqueous solutions is thermodynamically unstable, so the chemistry of U specie in aqueous solutions is very limited, and its compounds are mainly prepared by “dry” methods (Yusov et al. 2005). An example of a compound isolated from aqueous solutions is potassium U(III) sulphate, $K_5U(SO_4)_4$, created by adding a U(III) solution to a saturated solution of K_2SO_4 in H_2SO_4 , followed by separation through centrifugation and washing of the precipitate (Yusov

et al. 2005). This U(III) compound can be stored for over a month in dry air (Yusov et al. 2005). However, dissolved U(III) tends to oxidize to U(IV) in most reducing environments in nature (Gavrilescu et al. 2009). U(V) has also been considered an unstable and transient state that occurs only in small proportions over a limited range of E_H and disproportionates to tetra- and hexavalent states (Gavrilescu et al. 2009). However, some studies have demonstrated the U(V) stabilization in aqueous conditions using a polydentate aminocarboxylate ligand (Faizova et al. 2018). In oxidizing environments, U tends to be present in its U(VI) oxidation state, mainly as the uranyl ion (UO_2^{2+}) (Gavrilescu et al. 2009). U(VI) has the ability to form easily complexes with calcium, magnesium, and/or carbonate, increasing its solubility and mobility, thus increasing its bioavailability and, consequently, its toxicity (Nolan et al. 2021). In contrast, U(IV) is stable under reducing conditions and is considered relatively immobile, as it forms poorly soluble minerals such as uraninite (UO_2) (Gavrilescu et al. 2009; Nolan et al. 2021). Since these minerals are poorly soluble, they have lower bioavailability and, therefore, are less toxic.

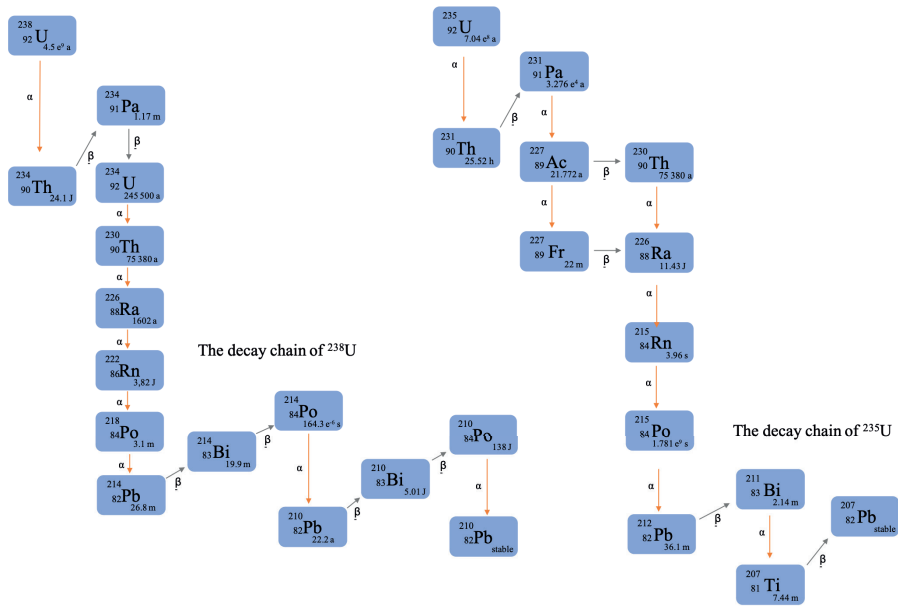


Figure 2. The radioactive decay pathways of ^{235}U and ^{238}U . Figure adapted from Elafia and co-authors (2024). a: years; J: days; h: hours; m: minutes; s: seconds.

3. Natural Occurrence of U Minerals

U is ubiquitous in nature, found in soils, surface waters, and groundwater. The Earth's crust contains around 2.8 mg of U per kilogram, while in rivers, a worldwide average of 0.3 $\mu\text{g U/l}$ has been reported (Smedleya and Kinniburgh 2023). However, in rivers in Germany, a range of 0.23 $\mu\text{g U/l}$ to 3.5 $\mu\text{g U/l}$ was measured (Mangini et al. 1979). Around 3.3 $\mu\text{g U/l}$ are found in open seawater, while typically less than 5 $\mu\text{g U/l}$ are present in groundwater. Nonetheless, elevated levels can be observed in both surface water and groundwater, with a variation of about six orders of magnitude, ranging up to milligrams of U per litre (Smedleya and Kinniburgh 2023). However, human activities have caused significant increases in U concentration in specific areas (Gavrilescu et al. 2009).

In nature, U exists in the form of complex minerals, and the primary factor controlling its formation is the redox state of the surrounding environment. More than 250 minerals containing U have been described (Campbell et al. 2015; Smedleya and Kinniburgh 2023). Table 1 summarizes the main U minerals. Minerals containing U(VI) are more abundant than those with U(IV), and so far, only one mineral with U(V) has been documented, named “wyar-tite” (Burns and Finch 1999; Smedleya and Kinniburgh 2023). U(IV)-containing minerals generally occur as oxides or primary silicates that form covalent bonds with U(IV), resulting in poorly soluble minerals (Bowell et al. 2011; Cumberland et al. 2016). The main minerals include uraninite (UO_2), coffinite ($\text{U}(\text{SiO}_4)_{1-x}(\text{OH})_{4x}$), and brannerite (UTi_2O_6). Conversely, U(VI) minerals are often generated as results of replacements of primary U(IV) minerals and are characterized by the numerous hydrated minerals formed such as phosphates, silicates, vanadates, carbonates, arsenates, and hydrated uranyl molybdates (Smedleya and Kinniburgh 2023). The most common U(VI) minerals are autunite ($\text{Ca}(\text{UO}_2)_2(\text{PO}_4)_2 \cdot 10\text{--}12\text{H}_2\text{O}$) and uranophane ($\text{Ca}(\text{UO}_2)_2\text{SiO}_3(\text{OH})_2 \cdot 5\text{H}_2\text{O}$).

Table 1. Main U minerals classified according to oxidation state (IV, V and VI). Table adapted from Smedleya and Kinniburgh (2023).

Mineral	Formula
U(IV) minerals	
Uraninite	UO_2
Pitchblende	U_3O_8
Coffinite	$\text{U}(\text{SiO}_4)_{1-x}(\text{OH})_{4x}$
Brannerite	UTi_2O_6
Davidite	$(\text{La,Ce})(\text{Y,U,Fe})(\text{Ti,Fe})_{20}(\text{O,OH})_{38}$
Betafite	$(\text{Ca,U})_2(\text{Nb,Ti})_2\text{O}_6\text{OH}$
Uranothorite	$(\text{U,Th})\text{SiO}_4$
Thucholite	Uraninite with hydrocarbons
U(V) minerals	
Wyartite	$\text{CaU}(\text{UO}_2)_2(\text{CO}_3)\text{O}_4(\text{OH})(\text{H}_2\text{O})_7$
U(VI) minerals	
Autunite	$\text{Ca}(\text{UO}_2)_2(\text{PO}_4)_2 \cdot 10\text{--}12\text{H}_2\text{O}$
Metaautunite	$\text{KCa}(\text{H}_3\text{O})_3(\text{UO}_2)_7(\text{PO}_4)_4\text{O}_4 \cdot 6\text{--}8\text{H}_2\text{O}$
Saléeite	$\text{Mg}(\text{UO}_2)_2(\text{PO}_4)_2 \cdot 10\text{H}_2\text{O}$
Torbernite	$\text{Cu}(\text{UO}_2)_2(\text{PO}_4)_2 \cdot 12\text{H}_2\text{O}$
Uranocircite	$\text{Ba}(\text{UO}_2)_2(\text{PO}_4)_2 \cdot 8\text{--}10\text{H}_2\text{O}$
Renardite	$\text{Pb}(\text{UO}_2)_2(\text{PO}_4)_2(\text{OH})_4 \cdot 7\text{H}_2\text{O}$
Metaankoleite	$\text{KUO}_2\text{PO}_4 \cdot 4\text{H}_2\text{O}$
Coconinoite	$\text{Fe}_2\text{Al}_2(\text{UO}_2)_2(\text{PO}_4)_4(\text{SO}_4)(\text{OH})_2 \cdot 20\text{H}_2\text{O}$
Uranophane	$\text{Ca}(\text{UO}_2)_2(\text{SiO}_3(\text{OH})_2) \cdot 5\text{H}_2\text{O}$
Boltwoodite	$\text{HK}(\text{UO}_2)\text{SiO}_4 \cdot 1.5\text{H}_2\text{O}$
Slodowskite	$\text{Mg}(\text{UO}_2)_2(\text{HSiO}_4)_2 \cdot 5\text{H}_2\text{O}$
Soddyite	$(\text{UO}_2)_2\text{SiO}_4 \cdot 2\text{H}_2\text{O}$
Schoepite	$(\text{UO}_2)_8\text{O}_2(\text{OH})_{12} \cdot 12\text{H}_2\text{O}$
Metaschoepite	$(\text{UO}_2)_8\text{O}_2(\text{OH})_{12} \cdot 10\text{H}_2\text{O}$
Bequerelite	$\text{Ca}[(\text{UO}_2)_3\text{O}_2(\text{OH})_3]_2 \cdot 8\text{H}_2\text{O}$
Carnotite	$\text{K}_2(\text{UO}_2)_2(\text{VO}_4)_2 \cdot 1\text{--}3\text{H}_2\text{O}$
Tyuyamunite	$\text{Ca}(\text{UO}_2)_2\text{V}_2\text{O}_8 \cdot 5\text{--}8\text{H}_2\text{O}$
Zeunerite	$\text{Cu}(\text{UO}_2)_2(\text{AsO}_4)_2 \cdot 8\text{--}10\text{H}_2\text{O}$
Umohoite	$(\text{UO}_2)\text{MoO}_4 \cdot 2\text{H}_2\text{O}$
Liebigite	$\text{Ca}_2\text{UO}_2(\text{CO}_3)_3 \cdot 10\text{H}_2\text{O}$
Rutherfordine	UO_2CO_3

4. U Extraction Methods

U is typically more abundant in the Earth's crust compared to the upper mantle and is often more concentrated in intrusive igneous rocks of silicic and alkaline composition, while being less common in mafic rocks (Campbell et al. 2015; Smedleya and Kinniburgh 2023). Weathering and metamorphism crustal processes can increase the concentration of U (Plant et al. 1999). Processes occurring in the Earth's crust are primarily responsible for U enrichment and the formation of mineral deposits. Often, minerals originate from elevated concentrations present in residues resulting from igneous cooling and crystallization, as well as water interacting with these residues (Plant et al. 1999; Campbell et al. 2015).

U ore deposits have been classified into 15 categories, considering their geological context and economic significance (NEA/IAEA 2022). These categories include sandstone deposits, proterozoic unconformity deposits, polymetallic Fe-oxide breccia complex deposits, paleo-quartz-pebble conglomerate deposits, granite-related, metamorphite, intrusive deposits, volcanic-related deposits, metasomatic deposits, surficial deposits, carbonate deposits, collapse breccia-type deposits, phosphate deposits, lignite and coal, and black shale (NEA/IAEA 2022). The predominant minerals in these deposits vary depending on the geological environment in which they formed. Among the most common U minerals in economic deposits are uraninite, coffinite, and brannerite, as well as a variety of alteration products of these minerals.

Therefore, U mining is a fundamental process in the extraction and production of U. However, for U ore deposits, the choice of extraction methods and processing options is highly specific to the deposit and depends on many variables, such as the quality and quantity of the ore, the shape and depth of the ore deposit, specific environmental conditions at the site, and a range of other factors (NEA/IAEA 2022).

There are two types of conventional mining processes: open-pit mining, and underground mining, which will be detailed later on. These mining technologies can be used individually or combined. For example, some mines start as open-pit operations and later continue as underground

operations to reach deeper deposits underground (NEA/IAEA 2022). Both types of mining have varied in terms of productivity, costs, and availability. There are also other more innovative mining methods such as *In Situ Recovery* (ISR), and heap leaching. ISR has become one of the most widely used mining methods worldwide (NEA/IAEA 2022).

4.1. Open-pit mining

Open-pit mining is a mineral extraction method that involves removing large amounts of material from the Earth's surface to have access to mineral deposits located near the surface (Fig. 3). The closer the mineral deposit is to the surface, the more profitable the mining process will be as long as the mining cost does not exceed the value of the ore. This method is used to extract a wide variety of minerals, including gold (Au), copper (Cu), U, and many others. It is one of the historically most used methods and in 2021 accounted for 17.1% of U extraction methods worldwide (NEA/IAEA 2022). This type of mining has significant environmental impacts, including the destruction of natural habitats and alteration of landscapes. Additionally, it generates large amounts of waste that can contaminate soil, water, and air.



Figure 3. Former Lichtenberg U open-pit mine in 1991 (WISMUT GmbH, Ronneburg, Germany) (WISMUT GmbH Umweltbericht 2024).

4.2. Underground mining

Underground mining involves drilling shafts, tunnels, and underground galleries to access mineral deposits located at greater depths (Fig. 4). This method is used when mineral deposits are not economically or safely accessible through open-pit mining. Underground mining is more expensive than open-pit mining as it involves the construction and maintenance of safe underground infrastructure, considering important aspects such as ventilation systems to ensure air quality for workers and ground control to prevent rock collapse in a mined cavity. Although underground mining can be more expensive, it offers environmental and safety benefits and is essential for exploiting mineral deposits at greater depths. In 2021, underground mining accounted for 15.2% of global production by production method (NEA/IAEA 2022).



Figure 4. Former underground U mine in Pöhla (WISMUT GmbH, Germany).

4.3. *In situ* Recovery (ISR)

In Situ Recovery (ISR), also known as *In Situ* Leaching (ISL), is an innovative method of mineral extraction used particularly in the extraction of U and other industrial metals. Unlike conventional underground or open-pit mining methods, ISR allows minerals to be extracted without the need to excavate large amounts of rock or soil. This process involves extracting U by dissolving it directly from the minerals containing it. This is achieved by injecting a leaching solution into the mineral deposit, followed by pumping the dissolved U into an impregnated solution to the surface, where the metal can be recovered. The leaching solution can be either alkaline or acidic, depending on the mineralogical or geochemical properties of the deposit being treated. This method minimizes surface disturbance and avoids the generation of tailings or sterile rock. However, it is necessary for the deposit rock structure to be permeable (commonly sandstone) and have an underlying impermeable confining layer (such as clay) beneath the mineralization. According to NEA/IAEA (2022), it accounted for 63.3% of global production.

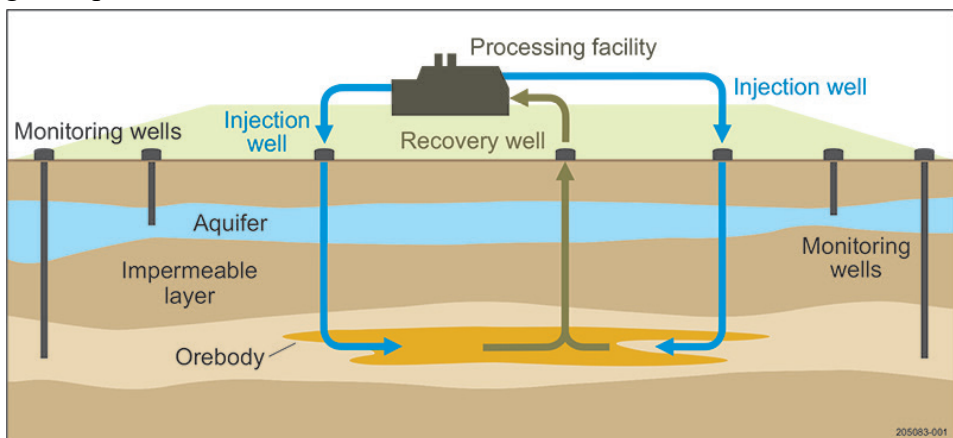


Figure 5. Conceptual model of an *In Situ* Recovery mining process (Energy&Mining/SAGOVAU).

4.4. Heap leaching

Heap leaching is a mineral extraction method widely used in the mining industry to recover valuable metals such as Au, silver (Ag), and Cu, among others (Tuovinen et al. 2018). Although it is most commonly associated with the extraction of precious metals, it has also been applied in U extraction

(Campbell et al. 2015). The heap leaching process involves the extraction of minerals found in large piles, which contain low-grade material, i.e., with relatively low concentrations of the metal of interest. This method is especially useful when the mineralization is not rich enough to justify the construction and operation of a conventional processing plant. In heap leaching, the U-containing mineral is stacked and sprayed with a fluid that leaches the metal over several months. Currently, this process is applied to crushed minerals, and modern heaps are designed with double containment measures, and groundwater monitoring to prevent soil contamination. Interestingly, micro-organisms play an important role in the heap leaching process, especially in the leaching of metallic minerals such as Cu and Au. This approach, known as bioleaching (or bioheap leaching), uses micro-organisms to accelerate the release of valuable metals from minerals and increase the efficiency of the leaching process. An interesting group is the bacteria of the genus *Acidithiobacillus*. Most of the attention on biological leaching in heaps has focused on *Acidithiobacillus ferrooxidans* and *Acidithiobacillus thiooxidans* for the recovery of Au, Cu, and Molybdenum (Mo) (Campbell et al. 2015). Likewise, Li and co-authors (2023) described the potential of *A. ferrooxidans*, *A. thiooxidans*, and *L. ferriphilum* for U recovery through biological heap leaching. Heap leaching offers key benefits: it avoids fine grinding, uses minimal water, and simplifies remediation by eliminating tailings deposits. Despite these advantages, it accounts for less than 0.1% of global production.

Various methods exist for obtaining U, including recovery as a by-product during the production of metals like Au, Cu, or nickel (Ni). U is also extracted for environmental and product purity reasons, such as in phosphoric acid fertilizers or Cu production. While U extraction traditionally occurs from rock formations, U ore deposits are limited. However, the Nuclear Energy Agency suggests that oceans contain around 4,500 million tons of U, far exceeding land-based reserves. Yet, extracting these ions poses challenges due to insufficient surface area in existing materials. Nonetheless, Chen et al. (2023) have designed an effective method using flexible porous organic polymer electrodes, offering promising prospects for electrochemical U

extraction from seawater, ensuring future supply.

After extraction, U ore undergoes processing at a hydrometallurgical facility to eliminate impurities. The choice of hydrometallurgical process is contingent upon the ore and its host rock, considering environmental, economic, and safety aspects.

5. Utilities and production of U

In its beginnings, the demand for U far exceeded the initial uses attributed to this element, including the colouring of glass and ceramics. However, once nuclear fission was discovered, the economic importance of U increased enormously. Nowadays, the primary commercial use of U is to produce fuel for nuclear reactors. Over the last 60 years, U has become one of the world's most important element.

Due to the increasing number of nuclear power plants and the growing demand for energy, a rising global and annual production of U is expected. According to the World Nuclear Association report (WNA 2021), currently around 15 countries stand out as the main contributors to U production, with nearly two-thirds of the global production of U minerals originating from Kazakhstan, Canada, and Australia (Table 2). In 2022, Kazakhstan led U production from mines, accounting for 43% of the world's supply, followed by Canada with 15% and Namibia with 11% (Figure 6). According to estimates from the World Nuclear Association, the global production of U by the main countries is distributed as follows: Kazakhstan (43.01%), Canada (14.89%), Namibia (11.38%), Australia (9.23%), Uzbekistan (6.68%), Russia (5.08%), Niger (4.09%), China (3.44%), India (1.22%), South Africa (0.40%), Ukraine (0.20%), United States (0.15%), Pakistan (0.09%), Brazil (0.09%), Iran (0.04%). Historically, the main producers of U in the European Union (EU) have been Germany, the Czech Republic, and France.

5.1. Czech Republic

U extraction started post-World War II in the Czech side of the Ore Mountains, mainly around Jáchymov. Production peaked between 1955 and 1988, totalling 102,245 tons by 1992. Příbram was a significant province, producing 38.9% of the U until its closure in 2017 (NEA/IAEA 2022).

5.2. France

Once the largest U producer in Western Europe, France's production hit its apex in 1988 at 3,394 tons, meeting half its reactor demand domestically. However, depleted deposits and high costs led to closures in 1995 (WISE 1995). Orano, previously Areva, ceased exploration in 1999 but operates overseas since 2020, particularly in Canada, Gabon, Kazakhstan, Mongolia, Namibia, and Niger (NEA/IAEA 2022)

5.3. Germany

After World War II, eastern Germany was considered the third major U mining province in Europe. Wismut, the mining company, produced around 220,000 tons of U until 1990 (WISE 1995). German reunification ceased extraction, leading to closure and remediation work by Wismut. Mining activities primarily occurred in the Federal States of Saxony and Thuringia, with key locations including Schneeberg, Oberschlema, Aue-Schlema-Alberoda, Königstein, Pöhla, Freital, Zobes/Bergen, Johanngeorgenstadt, Schwarzenberg, Auerbach/Vogtl, Annaberg-Buchholz, Bärenstein-Niederschlag, Marienberg, Bärenhecke, Niederpöbel, Johnsbach, Freiburger Revier, Dresden-Gittersee (in Saxony), and Ronneburg/Gera, Greiz, Dittrichshütte, Steinach, Schleusingen (in Thuringia).

Nowadays, in the EU, U production has been declining over the years. Primary U production in the EU for 2020 came only from the Czech Republic, which produced 28 tons of U through ISL (NEA/IAEA 2022). The total reported production of the EU in 2020 was 44 tons of U, a 13% increase compared to the 39 tons of U reported for 2018. The EU U-production should continue to decrease as U recovery from mining remediation declines as remediation progresses (NEA/IAEA 2022). The Czech Republic recovered 6 tons of U in the ongoing treatment of mine water in remediation activities, while Germany contributed 7 tons of U, only from mining remediation activities in 2020 (NEA/IAEA 2022).

Table 2. Annual U production from 2013 to 2022 from mines in major producing countries (tonnes of U). The data were obtained from the World Nuclear Association (WNA 2021).

Country	2013	2014	2015	2016	2017	2018	2019	2020	2021	2022
Kazakhstan	22451	23127	23607	24689	23321	21705	22808	19477	21819	21227
Canada	9331	9124	13325	14039	13116	7001	6938	3885	4693	7351
Namibia	4323	3255	2993	3654	4224	5525	5476	5413	5753	5613
Australia	6350	5001	5654	6315	5882	6517	6613	6203	4192	4553
Uzbekistan (est.)	2400	2400	2385	3325	3400	3450	3500	3500	3520	3300
Russia	3135	2990	3055	3004	2917	2904	2911	2846	2635	2508
Niger	4518	4057	4116	3479	3449	2911	2983	2991	2248	2020
China (est.)	1500	1500	1616	1616	1692	1885	1885	1885	1600	1700
India (est.)	385	285	385	385	421	423	308	400	600	600
South Africa (est.)	531	573	393	490	308	346	346	250	192	200
Ukraine	922	926	1200	808	707	790	800	744	455	100
USA	1792	1919	1256	1125	940	582	58	6	8	75
Pakistan (est.)	45	45	45	45	45	45	45	45	45	45
Brazil	192	55	40	44	0	0	0	15	29	43
Iran (est.)	0	0	38	0	40	71	71	71	21	20
Czech Republic	215	193	155	138	0	0	0	0	0	0
Romania	77	77	77	50	0	0	0	0	0	0
France	5	3	2	0	0	0	0	0	0	0
Germany	27	33	0	0	0	0	0	0	0	0
Malawi	1132	369	0	0	0	0	0	0	0	0
Total world	59331	56041	60304	63207	60514	54154	54742	47731	47808	49355

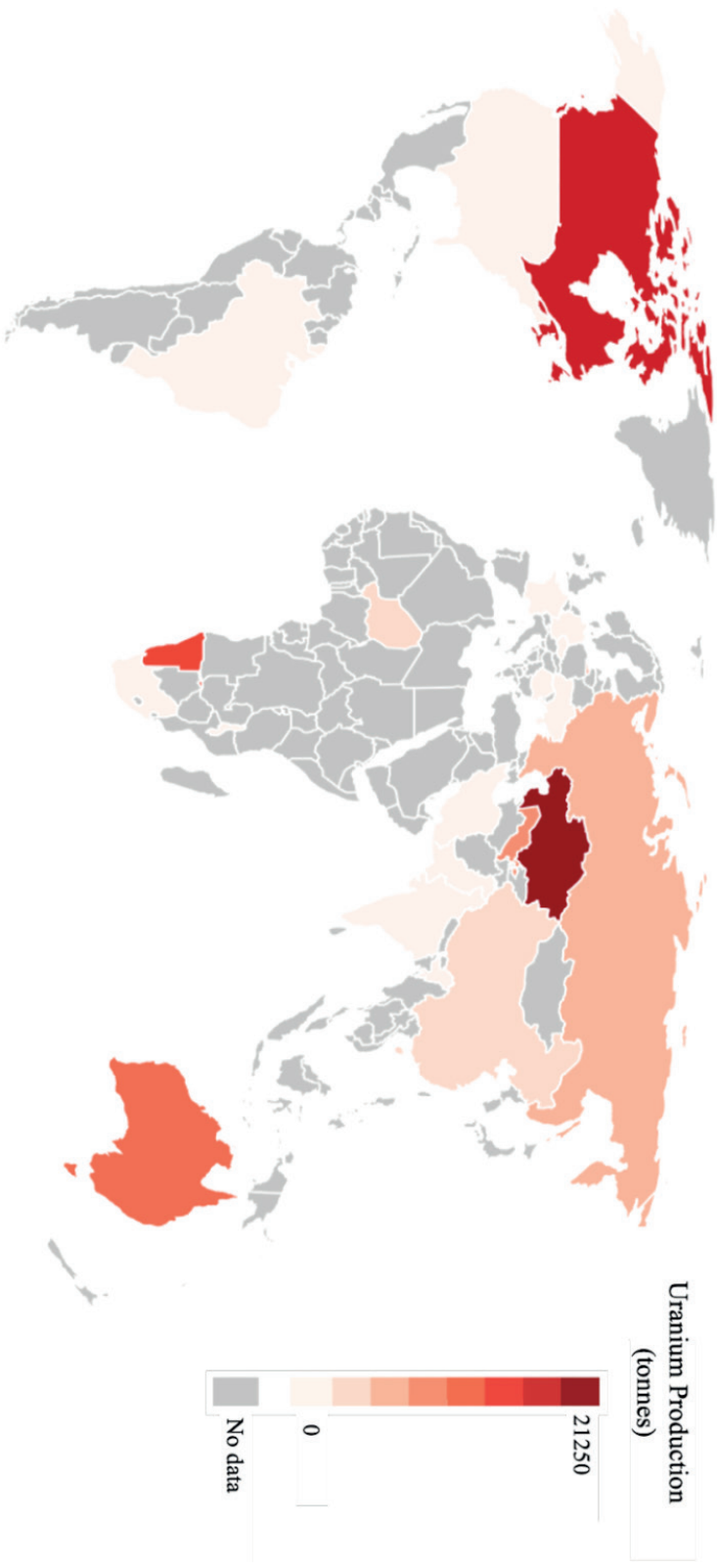


Figure 6. Global heat map for U production in different countries in 2022. The data were obtained from the World Nuclear Association (WNA 2021) and normalised. Countries with insufficient data for the prediction are shown in grey.

6. U Contamination and potential health risks

U is naturally distributed worldwide, following its natural cycle, which can be influenced by various factors like coastal erosion, river inputs, and wind transport, thereby altering its distribution (Shumilin et al. 2012). However, in recent decades, anthropogenic activities have been responsible for increasing the concentration of U in specific areas. The presence of U and heavy metals has led to significant degradation of some ecosystems. Anthropogenic U contamination is associated with human activities such as U mining and milling, industrial use in nuclear power plants and nuclear weaponry, as well as intensive agriculture, where phosphate fertilizers can significantly contribute to the presence of U (Smedleya and Kinniburgh 2023).

The issue of groundwater contamination poses a serious concern related to U mining operations. U presents both chemical and radiological risks that can be toxic to humans and other organisms. Generally, chemical toxicity is more prevalent compared to radioactivity in this context. The toxicity of U is primarily linked to its oxidation state and the formation of soluble species, with U(VI) being the most hazardous oxidation state. In oxidizing environments, U exists as mobile U(VI), where the uranyl ion is the predominant form (Banala et al. 2021). It is recognized that this form is soluble, bioavailable, and therefore more toxic. *In vivo* studies have reported that the uranyl ion has the capacity to cause kidney damage, acting as a nephrotoxin (Anke et al. 2009). Furthermore, radiation energy deposited in the body can cause DNA damage and increase the risk of cancer (Mukherjee et al. 2012; Park and Jiao 2014). It is estimated that the human body naturally contains around 90 µg to 100 µg of U, with daily average intake through food ranging from 0.7 to 15.3 µg. Within a week, approximately 90% to 95% of ingested U is rapidly excreted through the kidneys in urine, while a portion is retained and accumulates mainly in bones, kidneys, and liver (Priest 2001; Meinrath et al. 2003; Wang et al. 2019; Ma et al. 2020). Moreover, U can also influence xenobiotic metabolism, the brain, the reproductive system, the antioxidant system, and intestinal inflammatory pathways (Gandhi et al 2022). It is imperative to

address solutions to prevent this environmental problem and mitigate the risks associated with U exposure.

7. Environmental remediation of U: technologies

Following the gradual cessation of U mining, environmental remediation projects were initiated in impacted areas with the aim of restoring environments and preventing risks to human health and other organisms.

In mining, milling, and disposal activities, U is seldom the sole environmental concern. Coexisting elements include arsenic (As), selenium (Se), molybdenum (Mo), iron (Fe), sulphur (S), and magnesium (Mg), among others. Additionally, radionuclides like thorium (^{230}Th), radium (^{226}Ra), and lead (^{210}Pb) from the decay series of ^{238}U may be present. When addressing remediation and disposal, it is essential to consider the biogeochemistry of these elements. Effective U contamination solutions might mobilize other elements into surface or groundwater (Campbell et al. 2015).

The remediation of U-contaminated water can be achieved using different treatment technologies. Options include *in situ* and *ex situ* methods, based on traditional physicochemical and innovative biological strategies. Each method has limitations and strengths, but the applicable approach depends on site conditions. Multiple technologies are often used together, acknowledging that no single or combined solution can address all contamination in underground environments.

Chemical remediation of U involves specific methods and reagents to reduce contamination in groundwater or other sources by changing its chemical speciation. In the case of U, the main methodologies include chemical separation, ion exchange, chemical precipitation, and permeable reactive barriers (Smedley and Kinniburgh 2023). On the other hand, physical remediation technologies are *ex situ* processes that require the construction and operation of a groundwater extraction and injection system. The main physical methodologies for U remediation are membrane filtration (reverse osmosis and microfiltration) and adsorption (Dinis and Fiúza 2021). Adsorption is a widely studied, common, and more efficient method for environmental remediation (Banala et al. 2021; Dinis and Fiúza 2021; Smedley and Kinniburgh 2023). Both technologies generate waste that

requires additional treatment, storage, or disposal. Therefore, additional treatment or disposal of the generated contaminated waste will be needed (Dinis and Fiúza 2021). Conventional remediation methods, focusing on physical, chemical, or combined approaches, are expensive, complex, environmentally unfriendly, and ineffective for low U concentrations. For example, costs for treating contaminated acidic water from the Osamu Utsumi U mine (Brazil) have been reported to range from US\$ 200,000 to US\$ 250,000 per month for a volume of 216,000 m³, using calcium hydroxide and flocculants (Nóbrega et al. 2008, Coelho et al. 2020). In view of these challenges, bioremediation emerges as a highly promising strategy to rehabilitate contaminated environments due to its effectiveness and cost savings. According to Zhu and Chen (2009), the approximate cost of rehabilitating one acre of soil using conventional methods is around US\$ 250,000, while treating one acre of soil through phytoremediation varies between 60,000 and US\$ 100,000. In addition to cost reduction, bioremediation offers simpler application and greater efficacy for low concentrations of U (Sanchez-Castro et al. 2021; Newman-Portela et al. 2024).

8. U bioremediation

U bioremediation consists on the use of living organisms such as bacteria, archaea, fungi, and plants (Kalin et al. 2005; Gadd and Fomina 2011; Chen et al. 2021; You et al. 2021) to remove U in the environment, such as soils and groundwater. These organisms can interact with U, transforming it into less soluble and toxic forms. Bioremediation is considered a more sustainable and less invasive environmental remediation technology than other traditional technologies. Additionally, it is notably more effective for low U concentrations (Sánchez-Castro et al. 2021; Newman-Portela et al. 2024).

Different studies reported that in U-rich environments, U itself can exert selective pressure favouring the enrichment of heavy metal and U-tolerant microbial community (Rastogi et al. 2010; Campbell et al. 2015), and sometimes leading to reduced microbial diversity (Rastogi et al. 2010; Kenarova et al. 2014). Research on microbial communities

in U-contaminated environments not only helps to understand microbial adaptation mechanisms to heavy metals and radionuclides but also provides new insights for the design of efficient U-contaminated environment bioremediation strategies through native microbial communities.

In recent years, several studies have characterized the microbial community using culture-independent techniques to study total microbial community such as 16S rRNA gene sequencing. These results identified bacterial populations that prevail in different contaminated environments such as soils or sediments (Xiao et al. 2019), and in surface or groundwater (Coral et al. 2018; Jroundi et al. 2020; Newman-Portela et al. 2024). The main identified bacterial phyla are Firmicutes, Actinobacteria, Proteobacteria, Acidobacteria, Bacteroidetes, Nitrospirae, Campylobacteria, Chloroflexi, Verrucomicrobia, Cyanobacteria, and Desulfobacterota. These phyla harbour a number of bacteria with high bioremediation potential based on their interaction mechanisms with U (Islam and Sar 2011; Rastogi et al. 2010; Xiao et al. 2019; Akob et al. 2007; Cho et al. 2012; Coral et al. 2018; Jroundi et al. 2020; Newman-Portela et al. 2024). Nevertheless, it has been demonstrated that U(VI)-reducing bacteria primarily belong to three phyla, namely Proteobacteria, Firmicutes, and Actinomycetes (Zeng et al. 2020; You et al. 2021).

Many studies have reported the presence of taxa belonging to the Proteobacteria and Acidobacteria phyla that are able to survive in oligotrophic environments playing a very important role in U immobilization in sediments or groundwater contaminated with U (Brodie et al. 2006; Akob et al. 2007; Rastogi et al. 2010; Zhu et al. 2023; Zachara et al. 2013). Suriya and co-authors (2017) identified a high abundance of *Desulfovibrio* (Proteobacteria) in U-contaminated sediments in the Cauvery River (India). *Desulfovibrio* is a sulphate-reducing bacteria (SRB) with the ability to reduce U and form uraninite (Wall and Krumholz 2006, Zeng et al. 2020). Environmental remediation experiments conducted in a contaminated area in Oak Ridge (USA) revealed the presence of several genera, including U(VI) reducers such as *Desulfovibrio*, *Geobacter*, *Anaeromyxobacter*, *Desulfosporosinus*, and *Acidovorax*. *Geobacter* (Proteobacteria), an iron-

reducing bacteria, is closely associated with the reduction of U(VI) to U(IV). *Shewanella* (Proteobacteria), *Desulfovibrio*, and *Geobacter* have frequently been identified in sediments contaminated with radionuclides (Rastogi et al. 2010; Spain and Krumholz 2011). These micro-organisms thrive in nutrient-poor environments, show resistance to heavy metals, and play an important role in the immobilization and remediation of U (Suzuki et al. 2003; Li et al. 2017a). *Desulfovibrio*, and *Geobacter* commonly dominate over other groups in U-contaminated sites (You et al. 2021). *Arthrobacter* and *Microbacterium* (both Actinobacteria) have also been identified in various radionuclide-contaminated sites and are acknowledged for their ability to reduce substantial quantities of U in environments enriched with heavy metals (Islam and Sar 2016; You et al. 2021).

Indirectly, other micro-organisms belonging to the Campylobacterota phylum linked to the nitrogen and sulphur cycle show an important role. Newman-Portela and co-authors (2024) reported a high dominance of *Sulfuricurvum*, *Sulfurovum*, and *Sulfurimonas* in former mine waters contaminated with U. These genera could play a key role in maintaining the stability of reduced U species by coupling nitrate reduction to sulphur compound oxidation, and thereby promoting the growth of metal-reducing micro-organisms. In addition, *Clostridium acetobutylicum* (Firmicutes) may reduce U(VI) by forming U(IV) precipitates (Vecchia et al. 2010).

In addition to bacteria, there are other micro-organisms such as fungi capable of adapting to contaminated environments. Mumtaz and co-authors (2013) reported insights on how fungi are able to tolerate higher concentrations of U than bacteria under laboratory conditions. The main fungal phyla identified in U-contaminated environments are Ascomycota and Basidiomycota. These fungi stand out as the most widely studied and diverse fungal phyla (Naranjo-Ortiz and Gabaldon 2019). Coelho et al. (2021) reported through culture-dependent techniques the genera *Talaromyces*, *Aspergillus*, *Pochonia*, *Umbelopsis*, *Metarhizium*, *Gongronella*, *Purpureocillium*, *Mucor*, and *Trichoderma* from the Osamu Utsumi U mine (Brazil). On the other hand, Newman-Portela et al. (2024) reported identification through

internal transcribed spacer (ITS) amplification of the genera *Cadophora*, *Acremonium*, *Aspergillus*, and *Penicillium*, among others. Furthermore, the capability of fungi to degrade complex organic molecules into low weight organic compounds could be used as electron donors and carbon sources for the growth of metal-reducing bacteria. Microbes employ multiple mechanisms to immobilize U, reducing its toxicity via stable mineral phases: biosorption, bioaccumulation, biomineralization, and bioreduction. Leveraging these characteristics, micro-organisms offer potential for remediating U-contaminated sites and sites contaminated by other heavy metals. In U bioremediation, the primary strategies are biomineralization for oxic environments and bioreduction for anoxic environments.

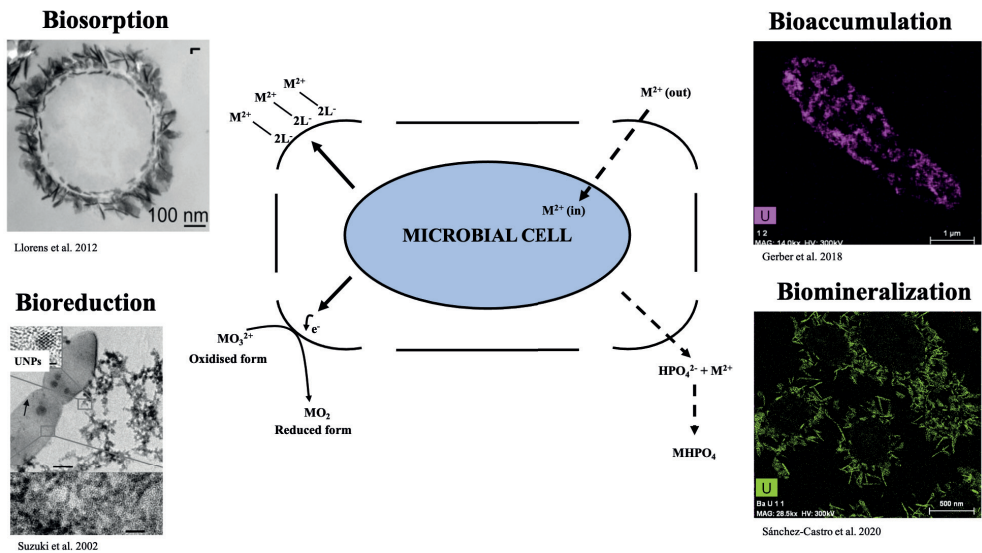


Figure 7. Schematic representation of the mechanisms to immobilize U used by micro-organisms: biosorption, bioaccumulation, bioreduction and biomineralization. Image adapted from Vaughan and Lloyd (2011).

8.1. U Biosorption

Biosorption is a passive process that sequesters and concentrates metallic species through physicochemical mechanisms. It occurs independently of metabolism, as specific functional groups (e.g., carboxyl, amine, hydroxyl, phosphate, sulfhydryl) naturally present on microbial cell surfaces interact

with metals (Gadd 2004; Banala et al. 2021). Common biosorbents include bacteria, fungi, algae, plant and animal biomass, among others. Sorption is a term encompassing both adsorption and absorption (Banala et al. 2021). However, adsorption is a two-dimensional process where molecules of the substance being retained attach to the surface of the biosorbent material, forming a layer. On the other hand, absorption occurs as a three-dimensional process, in which molecules of the substance to be retained are introduced and dispersed within the biosorbent material, reaching its internal structure (Banala et al. 2021). Biosorption is a fast process and can be influenced by the organism used and environmental conditions (pH, temperature, agitation, incubation time, and metal concentration).

8.2. U Intracellular Bioaccumulation

Bioaccumulation consists in the internalization of metals through the cell membrane into the cellular inner side (cytoplasm). This process is energy-dependent, i.e., metabolically active (Banala et al. 2021). Bioaccumulation involves two distinct phases. In the first phase, fast biosorption occurs on the surface. Then, in the second phase, active transport of the absorbed metal into the cell interior takes place, a process that requires higher energy consumption. U does not play any known biological function, and so far, no transporter proteins responsible for its entry into the cell interior have been identified (Banala et al. 2021). However, U can concentrate inside the cell due to increased permeability of the cell membrane or specific Fe transporters (Gallois et al. 2018).

8.3. U Biomineralization

Biomineralization is a process by which metals precipitate through complexation with inorganic ligands such as phosphates, mediated by an enzymatic process (Martínez-Rodríguez et al. 2021). Microbial phosphatase enzymes hydrolyse organic phosphate into inorganic phosphate, which forms an insoluble precipitate as a metal phosphate (Martínez-Rodríguez et al. 2021; Banala et al. 2021). Regarding U, three types of processes for U biomineralization have been identified: (I) metabolism-induced biomineralization, (II) extracellular precipitation, and (III) surface cell

precipitate formation through phosphate mineral nucleation (Jiang et al. 2020; Banala et al. 2021).

8.4. U Bioreduction

Metal bioreduction typically involves converting soluble metals into less soluble forms, reducing their mobility depending on the metal and its oxidation state. For example, in the case of U, hexavalent U is typically reduced to tetravalent U, forming an insoluble precipitate of U(IV) such as uraninite. U-reducing micro-organisms are ubiquitous, and microbial reduction of U was initially reported in 1962 in *Micrococcus lactilyticus* (reclassified as *Veillonella alcalescens*), but it was mostly recognized through Lovely's research in the early 1990s (Woolfolk and Whiteley 1962; Lovley et al. 1991; Banala et al. 2021). Before this time, it was believed that the process occurred abiotically rather than through direct reduction by micro-organisms. Nowadays, numerous prokaryotes have been identified with the ability to reduce hexavalent U. The most notable include archaea such as *Pyrobaculum islandicum* (Kashefi and Lovley 2000), sulphate-reducing bacteria such as *Desulfovibrio*, *Desulfosporosinus*, *Desulfotomaculum*, and *Desulfobacterium* (Spear et al. 2000; Suzuki et al. 2003; Payne et al. 2002; Tapia-Rodriguez et al., 2010; Akob et al. 2012; Zeng et al. 2020), iron-reducing bacteria from the *Geobacteraceae* family with lineages like *Geobacter uraniireducens*, *Geobacter daltonii*, and *Geobacter uraniireducens* (Holmes et al. 2009; Banala et al. 2021; You et al. 2021), and fermentative bacteria such as *Clostridium* (Francis et al. 1991, 1994; Gao and Francis, 2008; Tapia-Rodriguez et al. 2010; Vecchia et al. 2010). Moreover, other bacteria like *Thermus scotoeductus* SA-01, *Anaeromyxobacter dehalogenans* strain 2CP-C, *Bacillus* sp. dwc-2, and denitrifying *Pseudomonas* sp. have been reported to reduce U (Barton et al. 1996; Cason et al. 2012; Wu et al. 2006; Li et al. 2017a; Li et al. 2017b). The pathway of U reduction, the enzymes or genes responsible, and the number of electrons involved have not been well established. U(VI) is mostly reduced through a process of direct enzymatic reduction, where bacteria use electrons from organic/inorganic substrates to convert the oxidized and soluble forms of U(VI) into reduced and insoluble U(IV).

Additionally, U(VI) can also be reduced through an indirect reduction process, where bacteria first reduce substrates to secondary metabolites that then facilitate the reduction of U(VI) (Banala et al. 2021; You et al. 2021). It has generally been accepted that the reduction of U(VI) is a two-electron reduction process. However, recent research has indicated that the reduction of U(VI) by *Geobacter sulfurreducens* or *Shewanella oneidensis* MR-1 is initially reduced to U(V) by one electron and then to U(IV) by disproportionation or through further reduction of U(V) (Lloyd and Renshaw 2005; Vettese et al. 2020; Banala et al. 2021; You et al. 2021). Recently, Hilpmann and co-authors (2023) suggested a potential single-electron reduction mechanism of U(VI) in *Desulfosporosinus hippei* DSM 8344^T based on the identification of U(V).

Although U precipitation can occur through either two-electron or one-electron reduction, studies indicate that the reduction site may include extracellular space, outer membrane surface, or periplasm. However, the mechanisms and enzymes involved in U reduction differ among different micro-organisms. The process of U(VI) reduction involves the participation of the outer membrane and periplasmic cytochromes, with the latter being the main component of the terminal reductase complex. Although these elements play a key role, the degree of cytochrome involvement may vary among organisms (You et al. 2021). In *Geobacter*, a variety of genes codifying of multiheme cytochrome proteins are present in its genome, but not all participate in U reduction. The deletion of certain cytochromes, such as *OmcZ*, can significantly affect the rate of U(VI) reduction, while others, such as *OmcB*, have a lesser impact (Orellana et al. 2013). In *Shewanella*, the outer membrane cytochrome *MtrC* is crucial for U(VI) reduction, while others, such as *MtrF*, have little effect (Marshall et al. 2006). On the other hand, in *Desulfovibrio* species, the type 1 tetraheme cytochrome c3 participates in U reduction (Payne et al. 2004).

Since most type c cytochromes are located in the periplasm or outer membrane, they can only mediate U(VI) reduction when they are very close to the cell surface. Therefore, some bacteria possess both type c cytochromes and highly conductive extracellular pili (You et al. 2021).

These components enable bacteria to reduce U(VI) even at significant distances from the cell. The transfer of electrons from pili to U(VI) has been a subject of controversy, although cytochromes are believed to play a significant role in this process. *Geobacter* can reduce U(VI) via pili (Cologgi et al. 2011).

Some bacteria use extracellular electron shuttle molecules (ES) to transfer electrons to U(VI) at a distance, alleviating the need for direct contact between U(VI) and cellular electron acceptors (You et al. 2021). The process of ES-mediated extracellular electron transfer is straightforward: the oxidized electron shuttle molecule (ESox) accepts electrons and then, in its reduced state (ESred), transfers electrons to another extracellular electron acceptor, such as U(VI) (You et al. 2021). *Shewanella* is capable of secreting ES molecules, unlike *Geobacter* (Canstein et al. 2008; You et al. 2021).

Bioreduction emerges as a promising alternative to other techniques like biosorption or bioaccumulation for addressing the bioremediation of U-contaminated areas in an anoxic atmosphere. Furthermore, when the area to be treated is amended with electron donors, submicromolar level bioreduction can be achieved (Banala et al. 2021). Amendment with nutrients or electron donors is an increasingly accepted practice to stimulate the growth of U-reducing micro-organisms capable of immobilizing dissolved U *in situ* or *ex situ*. In both laboratory and field studies, various electron donors have been used to promote the growth and activity of U-reducing bacteria, including acetate, lactate, ethanol, methanol, hydrogen, glycerol, glucose, toluene, pyruvate, fumarate, and emulsified vegetable oils, among others (Anderson et al. 2003; Istok et al. 2004; Marshall et al. 2009; Finneran et al. 2002; Cárdenas et al. 2008; Shelobolina et al. 2008; Wu et al. 2006, 2007; Luo et al. 2007; Madden et al. 2007; Gihring et al. 2011; Newsome et al. 2015).

Many environmental factors influence *in situ* bioreduction processes, such as microbial community populations, E_H , pH, organic substrates, and the presence of other contaminants. Therefore, it is important to select the appropriate electron donor to bio-stimulate the community. An example

of *in situ* U bioremediation is the construction of a test field at the Rifle Colorado Base (USA). Anderson et al. (2003) conducted *in situ* acetate injection experiments at the Rifle Colorado Base, observing a rapid decrease in U(VI) after injection, with *Geobacter* being more effective than sulphate-reducing bacteria. Williams et al. (2011) showed that the initial U(VI) removal was independent of amendment, but its subsequent increase indicated the importance of electron donor oxidation in maintaining U(VI) reduction. Istok et al. (2004) found that a low concentration of nitrate favoured U(VI) reduction, while a high concentration inhibited this process due to higher thermodynamic competition for the electron donor

8.4.1. Tetravalent U

Initially, it was believed that microbial reduction of U(VI) to U(IV) only forms insoluble crystalline U such as uraninite (UO_2). However, it was later discovered that non-crystalline U(IV) species (NCU(IV)) could also be produced, also referred to as “monomeric U(IV),” “mononuclear U(IV),” and “molecular U(IV)” (Bernier-Latmani et al. 2010; Bhattacharyyala et al. 2017). A study by Bargar et al. (2013) showed the formation of NCU(IV) in a shallow aquifer contaminated with U during microbial bioremediation with acetate as an electron donor. Furthermore, Bhattacharyyala et al. (2017) reported that NCU(IV) is the dominant U species in undisturbed rolling front deposits in Wyoming (USA), while uraninite and U(VI) represent only minor components. NCU(IV) is less stable due to its amorphous nature and more reactive, which may compromise remediation efforts (Loreggian et al. 2020). Newsome et al. (2015) proposed that NCU(IV) may age into crystalline UO_2 , although recent studies suggest that NCU(IV) persists for over a year, possibly due to differences in sediment conditions used (Loreggian et al. 2020). Several authors have demonstrated the reoxidation to U(VI) of biogenic uraninite when exposed to oxidizing agents such as oxygen, making it an impractical bioremediation strategy. Additionally, nitrate, manganese oxides, and iron oxides also facilitated U reoxidation (Abdelouas et al. 2000, Finneran et al. 2002, Fredrickson et al. 2002; Istok et al. 2004). Additionally, to address the weaknesses of microbial reduction of U(VI) to U(IV), approaches such as bio-stimulation

with an organophosphate compound (Glycerol-P) that bacteria break down to release orthophosphate, thereby precipitating insoluble U phosphate minerals of reduced crystalline U(IV) have been proposed (Newsome et al. 2015).

8.4.2. Pentavalent U

While traditionally U(V) has been considered as an unstable and transitory oxidation state during the reduction of U(VI) to U(IV), advances in spectroscopic techniques, such as High Energy Resolution-X-ray Absorption Near Edge Structure Spectroscopy, have facilitated its possible identification in recent years (Hilpmann et al. 2023). U(V) is a transient form, but the aqueous ion UO_2^+ has been identified in the laboratory and can be stabilized by a uranyl carbonate complex (Mizuoka et al. 2005). Kubicki et al. (2009) reported the stability of the U(V) species $\text{UO}_2(\text{CO}_3)_3^{5-}$ for up to 2 hours in aqueous solutions and up to 2 weeks when sealed in a cuvette. In nature, U(V) can form but quickly disproportionates to U(IV) or U(VI), making it significantly unstable and rare. Nevertheless, Crean et al. (2020) reported the long-term stability (>25 years) of the U(V) species as UFeO_4 under environmental, oxic, and variable humid conditions. Additionally, pentavalent U has begun to be reported as intermediates in microbial reactions of U(VI) reduction. As mentioned earlier, in microbial reduction of U(VI) carried out by *G. sulfurreducens*, *S. oneidensis* MR-1, and *D. hippel* DSM 8344^T, U(V) species as a transition phase before its complete reduction to U(IV) through additional U(V) reduction or disproportionation has been identified. However, its transformation mechanism is not clear. Interestingly, Renshaw et al. (2005) used NpO_2^+ as a chemically analogous species of U(V), where Np is present as Np(V) and is stable with respect to disproportionation, faced *G. sulfurreducens*. Their results did not report reduction, suggesting that U(V) disproportionation to the U(IV) product during reduction is more likely. To date, the stabilization of U(V) by microbes has not been reported. However, Faizova et al. (2018) demonstrated the stabilization of U(V) in aqueous conditions using a polydentate aminocarboxylate ligand.

9. References

- Abdelouas A, Werner L, Weiliang G, Eric HN, Betty AS, Bryan JT (2000) Biological reduction of uranium in groundwater and subsurface soil. *Science of The Total Environment*. 250(1-3):21–35. [https://doi.org/10.1016/s0048-9697\(99\)00549-5](https://doi.org/10.1016/s0048-9697(99)00549-5)
- Akob DM, Lee SH, Sheth M, Küsel K, Watson DB, Palumbo AV, Kostka JE, Chin KJ (2012) Gene expression correlates with process rates quantified for sulfate- and Fe(III)-reducing bacteria in U(VI)-contaminated sediments. *Frontiers in Microbiology*. 3(280):1–14. <https://doi.org/10.3389/fmicb.2012.00280>
- Akob DM, Mills HJ, Kostka JE (2006) Metabolically Active Microbial Communities in Uranium- Contaminated Subsurface Sediments. *FEMS Microbiology Ecology*. 59(1):95–107. <https://doi.org/10.1111/j.1574-6941.2006.00203.x>
- Anderson RT (2006) DOE Genomics: Applications to *In Situ* Subsurface Bioremediation. *Remediation*. 17(1):23–38. <https://doi.org/10.1002/rem.20110>
- Anke M, Seeber O, Müller R, Schäfer U, Zerull J (2009) Uranium transfer in the food chain from soil to plants, animals and man. *Geochemistry*. 69(2):75–90. <https://doi.org/10.1016/j.chemer.2007.12.001>
- Banala UK, Indradyumna Das NPI, Toleti SR (2021) Microbial interactions with uranium: towards an effective bioremediation approach. *Environmental Technology And Innovation*. 21:101254. <https://doi.org/10.1016/j.eti.2020.101254>
- Bargar JR, Williams KH, Campbell KM, Long PE, Stubbs JE, Suvorova EI, Giammar DE, Blue LY, Bernier-Latmani R (2013) Uranium redox transition pathways in acetate-amended sediments. *Proceedings of the National Academy of Sciences of the United States of America*. 110(12):4506–4511. <https://doi.org/10.1073/pnas.1219198110>
- Bem H and Bou-Rabee F (2004) Environmental and health consequences of depleted uranium use in the 1991 Gulf War. *Environment International*. 30:123–134. [https://doi.org/10.1016/S0160-4120\(03\)00151-X](https://doi.org/10.1016/S0160-4120(03)00151-X)
- Bernier-Latmani R, Veeramani H, Dalla Vecchia E, Junier P, Lezama-Pacheco JS, Suvorova EI, Sharp JO, Wigginton NS, Bargar JR (2010) Non-Uraninite products of microbial U(VI) reduction. *Environmental Science and Technology* 44(24):9456–9462. <https://doi.org/10.1021/es101675a>
- Bhattacharyya A, Campbell KM, Kelly SD, Roebbert Y, Weyer S, Bernier-Latmani R, Borch T (2017) Biogenic Non-Crystalline U (IV) Revealed as Major Component in

- Uranium Ore Deposits. *Nature Communications*. 8(4):1–8. <https://doi.org/10.1038/ncomms15538>
- Bowell RJ, Grogan J, Hutton-Ashkenny M, Brough C, Penman K, Sapsford DJ (2011) Geometallurgy of Uranium Deposits. *Minerals Engineering*. 24(12):1305–1313. <https://doi.org/10.1016/j.mineng.2011.05.005>
- Brodie EL, DeSantis TZ, Joyner DC, Baek SM, Larsen JT, Andersen GL, Hazen TC, Richardson PM, Herman DJ, Tokunaga TK, Wan JM, Firestone MK (2006) Application of a high-density oligonucleotide microarray approach to study bacterial population dynamics during uranium reduction and reoxidation. *Applied and Environmental Microbiology*. 72(9):6288–6298. <https://doi.org/10.1128/AEM.00246-06>
- Burns PC and Finch RJ (1999) Wyartite: crystallographic evidence for the first pentavalent-uranium mineral. *American Mineralogist*. 84(9):1456–1460. <https://doi.org/10.2138/am-1999-0926>
- Campbell KM, Gallegos TJ, Landa ER (2015) Applied geochemistry biogeochemical aspects of uranium mineralization, mining, milling, and remediation. *Applied Geochemistry*. 57: 206–235. <https://doi.org/10.1016/j.apgeochem.2014.07.022>
- Cardenas E, Wu WM, Leigh MB, Carley J, Carroll S, Gentry T, Luo J, Watson D, Gu B, Ginder-Vogel M, Kitanidis PK, Jardine PM, Zhou J, Criddle CS, Tiedje JM (2008) Microbial communities in contaminated sediments, associated with bioremediation of uranium to submicromolar levels. *Applied and Environmental Microbiology*. 74(12):3718–3729. <https://doi.org/10.1128/AEM.02308-07>
- Carvalho FP (2011) Marie Curie and the discovery of radium. In: B. Merkel and M. Schipek (Eds.). *The new uranium mining boom. challenge and lessons learned*, (Berlin: Springer-Verlag): 3–13. Retrieved from: <https://link.springer.com/book/10.1007/978-3-642-22122-4>
- Cason ED, Piater LA, Van Heerden E (2012) Chemosphere Reduction of U(VI) by the Deep Subsurface Bacterium, *Thermus Scotoductus* SA-01, and the Involvement of the ABC Transporter Protein. *Chemosphere*. 86(6):572–77. <https://doi.org/10.1016/j.chemosphere.2011.10.006>
- Chen D, Li Y, Zhao X, Shi M, Shi X, Zhao R, Zhu G (2023) Self-Standing porous aromatic framework electrodes for efficient electrochemical uranium extraction. *ACS Central*

Science. 9(12):2326-2332. <https://doi.org/10.1021/acscentsci.3c01291>

Chen L, Liu J, Zhang W, Zhou J, Luo D, Li Z (2021) Uranium(U) Source, Speciation, Uptake, Toxicity and Bioremediation Strategies in Soil-Plant System: A Review. Journal of Hazardous Materials. 413:125319. <https://doi.org/10.1016/j.jhazmat.2021.125319>

Cho K, Zholi A, Frabutt D, Flood M, Floyd D, Tiquia SM (2012) Linking bacterial diversity and geochemistry of uranium-contaminated groundwater. Environmental Technology. 33(13-15):162916-40. <https://doi.org/10.1080/09593330.2011.641036>

Coelho E, Alves T, Cotrim M, Mullan TK (2020) Chemosphere Resistant Fungi Isolated from Contaminated Uranium Mine in Brazil Shows a High Capacity to Uptake Uranium from Water. Chemosphere. 248:126068. <https://doi.org/10.1016/j.chemosphere.2020.126068>

Cologgi DL, Lampa-Pastirk S, Speers AM, Kelly SD, Reguera G (2011). Extracellular Reduction of Uranium via *Geobacter* Conductive Pili as a Protective Cellular Mechanism. Proceedings of the National Academy of Sciences of the United States of America. 108(37):15248-15252. <https://doi.org/10.1073/pnas.1108616108>

Coral T, Descostes M, De Boissezon H, Bernier-Latmani R, Felipe L de Alencastro, y Rossi P (2018) Microbial Communities Associated with Uranium In-Situ Recovery Mining Process Are Related to Acid Mine Drainage Assemblages. Science of the Total Environment. 628–629:26–35. <https://doi.org/10.1016/j.scitotenv.2018.01.321>

Crean DE, Stennett MC, Livens FR, Grolimund D, Borca CN, Hyatt NC (2020) Multimodal X-ray microanalysis of a $UFeO_4$: evidence for the environmental stability of ternary U(V) oxides from depleted uranium munitions testing. Environ. Environmental Science: Processes & Impacts. 22(7):1577–1585. <https://doi.org/10.1039/d0em00243g>

Cumberland SA, Douglas G, Grice K y Moreau JW (2016) Uranium Mobility in Organic Matter-Rich Sediments: A Review of Geological and Geochemical Processes. Earth-Science Reviews. 159:160–85. <https://doi.org/10.1016/j.earscirev.2016.05.010>

Dinis MdL and Fiúza A. (2021) Mitigation of Uranium Mining Impacts-A Review on Groundwater Remediation Technologies. Geosciences. 11(6):250. <https://doi.org/10.3390/geosciences11060250>

Elafia Z, Didi A, Hilal I, Amsil H, Bounouira H (2024) In-Depth Study of Radioactive Isotope Profiles ^{234}U , ^{235}U , and ^{238}U in Earth Samples from the Missouri Region,

- Morocco: A Detailed Exploration of Nuclear Activity. Iranian Journal of Science. 0123456789. <https://doi.org/10.1007/s40995-024-01587-y>
- Energy & Mining - Government of South Australia (Energy&Mining/SAGOVAU) (2024) Date of access: February 01, 2024. Retrieved from <https://www.energymining.sa.gov.au/industry/minerals-and-mining/mining/major-projects-and-mining-activities/in-situ-recovery-ISR-mining>
- Faizova R, Scopelliti R, Chauvin AS, Mazzanti M (2018) Synthesis and Characterization of a Water Stable Uranyl(V) Complex. Journal of the American Chemical Society 140(42):13554–13557. <https://doi.org/10.1021/jacs.8b07885>
- Finneran KT, Housewright ME, Lovley DR (2002) Multiple influences of nitrate on uranium solubility during bioremediation of uranium-contaminated subsurface sediments. Environmental Microbiol. 4(9):510-506. <https://doi.org/10.1046/j.1462-2920.2002.00317.x>
- Francis AJ, Dodge CJ, Gillow JB, Cline JE (1991) Microbial Transformations of Uranium in Wastes. Radiochimica Acta. 52-53(2):311-316. <https://doi.org/10.1524/ract.1991.5253.2.311>
- Francis AJ, Dodge CJ, Lu F, Halada GP, Clayton CR (1994) XPS and XANES Studies of Uranium Reduction by *Clostridium* sp. Environmental Science & Technology 28(4):636-639. <https://doi.org/10.1021/es00053a016>
- Fredrickson JK, Zachara JM, Kennedy DW, Liu C, Duff MC, Hunter DB y Dohnalkova A. (2002) Influence of Mn oxides on the reduction of uranium(VI) by the metal-reducing bacterium *Shewanella putrefaciens*. Geochimica et Cosmochimica Acta. 66(18):3247-3262. [https://doi.org/10.1016/S0016-7037\(02\)00928-6](https://doi.org/10.1016/S0016-7037(02)00928-6)
- Gadd GM (2004) Microbial influence on metal mobility and application for bioremediation. Geoderma. 122(2–4):109-119. <https://doi.org/10.1016/j.geoderma.2004.01.002>
- Gadd GM, and Fomina M (2011) Uranium and Fungi. Geomicrobiology Journal. 28(5-6):471-482. <https://doi.org/10.1080/01490451.2010.508019>
- Gallois N, Alpha-Bazin B, Ortet P, Barakat M, Piette L, Long J, Berthomieu C, Armengaud J, Chapon V (2018) Proteogenomic Insights into Uranium Tolerance of a Chernobyl's *Microbacterium* Bacterial Isolate. Journal of Proteomics. 177: 148–57. <https://doi.org/10.1016/j.jprot.2017.11.021>

- Gandhi TP, Sampath PV, Maliyekkal SM (2022) A Critical Review of Uranium Contamination in Groundwater: Treatment and Sludge Disposal. *Science of the Total Environment*. 825:153947. <https://doi.org/10.1016/j.scitotenv.2022.153947>
- Gao W and Francis AJ (2008) “Reduction of Uranium(VI) to Uranium(IV) by *Clostridia*. *Applied and Environmental Microbiology*. 74(14):4580–4584. <https://doi.org/10.1128/AEM.00239-08>
- Gavrilescu M, Pavel LV, Cretescu I (2009) Characterization and Remediation of Soils Contaminated with Uranium. 163(2–3):475–510. <https://doi.org/10.1016/j.jhazmat.2008.07.103>
- Gerber U, Hübner R, Rossberg A, Krawczyk-Bärsch E, Merroun ML (2018) Metabolism-dependent bioaccumulation of uranium by *Rhodospiridium toruloides* isolated from the flooding water of a former uranium mine. *PLoS One*. 13(8):e0201903. <https://doi.org/10.1371/journal.pone.0201903>
- Gihring TM, Zhang G, Brandt CC, Brooks SC, Campbell JH, Carroll S, Criddle CS, Green SJ, Jardine P, Kostka JE, Lowe K, Mehlhorn TL, Overholt W, Watson DB, Yang Z, Wu WM, Schadt CW (2011) A Limited Microbial Consortium Is Responsible for Extended Bioreduction of Uranium in a Contaminated Aquifer. *Applied and Environmental Microbiology*. 77(17):5955–5965. <https://doi.org/10.1128/AEM.00220-11>
- Hilpmann S, Rossberg A, Steudtner R, Drobot B, Hübner R, Bok F, Prieur D, Bauters S, Kvashnina KO, Stumpf T, Cherkouk A (2023) Presence of Uranium(V) during Uranium(VI) Reduction by *Desulfosporosinus Hippei* DSM 8344T. *Science of the Total Environment*. 875:162593. <https://doi.org/10.1016/j.scitotenv.2023.162593>
- Holmes DE, O’Neil RA, Chavan MA, Guessan LAN, Vrionis HA, Perpetua LA, Larrahondo MJ, DiDonato R, Liu A Lovley DR (2009) Transcriptome of *Geobacter uraniireducens* growing in uranium-contaminated subsurface sediments, *The ISME Journal*. 3(2):216–230. <https://doi.org/10.1038/ismej.2008.89>
- Islam E, and Sar P (2011) Culture-Dependent and Independent Molecular Analysis. *Journal of Basic Microbiology*. 51(4):372–384. <https://doi.org/10.1002/jobm.201000327>
- Istok JD, Senko JM, Krumholz LR, Watson D, Bogle MA, Peacock A, Chang Y-J, White DC (2004) *In Situ* Bioreduction of Technetium and Uranium in a Nitrate-Contaminated Aquifer. *Environmental Science & Technology*. 38(2):468-475.

<https://doi.org/10.1021/es034639p>

Jiang L, Liu X, Yin H, Liang Y, Liu H, Miao B (2020) Ecotoxicology and environmental safety the utilization of biomineralization technique based on microbial induced phosphate precipitation in remediation of potentially toxic ions contaminated Soil: A Mini Review. *Ecotoxicology and Environmental Safety*. 191:110009. <https://doi.org/10.1016/j.ecoenv.2019.110009>

Jroundi F, Descostes M, Povedano-Priego C, Sánchez-Castro I, Suvannagan V, Grizard P y Merroun ML (2020) Profiling native aquifer bacteria in a uranium roll-front deposit and their role in biogeochemical cycle dynamics: insights regarding *in situ* recovery mining. *Science of the Total Environment*. 721:137758. <https://doi.org/10.1016/j.scitotenv.2020.137758>

Kalin M, Wheeler WN, Meinrath G (2005) The removal of uranium from mining waste water using algal/microbial biomass. *Journal of Environmental Radioactivity*. 78(2):151–77. <https://doi.org/10.1016/j.jenvrad.2004.05.002>

Kashefi K and Lovley DR (2000) Reduction of Fe(III), Mn(IV), and toxic metals at 100 degrees C by *Pyrobaculum islandicum*. *Applied and Environmental Microbiology*. 66(3):1050-1056. <https://doi.org/10.1128/aem.66.3.1050-1056.2000>

Kenarova A, Radeva G, Traykov I, Boteva S (2014) Ecotoxicology and environmental safety community level physiological profiles of bacterial communities inhabiting uranium mining impacted sites. *Ecotoxicology and Environmental Safety*. 100: 226–232. <https://doi.org/10.1016/j.ecoenv.2013.11.012>

Khani MH (2011) Uranium Biosorption by *Padina* sp. Algae Biomass: Kinetics and Thermodynamics. *Environmental Science and Pollution Research*. 18:1593–1605. <https://doi.org/10.1007/s11356-011-0518-0>

King HM (2024) Uraninite - A radioactive mineral and the most important source of uranium. Date of access: February 01, 2024. Retrieved from <https://geology.com/minerals/uraninite.shtml>

Kubicki JD, Halada GP, Jha P, Phillips BL (2009) Quantum mechanical calculation of aqueous uranium complexes: carbonate, phosphate, organic and biomolecular species. *Chemistry Central Journal*. 18(3):10. <https://doi.org/10.1186/1752-153x-3-10>

- Lakaniemi AM, Douglas GB, Kaksonen AH (2019) Engineering and kinetic aspects of bacterial uranium reduction for the remediation of uranium contaminated environments. *Journal of Hazardous Materials*. 5(371):198-212. <https://doi.org/10.1016/j.jhazmat.2019.02.074>
- Li X, Meng D, Li J, Yin H, Liu H, Liu X, Cheng C, Xiao Y, Liu Z, Yan M (2017a) Response of soil microbial communities and microbial interactions to long-term heavy metal contamination. *Environmental Pollution*. 231(1):908-917. <https://doi.org/10.1016/j.envpol.2017.08.057>
- Li X, Ding C, Liao J, Du L, Sun Q, Yang J, Yang Y, Zhang D, Tang J, Liu N (2017b) Microbial reduction of uranium (VI) by *Bacillus* sp. dwc-2: A macroscopic and spectroscopic study. *Journal of Environmental Sciences (China)*. 53:9-15. <https://doi.org/10.1016/j.jes.2016.01.030>
- Li Q, Yang Y, Ma J, Sun J, Li G, Zhang R, Cui Z, Li T, Liu X (2023) Sulfur enhancement effects for uranium bioleaching in column reactors from a refractory uranium ore. *Front Microbiol*. 26(14):1107649. <https://doi.org/10.3389/fmicb.2023.1107649>
- Llorens I, Untereiner G, Jaillard D, Gouget B, Chapon V, Carriere M. (2012) Uranium interaction with two multi-resistant environmental bacteria: *Cupriavidus metallidurans* CH34 and *Rhodopseudomonas palustris*. *PLoS One*. 7(12):e51783. <https://doi.org/10.1371/journal.pone.0051783>
- Lloyd JR and Renshaw JC (2005) Bioremediation of radioactive waste: radionuclide-microbe interactions in laboratory and field-scale studies. *Current Opinion in Biotechnology*. 16(3):254-260. <https://doi.org/10.1016/j.copbio.2005.04.012>
- Loreggian L, Novotny A, Bretagne SL, Bartova B, Wang Y, Bernier-Latmani R (2020) Effect of Aging on the Stability of Microbially Reduced Uranium in Natural Sediment. *Environmental Science & Technology*. 54(1):613-620. <https://doi.org/10.1021/acs.est.8b07023>
- Lovley DR, Phillips EJP, Gorby YA, Landa ER (1991) Microbial reduction of uranium. *Nature*. (350):413-416. <https://doi.org/10.1038/350413a0>
- Ma M, Wang R, Xu L, Xu M y Liu S (2020) Emerging health risks and underlying toxicological mechanisms of uranium contamination: Lessons from the past two decades. *Environment International*. 145(1):106107. <https://doi.org/10.1016/j.envint.2020.106107>

- Madden AS, Palumbo AV, Ravel B, Vishnivetskaya TA, Phelps TJ, Schadt CW, Brandt CC (2007) Donor-dependent extent of uranium reduction for bioremediation of contaminated sediment microcosms. *Journal of Environmental Quality*. 38(1):53-60. <https://doi.org/10.2134/jeq2008.0071>
- Mangini A, Sonntag C, Bertsch G, Müller E (1979) Evidence for a higher natural uranium content in world rivers. *Nature*. 278(1):337–339. <https://doi.org/10.1038/278337a0>
- Marshall JL and Marshall VR (2008) Rediscovery of the Elements: Jáchymov (Joachimsthal), Czech Republic. University of North Texas, The Hexagon, Winter. Retrieved from <http://large.stanford.edu/courses/2017/ph241/hasson2/docs/marshall.pdf>
- Marshall MJ, Beliaev AS, Dohnalkova AC, Kennedy DW, Shi L, Wang Z, Boyanov MI, Lai B, Kemner KM, McLean JS, Reed SB, Culley DE, Bailey VL, Simonson CJ, Saffarini DA, Romine MF, Zachara JM, Fredrickson JK (2006) c-Type cytochrome-dependent formation of U(IV) nanoparticles by *Shewanella oneidensis*. *PLoS Biology*. 4(9):e268. <https://doi.org/10.1371/journal.pbio.0040268>
- Marshall MJ, Dohnalkova AC, Kennedy DW, Plymale AE, Thomas SH, Löffler FE, Sanford RA, Zachara JM, Fredrickson JK, Beliaev AS (2009) Electron donor-dependent radionuclide reduction and nanoparticle formation by *Anaeromyxobacter dehalogenans* strain 2CP-C. *Environmental Microbiology*. 11(2):534-543. <https://doi.org/10.1111/j.1462-2920.2008.01795.x>
- Martínez-Rodríguez P, Sánchez-Castro I, Ojeda JJ, Abad MM, Descostes M, Merroun ML (2023) Effect of different phosphate sources on uranium biomineralization by the *Microbacterium* sp. Be9 strain: A multidisciplinary approach study. *Frontiers in Microbiology*. 13:1092184. <https://doi.org/10.3389/fmicb.2022.1092184>
- Meinrath A, Schneider P, Meinrath G (2003) Uranium ores and depleted uranium in the environment, with a reference to uranium in the biosphere from the Erzgebirge/Sachsen, Germany. *Journal of Environmental Radioactivity*. 64(2-3):175-193. [https://doi.org/10.1016/s0265-931x\(02\)00048-6](https://doi.org/10.1016/s0265-931x(02)00048-6)
- Mettler FA and Upton AC (2008) Chapter 9 - Uranium, Plutonium, and Radium. In: Saunders WD (Eds.). *Medical Effects of Ionizing Radiation (Third Edition)*: 423-436. <https://doi.org/10.1016/B978-0-7216-0200-4.10009-5>
- Mizuoka K, Grenthe I, Ikeda Y (2005) Structural and kinetic studies on uranyl(V) carbonate

complex using ¹³C NMR spectroscopy. *Inorganic Chemistry*. 44(13):4472-4474. <https://doi.org/10.1021/ic050308x>

Mukherjee A, Wheaton GH, Blum PH, Kelly RM (2012) Uranium extremophily is an adaptive, rather than intrinsic, feature for extremely thermoacidophilic *Metallosphaera* species. *Proceedings of the National Academy of Sciences of the United States of America*. 109(41):16702-16707. <https://doi.org/10.1073/pnas.1210904109>

Mumtaz S, Streten-Joyce C, Parry DL, McGuinness KA, Lu P, Gibb KS (2013) Fungi outcompete bacteria under increased uranium concentration in culture media. *Journal of Environmental Radioactivity*. 120:39-44. <https://doi.org/10.1016/j.jenvrad.2013.01.007>

Naranjo-Ortiz MA and Gabaldón T (2019). Fungal evolution: diversity, taxonomy and phylogeny of the Fungi. *Biological Reviews*, 94(6):2101-2137. <https://doi.org/10.1111/brv.12550>

NEA/IAEA (2022) Uranium Resources, Production and Demand: A Joint Report by the Nuclear Energy Agency and the International Atomic Energy Agency. Retrieved from: https://www.oecd-nea.org/jcms/pl_79960/uranium-2022-resources-production-and-demand?details=true

Newman-Portela AM, Krawczyk-Bärsch E, Lopez-Fernandez M, Bok F, Kassahun A, Drobot B, Steudtner R, Stumpf T, Raff J, Merroun ML (2024) Biostimulation of indigenous microbes for uranium bioremediation in former U mine water: multidisciplinary approach assessment. *Environmental Science and Pollution Research*. 31(5):7227-7245. <https://doi.org/10.1007/s11356-023-31530-4>

Newsome L, Morris K, Trivedi D, Bewsher A, Lloyd JR (2015) Biostimulation by Glycerol Phosphate to Precipitate Recalcitrant Uranium(IV) Phosphate. *Environmental Science & Technology*. 49(18):11070-8. <https://doi.org/10.1021/acs.est.5b02042>

Nóbrega FA, Lima HM, Leite AL (2008) Análise de múltiplas variáveis no fechamento de mina - Estudo de caso da pilha de estéril BF-4, Mina Osamu Utsumi, INB Caldas, Minas Gerais. *Mineração*. 61:197e202. <https://doi.org/10.1590/s0370-44672008000200014>

Nolan PJ, Bone SE, Campbell KM, Pan D, Healy OM, Stange M, Bargar JR, Weber KA (2021) Uranium(VI) attenuation in a carbonate-bearing oxic alluvial aquifer. *Journal*

- of Hazardous Materials. 412:125089. <https://doi.org/10.1016/j.jhazmat.2021.125089>
- Orellana R, Leavitt JJ, Comolli LR, Csencsits R, Janot N, Flanagan KA, Gray AS, Leang C, Izallalen M, Mester T, Lovley DR (2013) U(VI) reduction by diverse outer surface c-type cytochromes of *Geobacter sulfurreducens*. *Applied and Environmental Microbiology*. 79(20):6369-6374. <https://doi.org/10.1128%2FAEM.02551-13>
- Park DM and Jiao Y (2014) Modulation of medium pH by *Caulobacter crescentus* facilitates recovery from uranium-induced growth arrest. *Applied and Environmental Microbiology*. 80(18):5680-5688. <https://doi.org/10.1128%2FAEM.01294-14>
- Payne RB, Gentry DM, Rapp-Giles BJ, Casalot L, Wall JD (2002) Uranium reduction by *Desulfovibrio desulfuricans* strain G20 and a cytochrome c3 mutant. *Applied and Environmental Microbiology*. 68(6):3129-3132. <https://doi.org/10.1128%2FAEM.68.6.3129-3132.2002>
- Plant JA, Simpson PR, Smith B, Windley BF (1999) Uranium Ore Deposits-Products of the Radioactive Earth. In: Burns PC and Finch R (Eds.). *Uranium: Mineralogy, Geochemistry and the Environment*. *Reviews in Mineralogy*. 38:255-319. Retrieved from: <https://www.scirp.org/reference/referencespapers?referenceid=1975253>
- Priest ND (2001) Toxicity of depleted uranium. *The Lancet*. 357(9252):244-6. [https://doi.org/10.1016/s0140-6736\(00\)03605-9](https://doi.org/10.1016/s0140-6736(00)03605-9)
- Renshaw JC, Butchins LJ, Livens FR, May I, Charnock JM, Lloyd JR (2005) Bioreduction of uranium: environmental implications of a pentavalent intermediate. *Environmental Science & Technology*. 39(15):5657-5660. <https://doi.org/10.1021/es048232b>
- Sánchez-Castro I, Martínez-Rodríguez P, Jroundi F, Solari PL, Descostes M, Merroun ML (2020) High-efficient microbial immobilization of solved U(VI) by the *Stenotrophomonas* strain Br8. *Water Research*. 183:116110. <https://doi.org/10.1016/j.watres.2020.116110>
- Sánchez-Castro I, Martínez-Rodríguez P, Abad MM, Descostes M, Merroun ML (2021) Uranium removal from complex mining waters by alginate beads doped with cells of *Stenotrophomonas* sp. Br8: Novel perspectives for metal bioremediation. *Journal of Environmental Management*. 296:113411. <https://doi.org/10.1016/j.jenvman.2021.113411>
- Shelobolina ES, Vrionis HA, Findlay RH, Lovley DR (2008) *Geobacter uraniireducens* sp. nov., isolated from subsurface sediment undergoing uranium bioremediation.

International Journal of Systematic and Evolutionary Microbiology. 58(5):1075-1078. <https://doi.org/10.1099/ijs.0.65377-0>

Shumilin E, Rodríguez-Figueroa G, Sapozhnikov D, Sapozhnikov Y, Choumiline K (2012) Anthropogenic and authigenic uranium in marine sediments of the central Gulf of California adjacent to the Santa Rosalía mining region. *Archives of Environmental Contamination and Toxicology*. 63(3):309-322. <https://doi.org/10.1007/s00244-012-9776-1>

Smedley PL and Kinniburgh DG (2023) Uranium in natural waters and the environment: Distribution, speciation and impact. *Applied Geochemistry*. 148:105534. <https://doi.org/10.1016/j.apgeochem.2022.105534>

Spain AM and Krumholz LR (2011) Nitrate-Reducing Bacteria at the Nitrate and Radionuclide Contaminated Oak Ridge Integrated Field Research Challenge Site: A Review. *Geomicrobiology*. 28(5-6):418-429. <https://doi.org/10.1080/01490451.2010.507642>

Spear JR, Figueroa LA, Honeyman BD (2000) Modeling reduction of uranium U(VI) under variable sulfate concentrations by sulfate-reducing bacteria. *Applied and Environmental Microbiology*. 66(9):3711-21. <https://doi.org/10.1128/aem.66.9.3711-3721.2000>

Suriya J, Chandra Shekar M, Nathani NM, Suganya T, Bharathiraja S, Krishnan M (2017) Assessment of bacterial community composition in response to uranium levels in sediment samples of sacred Cauvery River. *Applied Microbiology and Biotechnology*. 101(2):831-841. <https://doi.org/10.1007/s00253-016-7945-2>

Suzuki Y, Kelly SD, Kemner KM, Banfield JF (2003) Microbial populations stimulated for hexavalent uranium reduction in uranium mine sediment. *Applied and Environmental Microbiology*. 69(3):1337-1346. <https://doi.org/10.1128/aem.69.3.1337-1346.2003>

Tapia-Rodríguez A, Luna-Velasco A, Field JA, Sierra-Alvarez R (2010) Anaerobic bioremediation of hexavalent uranium in groundwater by reductive precipitation with methanogenic granular sludge. *Water Research*. 44(7):2153-2162. <https://doi.org/10.1016/j.watres.2009.12.030>

Taylor DM and Taylor SK (1997) Environmental uranium and human health. *Reviews on Environmental Health*. 12(3):147-157. <https://doi.org/10.1515/reveh.1997.12.3.147>

- Tuovinen H, Pelkonen M, Lempinen J, Pohjolainen E, Read D, Solatie D, Lehto J (2018) Behaviour of Metals during Bioheap Leaching at the Talvivaara Mine, Finland. *Geosciences*. 8(2):66. <https://doi.org/10.3390/geosciences8020066>
- U.S.NRC (United States Nuclear Regulatory Commission) 2023 Date of access: February 01, 2024. Retrieved from <https://www.nrc.gov/reading-rm/basic-ref/glossary/natural-uranium.html>
- Vaughan DJ and Lloyd JR (2011) Mineral-organic-microbe interactions: Environmental impacts from molecular to macroscopic scales Interactions matière minérale-matière organique-microbe: impacts environnementaux de l'échelle moléculaire à l'échelle macroscopique. *Comptes Rendus Geoscience*. 343(2-3):140-159. <https://doi.org/10.1016/j.crte.2010.10.005>
- Vettese GF, Morris K, Natrajan LS, Shaw S, Vitova T, Galanzew J, Jones DL, Lloyd JR (2020) Multiple Lines of Evidence Identify U(V) as a Key Intermediate during U(VI) Reduction by *Shewanella oneidensis* MR1. *Environmental Science & Technology*. 54(4):2268-2276. <https://doi.org/10.1021/acs.est.9b05285>
- Von Canstein H, Ogawa J, Shimizu S, Lloyd JR (2008) Secretion of Flavins by *Shewanella* Species and Their Role in Extracellular Electron Transfer. *Applied and Environmental Microbiology*. 74(3):615-23. <https://doi.org/10.1128/AEM.01387-07>
- Wall JD and Krumholz LR (2006) Uranium reduction. *Annual Review of Microbiology*. 60:149-166. <https://doi.org/10.1146/annurev.micro.59.030804.121357>
- Wang X, Dai X, Shi C, Wan J, Silver MA, Zhang L, Chen L, Yi X, Chen B, Zhang D, Yang K, Diwu J, Wang J, Xu Y, Zhou R, Chai Z, Wang S (2019) A 3,2-Hydroxypyridinone-based Decorporation Agent that Removes Uranium from Bones In Vivo. *Nature Communication*. 10(1):2570. <https://doi.org/10.1038/s41467-019-10276-z>
- Long KH, Davis PE, Wilkins JA, N'Guessan MJ, Steefel AL, Yang CI, Newcomer L, Spane D, Kerkhof FA, McGuinness LJ, Dayvault L, Lovley DR (2011) Acetate Availability and its Influence on Sustainable Bioremediation of Uranium-Contaminated Groundwater. *Geomicrobiology Journal*. 28(5-6):519-539. <https://doi.org/10.1080/01490451.2010.520074>
- World information service on energy (WISE) (1995) Uranium production in Europe. Date of access: February 01, 2024. Retrieved from <https://www.wiseinternational.org/nuclear-monitor/439-440/1-uranium-production-europe>

- WISMUT GmbH Umweltbericht (2021) Date of access: February 01, 2024. Retrieved from https://www.wismut.de/en/ronneburg_lichtenberg-pit-mine.php
- WNA (World Nuclear Association) 2023 Date of access: February 01, 2024. Retrieved from <https://world-nuclear.org/information-library/nuclear-fuel-cycle/uranium-resources/the-cosmic-origins-of-uranium.aspx#:~:text=The%20Earth's%20uranium%20had%20been,of%20the%20Earth's%20heat%20flux>
- Woolfolk CA and Whiteley HR (1962) Reduction of inorganic compounds with molecular hydrogen by *Micrococcus lactilyticus*. I. Stoichiometry with compounds of arsenic, selenium, tellurium, transition and other elements. *Journal of Bacteriology*. 84(4):647-58. <https://doi.org/10.1128/jb.84.4.647-658.1962>
- Wu WM, Carley J, Gentry T, Ginder-Vogel MA, Fienen M, Mehlhorn T, Yan H, Caroll S, Pace MN, Nyman J, Luo J, Gentile ME, Fields MW, Hickey RF, Gu B, Watson D, Cirpka OA, Zhou J, Fendorf S, Kitanidis PK, Jardine PM, Criddle CS (2006a) Pilot-scale in situ bioremediation of uranium in a highly contaminated aquifer. 2. Reduction of U(VI) and geochemical control of U(VI) bioavailability. *Environmental Science & Technology*. 40(12):3986-3995. <https://doi.org/10.1021/es051960u>
- Wu Q, Sanford RA, Löffler FE (2006b) Uranium(VI) reduction by *Anaeromyxobacter dehalogenans* strain 2CP-C. *Applied and Environmental Microbiology*. 72(5):3608-3614. <https://doi.org/10.1128/AEM.72.5.3608-3614.2006>
- Xiao S, Zhang Q, Chen X, Dong F, Chen H, Liu M, Ali I (2019) Speciation Distribution of Heavy Metals in Uranium Mining Impacted Soils and Impact on Bacterial Community Revealed by High-Throughput Sequencing. *Frontiers in Microbiology*. 10:1867. <https://doi.org/10.3389/fmicb.2019.01867>
- You W, Peng W, Tian Z, Zheng M (2021) Uranium bioremediation with U(VI)-reducing bacteria. *Science of the Total Environment*. 798:149107. <https://doi.org/10.1016/j.scitotenv.2021.149107>
- Yusov AB, Shilov VP, Peretrukhin VF, Fedoseev AM (2007) Uranium(III) in aqueous solutions: Preparation, properties, synthesis of solid compounds. *Radiochemistry*. 49(1):1-13. <https://doi.org/10.1134/S1066362207010018>
- Zachara JM, Long PE, Bargar J, Davis JA, Fox P, Fredrickson JK, Freshley MD, Konopka AE, Liu C, McKinley JP, Rockhold ML, Williams KH, Yabusaki SB (2013) Persistence of uranium groundwater plumes: contrasting mechanisms at two DOE

sites in the groundwater-river interaction zone *Journal of Contaminant Hydrology*. 147:45-72. <https://doi.org/10.1016/j.jconhyd.2013.02.001>

Zeng T, Wang L, Zhang X, Song X, Li J, Yang J, Chen S, Zhang J (2020) Characterization of Microbial Communities in Wastewater Treatment Plants Containing Heavy Metals Located in Chemical Industrial Zones. *Int J Environ Res Public Health*. 19(11):6529. <https://doi.org/10.3390/ijerph19116529>

Zhu YG and Chen BD (2009) Chapter 8 Principles and Technologies for Remediation of Uranium-Contaminated Environments. In G. Voigt and S. Fesenko (edt.). *Radioactivity in the Environment*. 14:357-374. [https://doi.org/10.1016/S1569-4860\(08\)00208-8](https://doi.org/10.1016/S1569-4860(08)00208-8)

Zhu F, Zhao B, Min W and Li J (2023) Characteristics of groundwater microbial communities and the correlation with the environmental factors in a decommissioned acid in-situ uranium mine. *Frontiers in Microbiology*. 13:1078393. <https://doi.org/10.3389/fmicb.2022.1078393>



Photo by Joana Hahn



Objectives

OBJECTIVES


Human activities as mining and processing of ores generate several wastes, with uranium (U) being one of the most concerning as they cannot undergo microbial or chemical degradation, in contrast to organic contaminants. Since U is a radionuclide, which in enriched concentrations exhibits a major health threat, conventional remediation technologies (controlled flooding and a following long-lasting water treatment) are used to address this issue. However, these technologies show a high implementation cost and are not effective for low U concentrations. For nearly five decades, the application of bioremediation strategies has emerged as an effective method to immobilize inorganic contaminants. These strategies are based on the ability of microorganisms to interact with heavy metals through different mechanisms. The main objective of this PhD thesis was to characterize the chemistry and microbiology of the mine water from two flooded former U mines in the Ore Mountains, Germany, Schlema-Alberoda and Pöhla (Wismut GmbH), to design a bioremediation strategy based on the biostimulation of the U-reducing microbial community. To achieve this main objective, the following specific objectives were established:

1. Characterize geochemically the mine water of Schlema-Alberoda and Pöhla using a multidisciplinary approach, and the microbial community through sequencing of the bacterial 16S ribosomal RNA (rRNA) gene and the fungal internal transcribed spacer (ITS).
2. Describe and explore key metabolic pathways and activities related to the biogeochemical cycles of S, N, and C in the mine water of Schlema-Alberoda and Pöhla through metatranscriptomic analysis.
3. Isolate, molecularly identify, and biochemically characterize fungi from Schlema-Alberoda and Pöhla mine waters. Additionally, screen for fungal strains with U immobilization potential.

4. Design and optimize a U bioremediation approach based on stimulating the native bacterial community, from Schlema-Alberoda mine water, able to reduce U using glycerol as electron donor, as well as characterizing the U reduced products using spectroscopic and microscopic techniques.



Photo by Chokniti Khongchum

A vertical strip on the left side of the page shows a close-up, shallow depth-of-field photograph of a microscope. The focus is on the objective lens and eyepiece area, with the rest of the instrument and the background blurred. The lighting is soft and blue-toned.

Materials and Methods

MATERIALS AND METHODS

The Materials and Methods section aims to briefly describe the different methodologies used in this PhD thesis to achieve the previously mentioned objectives. For more detailed information on each of these methodologies and how they were used in each experiment, details are provided in the corresponding Materials and Methods section of the Chapter I to IV.

1. Sampling campaigns

Fresh mine water samples were collected from two subsurface flooded mine shafts located in Schlema-Alberoda (50°37'32.5"N, 12°40'52.4"E) and Pöhla (50°29'34.8"N, 12°49'07.1"E) during the years 2020, 2021, and 2022. These samples were obtained using water pumped to the surface. Mine water was extracted using sterile screw-capped bottles sterilized in an autoclave at an authorized and safe point within each mine. In Schlema-Alberoda, sampling was conducted through an external pipeline that transported water from inside the mine to the outside, while in Pöhla, it was done inside the mine using a pipeline directly connected to it. In both cases, the pipeline was properly purged before sampling, discarding several volumes of water to remove residual water and ensure the representativeness of the samples. Subsequently, the samples were transported to the laboratory at a temperature of 4°C and stored in a refrigerator at the same temperature until further processing.

2. Characterization of the microbial community in the mine water

The total DNA extraction was carried out using a kit (DNeasy Power Water Kit, QIAGEN, Germany) and according to the manufacturer's protocol, with the temperature increase modification recommended by the manufacturer for obtaining fungal DNA. The DNA extracted was checked by agarose gel electrophoresis and DNA concentration was determined using Qubit Fluorometer 4.0 (Thermo Fisher Scientific, USA) according to the manufacturer's protocol. The samples were stored at -20 °C until DNA amplification. The hypervariable V3-V4 bacterial regions of the 16S rRNA gene was amplified using the primers 341F (5'-CCTACGGGNGGCWGCAG-3')

and 785R (5'-GACTACHVGGGTATCTAATCC-3') (Thijs et al. 2017). Fungal ITS gene amplification was performed using the primers ITS1F (5'-CTTGGTCATTTAGAGGAAGTAA-3') and ITS2R (5'-GCTGCGTTCTTCATCGATGC-3') (Op De Beeck et al. 2014). Then, PCR amplification, assembly, and sequencing of the libraries (Illumina Mi-Seq) were conducted at the laboratories of STAB-VIDA (Caparica, Portugal).

2.1 Bioinformatics and statistical analyses

FastQC was used for quality control of raw sequence data (Andrews 2010). 16S and ITS rRNA raw sequences obtained via Illumina MiSeq were analysed using QIIME2 (Caporaso et al. 2010; Bolyen et al. 2019). The DADA2 plugin was used to denoise the reads, and taxonomy was assigned using classifiers pretrained on SILVA and UNITE databases (Quast et al. 2013; Callahan et al. 2016; Nilsson et al. 2019). Amplicon Sequence Variants (ASVs) with at least 10 sequence reads were deemed dominant.

For statistical analyses, alpha and beta diversity analyses were conducted using MicrobiomeAnalyst (v4.1.3) (Dhariwal et al. 2017). Filters were applied to remove low-quality features, and ASVs with four read counts, representing 20% of the total counts, were retained. Chao1 and Shannon indexes were used for alpha diversity, while beta diversity was assessed using NMDS and PERMANOVA. PCA was conducted using PAST4 (v4.04) on Hellinger-transformed data, excluding taxa with <1% relative abundance (Harper 1999).

3. Metatranscriptomic study

Total RNA was extracted using a RNeasy PowerWater kit (QIAGEN, Germany) including on-column DNase digestion. RNA concentrations were quantified with a Qubit Fluorometer, and integrity was assessed using an Agilent 2100 Bioanalyzer at STAB-VIDA laboratories (Caparica, Portugal). RNA samples were used for library construction and metatranscriptome sequencing at STAB-VIDA, sequenced on an Illumina Novaseq platform.

3.1. Bioinformatics and statistical analyses

Illumina adapters and low-quality reads were removed using Cutadapt and Trimmomatic (Martin 2011; Bolger et al. 2014). SortMeRNA filtered remaining rRNA reads (Kopylova et al. 2014). Trinity assembled reads into transcripts, Prodigal 2.6.3 predicted functional genes, and Bowtie2 mapped reads for quantification (Hyatt et al. 2010; Grabherr et al. 2011; Langmead and Salzberg, 2012). Differential gene expression (DGE) was analysed with edgeR. GhostKOALA annotated DGE with KEGG Orthology, and KEGG decoder summarized pathway completeness (Kanehisa et al. 2016a, b; Graham et al. 2018). Heatmaps visualized differences in KEGG pathways. Volcano plots showed DGE involved in sulphate reduction. FeGenie identified iron reduction genes (Garber et al. 2020).

4. Molecular and biochemical characterization of isolated fungi

For the fungi isolation, fresh mine water was filtered through sterile membrane filters (Membrane Filter, MF-Millipore®, Germany). Each filter was divided into four pieces and placed on Potato Dextrose Agar (PDA) plates. After 7 days at 25 ± 2 °C, fungal mycelium emerged. Agar discs were transferred to fresh PDA medium and incubated for 5 days until pure colonies formed. Pure colonies were stored at 4 °C on PDA and malt extract agar.

4.1. Molecular characterization

DNA extraction from each isolated colony was carry out following the protocol described by Martín-Platero et al. (2007) and modified as reported in Povedano-Priego et al. (2024). Sample quality and concentration were evaluated using agarose gel electrophoresis and the Qubit dsDNA BR Assay kit on the Qubit Fluorometer 4.0 (Thermo Fisher Scientific, USA), respectively.

For PCR amplification, the primers ITS-1 (5'-TCCGTAGGTGAACCTGCGG-3') and ITS-4 (5'-TCCTCCGCTTATTGATATGC-3'), were used to amplify ~600-base pair (bp) fragments of the ITS region. DNA amplicon concentrations were quantified using the Qubit dsDNA BR Assay kit on the Qubit Fluorometer

4.0. Purified PCR products were sequenced by Sanger sequencing at the *Instituto de Parasitología y Biomedicina López Neyra* (IPBLN) Genomics Facility (CSIC, Granada, Spain). Sequences were edited and aligned using BioEdit (v7.09) (Hall 1999). BLAST was used to identify the isolated strains by comparing them with NCBI GenBank accessions.

4.2 Enzymatic activity characterization

The enzymatic activities of the isolated fungal strains, including cellulase, amylase, laccase, and lignin peroxidase (LiP), were evaluated using different culture medium. Cellulase activity was studied using solid carboxymethylcellulose (CMC) medium, LiP activity was assessed on agar-malt medium supplemented with sawdust, laccase activity was tested on Kirk solid medium amended with ABTS (2,2'-azino-bis(3-ethylbenzothiazoline-6-sulphonic acid)) (Kirk et al. 1986), and amylase activity was determined on starch agar solid medium. In addition, *API® 20 ZYM* test (BioMérieux, France) a semi-quantitative test designed to evaluate the activity of nineteen hydrolytic enzymes, was used. Further information regarding the preparation of the culture medium, testing procedures, incubation times, and conditions can be found in Chapter IV.

5. Geochemical characterization of the mine waters

To determine the concentration of cations (Na, K, Mg, Ca, Al, Si, P, Mn, Fe, As, Ba, Th, U) in the studied water samples, inductively coupled plasma mass spectrometry (ICP-MS, ELAN 9000, PerkinElmer, Germany) was used. On the other hand, high-performance ion chromatography (HPIC, Dionex Integrion, Thermo Fisher Scientific, USA) was used to analyse the anions (NO_2^- , NO_3^- , PO_4^{3-} , SO_4^{2-} , Cl^-). Additionally, total inorganic/organic carbon (TIC/TOC), dissolved organic carbon (DOC), and nitrogen were quantified by a Multi N/C 2100S (Analytik Jena, Germany).

6. Prediction and determination of soluble U species

6.1. Thermodynamic calculation of the U speciation

To predict the dominant U species under environmental conditions in both mine waters and to predict the potential reduction of U under experimental

conditions, Pourbaix diagrams were calculated using analytical data and the Geochemist's Workbench (GWB) geochemical speciation code, version 17.0.1/Act2. GWB is an integrated geochemical modelling package used for balancing chemical reactions, calculating stability diagrams and equilibrium states of natural waters, tracking reaction processes, modelling reactive transport, plotting the results of these calculations, and storing related data. The thermodynamic database used was ThermoChimie Version 10.a. (Giffaut et al. 2014; Grivé et al. 2015).

6.2. Cryo-time-resolved laser fluorescence spectroscopy (Cryo-TRLFS)

Cryo-TRLFS is a useful technique for identifying certain actinide species resulting from different biogeochemical processes (Collins et al. 2011; Steudtner et al. 2011). In general terms, cryo-TRLFS distinguishes between different chemical species of a fluorescent metal ion by analysing different excitation and emission spectra, as well as associated decay lifetimes. This technique is non-destructive and does not alter the chemical composition of the sample. Furthermore, conducting measurements at cryogenic temperatures (-120°C) significantly enhances the intensity and resolution of the luminescence spectra due to reduced quenching effects from ligands and/or water (Steudtner et al. 2011). The main advantage of cryo-TRLFS over other advanced spectroscopic techniques lies in its ability to determine metal speciation at environmentally relevant concentrations ranging from micromolar to picomolar levels (Collins et al. 2011). Therefore, in our study, we used cryo-TRLFS to identify soluble forms of U(VI) present in the mine water of Schlemma-Alberoda and Pöhla mines contaminated with low U concentrations. For this purpose, the luminescence of soluble U(IV) in cryogenic conditions was measured using a Nd:YAG pulsed laser system (Continuum Inlite series, Continuum, USA). The luminescence spectra were detected using an iHR550 spectrograph and an intensified CCD-camera system (HORIBA Jobin Yvon, Edison, USA). Finally, data were evaluated using the software OriginPro v9.7 2020 (OriginLab Corporation, USA). Collected spectra were analysed by parallel factor analysis (PARAFAC) (Andersson and Bro 2000; Drobot et al. 2015). A more detailed description of the experimental design and the evaluation of the data can be found in

Chapter I.

7. Experimental design of microcosms

The assessment of the bioremediation potential of the indigenous U-reducing microbial community from the Schlema-Alberoda mine water was carried out using microcosms-based experiment incubated at anoxic conditions. Two-liter serum bottles were filled with fresh mine water from Schlema-Alberoda and supplemented with the electron donor (Fig. 1). Additionally, to assess the significant implication of biological processes in U reduction, control microcosms were simultaneously conducted. In one set of microcosms, mine water without amendment was used as control, while in another set of control microcosms, mine water was sterilized (autoclaved) and amended with the electron donor. Microcosms were incubated at $28 \pm 2^\circ\text{C}$ in the dark.

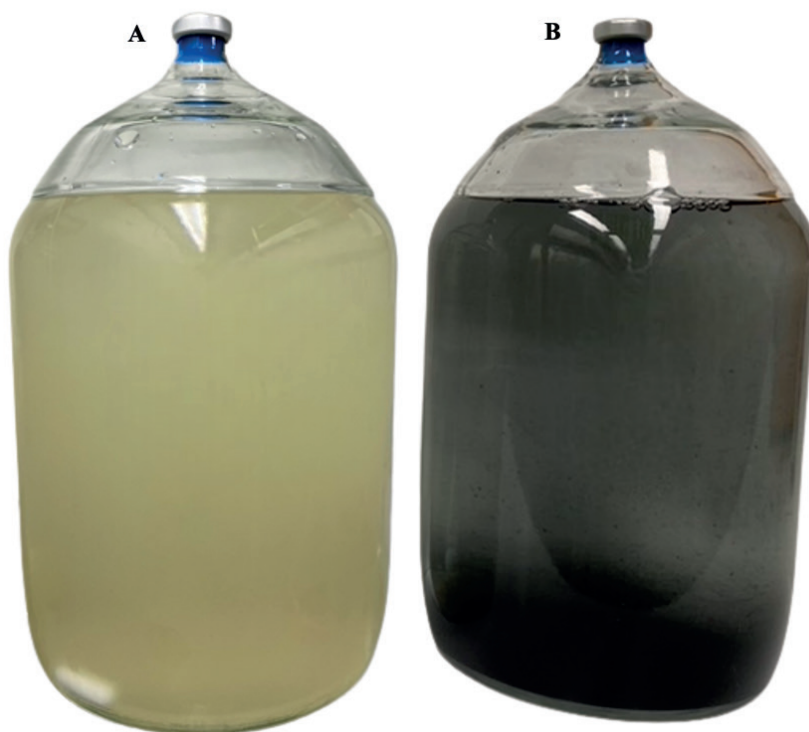


Figure 1. Microcosms amended with the electron donor (glycerol) at the beginning of the experiment (A), and at the end of the experiment (B).

8. Characterisation of reduced U products in the microcosms

8.1. UV-Visible (UV/VIS) spectroscopy

UV/VIS spectroscopy is a simple, versatile, non-destructive, and cost-effective analytical technique. This technique is used to measure the absorption of light in the ultraviolet and visible regions of the electromagnetic spectrum by a sample. It is based on the principle that absorbing molecules absorb light at specific wavelengths, allowing for the identification and quantification of substances present in the sample (Khalid et al. 2024). UV-VIS is a technique applicable to a wide range of research disciplines, including pharmaceuticals, environmental science, and many others. In our work, we used UV-VIS spectroscopy to obtain evidence of the presence and formation of U(IV). For this purpose, we use a Cary 5G UV/VIS-NIR spectrophotometer (Varian, U.S.). Details regarding sample preparation and measurements can be found in Chapter III.

8.2. Powder X-ray diffraction (PXRD)

PXRD is an analytical technique that allows for a rapid and non-destructive analysis of the sample. This technique is based on the diffraction of X-rays by atoms within a crystal. When a beam of X-rays hits a crystal, the atoms in the crystal lattice scatter the X-rays in different directions. This scattering results in a characteristic pattern of intensity peaks as a function of scattering angle, which can be recorded in the form of a diffractogram. PXRD is used to identify crystalline phases present in a sample, determine the crystal structure, quantify the amount of each phase present, study changes in the crystal structure under different conditions (such as temperature or pressure), and characterize unknown materials. In this PhD thesis, PXRD was used to characterize the possible crystalline phases present in the black precipitate during the U reduction. To achieve this objective, we used a MiniFlex 600 Powder X-ray diffractometer (Rigaku, Tokyo, Japan) equipped with a Cu K α X-ray source (40 keV/15 mA operation for X-ray generation) and the D/teX Ultra 1D silicon strip detector in the Bragg–Brentano θ – 2θ geometry at a scanning speed of 2 degrees per min. Chapter III contains further details on the procedures involved in sample preparation and measurements.

8.3. Extended X-ray absorption fine structure (EXAFS) and Energy-resolution fluorescence-detected X-ray absorption near-edge structure (HERFD-XANES)

Synchrotron radiation-based techniques, EXAFS, and HERFD-XANES were employed to obtain a more detailed description of the chemical structure(s) present in the bulk samples, as well as their oxidation state. EXAFS spectroscopy provides structural information about a sample by way of the analysis of its X-ray absorption spectrum. It allows determining the chemical environment of a single element in terms of the number and type of its neighbours, inter-atomic distances and structural disorders. Meanwhile HERFD-XANES, provides information about the oxidation states of the atoms.

The black precipitate, resulting from the reduction of U in the microcosms, was collected and analysed at the BM20-Rossendorf Beamline (ROBL) of the European Synchrotron Radiation Facility (ESRF) in Grenoble, France (Fig. 2). ROBL-II provides four different experimental stations to investigate actinide and other alpha- and beta-emitting radionuclides at the new EBS storage ring of ESRF within an energy range of 3 to 35 keV (Scheinost et al. 2021). The storage ring was operated in the multi-bunch filling mode at 6 GeV with a current of 200 mA. In order to characterize the reduced products of U in the black precipitate, we performed fluorescence EXAFS measurements at the U L₃-edge (Lee et al. 1981), and HERFD-XANES measurements at the U M₄-edge (Kvashnina et al. 2013).



Fig. 2. European Synchrotron Radiation Facility (ESRF) in Grenoble, France. Image retrieved from <https://blogs.helmholtz.de/researchintheworld/2016/06/die-feinen-unterschiede/>

U L_3 -edge EXAFS measurements utilized a Si(111) double crystal monochromator and Rh-coated mirrors to filter the X-ray beam. Fluorescence signals were detected with an 18-element Ge-detector, while a Y metal foil's absorption spectrum provided energy calibration. Gas-filled ionization chambers measured photon flux and foil absorption. Each sample underwent 6-9 energy scans averaged for data analysis. Measurements were conducted cryogenically using a closed cycle He-cryostat, with the ionization potential set to 17.185 keV for photoelectron wave vector calculation. HERFD spectra were recorded using a Johann-type X-ray emission spectrometer in vertical Rowland geometry, equipped with a silicon drift X-ray detector. Incident energy was controlled by a Si(111) double-crystal monochromator. Calibration relied on HERFD spectra of a reference compound, setting U HERFD-XANES maximum energy at 3725 eV. The spectrometer had five crystal analyzers using Si(220), focusing on the U M_4 -edge (Fig. 3). Helium-filled bags minimized air absorption. Energy resolution was around 1 eV. Spectra were recorded with a 0.2 eV

step and 3-second counting time per point, with each spectrum lasting approximately 6 minutes for U. Averaging 4–10 spectra were collected per sample enhanced signal-to-noise ratio.

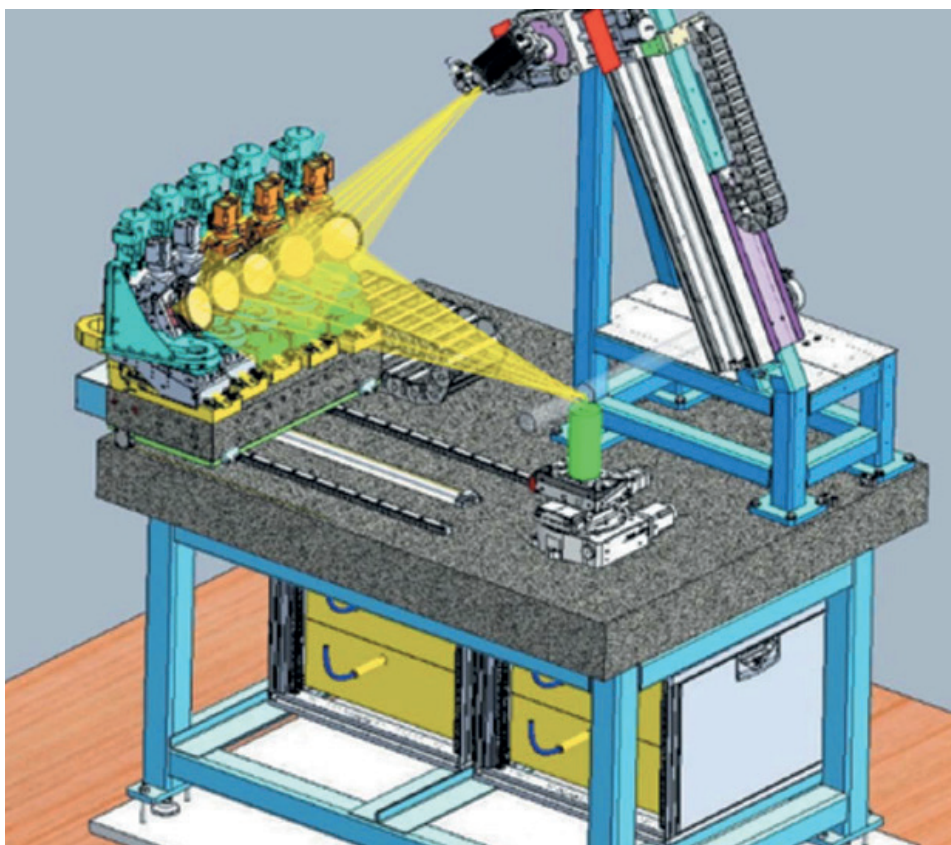


Fig. 3. Schematic drawing of the five-crystal of the HERFD-XANES. Figure from Scheinost et al. (2021).

Finally, data were evaluated using the software EXAFSPAK, target factor analysis (TFA) and iterative target transformation factor analysis (ITFA) (George 1995; Rossberg et al. 2003)

8.4. Microscopic methodologies

The combination of Transmission Electron Microscopy (TEM) and Scanning Electron Microscopy (SEM) techniques allows a comprehensive analysis of nanoparticles, resulting from U reduction, in terms of their size, shape, composition, crystalline structure, and surface properties. This is essential for understanding the nature of the nanoparticles and investigating the interaction mechanisms of U with micro-organisms. Details on sample

preparation for the different microscopic techniques can be found in the Materials and Methods section of Chapter III and IV.

8.4.1. FEI Titan High-Resolution Transmission Electron Microscopy (HRTEM)

The High-Angle Annular Dark Field Scanning Transmission Electron Microscope (HAADF-STEM, FEI TITAN G2 80–300, University of Granada, Spain) operating at an acceleration voltage of 300 kV, along with a MegaViewIII camera under standard operating conditions with a liquid nitrogen anticontaminator in place, were utilized (Fig. 4). In addition, Energy-Dispersive X-Ray Spectroscopy (EDXS), Selected Area Electron Diffraction (SAED), and Fast Fourier Transform (FFT) were used for the characterization of the U reduced products.

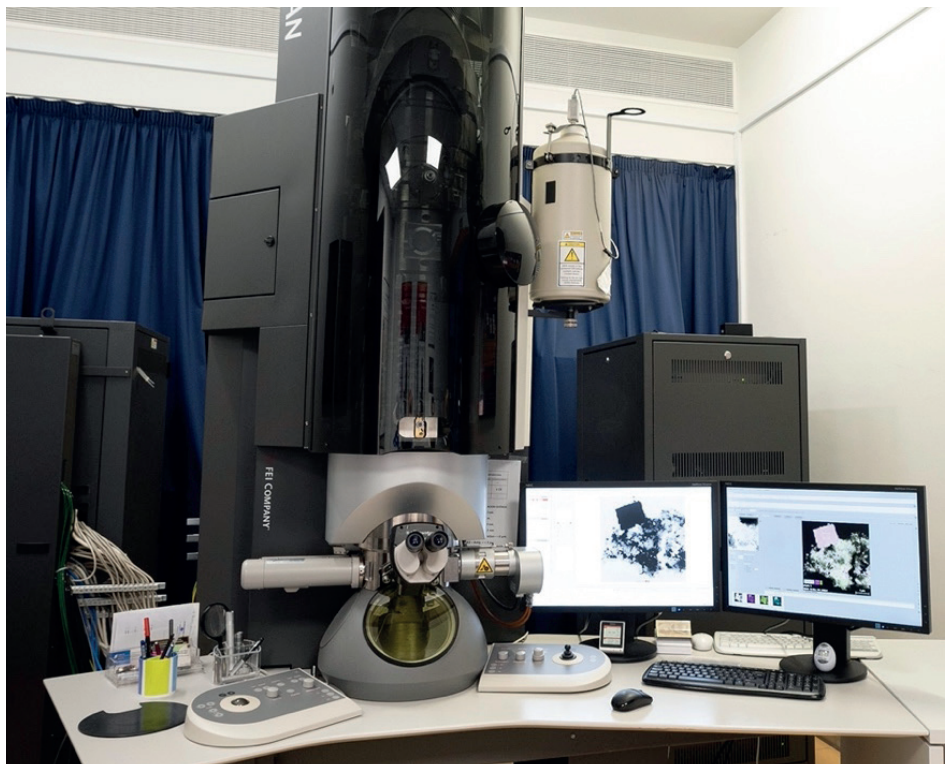


Fig. 4. High-Angle Annular Dark Field Scanning Transmission Electron Microscope (HAADF-STEM, FEI TITAN G2 80–300, University of Granada, Spain). Image retrieved from <https://intranet-cic.ugr.es/servicios-y-unidades/ficha.php?codServicio=6&unidad=28#>

8.4.2. Hitachi S-4800 High-Resolution Scanning Electron Microscope (HRSEM)

The High-Resolution Scanning Electron Microscope (Hitachi S-4800, Helmholtz-Zentrum Dresden-Rossendorf, Germany) was used in combination with an energy-dispersive X-ray spectroscopy (EDXS) microanalysis system to characterize the black precipitate of the microcosms with secondary electron (SE) and backscattered electron (BSE) detectors using a voltage of 5–30 kV.

8.4.3. Zeiss SUPRA40VP Variable Pressure Field Emission Scanning Electron Microscope (VPFESEM)

The Field Emission Scanning Electron Microscopy (Zeiss SUPRA40VP, University of Granada) equipped with SE (InLens) and BSE detectors (Zeiss SMT) coupled to EDXS microanalysis was used to study the interaction mechanisms of fungi with U and Se.

9. References

- Andersson CA and Bro R (2000) The *N*-way Toolbox for MATLAB. *Chemometrics and Intelligent Laboratory Systems*. 52(1):1-4. [https://doi.org/10.1016/S0169-7439\(00\)00071-X](https://doi.org/10.1016/S0169-7439(00)00071-X).
- Andrews (2010) *FastQC*: quality control tool for high throughput sequence data. Date of access: February 02, 2022. Retrieved from <http://www.bioinformatics.babraham.ac.uk/projects/fastqc>
- Bolger AM, Lohse M, Usadel B (2014) Trimmomatic: a flexible trimmer for Illumina sequence data. *Bioinformatics*. 30(15):2114-2120. <https://doi.org/10.1093/bioinformatics/btu170>
- Bolyen E, Rideout JR, Dillon MR, Bokulich NA, Abnet CC, Al-Ghalith GA, Alexander H, Alm EJ, Arumugam M, Asnicar F, Bai Y, Bisanz JE, Bittinger K, Brejnrod A, Brislawn CJ, Brown CT, Callahan BJ, Caraballo-Rodríguez AM, Chase J, Cope EK, Da Silva R, Diener C, Dorrestein PC, Douglas GM, Durall DM, Duvallet C, Edwardson CF, Ernst M, Estaki M, Fouquier J, Gauglitz JM, Gibbons SM, Gibson DL, Gonzalez A, Gorlick K, Guo J, Hillmann B, Holmes S, Holste H, Huttenhower C, Huttley GA, Janssen S, Jarmusch AK, Jiang L, Kaehler BD, Kang KB, Keefe CR, Keim P, Kelley ST, Knights D, Koester I, Kosciulek T, Kreps J, Langille MGI, Lee J, Ley R, Liu YX, Loftfield E, Lozupone C, Maher M, Marotz C, Martin BD, McDonald D, McIver LJ, Melnik AV, Metcalf JL, Morgan SC, Morton JT, Naimey AT, Navas-Molina JA, Nothias LF, Orchanian SB, Pearson T, Peoples SL, Petras D, Preuss ML, Pruesse E, Rasmussen LB, Rivers A, Robeson MS, Rosenthal P, Segata N, Shaffer M, Shiffer A, Sinha R, Song SJ, Spear JR, Swafford AD, Thompson LR, Torres PJ, Trinh P, Tripathi A, Turnbaugh PJ, Ul-Hasan S, Van der Hooft JJJ, Vargas F, Vázquez-Baeza Y, Vogtmann E, Von Hippel M, Walters W, Wan Y, Wang M, Warren J, Weber KC, Williamson CHD, Willis AD, Xu ZZ, Zaneveld JR, Zhang Y, Zhu Q, Knight R, Caporaso JG (2019) Reproducible, interactive, scalable and extensible microbiome data science using QIIME 2. *Nature Biotechnology*. 37(8):852–857. <https://doi.org/10.1038/s41587-019-0209-9>
- Callahan BJ, Mcmurdie PJ, Rosen MJ, Han WH, Johnson AJ, Holmes SP (2016) DADA2: High resolution sample inference from amplicon data. *Nature Methods*. 13(7):581–583. <http://dx.doi.org/10.1101/024034>
- Caporaso JG, Kuczynski J, Stombaugh J, Bittinger K, Bushman FD, Costello EK, Fierer

- N, Peña AG, Goodrich JK, Gordon JI, Huttley GA, Kelley ST, Knights D, Koenig JE, Ley RE, Lozupone C A, McDonald D, Muegge BD, Pirrung M, Reeder J, Sevinsky JR, Turnbaugh PJ, Walters WA, Widmann J, Yatsunenko T, Zaneveld J, Knight R (2010) QIIME allows analysis of high-throughput community sequencing data. *Nature Methods*. 7(5):335-336. <https://doi.org/10.1038/nmeth.f.303>
- Collins RN, Saito T, Aoyagi N, Payne TE, Kimura T, Waite TD (2011) Applications of time-resolved laser fluorescence spectroscopy to the environmental biogeochemistry of actinides. *Journal of Environmental Quality*. 40(3):731-41. <https://doi.org/10.2134/jeq2010.0166>
- Dhariwal A, Chong J, Habib S, King IL, Agellon LB, Xia J (2017) MicrobiomeAnalyst: A web-based tool for comprehensive statistical, visual and meta-analysis of microbiome data. *Nucleic Acids Research*. 45(W1):W180–W188. <https://doi.org/10.1093/nar/gkx295>
- Drobot B, Steudtner R, Raff J, Geipel G, Brendler V, Tsushima S (2015) Combining luminescence spectroscopy, parallel factor analysis and quantum chemistry to reveal metal speciation - A case study of uranyl(VI) hydrolysis. *Chemical Science*. 6:964–972. <https://doi.org/10.1039/c4sc02022g>
- Garber AI, Nealson KH, Okamoto A, McAllister SM, Chan CS, Barco RA, Merino N (2020) FeGenie: A Comprehensive Tool for the Identification of Iron Genes and Iron Gene Neighborhoods in Genome and Metagenome Assemblies. *Frontiers in Microbiology*. <https://doi.org/10.3389/fmicb.2020.00037>
- George GN and Pickering IJ (1995) EXAFSPAK: A Suite of Computer Programs for Analysis of X-Ray Absorption Spectra. Stanford Synchrotron Radiation Laboratory. https://scholar.google.com/scholar_lookup?title=EXAFSPAK%3A%20A%20Suite%20of%20Computer%20Programs%20for%20Analysis%20of%20X-Ray%20Absorption%20Spectra.&publication_year=1993&author=G.N.%20George&author=I.J.%20Pickering
- Giffaut E, Grivé M, Blanc P, Vieillard P, Colàs E, Gailhanou H, Gaboreau S, Marty N, Madé B, Duro L (2014) Andra thermodynamic database for performance assessment: ThermoChimie. *Applied Geochemistry*. 49:225–236. doi.org/10.1016/j.apgeochem.2014.05.007
- Grabherr MG, Haas BJ, Yassour M, Levin JZ, Thompson DA, Amit I, Adiconis X, Fan L, Raychowdhury R, Zeng Q, Chen Z, Mauceli E, Hacohen N, Gnirke A, Rhind N, di

- Palma F, Birren BW, Nusbaum C, Lindblad-Toh K, Friedman N, Regev A (2011) Full-length transcriptome assembly from RNA-Seq data without a reference genome. *Nature Biotechnology*. 29(7):644-652. <https://doi.org/10.1038/nbt.1883>
- Graham ED, Heidelberg JF, Tully BJ (2018) Potential for primary productivity in a globally-distributed bacterial phototroph. *ISME Journal*. 12(7):1861-1866. <https://doi.org/10.1038/s41396-018-0091-3>
- Grivé M, Duro L, Colàs E, Giffaut E (2015) Thermodynamic data selection applied to radionuclides and chemotoxic elements: an overview of the ThermoChimie-TDB. *Applied Geochemistry*. 55:85-94. doi.org/10.1016/j.apgeochem.2014.12.017
- Hall TA (1999). BioEdit: a user-friendly biological sequence alignment editor and analysis program for Windows 95/98/NT. *Nucleic Acids Symposium Series*, 41(41):95-98. Date of access: February 11, 2024. Retrieved from https://www.academia.edu/2034992/BioEdit_a_user_friendly_biological_sequence_alignment_editor_and_analysis_program_for_Windows_95_98_NT
- Harper DAT (ed.) 1999 Numerical Palaeobiology. John Wiley and Sons, New York. doi:10.1017/S0016756800334410
- Hyatt D, Chen GL, Locascio PF, Land ML, Larimer FW, Hauser LJ (2010) Prodigal: prokaryotic gene recognition and translation initiation site identification. *BMC Bioinformatics*. 11:119. <https://doi.org/10.1186/1471-2105-11-119>
- Kanehisa M, Sato Y, Kawashima M, Furumichi M, Tanabe M (2016a) KEGG as a reference resource for gene and protein annotation. *Nucleic Acids Research*. 44(D1):D457-462. <https://doi.org/10.1093/nar/gkv1070>
- Kanehisa M, Sato Y, Morishima K (2016b) BlastKOALA and GhostKOALA: KEGG Tools for Functional Characterization of Genome and Metagenome Sequences. *Journal of Molecular Biology*. 428(4):726-731. <https://doi.org/10.1016/j.jmb.2015.11.006>
- Khalid K, Ishak R, Chowdhury ZZ (2024) Chapter 15 - UV-Vis spectroscopy in non-destructive testing. *Non-Destructive Material Characterization Methods*. 391-416. <https://doi.org/10.1016/B978-0-323-91150-4.00021-5>
- Kirk TK, Croan S, Tien M, Murtagh KE, Farrel RL (1986). Production of multiple ligninases by *Phanerochaete chrysosporium*: effect of selected growth conditions and use of a mutant strain. *Enzyme and Microbial Technology*. 8:27-32. [https://doi.org/10.1016/0141-0296\(86\)90021-5](https://doi.org/10.1016/0141-0296(86)90021-5)

[org/10.1016/0141-0229\(86\)90006-2](https://doi.org/10.1016/0141-0229(86)90006-2)

- Kopylova E, Noé L, Touzet H (2012) SortMeRNA: fast and accurate filtering of ribosomal RNAs in metatranscriptomic data. *Bioinformatics*. 28(24):3211-3217. <https://doi.org/10.1093/bioinformatics/bts611>
- Kvashnina KO, Butorin SM, Martin P, Glatzel P (2013) Chemical State of Complex Uranium Oxides. *Physical Review Letters*. 111(25):1–5. <https://doi.org/10.1103/PhysRevLett.111.253002>
- Langmead B and Salzberg SL (2012) Fast gapped-read alignment with Bowtie 2. *Nature Methods*. 9(4):357-359. <https://doi.org/10.1038/nmeth.1923>
- Lee PA, Citrin PH, Eisenberger P, Kincaid BM (1981) Extended X-Ray Absorption Fine Structure Its Strengths and Limitations as a Structural Tool. *Reviews of Modern Physics*. 53(4):769–806. <https://doi.org/10.1103/RevModPhys.53.769>
- Martin M (2011) Cutadapt Removes Adapter Sequences from High-Throughput Sequencing Reads. *EMBnet Journal*. 17:10-12. <https://doi.org/10.14806/ej.17.1.200>
- Martín-Platero AM, Valdivia E, Maqueda M, Martínez-Bueno M (2007) Fast, convenient, and economical method for isolating genomic DNA from lactic acid bacteria using a modification of the protein “salting-out” procedure. *Analytical Biochemistry*. 366(1):102-4. <https://doi.org/10.1016/j.ab.2007.03.010>
- Nilsson RH, Larsson KH, Taylor AFS, Bengtsson-Palme J, Jeppesen TS, Schigel D, Kennedy P, Picard K, Glöckner FO, Tedersoo L, Saar I, Kõljalg U, Abarenkov K. (2019) The UNITE database for molecular identification of fungi: Handling dark taxa and parallel taxonomic classifications. *Nucleic Acids Research*. 47(D1): D259–D264. <https://doi.org/10.1093/nar/gky1022>
- Op De Beeck M, Lievens B, Busschaert P, Declerck S, Vangronsveld J, Colpaert JV (2014) Comparison and validation of some ITS primer pairs useful for fungal metabarcoding studies. *PLoS ONE*. 9(6):e97629. <https://doi.org/10.1371/journal.pone.0097629>
- Povedano-Priego C, Fadwa J, Morales-Hidalgo M, Pinel-Cabello M (2024) Unveiling Fungal Diversity in Uranium and Glycerol-2-Phosphate-Amended Bentonite Microcosms: Implications for Radionuclide Immobilization within the Deep Geological Repository System. *Science of the Total Environment*. 908: 168284. <https://doi.org/10.1016/j.scitotenv.2023.168284>

- Quast C, Pruesse E, Yilmaz P, Gerken J, Schweer T, Yarza P, Peplies J, Glöckner FO (2013) The SILVA ribosomal RNA gene database project: Improved data processing and web-based tools. *Nucleic Acids Research*, 41(D1):D590–D596. <https://doi.org/10.1093/nar/gks1219>
- Rossberg A, Reich T, Bernhard G (2003) Complexation of Uranium(VI) with Protocatechuic Acid-Application of Iterative Transformation Factor Analysis to EXAFS Spectroscopy. *Analytical and Bioanalytical Chemistry*. 376(5):631–38. <https://doi.org/10.1007/s00216-003-1963-5>
- Scheinost AC, Claussner J, Exner J, Feig M, Findeisen S, Hennig C, Kvashnina KO, Naudet D, Prieur D, Rossberg A, Schmidt M, Qiu C, Colomp P, Cohen, C, Dettona E, Dyadkin V, Stumpf T (2021) ROBL-II at ESRF: A Synchrotron Toolbox for Actinide Research. *Journal of Synchrotron Radiation*. 28:333–349. <https://doi.org/10.1107/S1600577520014265>
- Stedtner R, Sachs S, Schmeide K, Brendler V, Bernhard G (2011) Ternary uranium(VI) carbonate humate complex studied by cryo-TRLFS. *Radiochimica Acta*. 99(11): 687–692. <https://doi.org/10.1524/ract.2011.1861>
- Thijs S, De Beeck MO, Beckers B, Truyens S, Stevens V, Van Hamme JD, Weyens N, Vangronsveld J (2017) Comparative evaluation of four bacteria-specific primer pairs for 16S rRNA gene surveys. *Frontiers in Microbiology*. 8(494):1–15. <https://doi.org/10.3389/fmicb.2017.00494>



Underground mine gallery.
Photo by I.L.Pixel

Chapter I:

Biostimulation of Indigenous Microbes for Uranium Bioremediation in Former U Mine Water: Multidisciplinary approach assessment.

AUTHORS:

Antonio M. Newman-Portela^{1,2*}, Evelyn Krawczyk-Bärsch²,
Margarita Lopez-Fernandez¹, Frank Bok², Andrea Kassahun³,
Björn Drobot², Robin Steudtner², Thorsten Stumpf², Johannes
Raff², Mohamed L. Merroun¹

¹Department of Microbiology, Faculty of Science, University of Granada, Avda.
Fuentenueva s/n, 18071 Granada, Spain.

²Institute of Resource Ecology, Helmholtz-Zentrum Dresden-Rossendorf, Bautzner
Landstraße 400, 01328 Dresden, Germany.

³WISMUT GmbH, Jagdschänkenstraße 29, 09117 Chemnitz, Germany.

This chapter has been published in *Environmental Science and Pollution
Research*: Newman-Portela, A.M., et al. (2024). *Environ Sci Pollut Res Int.*
31(5):7227-7245. <https://doi.org/10.1007/s11356-023-31530-4>

IF: 5.8 / Q1

KEYWORDS: Mine water; uranium; bacterial communities; fungal communities; bioremediation; electron donors; glycerol; bioreduction

ABSTRACT

Characterizing uranium (U) mine water is necessary to understand and design an effective bioremediation strategy. In this study, water samples from two former U-mines in East Germany were analysed. The U and sulphate (SO_4^{2-}) concentrations of Schlema-Alberoda mine water (U: 1 mg/l; SO_4^{2-} : 335 mg/l) were 2 and 3 order of magnitude higher than those of the Pöhla sample (U: 0.01 mg/l; SO_4^{2-} : 0.5 mg/l). U and SO_4^{2-} seemed to influence the microbial diversity of the two water samples. Microbial diversity analysis identified U(VI)-reducing bacteria (e.g., *Desulfurivibrio*) and wood-degrading fungi (e.g., *Cadophora*) providing as electron donors for the growth of U-reducers. U-bioreduction experiments were performed to screen electron donors (glycerol, vanillic acid, and gluconic acid) for Schlema-Alberoda U-mine water bioremediation purpose. Thermodynamic speciation calculations show that under experimental conditions, U(VI) is not coordinated to the amended electron donors. Glycerol was the best-studied electron donor as it effectively removed 99% of soluble U, 95% of Fe, and 58% of SO_4^{2-} from the mine water, probably by biostimulation of indigenous microbes. Vanillic acid removed 90% of U, and no U removal occurred using gluconic acid.

1. Introduction

Uranium (U) mining and processing have their origins in the second half of the 20th century in East Germany, mainly in the Federal States of Saxony and Thuringia (Bernhard et al. 1998; Albrecht 2017). Intense mining activities are a major source of soluble U, which can migrate into surrounding aquifers, representing a significant environmental and human health threat (Jroundi et al. 2020; Lopez-Fernandez et al. 2021). It is well known that U toxicity depends upon its chemical speciation, which is in turn controlled by abiotic and biotic processes. Therefore, understanding the U speciation in mine water from mines is essential to predict possible U migration in the environment and to design efficient remediation technologies (Newsome et al. 2014).

Conventional remediation strategies have focused on physical and chemical processes such as controlled flooding of mine galleries, permeable reactive multi-barriers, chemical precipitation and solvent extraction, amongst others. However, these approaches are time consuming, economically infeasible, and not very effective for very low U concentrations (Sánchez-Castro et al. 2021; Banala et al. 2021). These remediation technologies should meet the set water quality regulatory standard for beneficial reuse of the U mine water for different purposes (e.g., irrigation, especially in water-stressed regions in the world) within the concept of circular economy (Annandale et al. 2017). Bioremediation of U based on the interaction of biological agents (e.g., plants, algae, fungi, and bacteria) with this radionuclide could be considered as an innovative and promising alternative (Kalin et al. 2005; Gadd and Fomina 2011; Chen et al. 2021; You et al. 2021). Micro-organisms can interact with U through mechanisms such as biomineralization, enzymatic reduction, biosorption and intracellular accumulation, altering its speciation and playing an important role in the solubility and mobility of this radionuclide in aquatic environments (Merroun and Selenska-Pobell 2008; Gallois et al. 2018; Lopez-Fernandez et al. 2021; You et al. 2021). U bioremediation strategies are mainly based on U phosphate biomineralization under aerobic conditions (Jroundi et al. 2007; Krawczyk-Bärsch et al. 2015; Sánchez-Castro et al. 2020; Martínez-

Rodríguez et al. 2023), and bioreduction under anaerobic conditions (Lovley et al. 1991; Phillips et al. 1995; Newsome et al. 2014).

Biological enzymatic reduction of U(VI) to U(IV) has been the objective of several research studies over recent decades in U-contaminated groundwater masses (Lovley et al. 1991; You et al. 2021). In terrestrial environments, U usually occurs in either the hexavalent or tetravalent oxidation state. Hexavalent U (U(VI)) is soluble, mobile and therefore bioavailable in oxic conditions. However, tetravalent U (U(IV)) is insoluble and immobile, substantially decreasing its bioavailability along with its potential toxicity (Krawczyk-Bärsch et al. 2018; Lopez-Fernandez et al. 2021). The immobilization of highly soluble U(VI) (e.g., UO_2^{2+}) to the insoluble U(IV) mineral, such as uraninite (UO_2), occurs through bacterial reduction under anoxic conditions.

This transition could occur as a direct process, where U(VI) acts as a final electron acceptor, or as an indirect process, coupled to the microbial reduction of Fe(III) (Liu et al. 2007; You et al. 2021). In a natural environment, this reduction process is not carried out by a single microorganism, but rather a microbial consortium including U reducing bacteria, generating optimal conditions for biological reduction to take place. For instance, fungi are widely distributed in former mines, which have been treated by controlled flooding (Arnold et al. 2011; Kassahun et al. 2018) and are considered as a source of electron donors needed for the U bioreduction. Heterotrophic microbes (e.g., fungi) in a mine gallery degrade wood and consume oxygen, producing organic compounds such as saccharic acids, glycerol, and vanillin. These compounds can serve as electron donors for U reducing bacteria (Baraniak et al. 2002; Haq et al. 2022). Fungi have also been identified in such contaminated environments and contribute to many biogeochemical transformations (Gadd and Fomina 2011; Passarini et al. 2022). It is well documented that fungi can interact with U, mainly by biomineralization and biosorption processes (Schaefer et al. 2021). In addition, fungi are good metal chelators forming metal-organic complexes through the secretion of low-molecular-weight carboxylic acids (oxalic, succinic, malic and formic acids) (Gadd and Fomina 2011).

Different studies on *in situ* U bioreduction have been conducted at different mining sites to optimize the process and to study large-scale microbial reduction of U (Anderson et al. 2003; Istok et al. 2004). However, very few studies have reported the remediation of U contaminated sites at very low U concentrations (0.01–1 mg/l). Here, we describe the U-reduction potential of naturally occurring microbes in mine water from two former German U mines (Schlema-Alberoda and Pöhla, Wismut GmbH) for bioremediation in the concentration range between 1 mg/l and 0.01 mg/l. These low U concentrations resulted from controlled flooding-based remediation strategies applied to the mine water from these two U mines during Wismut remediation activities (Hiller and Schuppan 2008; Schuppan and Hiller 2012). According to the World Health Organization (WHO), the maximum admissible concentration of U in drinking water is limited to 0.03 mg/l (Frisbie et al. 2013; Ansoberlo et al. 2015; WHO 2022). This concentration may vary amongst European Union member states (Garboś and Świącicka 2015) and 0.5 mg/l when discharged into the aqueous environment (Wismut GmbH Umweltbericht 2021).

The main objective of the present study was to characterize the geochemistry, structure and composition of the microbial community of mine water from the two former U mines in order to assess the U-bioremediation potential of the native microbial community. Exploring the links between the geochemistry and microbial diversity of U mine water will provide insights into how microbial communities survive and thrive in such extreme contaminated environments and help designing efficient bioremediation strategies. The second objective was to screen for optimal electron donors (glycerol, gluconic acid, and vanillic acid) to be used as biostimulators for the growth of U-reducing bacteria in the studied mine water. Gluconic acid and vanillic acid were identified in the studied mine water as wood-decay products (Baraniak et al. 2002). For comparison purpose, glycerol was used as reference electron donor previously described for its suitability for U removal by U reducing bacteria (Madden et al. 2007; Newsome et al. 2015; Coral et al. 2022).

2. Materials and methods

2.1. Site description

Uranium was discovered in the Ore Mountains, a mountain range on the border between Saxony (Germany) and Bohemia (Czech Republic). The Schlema-Alberoda mine was one of the most important Wismut mining sites. From 1946 to the beginning of 1991, about 80000 t of U were extracted, left behind a sub-surface mine area at a depth of 1800 m and a volume of 35 million m³ (Meyer et al. 2008; Hiller and Schuppan 2008; WISMUT GmbH Brochure 2015). Another important Wismut mining activity site located in this area was the Pöhla mine with a depth of 600 m below the surface and a volume of 1.5 million m³. This uranium deposit was only partially mined and produced around 1200 t of U from 1967 to 1990 (Schuppan and Hiller 2012).

After the cessation of active mining, flooding by inflowing infiltration water has been carried out and controlled in the Wismut mine of Schlema-Alberoda and Pöhla since 1991.

2.2 Mine water sampling description

Fresh mine water samples were collected from two flooded subsurface mine shafts: 1) Schlema-Alberoda (50°37'32.5"N, 12°40'52.4"E) and 2) Pöhla (50°29'34.8"N, 12°49'07.1"E) in August and September 2020, respectively, by using the water, which is pumped to the surface. Since the major part of the flooding of the mines were completed in 1995 (Pöhla) and 2008 (Schlema-Alberoda), strong changes in the flow velocity of the subsurface water bodies are no longer expected. A total of 13 L of mine water were sampled per mine in sterile autoclaved screw-capped bottles at an authorised and secure point at each mine. Sampling at Schlema-Alberoda was conducted through an external pipe where water was pumped from inside the mine to the outside. At Pöhla, sampling was carried out inside the mine, through a pipe connected to the mine. In both mines, samples were taken after properly purging the pipe, discarding several water volumes in order to eliminate the residual water to obtain representative samples. The samples were transported to the laboratory at 4 °C and stored in a refrigerator at the same temperature on arrival until further processing.

2.3 Mine water chemistry characterization

Different physicochemical parameters of water from the two mines were determined to link the microbial diversity and the geochemistry of the studied water samples. Mine water temperature was measured *in situ* using a conventional thermometer. pH and redox potential (E_H) were determined *in situ* using a pH meter 3110 (WTW, Germany) with a BlueLine 16 pH microelectrode (Schott Instruments, Germany) and a micro redox electrode with platinum ring (ORP electrode, Mettler-Toledo InLab, Spain).

For the determination of the geochemical parameters, aliquots of each mine water were centrifuged at 4,020 x g for 15 minutes (Hettich EBA 21, Germany) prior to the analysis. A volume of 50 mL was acidified with nitric acid (HNO_3) and used to measure the total concentration of cations (Na, K, Mg, Ca, Al, Si, P, Mn, Fe, As, Ba, Th, U) by Inductively Coupled Plasma Mass Spectrometry (ICP-MS, ELAN 9000, PerkinElmer, Germany). Furthermore, an aliquot of 15 mL was taken to measure the total concentration of anions (NO_2^- , NO_3^- , PO_4^{3-} , SO_4^{2-} , Cl^-) by High Performance Ionic Chromatography (HPIC, Dionex Integriion, Thermo Fisher Scientific, USA). Total inorganic/organic carbon (TIC/TOC), dissolved organic carbon (DOC), and nitrogen were also quantified (Multi N/C 2100S, Analytik Jena, Germany).

2.4 Thermodynamic calculation of the U speciation of the mine water

The analytical data, which were obtained from the untreated Schlema-Alberoda and Pöhla mine water, were used to calculate the predominant fields of the possible U species present in the environmental conditions. The Pourbaix diagrams were calculated using the geochemical speciation code Geochemist's Workbench, version 17.0.1/Act2. The thermodynamic database used was the ThermoChimie database Version 10.a (Giffaut et al. 2014; Grivé et al. 2015).

In addition, abiotic controls consisted of sterile (autoclaved) mine water samples from Schlema-Alberoda amended with 10 mM glycerol, vanillic, and gluconic acid to investigate whether these electron donors affect the mine water chemistry. After 128 days, the analytical data of the microcosms

were used for thermodynamic speciation calculation using the analogue database, data from the literature (Vulpius et al. 2006 for vanillic acid; Zhang et al. 2008 and Sawyer et al. 1964 for gluconic acid), and the geochemical speciation code in the Geochemist's Workbench (version 17.0.1/Act2).

2.5 Cryo-time-resolved laser fluorescence spectroscopy (cryo-TRLFS) studies of mine water

Aliquots of 2 mL in plastic single-use cuvettes (Rotilabo, Carl Roth, Germany) were immediately shock frozen with liquid nitrogen and stored at $-20\text{ }^{\circ}\text{C}$. These aliquots were used to determine soluble U(VI) species in the water from both U mines by cryo-TRLFS. Cryo-TRLFS is a non-destructive technique and it does not change the chemical composition of the mine water. All the measurements were carried out under cryogenic conditions. The luminescence of soluble U(IV) in cryogenic conditions was measured with a laser energy of $300\text{ }\mu\text{J}$, frequency quadruplication at 266 nm, pulse width of 5 – 8 ns, and a frequency of 10 Hz using a Nd:YAG pulsed laser system (Continuum Inlite series, Continuum, USA). The luminescence spectra were detected using an iHR550 spectrograph and an intensified CCD-camera system (HORIBA Jobin Yvon, Edison, USA) in a wavelength range from 350 to 650 nm. The intrinsic luminescence properties of U(VI) are of great advantage for label-free U(VI) speciation studies. The disadvantage is quenching, caused by ligands (e.g., Cl^- or CO_3^{2-}). In order to reduce this quenching, the measurements were performed at a low temperature (-120°C) (Steudtner et al. 2011). Data were evaluated using the software OriginPro v9.7 2020 (OriginLab Corporation, USA). Collected spectra were analysed by parallel factor analysis (PARAFAC) (Andersson and Bro 2000; Drobot et al. 2015).

2.6 Molecular analysis of the microbial communities

2.6.1 DNA extraction and rRNA gene sequencing

From each mine, a total of 13 L were collected in several sterile glass bottles and transported to the laboratory for all the analyses. For DNA analysis, 800 mL of mine water were filtered through sterile $0.45\text{ }\mu\text{m}$ and $0.20\text{ }\mu\text{m}$ pore size membrane (Membrane Filter, MF-Millipore[®],

Germany) filters. The filters were immediately frozen at $-20\text{ }^{\circ}\text{C}$. Three biological replicates per mine water sample were analysed. Each filter was cut into four pieces and each piece was aseptically placed in a 5 mL sterile screw-cap tube from the DNA extraction kit (DNeasy Power Water Kit, QIAGEN, Germany). DNA extraction was carried out according to the manufacturer's protocol, with the temperature increase modification recommended by the manufacturer for obtaining fungal DNA. The DNA extraction was checked by agarose gel electrophoresis (0.75% w/v) and DNA concentration was determined using Qubit Fluorometer 4.0 (Thermo Fisher Scientific, USA) according to the manufacturer's protocol. The samples were stored at $-20\text{ }^{\circ}\text{C}$ until DNA amplification. After quality control, three out of the four DNA extractions from each filter were designated for further analysis. The DNA extracted from the filter pieces was pooled into a single 1.5 mL low-retention tube and considered as one biological replicate. The bacterial 16S rRNA gene was amplified using the forward primer 341F (5'-CCTACGGGNGGCWGCAG-3') and the reverse primer 785R (5'-GACTACHVGGGTATCTAATCC-3'), targeting the hypervariable V3-V4 regions (Thijs et al. 2017). Fungal ITS gene amplification was performed using the forward primer ITS1F (5'-CTTGGTCATTTAGAGGAAGTAA-3') and the reverse primer ITS2R (5'- GCTGCGTTCTTCATCGATGC -3') (Op De Beeck et al. 2014).

PCR amplification, assembly, and sequencing of the libraries (Illumina Mi-Seq) were carried out in the STAB-VIDA laboratories (STAB-VIDA, Caparica, Portugal, <https://www.stabvida.com/es>).

2.6.2 Molecular data analysis

FastQC was used for quality control of the raw sequence data (Andrews 2010). 16S and ITS rRNA raw sequences obtained by Illumina MiSeq were analysed by QIIME2 v2020.8 (Quantitative Insights into Microbial Ecology) (Caporaso et al. 2010; Bolyen et al. 2019). DADA2 (Divisive Amplicon Denoising Algorithm 2) plugin was used to denoise the reads (trimming and truncating low quality regions; dereplicating the reads and filtering chimeras) (Callahan et al. 2016). Then, the reads were organized

into Amplicon Sequence Variants (ASVs). Taxonomy was assigned based on a scikit-learn classifier pre-trained on SILVA (release 138 QIIME) for bacterial sequences (Quast et al. 2013) and UNITE (release 8.2) for fungal sequences (Nilsson et al. 2019) with a clustering threshold of 97% similarity. ASVs containing at least 10 sequence reads were considered as the dominant ASVs.

2.6.3 Statistical analysis

Alpha and beta diversity analyses were performed on MicrobiomeAnalyst (v4.1.3) (<https://www.microbiomeanalyst.ca/> (accessed on 01 February 2022) (Dhariwal et al. 2017). To remove low quality and/or uninformative features that could be associated with sequencing errors or low-level contamination, a low count filter and a low variance filter were implemented on the data. ASVs with four read counts and representing 20% of the total counts were kept. The variance of read counts was assessed using the interquartile range, and any ASVs with a percentage of counts below the cut-off (>10%) were excluded. In addition, the data were rarefied to the minimum library size. The microbiome was explored at the genus and phylum level but only the results at genus level are shown in this publication. Statistical results at phylum level can be found in the supplementary material. Chao1 and Shannon indexes were used to study alpha diversity. The statistical significance of the indexes was tested using the Kruskal-Wallis test. Beta diversity was also explored in a non-metric multidimensional scaling (NMDS) matrix and Permutational analysis of variance (PERMANOVA) by Bray-Curtis dissimilarities. PAST4 (v4.04) was used to perform principal component analysis (PCA) of the Hellinger-transformed data using the relative abundances of the taxonomic composition at phylum and genus level of the two samples (three biological replicates per sample), excluding taxa with a relative abundance below 1% (Harper 1999).

2.6.4 Data availability statement

Raw sequences used in this study are available in the Sequence Reads Archive (SRA) in the NCBI database under accession number PRJNA973613.

2.7. Microbial uranium reduction: screening for suitable electron donors

To assess the potential of the indigenous microbial communities in Schlema-Alberoda mine water to remove soluble U(VI), biostimulation microcosm experiments of U reduction were set up. Glass serum bottles (1 L) were used for microcosms, filled with fresh Schlema-Alberoda mine water. Three different organic compounds were used singly as electron donors at 10 mM: glycerol (ROTIPURAN, Germany), vanillic acid or 4-Hydroxy-3-methoxybenzoic acid (ACROS ORGANICS, USA), and gluconic acid sodium salt (ACROS ORGANICS, USA). These last two electron donors are particularly considered as typical wood-decaying products (Baraniak et al. 2002). The walls inside the mine are lined with wood, so the wood degradation products could be used as potential natural electron donors for microbial U reduction after controlled flooding of the mine. Glass serum bottles were degassed with nitrogen under sterile conditions and incubated (unshaken) at 28 (± 1) °C in the dark. To assess the key role of U reducing micro-organisms in this enzymatic process, controls were also considered. Untreated mine water was used as a control sample, as well as sterilised (autoclaved) mine water amended with electron donors. For the sampling, aliquots were taken carefully and slowly with a needle of a suitable length from the middle of the bottles to avoid touching the bottom and without disturbing the supernatant. This was done at the beginning and at the end of the experiment to measure changes in the total concentration of anions and cations. The aliquot was centrifuged at 4,020 x g for 15 minutes with a centrifuge (Hettich EBA 21, Germany), which was inside the anaerobic chamber.

In addition, U, As, and SO_4^{2-} concentrations were monitored over a period of 128 days, all by ICP-MS and HPIC. Furthermore, variations in E_H and pH parameters were monitored by the same methodology as mentioned in 2.3.

3. Results

3.1 Geochemical characteristics of mine waters

The mine waters of Schlema-Alberoda and Pöhla were pH-circumneutral (6.6 and 7.3). The relatively low E_H (+139 mV and -91 mV, respectively) indicate that reducing conditions existed in both samples. A high electrical conductivity (EC) was determined in the Schlema-Alberoda mine water (1.52 mS/cm) compared with the Pöhla sample (0.56 mS/cm), which is probably due to the higher concentration of dissolved ions, such as Na (99.5 mg/l and 31.4 mg/l), Mg (71.2 mg/l and 15.1 mg/l), and Ca (115 mg/l and 49.1 mg/l) (Table 1). Since the beginning of the monitoring of the Pöhla mine water by the Wismut GmbH, the U concentration decreased from 4.9 mg/l (Schuppan and Hiller 2012) to values around 0.01 mg/l. In contrast, the water from the Schlema-Alberoda mine still showed 1 mg/l U at the time of sampling. The As concentration has increased in both mines since the beginning of the flooding until our sampling from 0.1 mg/l (Schuppan and Hiller 2012) to approximately 1 mg/l. The determination of the anions showed relatively high SO_4^{2-} values in the water of Schlema-Alberoda mine in contrast to the Pöhla water. The concentrations of NO_2^- , NO_3^- , and PO_4^{3-} were low in both samples. The mine water from Pöhla showed a low Cl^- concentration (3.36 mg/l). Conversely, the value determined in the water from Schlema-Alberoda was 15 times higher at 56.1 mg/l. The determination of dissolved organic carbon (DOC) and total organic carbon (TOC) showed similarly low values for the water from both mines. The values for total inorganic carbon (TIC) (96.6 mg/l and 53.2 mg/l), on the other hand, were high in both the samples. In particular, TIC content in the mine water from the Schlema-Alberoda mine was two times higher than that from the Pöhla mine. The value for total nitrogen (TN) was below the detection limit in both mines.

Table 1. Chemistry of the Schlema-Alberoda and Pöhla mine water.

	Schlema-Alberoda	Pöhla
Sampling date	11.08.2020	23.09.2020
pH	7.3 ±0.1	6.6 ±0.1
E _H [mV]	139 ±20	- 91 ±20
EC [mS/cm]	1.52	0.56
Temp. [°C]	24 ±1	18 ±1
Cations [mg/L]		
Na	99.5 ±1.44	31.4 ±0.26
Mg	71.2 ±1.91	15.1 ±0.6
Al	< 0.01	< 0.01
Si	7.76 ±0.14	10.4 ±0.97
K	10 ±0.17	5.46 ±0.08
Ca	115 ±6.43	49.1 ±1.68
Mn	1.44 ±0.004	0.17 ±0.002
Fe	0.99 ±0.038	0.01 ±0.0004
As	0.92 ±0.017	1.15 ±0.01
Ba	0.03 ±0.0004	1.79 ±0.015
Th	< 0.001	0.002 ±0.0002
U	1.05 ±0.05	0.01 ±0.0001
Anions [mg/L]		
Cl ⁻	56.1 ±1.57	3.36 ±0.1
NO ₂ ⁻	< 0.05	< 0.05
NO ₃ ⁻	< 0.05	0.075 ±0.003
PO ₄ ³⁻	0.399 ±0.01	0.1 ±0.01
SO ₄ ²⁻	335 ±2.68	0.5 ±0.015
[mg/L]		
TIC	96.6 ±3.53	53.2 ±0.29
TOC	9.5 ±0.03	4.8 ±0.15
DOC	9.2 ±0.04	4.9 ±0.11
TN	< 0.1	< 0.5

TIC: total inorganic carbon; TOC: total organic carbon; TN: total nitrogen; EH: redox potential; EC: conductivity, Standard deviation with n=3.

3.2 Thermodynamic calculation

For the thermodynamic calculation of the predominance fields of uranium species, the analytical data of the Schlema-Alberoda and Pöhla mine water were used. The constructed corresponding Pourbaix diagrams (Fig. 1) were similar. Both mine water show an aqueous calcium uranyl carbonate species in the area characterized by a higher pH and a higher E_H limit, moving from +130 mV at pH 6.2 to -250 mV at pH 11 for the Schlema-Alberoda mine water and to -270 mV at pH 11.6 for the Pöhla mine water. Due to the 100-fold lower U concentration in the Pöhla mine water, a precipitation of bequerellite was not predicted and the stability ranges of clarkeite and uranophane were smaller than Schlema-Alberoda mine water. The stability range of uraninite as a U(IV) mineral was, however, comparatively the same, since in both mine waters under reducing conditions the saturation limit of uraninite (Neck and Kim 2001) was exceeded, and mineral formation occurred. The plotting of the measured pH and E_H values into the calculated Pourbaix diagrams showed that $\text{Ca}_2\text{UO}_2(\text{CO}_3)_3(\text{aq})$ existed under the geochemical conditions in the Schlema-Alberoda mine water, whereas in the Pöhla mine water the formation of uraninite was predicted to occur due to the much lower E_H value.

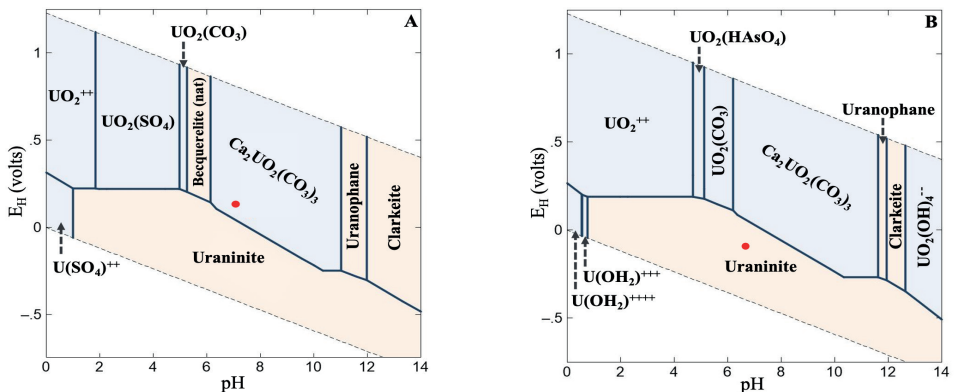


Fig. 1. Pourbaix diagrams for the Schlema-Alberoda (A) and Pöhla mine water (B) after thermodynamic calculation using the geochemical speciation code Geochemist's Workbench Version 17.0.1/Act2 and the analytical data. E_H and pH values of the mine waters were plotted into the diagrams (red points).

3.3 Determination of U species from cryo-TRLFS using PARAFAC analysis

Previous U(VI) speciation modelling calculations represent an estimation of the real environmental conditions. Therefore, cryo-TRLFS was used to confirm the obtained U speciation. In the Pöhla mine water, no U signal was identified due to the low U concentration of 0.01 mg/l. However, in the Schlema-Alberoda mine water, the corresponding U(VI) spectrum was clearly identified (Fig. 2). To get an accurate insight into U(VI) speciation, the data were analysed using PARAFAC, providing information on the total number of U(VI) species present after deconvolution. The results provided two different U(VI) species. The first PARAFAC extracted species showed fluorescence bands at 479.5 nm, 500.0 nm, 521.5 nm, 544.7 nm and 571.1 nm, matching with the fluorescence bands of the $\text{Ca}_2\text{UO}_2(\text{CO}_3)_3(\text{aq})$ species mentioned by Bernhard and co-authors (1998). The second species showed a slight shift of the emission bands to higher energies (lower wavelength). These bands at 478 nm, 498 nm, 519 nm, 542 nm, and 568 nm matched well with the uranyl carbonate complex $\text{UO}_2(\text{CO}_3)_3^{4-}$ (Wang 2004).

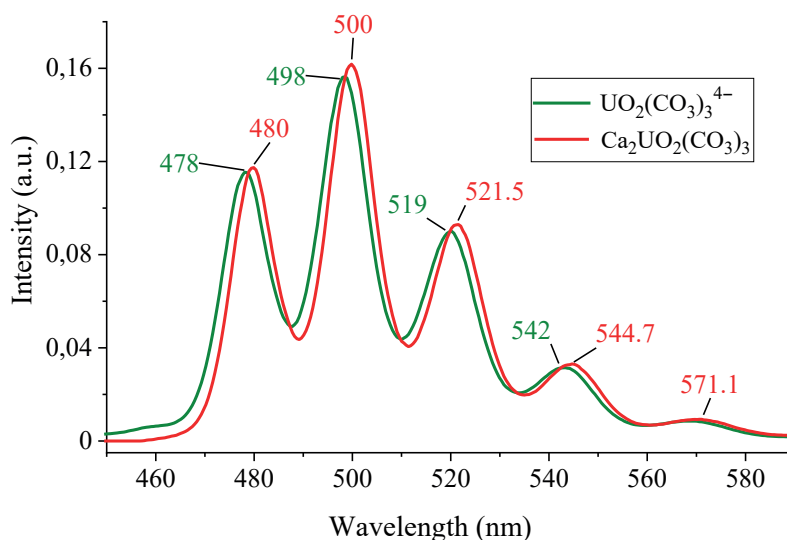


Fig. 2. Deconvoluted spectra of the extracted aqueous species $\text{Ca}_2\text{UO}_2(\text{CO}_3)_3$ and $\text{UO}_2(\text{CO}_3)_3^{4-}$ of the Schlema-Alberoda mine water with determined emission wave lengths in the peak maxima.

3.4 Microbial diversity analysis

3.4.1 Alpha and beta diversity

Species richness and diversity in the bacterial and fungal communities were examined (Table 1S) by analysing the average relative abundances of ASVs using the species richness estimate (Chao1) and Shannon (H') diversity indexes for each sample. Moreover, beta-diversity analysis was performed through PERMANOVA and NMDS analysis, based on the Bray-Curtis index (Fig. 2SA, B).

Chao1 revealed a high richness in the bacterial community at genus level in both mine water, with no significant differences ($p>0.1$) between them. In addition, a high bacterial diversity was observed by Shannon's index, ranging from 2.540 – 2.699 in Schlema-Alberoda mine and 3.064 – 3.123 in Pöhla mine (Table 1S). The Shannon's index showed a high fungal diversity in Pöhla mine water compared with Schlema-Alberoda mine water, the diversity values revealed a less diverse fungal community. However, the differences were still not significant ($p>0.1$). For all the indexes, as expected, the values between replicates were similar.

Beta diversity revealed non-significant differences ($p>0.1$) in bacterial (PERMANOVA, F: 114.17; R-squared: 0.96615; p: 0.1) and fungal (PERMANOVA, F: 21.232; R-squared: 0.84147; p: 0.1) community structure and abundance at genus level. Non-metric multidimensional scaling ordination (NMDS) based on Bray-Curtis dissimilarity matrices visualized the variation in bacterial (Stress: 0) and fungal (Stress: 9.211e-05) community composition between samples (Fig. 2SA, B). NMDS revealed no clear correlations between the compared microbial communities.

3.4.2 In situ bacterial community composition and structure

A total of 1,825,744 raw sequences reads from the bacterial 16S rRNA gene were obtained after sequencing. An average of 268,112 raw sequences corresponded to the Schlema-Alberoda mine water and an average of 340,469 to the Pöhla water. Platform QIIME2™ (v2020.8) was used to analyse the sequences. Finally, 2,611 ASVs were identified in total. Sequences were consistently affiliating to the following phyla for the water from both mines:

Campilobacterota (49.11%), Proteobacteria (19.38%), Patescibacteria (8.60%), Verrucomicrobiota (5.04%), Nitrospirota (4.12%), Chloroflexi (4.01%), Actinobacteriota (2.11%) and Desulfobacterota (2.03%) (Fig. 3). Planctomycetota, Acidobacteriota, Bacteroidota, Acetothermia and Firmicutes were also identified at a relative abundance of 1%.

A total of 377 different bacterial genera were identified. The Pöhla mine water was dominated by the genus *Sulfurovum* (24.94%), followed by *Sulfuricurvum* (19.57%), an uncultured genus of the class *Thermodesulfovibrionia* (6.65%), an unidentified genus of the family *Gallionellaceae* (4.56%), *Candidatus Omnitrophus* (3.39%), *Gallionella* (3.35%), *Sulfuritaela* (3.21%), *Thiovirga* (2.61%), *Candidatus Moranbacteria* (2.29%), an unidentified genus of the family *Rhodocyclaceae* (2.12%), GIF9 (1.80%), WCHB1-81 (1.56%), *Parcubacteria* (1.18%) and *Sideroxydans* (1.17%) (Fig. 3). Similarly, *Sulfuricurvum* (24.71%), an unidentified genus of the family *Gallionellaceae* (7.66%), *Candidatus Omnitrophus* (5.93%), *Gallionella* (1.74%), *Sulfurovum* (1.07%), amongst others with an occurrence of <1% were identified in the Schlema-Alberoda mine water (Fig. 3). However, the Schlema-Alberoda samples were strongly dominated by the genus *Sulfurimonas* (30.68%). Uncultured genus of the family *Hydrogenophilaceae* (5.82%) and *Desulfurivibrio* (2.66%), were identified in the Schlema-Alberoda samples with a much lower occurrence compared to the Pöhla samples.

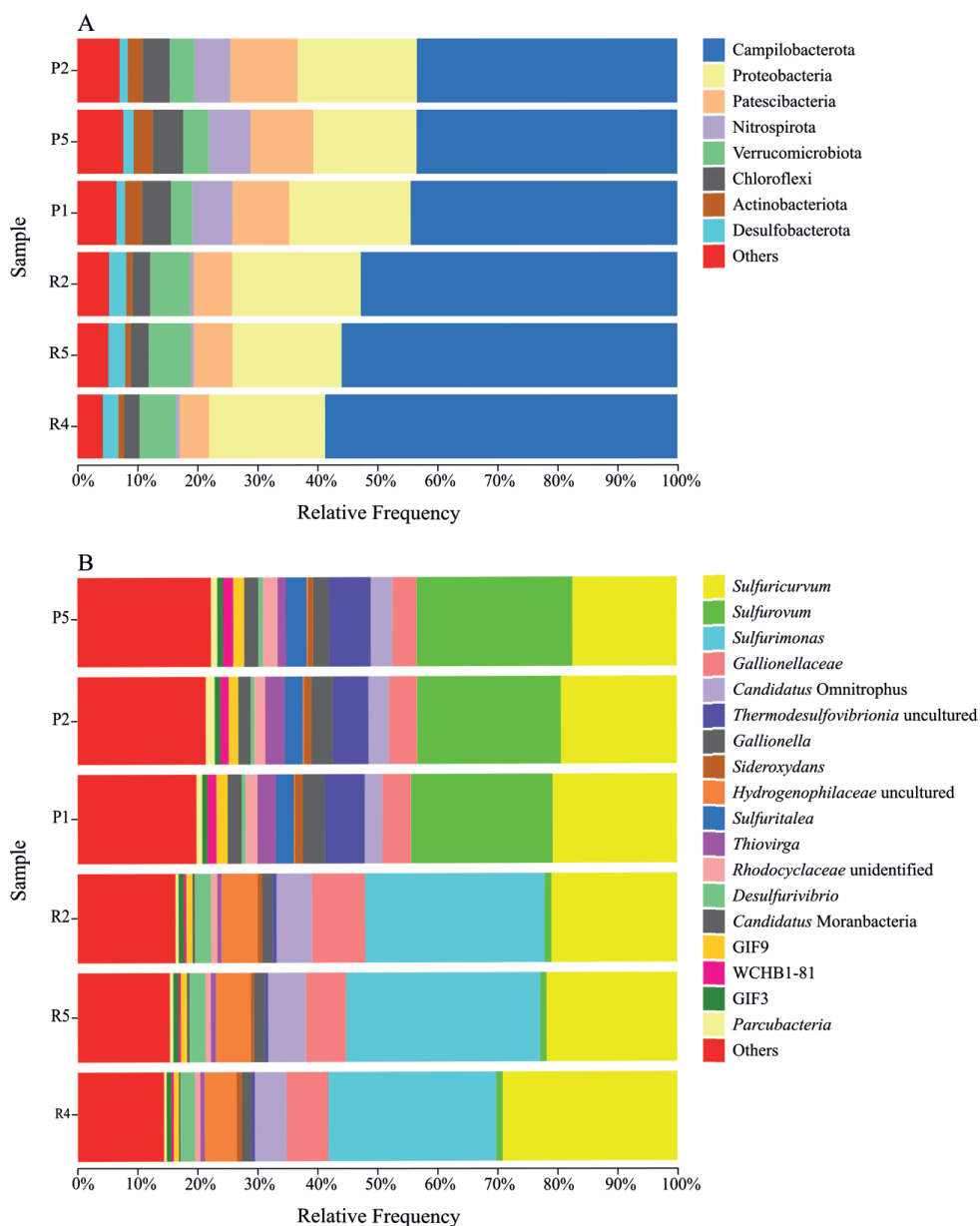


Fig. 3. Barplot of the taxonomic distribution of bacterial diversity in the water samples from the Pöhla (P5; P2; P1) and Schlema-Alberoda mines (R2; R5; R4) at phylum (A) and genus (B) level. Each sample comprises three replicates. Only the phyla and genera identified in the three samples with >1% relative abundance were included, while the remaining ones were included in “others”.

3.4.3 In situ fungal community composition and structure

The size of the fungal community was estimated by amplifying the ITS1 region of the rRNA gene, obtaining a total of 1,139,998 raw sequences reads. An average of 221,632 raw sequences corresponded to the Schlema-Alberoda mine water and an average of 158,366 to the Pöhla samples. A total of 373 ASVs were identified. At phylum level (Fig. 4), Ascomycota was strongly represented in the water from both mines with an average percentage of 79.75% in the Pöhla samples and 96.05% in the Schlema-Alberoda samples. In addition, Basidiomycota constituted 18.87% and 3.82%, respectively. The phylum Rozellomycota was mainly identified in the Pöhla water with an average occurrence of 1.30%.

In addition, a total of 119 different genera were identified in the mine water. The fungal community in the Pöhla mine water (Fig. 4) was characterized by *Acremonium* (29.66%), followed by an unidentified genus of the family *Fomitopsidaceae* (15.86%), *Lecanicillium* (14.42%), an unidentified genus of the order *Neodevriesia* (8.54%), *Helotiales* (7.94%), an unidentified genus of the class *Sordariomycetes* (6.91%), *Cyphellophora* (6.08%), an unidentified fungi genus (4.73%), *Aspergillus* (3.11%) and an unassigned fungi genus (2.49%). In contrast, the fungal community in Schlema-Alberoda (Fig. 4) was quite different compared to the Pöhla samples. The Schlema-Alberoda mine water was strongly dominated by the genus *Cadophora* (85.32%), followed by *Paraphoma* (8.80%), *Exophiala* (2.35%), *Cystobasidium* (1.37%) and *Penicillium* (1.30%).

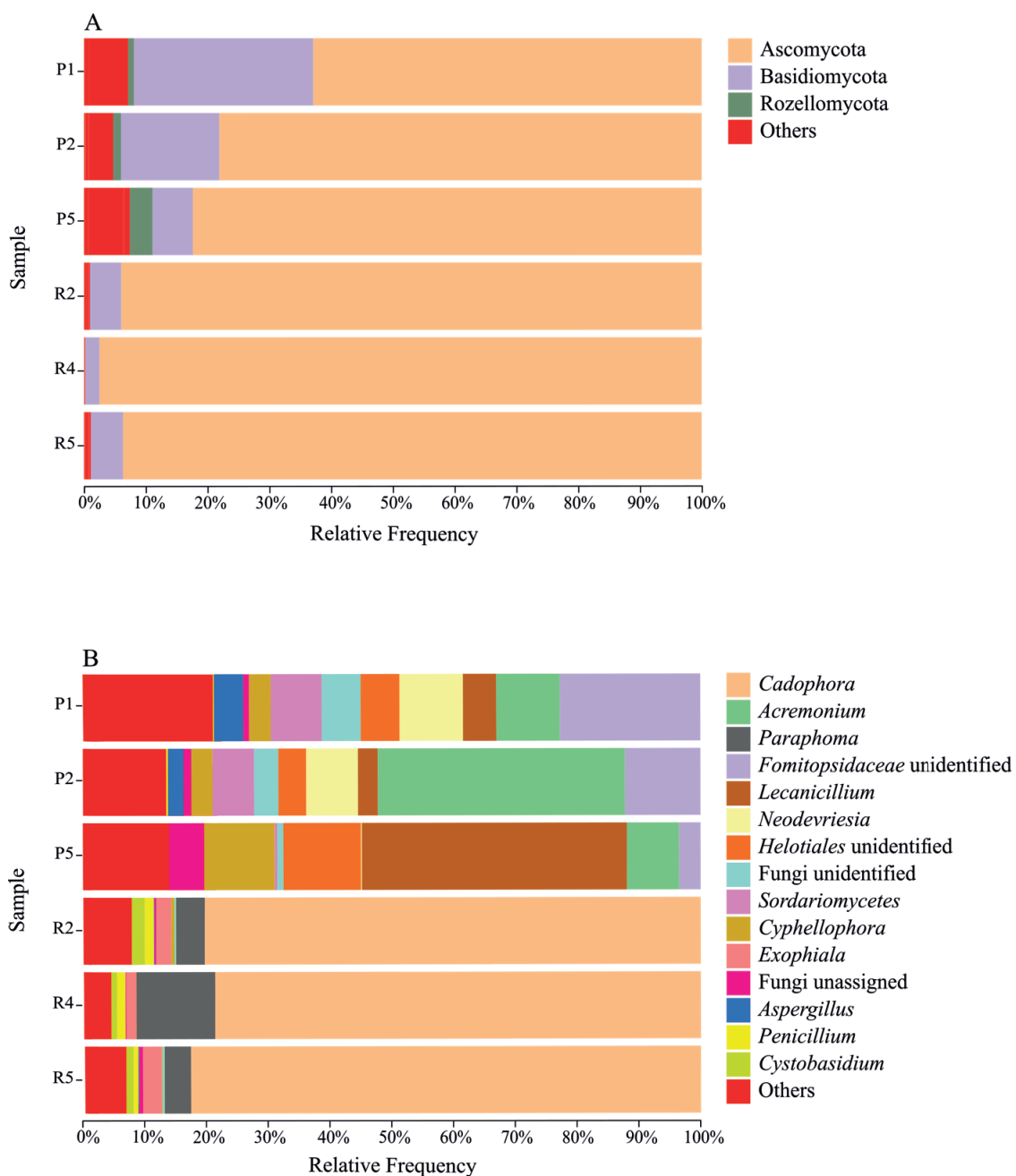


Fig. 4. Taxonomic distribution of fungal diversity in the mine water from Pöhla (P1; P2; P5) and Schlema-Alberoda (R2; R4; R5) at phylum (A) and genus (B) level. Each sample comprises three replicates. Only phyla and genera identified in the three samples with >1% relative abundance were included, while the remaining genera were included in “others”.

3.4.4 Linking the microbial communities to the geochemical mine water parameters

PCA of the abundance matrices at the phylum and genus level (Fig. 3S and 4S, respectively) clearly showed a division between the major bacterial and fungal phyla in both mine waters. PCA at genus level showed the main influence of *Sulfurimonas* in Schlema-Alberoda and *Sulfurovum* in Pöhla. Interestingly, *Sulfuricurvum* influenced both mine waters. An unidentified genus of the family *Gallionellaceae* also showed a more pronounced effect on Schlema-Alberoda mine water. In addition, an uncultivable genus of the family *Thermodesulfovibrionia* had an influence on Pöhla mine water. In the PCA analysis, we did not observe major influences of specific fungal taxa on Schlema-Alberoda mine water, except for *Cadophora*, which had a slight impact. Conversely, in the Pöhla mine water, it was characterized primarily by the presence of *Acremonium*, followed by the influence of an unidentified genus of the family *Fomitopsidaceae*. In addition, we observed that bacterial and fungal groups plot together with the mines.

3.5 Biostimulation of U-reducing bacteria: effect of electron donors

In this study it was observed that the water from both mines exhibited different U(VI) concentrations. The water from the Pöhla mine had a U(VI) concentration of 0.01 mg/l, that fits very closely to the allowed limit for drinking water in Germany (WHO 2022; Garboś and Świącicka 2015). However, the water from the Schlema-Alberoda mine presented higher U(VI) concentrations of about 1 mg/l, which should be decreased to the permitted levels. As a complement to the existing chemical treatment for the multiple mine water pollutants, the biostimulation of U(VI) reducing bacteria activity could lead to the removal of soluble U(VI) as U(IV) mineral phases within the mine. Therefore, preliminary U mine water bioreduction microcosms were designed and implemented using Schlema-Alberoda mine water (Table 1) amended with different electron donors (glycerol, vanillic acid and gluconic acid) in triplicates. The chemistry of the U mine water was determined at the beginning and at end of the experiment. In addition, a monitoring of the U(VI), As and SO_4^{2-} concentrations, the E_H and pH values were carried out during the experiments (Table 2).

Small changes in pH were observed, from circumneutral (pH 7.32) in the original mine water to slightly alkaline (pH 8) in the glycerol and gluconic acid amended microcosms. No difference in the pH of the sample amended with vanillic acid was noticed and it remained circumneutral. An increase in the pH of the control samples was also observed. Differences in E_H values compared to the initial conditions was detected in all the microcosms. At the end of the experiment, whilst the E_H of mine water microcosms amended with glycerol and gluconic acid reached very low values (-246 ± 20 mV and -248 ± 20 mV, respectively), the vanillic acid supplemented microcosm showed a higher E_H ($+218 \pm 20$ mV) than the original mine water. However, the E_H of the controls increased considerably to $+397 \pm 20$ mV.

Table 2. Analysis of the most important cations and anions as well as the physico-chemical parameters of the original Schlema-Alberoda mine water during sampling and at the end of the microcosm experiment after the amendment of various electron donors.

	SA	SAC	SA+G	ASA+G	SA+V	ASA+V	SA+K	ASA+K
pH	7.32	7.98	7.99	8.72	7.00	8.63	8.01	9.11
E_H [mV]	139	397	-246	333	218	330	-248	321
Cations								
[mg/L]								
Fe	0.99	0.60	0.05	0.11	0.32	1.19	0.35	2.47
As	0.92	0.97	0.46	0.65	0.40	1.13	0.17	0.58
U	1.1	1.15	0.01	0.70	0.10	1.25	1.37	0.62
Anions								
[mg/L]								
SO_4^{2-}	335	325	141	336	338	349	144	348

SA: Schlema-Alberoda mine water during sampling; SAC: Schlema mine water after 128 days; SA+G: Schlema mine water + 10 mM glycerol; ASA+G: autoclaved Schlema mine water + 10 mM glycerol; SA+V: Schlema mine water + 10 mM vanillic acid; ASA+V: autoclaved Schlema mine water + 10 mM vanillic acid; SA+K: Schlema mine water + 10 mM gluconic acid; ASA+K: autoclaved Schlema mine water + 10 mM gluconic acid; EH: Redox potential.

Figure 5 shows changes in the concentrations of U(VI), As and SO_4^{2-} in the U mine water amended with the studied electron donors for 128 days. The concentration of dissolved U(VI) varies remarkably in the microcosms. The addition of glycerol to the microcosm led to a considerable decrease of the U(VI) concentration during the experiment. A reduction of 43% was

already determined after 24 days. After 92 days, U(VI) was only detectable in small amounts, indicating a U(VI) reduction of 99%. Since it was not possible to collect samples between day 27 and day 92, it is unknown when exactly the U(VI) concentration decreased to 1%. In the microcosm supplemented with vanillic acid, the aqueous U concentration reduction was faster at the beginning of the experiment. Already on day 8, there was a considerable decrease of 76%. At the end of the experiment a notable U(VI) concentration decrease of 91% was also determined. In the gluconic acid microcosm, however, no U(VI) concentration decrease was observed. The SO_4^{2-} concentration decreased markedly after 27 days in the experiments with glycerol and gluconic acid. At the end of the experiment, a decrease of 58% and 57%, respectively, was determined. In contrast, using vanillic acid, no changes were observed. Both total Fe and As showed a notable decrease in their concentrations in each microcosm.

The addition of glycerol to the mine water resulted in a decrease of about 95% of total Fe at the end of the experiment. In regards to As, the use of gluconic acid resulted in an 82% reduction of this oxyanion from the mine water, whereas when glycerol and vanillic acid were used, the removal rates of As were 50% and 43%, respectively. In brief, glycerol seems to show better results as an electron donor to stimulate the U-reducing bacterial community of the Schlema-Alberoda mine water than vanillic acid and gluconic acid.

The thermodynamic speciation calculation of abiotic controls of sterile (autoclaved) Schlema-Alberoda mine water amended with vanillic acid and gluconic acid showed that both electron donors do not affect the mine water chemistry under the given physicochemical conditions (Fig. 1S) since no complexation with U(VI) was predicted. U(VI) is neither coordinated to vanillic acid, nor to gluconic acid at the given pH of 8.63 and 9.11, respectively, at the end of the experiments. Strong calcium-uranyl-carbonate complexes such as $\text{Ca}_2\text{UO}_2(\text{CO}_3)_3$ and $\text{CaUO}_2(\text{CO}_3)_3^{2-}$ dominated the U speciation completely. Concerning glycerol, there were no thermodynamic data for complexation with U(VI). However, no formation of U(VI)-glycerol complexes were expected since glycerol has only three hydroxyl groups that do not deprotonate in aqueous solutions (Yu et al. 2021).

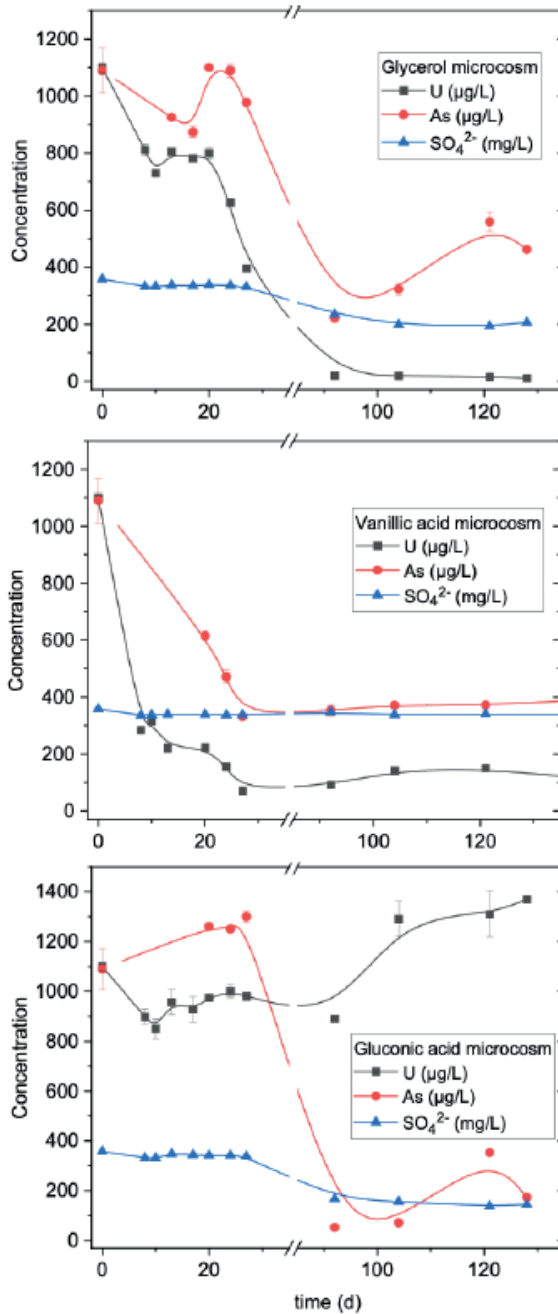


Fig. 5. Changes in the kinetic of U, As and SO₄²⁻ by biostimulation of the native community of micro-organisms after the addition of electron donors (glycerol, gluconic acid and vanillic acid).

4. Discussion

4.1 Geochemical characteristics of the mine water

Studies on dammed or collected water from technical processes, such as the flooded mine water, often show a diverse and relevant microbial community, which could have a deep impact on the overall biogeochemical cycles of the elements in mine water and on its quality. In general, flooded mine water quality is determined by the solubility of the minerals from the mine and by chemical changes due to oxidation of the exposed ore and host rock (Bernhard et al. 1996). In addition, the methodology used during mineral extraction may also influence mine-water quality (e.g., acidification of host rock for ore extraction) (Arnold et al. 2011). Water from both mines (Schlema-Alberoda and Pöhla) showed a circumneutral pH. The Schlema-Alberoda water is characterized by a much higher SO_4^{2-} concentration (335 mg/l) compared to that of the Pöhla sample (0.5 mg/l). The supply of SO_4^{2-} is not limited due to the presence of sulphide mineralization. Nevertheless, we believe that the SO_4^{2-} quantity is insufficient to induce acidification within the system. The presence of multiple carbonates creates an excess of neutralization, which hinders the acidification of the water via the sulphide supply from the existing sulphide ores, as it was previously described by Hiller and Schuppan (2008). Ongoing studies are currently underway to investigate the reasons behind the higher SO_4^{2-} concentration in Schlema-Alberoda compared to Pöhla mine water. The higher concentrations of Mg, Na, K and Ca observed in the Schlema-Alberoda samples may originate from the chemical or microbiological alteration of granite (containing feldspar and plagioclase minerals) or dolomite (calcium magnesium carbonate) as described by Naumov et al. (2017) in the Schlema-Alberoda mine. Differences in E_{H} values may be due to the architecture of the Pöhla mine, being probably more “hermetic” than the Schlema-Alberoda mine, where infiltration of rainwater and O_2 are possible. The considerably high As concentrations in both mines are probably caused by oxidation of the arsenic minerals in the ore veins, according to Paul et al. (2013).

The chemical behaviour of the uranyl ion in natural waters may be partly influenced by pH, E_{H} , and dissolved ions (Bernhard et al. 1998).

Thermodynamic calculations predicted a calcium uranyl carbonate complex $[\text{Ca}_2\text{UO}_2(\text{CO}_3)_3(\text{aq})]$ such as the dominant species in the Schlema-Alberoda mine water. By cryo-TRLFS measurements of the Schlema-Alberoda mine water combined with PARAFAC, two species were detected. We observed an analogy in the positions for $\text{Ca}_2\text{UO}_2(\text{CO}_3)_3(\text{aq})$ complexes. A slight shift of the fluorescence bands to the left for the second one matches with a uranyl carbonate complex $[\text{UO}_2(\text{CO}_3)_3^{4-}]$ (Wang et al. 2004). Furthermore, our results are consistent with those of Bernhard et al. (1996, 1998, 2001), where calcium uranyl carbonate complex was reported as the major species in the Schlema-Alberoda water. Because of extremely low U concentrations in the Pöhla samples (0.01 mg/l), no detectable U signal was obtained by cryo-TRLFS measurements. On the other hand, by thermodynamic calculation of the predominance fields of U species, U is expected to form U(IV)-species, with uraninite as the end member.

4.2 Impact of microbial populations on mine water biogeochemical processes

It is well known that the microbial community structure and function of U mine water are shaped by physicochemical factors such as pH, total organic carbon (TOC), dissolved oxygen (DO), concentrations of anions (e.g., NO_3^- , SO_4^{2-}), cations (e.g., Fe, Mn) and toxic heavy metals/metalloids (e.g., U, Pb, As). Schippers et al. (1995), Fields et al. (2005) and Shuaib et al. (2021) showed that heavy metal and radionuclide contamination reduce the microbial diversity of the environment. In this study, it was observed that the richness and diversity of the bacterial and fungal communities in the mine water from Schlema-Alberoda were lower compared to the mine water from Pöhla. These results align with those of prior cited studies, as the aqueous U(VI) concentration in Schlema-Alberoda is a hundred times higher than that in the Pöhla mine.

4.2.1 *In situ* bacterial community composition and structure

The bacterial community composition of water from both U mines displayed similarities at phylum level compared to that of other U-contaminated environments previously reported (Rastogi et al. 2010a, b; Zeng et al. in

2019; Lusa et al. 2019). However, the bacterial community of Schlemma-Alberoda and Pöhla mine water exhibited a higher relative abundance of the following phyla: Proteobacteria, Patescibacteria, Verrucomicrobiota and Nitrospirota. Interestingly, Campylobacterota was highly represented, with an average relative abundance of 49.11% in both mine waters (Fig. 3). The representative of these bacterial phyla has evolved mechanisms of resistance and tolerance to environmental toxicity of heavy metals and radionuclides. In addition, they play a major role in the biogeochemical cycles of elements such as S, N, and Fe, which subsequently affect U. Bacteria involved in N/S redox cycling (nitrate reducers and sulphur oxidizers) from the phyla Campilobacterota and Proteobacteria were identified in water from both U mines. Abundant distribution of nitrate reducers and sulphur oxidizers from the genera *Sulfuricurvum*, *Sulfurovum* and *Sulfurimonas* of the phylum Campilobacterota in water from both U mine has been observed. They were reported to be distributed in heavy metals and radionuclide impacted environments (Chang et al. 2005; Shen et al. 2013; Zeng et al. 2019; Povedano-Priego et al. 2022) and to play a key role in the maintenance of reduced U species stability through coupling nitrate reduction to S-compound oxidation, and subsequently promote the growth of metal-reducing micro-organisms (e.g., Proteobacteria as SRB) (Chang et al. 2005; Huang et al. 2021). Nitrate might negatively influence the microbial reduction of U(VI). Nitrate, ferric ion and sulphate serve as thermodynamically more favourable final electron acceptors than U, and subsequently they would be reduced earlier than this radionuclide (Finneran et al. 2002). Therefore, anaerobic micro-organisms usually prefer nitrate as the first electron acceptor, followed by ferric iron and sulphate (Jroundi et al. 2020). In our study, the concentration of nitrate and nitrite remained below 0.07 mg/l, suggesting an adequate correlation of the microbial activity of these nitrate/nitrite reducers with the biogeochemical cycle of nitrogen. As pointed out in the PCA analysis, *Sulfuricurvum*, *Sulfurovum* and *Sulfurimonas* strongly influence both mine waters, playing an important role (Fig. 4S).

Proteobacterial nitrate reducers and sulphur oxidizers including *Sulfuritalea*,

Thiovirga and an unidentified genus of the family *Hydrogenophilaceae* also constitute a considerable proportion in water from both U mines. They are well known for surviving in oligotrophic environments, and previously reported for their ability to reduce and tolerate metals (You et al. 2021; Bärenstrauch et al. 2022). *Sulfuritalea* can reduce nitrate to molecular nitrogen under anoxic conditions and oxidize thiosulphate, elemental sulphur and hydrogen (Kojima and Fukui, 2011). Furthermore, *Thiovirga* is a sulphur oxidizer (Ito et al. 2005). Peng et al. (2020) reported the role of the *Hydrogenophilaceae* family as beneficial and important in the sulphur cycle. *Hydrogenophilaceae* is able to oxidize sulphide compounds (e.g., S^{2-} , HS^- and H_2S) to SO_4^{2-} , which could be used by SRB (Peng et al. 2020). Its role in the reduction of nitrate to nitrite in microaerophilic members has also been reported (Orlygsson and Kristjansson 2014). Highly increased sulphate concentrations were observed in the Schlema-Alberoda mine water compared to the Pöhla mine water. The high sulphate concentration could be correlated with the role of sulphur oxidizing bacteria (SOB). The increased SO_4^{2-} concentration could support the proliferation of SRB. For example, the phylum Desulfobacterota which contains several anaerobic genera of SRB including the genus *Desulfurivibrio*. *Desulfurivibrio* was mainly identified in the Schlema-Alberoda mine water where the sulphate concentration was higher (Jroundi et al. 2020). This is consistent with the assumption that SRB proliferated in the presence of higher sulphate concentrations. Moreover, an unidentified genus of the *Thermodesulfovibrionia* family (Nitrospirota) which couples H_2 oxidation to sulphate reduction was also identified in the water samples (Rempfert et al. 2017; Nothaft et al. 2021; Umezawa et al. 2021). The reduced products of sulphate as hydrogen sulphides are able to chemically reduce U(VI) as the Fe-reducing bacteria (FeRB) do (North et al. 2004).

In addition to Fe oxidizing bacteria, U mine water also harbour an unidentified genus of the family *Rhodocyclaceae* which include FeRB with the ability to reduce U(VI) (Cummings et al. 1999; Porsch et al. 2009). Fe(III) reduction products have been reported to be able to chemically reduce U(VI) as well (Lovley et al. 1993; North et al. 2004; Wilkins et al.

2006). The abundant distribution of FeOB and FeRB in Schlemma-Alberoda is correlated with its high Fe concentration. Furthermore, members of the *Rhodocyclaceae* family were reported to be able to grow lithotrophically by respiring U(VI) together with H₂ oxidation and to be responsible for U(VI) bioreduction coupled with organic electron donors (Zhou et al. 2014).

Furthermore, alongside the phyla involved in the biogeochemical cycle of S, Fe, N and U, microbial diversity analysis has unveiled the presence of bacterial communities described for their adaptation to extreme environments including U contaminated sites. Amongst them, the phylum reported as Patescibacteria has an ultra-small cell size, highly simplified membrane structures and a greatly reduced metabolism highly adapted to U-contaminated environments by so far unknown mechanisms (Tian et al. 2020; Povedano-Priego et al. 2022). Nayak et al. 2021 identified sequences of unclassified *Candidatus* Moranbacteria (Parcubacteria), in radon- and heavy-metal contaminated water. *Candidatus* Omnitrophus (Verrucomicrobiota) is a chemolithoautotrophic bacterial genus that thrives in anoxic environments. This genus and its phylum have been previously reported by other authors in different contaminated environments (Underwood et al. 2022). The role they play is unknown, but they have generally been associated with environments contaminated by low concentrations of U, and could become a possible indicator for monitoring these contaminations as reported by Mumtaz et al. 2018. 16S rRNA gene analysis is valuable for detecting microorganisms in an environment and can be useful in designing efficient remediation technologies. However, for a better understanding of the microbial role in biogeochemical processes, future metagenomics and/or metatranscriptomics studies are suitable for this purpose.

4.2.2 *In situ* fungal community composition and structure

The fungal diversity of water from both U mines was dominated by Ascomycota (phylum with the highest number of fungal genera) and Basidiomycota. Rozellomycota was mainly identified in the Pöhla water mass but had a low relative abundance. These results are in agreement with those reported by Zirnstein et al. (2012) and Harpke et al. (2022)

where these phyla were described in environments contaminated by U. Furthermore, Ascomycota, Rozellomycota and Basidiomycota, have been reported in previous studies as phyla that could potentially play a key role in the decomposition and degradation of lignocellulosic biomass (Young et al. 2018; Liu et al. 2022). At the genus level, the water samples from the two U mines were characterized by the distribution of genera that have been previously reported in heavy metal and radionuclide contaminated habitats. These include *Cadophora*, *Lecanicillium*, *Exophiala*, and unidentified genera of different taxa (e.g., order *Helotiales* (Ascomycota) and *Cystobasidium* (Basidiomycota), class *Sordariomycetes* (Ascomycota) and family *Fomitopsidaceae* (Basidiomycota) (Dos Santos Utmazian et al. 2007; Dirginčiute-Volodkiene and Pečiulyte 2011; Jasrotia et al. 2014; Văcar et al. 2021; Passarini et al. 2022). *Fomitopsis annosa* (*Fomitopsidaceae*) was reported to accumulate U (Nakajima and Sakaguchi 1993). To the best of our knowledge, this is the first study to describe the identification of genera such as *Neodevriesia* and *Cyphellophora* (Ascomycota) in these types of extreme environments. They are able to produce melanin, a substance that protects the cell and participates in the immobilization of metals and radionuclides such as U (Fogarty and Tobin 1996; Turick et al. 2008; Oh et al. 2021). The most representative genera based on their role in the removal and biomineralization of U phosphates were *Penicillium* and *Aspergillus* (Ascomycota) (Schaefer et al. 2021; Zhang et al. 2022). However, despite its high adaptive potential, *Penicillium* was poorly reported in the Schlema-Alberoda samples and *Aspergillus* in the Pöhla samples.

4.3 Changes in mine water geochemistry by microbial biostimulation

The inner walls of Schlema-Alberoda mine are covered with spruce and pine boards to prevent the collapse of the floors. Although no data are available on the type of wood in Pöhla mine, an abundance of conifers left by mining activities can be assumed for both mines. During mining, wood degradation through microbial activity (mainly fungi) was observed. With beginning of the flooding process, the mine water comes into contact with the wood, causing the further degradation processes. The natural and fungal-mediated decomposition of the wood releases cellulose and lignin

as well as low molecular weight molecules (carbohydrates, saccharic acids, vanillin, vanillic acid and gluconic acid, amongst others) that may act as electron donors for U-reducing bacteria (Ander et al. 1980; Hedges et al. 1988; Baraniak et al. 2002; Mansour et al. 2020). Glycerol has previously been reported by other authors as an electron donor, in addition to lactate, acetate, methanol, and others (Madden et al. 2007; Newsome et al. 2015). These electron donors might stimulate the growth of SRB of the phylum Desulfobacterota (e.g., *Desulfurivibrio*), distributed in minor proportions in the Schlema-Alberoda mine, that may play an important role in U(VI) reduction (Chang et al. 2001; Geissler and Selenska-Pobell 2005; Moon et al. 2010). Biostimulation is a simple and effective bioremediation strategy that has previously been reported *in situ* and at laboratory scale by other authors (Yabusaki et al. 2007; Williams et al. 2013; Xu et al. 2017). In order to study the potential of the natural microbial community in the reduction of U(VI) in Schlema-Alberoda mine water, we amended a set of anoxic mine water microcosms with three different electron donors (glycerol, gluconic acid and vanillic acid).

In terms of redox potential, the glycerol and gluconic acid amended microcosms became reduced reaching strong negative E_H values (-246/-248 mV) at the end of the experiment. These values are broadly in line with the redox couple sulphate reduction and are supported by the removal rate of sulphates of about 58% for both microcosms. In the case of glycerol system, the U and Fe removal ratio was of about 90 and 95%, respectively, indicating the efficiency of this electron donor as stimulant of microbial reduction of these elements as it was described in different works (Newsome et al. 2015). Nonetheless, no U removal was detected in the gluconic system, which could be explained by the fact that this electron donor is not suitable for microbial U reduction. Nevertheless, in the case of vanillic acid amended microcosm the positive E_H value (218 mV) does not promote sulphate reduction as no decrease on the concentration of this anion was observed at the end of the experiment. However, a decrease of Fe, As and U concentrations was observed. The Fe reduction could be due to microbial activity as the Fe redox couple is on line with the E_H value of the

studied system. The Fe reduction leads to the formation biogenic Fe oxides, which would remove U and As by co-precipitation and/or adsorption. At the end of the experiment, remarkable changes were observed in the microcosm doped with glycerol where U(VI) concentration was reduced by ~99%. The concentration of total Fe (~95% reduction), SO_4^{2-} (~58% reduction) and E_{H} were affected as well, mainly by glycerol. It suggests that biostimulation with glycerol could promote the growth of SRB and FeRB which may be involved in U(VI) reduction. Madden et al. (2007) and Newsome et al. (2015) reported similar U reduction rates using glycerol phosphate and glycerol. Glycerol seems to be the most efficient electron donor for the stimulation of bacterial populations with potential in the U removal and the bioremediation in Schlema-Alberoda mine water.

5. Conclusions

To sum up, our study aimed to characterize the geochemistry and the native microbial community of the water from two former U mines. In addition, we carried out a screening test for electron donors to be used for the design of future U bioremediation strategy based on the biostimulation of U-reducing bacteria. Microbial diversity analysis revealed the distribution of bacterial populations with a key role in the biogeochemical cycles of relevant element for U reduction (e.g., sulphate reducers, iron reducers, iron oxidizers, nitrate reducers and metal reducers). Thus, our results show that Fe and U, as well as SO_4^{2-} , could influence the differential diversity of the microbial community of the waters from the two mines as they are correlated with the biogeochemical cycles of these elements. In addition, mine water harbours wood degrading fungal communities providing potential electron donors, which promote the growth of U reducing bacteria. The elucidation of the overall bacterial diversity and the chemistry of the water from these mines could help the correct design of U bioremediation strategies.

The bioreduction of U(VI) in glycerol amended water from the Schlema-Alberoda mine based on the biostimulation of indigenous bacterial communities could be a viable alternative for U removal. We also observed that high levels of soluble U (99%), Fe (95%) and SO_4^{2-} (58%) are removed

by the use of glycerol as an electron donor. Glycerol probably stimulates the native micro-organism community by reducing soluble U(VI) to insoluble U(IV). Further ongoing studies will fully explore the U bioreduction processes through the microscopic and spectroscopic characterization of the reduced U solid phases and identification of the microbial communities actively involved in U removal.

References

- Albrecht H (2017) The heritage of Uranium Mining in the German-Czech Ore Mountains. *Entreprises et Histoire*. 87:88–106. <https://doi.org/10.3917/eh.087.0088>
- Ander P, Hatakka A, Eriksson, KE (1980) Vanillic acid metabolism by the white-rot fungus *Sporotrichum pulverulentum*. *Archives of Microbiology*. 125(3):189–202. <https://doi.org/10.1007/BF00446876>
- Anderson RT, Vrionis HA, Ortiz-Bernad I, Resch CT, Long PE, Dayvault R, Karp K, Marutzky S, Metzler DR, Peacock A, White DC, Lowe M, and Lovley, DR (2003) Stimulating the In Situ Activity of *Geobacter* Species to Remove Uranium from the Groundwater of a Uranium-Contaminated Aquifer. *Applied and Environmental Microbiology*. 69(10):5884–5891. <https://doi.org/10.1128/AEM.69.10.5884-5891.2003>
- Andersson CA and Bro R (2000) The *N*-way Toolbox for MATLAB. *Chemometrics and Intelligent Laboratory Systems*. 52(1):1-4. [https://doi.org/10.1016/S0169-7439\(00\)00071-X](https://doi.org/10.1016/S0169-7439(00)00071-X)
- Andrews (2010) *FastQC*: quality control tool for high throughput sequence data. Date of access: February 02, 2022. Retrieved from <http://www.bioinformatics.babraham.ac.uk/projects/fastqc>
- Annandale J, Burgess J, Tanner P (2017) Where there's muck there's brass: irrigated agriculture with mine impacted waters. *International Mine Water Assoc (IMWA) Conf. Mine Water and Circular Economy*. 915–922. Date of access: February 02, 2022. Retrieved from http://www.mwen.info/docs/imwa_2017/IMWA2017_Annandale_915.pdf
- Ansoborlo E, Lebaron-Jacobs L, Prat O (2015) Uranium in drinking-water: A unique case of guideline value increases and discrepancies between chemical and radiochemical guidelines. *Environment International*. 77:1–4. <https://doi.org/10.1016/j.envint.2014.12.011>
- Arnold T, Baumann N, Krawczyk-Bärsch E, Brockmann S, Zimmermann U, Jenk U, Weiß S (2011) Identification of the uranium speciation in an underground acid mine drainage environment. *Geochimica et Cosmochimica Acta*. 75:2200–2212. <https://doi.org/10.1016/j.gca.2011.01.037>

- Banala UK, Das NPI, Toleti SR (2021) Microbial interactions with uranium: Towards an effective bioremediation approach. *Environmental Technology and Innovation*. 21:101254. <https://doi.org/10.1016/j.eti.2020.101254>
- Baraniak L, Bernhard G, Nitsche H (2002) Influence of hydrothermal wood degradation products on the uranium adsorption onto metamorphic rocks and sediments. *Journal of Radioanalytical and Nuclear Chemistry*. 253(2):185–190. <https://doi.org/10.1023/A:1019657503952>
- Bärenstrauch M, Vanhove AS, Allégra S, Peuble S, Gallice F, Paran F, Lavastre V, Girardot F (2022) Microbial diversity and geochemistry of groundwater impacted by steel slag leachates. *Science of the Total Environment*. 843:156987. <https://doi.org/10.1016/j.scitotenv.2022.156987>
- Bernhard G, Geipel G, Brendler V, Nitsche H (1996) Speciation of Uranium in Seepage Waters of a Mine Tailing Pile Studied by Time-Resolved Laser-Induced Fluorescence Spectroscopy (TRLFS). *Radiochimica Acta*. 74:87–91. <https://doi.org/10.1524/ract.1996.74.special-issue.87>
- Bernhard G, Geipel G, Brendler V, Nitsche H (1998) Uranium speciation in waters of different uranium mining areas. *Journal of Alloys and Compounds*. 271–273: 201–205. [https://doi.org/10.1016/S0925-8388\(98\)00054-1](https://doi.org/10.1016/S0925-8388(98)00054-1)
- Bernhard G, Geipel G, Reich T, Brendler V, Amayri S, Nitsche H (2001) Uranyl(VI) carbonate complex formation: Validation of the $\text{Ca}_2\text{UO}_2(\text{CO}_3)_3(\text{aq})$ species. *Radiochimica Acta*. 89(8): 511-518. <https://doi.org/10.1524/ract.2001.89.8.511>
- Bolyen E, Rideout JR, Dillon MR, Bokulich NA, Abnet CC, Al-Ghalith GA, Alexander H, Alm EJ, Arumugam M, Asnicar F, Bai Y, Bisanz JE, Bittinger K, Brejnrod A, Brislawn CJ, Brown CT, Callahan BJ, Caraballo-Rodríguez AM, Chase J, Cope EK, Da Silva R, Diener C, Dorrestein PC, Douglas GM, Durall DM, Duvall C, Edwardson CF, Ernst M, Estaki M, Fouquier J, Gauglitz JM, Gibbons SM, Gibson DL, Gonzalez A, Gorlick K, Guo J, Hillmann B, Holmes S, Holste H, Huttenhower C, Huttley GA, Janssen S, Jarmusch AK, Jiang L, Kaehler BD, Kang KB, Keefe CR, Keim P, Kelley ST, Knights D, Koester I, Kosciolk T, Kreps J, Langille MGI, Lee J, Ley R, Liu YX, Lofthfield E, Lozupone C, Maher M, Marotz C, Martin BD, McDonald D, McIver LJ, Melnik AV, Metcalf JL, Morgan SC, Morton JT, Naimey AT, Navas-Molina JA, Nothias LF, Orchanian SB, Pearson T, Peoples SL, Petras D, Preuss ML, Pruesse E, Rasmussen LB, Rivers A, Robeson MS, Rosenthal P, Segata N, Shaffer M, Shiffer A, Sinha R, Song SJ, Spear JR, Swafford AD, Thompson LR,

- Torres PJ, Trinh P, Tripathi A, Turnbaugh PJ, Ul-Hasan S, Van der Hooft JJJ, Vargas F, Vázquez-Baeza Y, Vogtmann E, Von Hippel M, Walters W, Wan Y, Wang M, Warren J, Weber KC, Williamson CHD, Willis AD, Xu ZZ, Zaneveld JR, Zhang Y, Zhu Q, Knight R, Caporaso JG (2019) Reproducible, interactive, scalable and extensible microbiome data science using QIIME 2. *Nature Biotechnology*. 37(8):852–857. <https://doi.org/10.1038/s41587-019-0209-9>
- Callahan BJ, Mcmurdie PJ, Rosen MJ, Han WH, Johnson AJ, Holmes SP (2016) DADA2: High resolution sample inference from amplicon data. *Nature Methods*. 13(7):581–583. <http://dx.doi.org/10.1101/024034>
- Caporaso JG, Kuczynski J, Stombaugh J, Bittinger K, Bushman FD, Costello EK, Fierer N, Peña AG, Goodrich JK, Gordon JI, Huttley GA, Kelley ST, Knights D, Koenig JE, Ley RE, Lozupone C A, McDonald D, Muegge BD, Pirrung M, Reeder J, Sevinsky JR, Turnbaugh PJ, Walters WA, Widmann J, Yatsunencko T, Zaneveld J, Knight R (2010) QIIME allows analysis of high-throughput community sequencing data. *Nature Methods*. 7(5):335-336. <https://doi.org/10.1038/nmeth.f.303>
- Chang Y (2005) *In situ biostimulation of uranium reducing microorganisms at the Old Rifle UMTRA Site*. PhD diss., University of Tennessee. Date of access: February 11, 2023. Retrieved from http://trace.tennessee.edu/utk_graddiss/1895/
- Chang Y, Peacock AD, Long PE, Stephen JR, McKinley JP, Macnaughton SJ, Hussain AKMA, Saxton AM, White DC (2001) Diversity and characterization of sulfate-reducing bacteria in groundwater at uranium mill tailing site. *Applied and Environmental Microbiology*. 67(7):3149–3160. <https://doi.org/10.1128/AEM.67.7.3149-3160.2001>
- Chen L, Liu, J, Zhang W, Zhou J, Luo D, Li Z (2021) Uranium (U) source, speciation, uptake, toxicity and bioremediation strategies in soil-plant system: A review. *Journal of Hazardous Materials*. 413:125319. <https://doi.org/10.1016/j.jhazmat.2021.125319>
- Coral T, Placko AL, Beaufort D, Tertre E, Bernier-Latmani R, Descostes M, De Boissezon H, Guillon S, Rossi P (2022) Biostimulation as a sustainable solution for acid neutralization and uranium immobilization post acidic in-situ recovery. *Science of The Total Environment*. 822: 153597. <https://doi.org/10.1016/j.scitotenv.2022.153597>
- Cummings D E, Caccavo F, Spring S, Rosenzweig RF (1999) *Ferribacterium limneticum*, gen. nov., sp. nov., an Fe (III) -reducing microorganism isolated from mining-impacted freshwater lake sediments. *Archives of Microbiology*. 183–188. <https://doi.org/10.1007/s002030050001>

doi.org/10.1007/s002030050697

- Dhariwal A, Chong J, Habib S, King IL, Agellon LB, Xia J (2017) MicrobiomeAnalyst: A web-based tool for comprehensive statistical, visual and meta-analysis of microbiome data. *Nucleic Acids Research*. 45(W1):W180–W188. <https://doi.org/10.1093/nar/gkx295>
- Dirginčiute-Volodkiene V and Pečiulyte D (2011) Increased soil heavy metal concentrations affect the structure of soil fungus community. *Agriculturae Conspectus Scientificus*. 76(1): 27-33. Date of access: February 11, 2023. Retrieved from <https://acs.agr.hr/acs/index.php/acs/article/view/598>
- Dos Santos Utmazian MN, Schweiger P, Sommer P, Gorfer M, Strauss J, Wenzel WW (2007) Influence of *Cadophora finlandica* and other microbial treatments on cadmium and zinc uptake in willows grown on polluted soil. *Plant, Soil and Environment*. 53(4):158–166. <https://doi.org/10.17221/2310-pse>
- Drobot B, Steudtner R, Raff J, Geipel G, Brendler V, Tsushima S (2015) Combining luminescence spectroscopy, parallel factor analysis and quantum chemistry to reveal metal speciation - A case study of uranyl(VI) hydrolysis. *Chemical Science*. 6:964–972. <https://doi.org/10.1039/c4sc02022g>
- Fields MW, Yan T, Rhee SK, Carroll SL, Jardine PM, Watson DB, Criddle CS, Zhou J (2005) Impacts on microbial communities and cultivable isolates from groundwater contaminated with high levels of nitric acid-uranium waste. *FEMS Microbiology Ecology*. 53:417–428. <https://doi.org/10.1016/j.femsec.2005.01.010>
- Finneran KT, Anderson RT, Nevin KP, Lovley DR (2002) Potential for bioremediation of uranium-contaminated aquifers with microbial U(VI) reduction. *Soil and Sediment Contamination*. 11(3):339–357. <https://doi.org/10.1080/20025891106781>
- Fogarty RV and Tobin JM (1996) Fungal melanins and their interactions with metals. *Enzyme and Microbial Technology*. 19:311–317. [https://doi.org/10.1016/0141-0229\(96\)00002-6](https://doi.org/10.1016/0141-0229(96)00002-6)
- Frisbie SH, Mitchell EJ, Sarkar B (2013) World Health Organization increases its drinking-water guideline for uranium. *Environmental Sciences: Processes and Impacts*. 15:1817–1823. <https://doi.org/10.1039/c3em00381g>
- Gadd GM and Fomina M (2011) Uranium and fungi. *Geomicrobiology Journal*. 28(5–6):471–482. <https://doi.org/10.1080/01490451.2010.508019>

- Gallois N, Alpha-Bazin B, Ortet P, Barakat M, Piette L, Long J, Berthomieu C, Armengaud J, Chapon V (2018) Proteogenomic insights into uranium tolerance of a Chernobyl's *Microbacterium* bacterial isolate. *Journal of Proteomics*. 177:148–157. <https://doi.org/10.1016/j.jprot.2017.11.021>
- Garboś S and Świecicka D (2015) Application of bimodal distribution to the detection of changes in uranium concentration in drinking water collected by random daytime sampling method from a large water supply zone. *Chemosphere*. 138:377–382. <https://doi.org/10.1016/j.chemosphere.2015.06.064>
- Geissler A and Selenska-Pobell S (2005) Addition of U(VI) to a uranium mining waste sample and resulting changes in the indigenous bacterial community. *Geobiology*. 3:275–285. <http://dx.doi.org/10.1111/j.1472-4669.2006.00061.x>
- Giffaut E, Grivé M, Blanc P, Vieillard P, Colàs E, Gailhanou H, Gaboreau S, Marty N, Madé B, Duro L (2014) Andra thermodynamic database for performance assessment: ThermoChimie. *Applied Geochemistry*. 49:225–236. doi.org/10.1016/j.apgeochem.2014.05.007
- Grivé M, Duro L, Colàs E, Giffaut E (2015) Thermodynamic data selection applied to radionuclides and chemotoxic elements: an overview of the ThermoChimie-TDB. *Applied Geochemistry*. 55:85-94. doi.org/10.1016/j.apgeochem.2014.12.017
- Haq IU, Hillmann B, Moran M, Willard S, Knights D, Fixen KR, Schilling, JS (2022) Bacterial communities associated with wood rot fungi that use distinct decomposition mechanisms. *ISME Communications*. 2:26. <https://doi.org/10.1038/s43705-022-00108-5>
- Harper DAT (ed.) 1999 *Numerical Palaeobiology*. John Wiley and Sons, New York. doi:10.1017/S0016756800334410
- Harpke M, Pietschmann S, Ueberschaar N, Krüger T, Kniemeyer O, Brakhage AA, Nietzsche S, Kothe E (2022) Salt and Metal Tolerance Involves Formation of Guttation Droplets in Species of the *Aspergillus versicolor* Complex. *Genes*. 13(9):1631. <https://doi.org/10.3390/genes13091631>
- Hedges JI, Blanchette RA, Weliky K, Devol AH (1988) Effects of fungal degradation on the CuO oxidation products of lignin: A controlled laboratory study. *Geochimica et Cosmochimica Acta*. 52(11):2717–2726. [153](https://doi.org/10.1016/0016-</p></div><div data-bbox=)

Hiller A and Schuppan W (2008) Geologie und Uranbergbau im Revier Schlema-Alberoda. Sächsisches Landesamt für Umwelt und Geologie (LfUG), Dresden. <https://publikationen.sachsen.de/bdb/artikel/12174>

Huang L, Bae HS, Young C, Pain AJ, Martin JB, Ogram A (2021) *Campylobacterota* dominate the microbial communities in a tropical karst subterranean estuary, with implications for cycling and export of nitrogen to coastal waters. *Environmental Microbiology*. 23(11):6749–6763. <https://doi.org/10.1111/1462-2920.15746>

Istok JD, Senko JM, Krumholz LR, Watson D, Bogle MA, Peacock A, Chang YJ, White DC (2004) In Situ Bioreduction of Technetium and Uranium in a Nitrate-Contaminated Aquifer. *Environmental Science and Technology*. 38(2):468–475. <https://doi.org/10.1021/es034639p>

Ito T, Sugita K, Yumoto I, Nodasaka Y, Okabe S (2005) *Thiovirga sulfuroxydans* gen. nov., sp. nov., a chemolithoautotrophic sulfur-oxidizing bacterium isolated from a microaerobic waste-water biofilm. *International Journal of Systematic and Evolutionary Microbiology*, 55(3):1059–1064. <https://doi.org/10.1099/ijs.0.63467-0>

Jasrotia P, Green SJ, Canion A, Overholt WA, Prakash O, Wafula D, Hubbard D, Watson, DB, Schadt CW, Brooks SC, Kostka JE (2014) Watershed-scale fungal community characterization along a pH gradient in a subsurface environment cocontaminated with uranium and nitrate. *Applied and Environmental Microbiology*. 80(6):1810–1820. <https://doi.org/10.1128/AEM.03423-13>

Jroundi F, Descostes M, Povedano-Priego C, Sánchez-Castro I, Suvannagan V, Grizard P, Merroun ML (2020) Profiling native aquifer bacteria in a uranium roll-front deposit and their role in biogeochemical cycle dynamics: Insights regarding in situ recovery mining. *Science of the Total Environment*. 721:137758. <https://doi.org/10.1016/j.scitotenv.2020.137758>

Jroundi F, Merroun ML, Arias JM, Rossberg A, Selenska-Pobell S, González-Muñoz MT (2007) Spectroscopic and microscopic characterization of uranium biomineralization in *Myxococcus xanthus*. *Geomicrobiology Journal*. 24(5):441–449. <https://doi.org/10.1080/01490450701437651>

Kalin M, Wheeler WN, Meinrath G (2005) The removal of uranium from mining waste

- water using algal/microbial biomass. *Journal of Environmental Radioactivity*. 78(2):151–177. <https://doi.org/10.1016/j.jenvrad.2004.05.002>
- Kassahun A, Hoth N, Paul M (2018) Mine Water Tracer Substances for Biogeochemical Processes in Flooded Uranium Mines. 635–640. Date of access: February 11, 2023. Retrieved from https://www.imwa.info/docs/imwa_2018/IMWA2018_Kassahun_635.pdf
- Kojima H and Fukui M (2011) *Sulfuritalea hydrogenivorans* gen. nov., sp. nov., a facultative autotroph isolated from a freshwater lake. *International Journal of Systematic and Evolutionary Microbiology*. 61(7):1651–1655. <https://doi.org/10.1099/ijs.0.024968-0>
- Krawczyk-Bärsch E, Gerber U, Müller K, Moll H, Rossberg A, Steudtner R, Merroun ML (2018) Multidisciplinary characterization of U(VI) sequestration by *Acidovorax facilis* for bioremediation purposes. *Journal of Hazardous Materials*. 347:233–241. <https://doi.org/10.1016/j.jhazmat.2017.12.030>
- Krawczyk-Bärsch E, Lütke L, Moll H, Bok F, Steudtner R, Rossberg A (2015) A spectroscopic study on U(VI) biomineralization in cultivated *Pseudomonas fluorescens* biofilms isolated from granitic aquifers. *Environmental Science and Pollution Research*. 22(6):4555–4565. <https://doi.org/10.1007/s11356-014-3671-4>
- Liu C, Jeon BH, Zachara JM, Wang Z (2007) Influence of calcium on microbial reduction of solid phase uranium(VI). *Biotechnology Bioengineering*. 97(6):1415–1422. <https://doi.org/10.1002/bit.21357>
- Liu Y, Zhang B, Zhang Y, Shen Y, Cheng C, Yuan W, Guo P (2022) Organic Matter Decomposition in River Ecosystems: Microbial Interactions Influenced by Total Nitrogen and Temperature in River Water. *Microbial Ecology*. 85:1236–1252. <https://doi.org/10.1007/s00248-022-02013-9>
- Lopez-Fernandez M, Jroundi F, Ruiz-Fresneda MA, Merroun ML (2021) Microbial interaction with and tolerance of radionuclides: underlying mechanisms and biotechnological applications. *Microbial Biotechnology*. 14(3):810–828. <https://doi.org/10.1111/1751-7915.13718>
- Lovley DR, Giovannoni SJ, White DC, Champine JE, Phillips EJP, Gorby YA, Goodwin S (1993) *Geobacter metallireducens* gen. nov. sp. nov., a microorganism capable of coupling the complete oxidation of organic compounds to the reduction of iron and

other metals. Archives of Microbiology. 159(4):336–344. <https://doi.org/10.1007/BF00290916>

Lovley DR, Phillips EJP, Gorby YA, Landa ER (1991) Microbial reduction of uranium. Nature. 350:413–416. <https://doi.org/10.1038/350413a0>

Lusa M, Knuutinen J, Lindgren M, Virkanen J, Bomberg M (2019) Microbial communities in a former pilot-scale uranium mine in Eastern Finland - Association with radium immobilization. Science of the Total Environment. 686:619-640. <https://doi.org/10.1016/j.scitotenv.2019.05.432>

Madden AS, Smith AC, Balkwill DL, Fagan LA, Phelps TJ (2007) Microbial uranium immobilization independent of nitrate reduction. Environmental Microbiology. 9(9):2321–2330. <https://doi.org/10.1111/j.1462-2920.2007.01347.x>

Mansour MMA, Hamed SAEKM, Salem, MZM, Ali HM (2020) Illustration of the effects of five fungi on *Acacia saligna* wood organic acids and ultrastructure alterations in wood cell walls by HPLC and TEM examinations. Applied Sciences. 10:2886. <https://doi.org/10.3390/APP10082886>

Martínez-Rodríguez P, Sánchez-Castro I, Ojeda JJ, Abad MM, Descostes M, Merroun ML (2023) Effect of different phosphate sources on uranium biomineralization by the *Microbacterium* sp. Be9 strain: A multidisciplinary approach study. Frontiers in Microbiology. 13:1092184. <https://doi.org/10.3389/fmicb.2022.1092184>

Merroun ML and Selenska-Pobell S (2008) Bacterial interactions with uranium: An environmental perspective. Journal of Contaminant Hydrology. 102(3–4): 285–295. <https://doi.org/10.1016/j.jconhyd.2008.09.019>

Meyer J, Paul M, Jenk U (2008) Mine Water Hydrology of the Schneeberg Mine (Saxony) Fifty Years after Flooding. Date of access: February 11, 2023. Retrieved from http://mwen.info/docs/imwa_2008/IMWA2008_169_Meyer.pdf

Moon HS, McGuinness L, Kukkadapu RK, Peacock AD, Komlos J, Kerkhof LJ, Long PE, Jaffé PR (2010) Microbial reduction of uranium under iron- and sulfate-reducing conditions: Effect of amended goethite on microbial community composition and dynamics. Water Research. 44(14):4015–4028. <https://doi.org/10.1016/j.watres.2010.05.003>

Mumtaz S, Streten C, Parry DL, McGuinness KA, Lu P, Gibb KS (2018) Soil uranium concentration at Ranger Uranium Mine Land Application Areas drives changes

- in the bacterial community. *Journal of Environmental Radioactivity*. 189:14–23. <https://doi.org/10.1016/j.jenvrad.2018.03.003>
- Nakajima A and Sakaguchi T (1993) Accumulation of uranium by basidiomycetes. *Applied Microbiology and Biotechnology*. 38(4):574–578. <https://doi.org/10.1007/BF00242958>
- Naumov GB, Vlasov BP, Golubev VN, Mironova OF (2017) The Schlemma–Alberoda five-element uranium deposit, Germany: An example of self-organizing hydrothermal system. *Geology of Ore Deposits*. 59(1):1–13. <https://doi.org/10.1134/S1075701517010056>
- Nayak T, De D, Karmakar P, Deb A, Dhal PK (2021) Microbial Communities of the Drinking Water With Gradient Radon Concentration Are Primarily Contributed by Radon and Heavy Metal Content. *Frontiers in Environmental Science*. 9:576400. <https://doi.org/10.3389/fenvs.2021.576400>
- Neck V and Kim JI (2001) Solubility and Hydrolysis of Tetravalent Actinides, *Radiochimica Acta*. 89:1-16. <https://doi.org/10.1524/ract.2001.89.1.001>
- Newsome L, Morris K, Lloyd JR (2014) The biogeochemistry and bioremediation of uranium and other priority radionuclides. *Chemical Geology*. 363:164–184. <https://doi.org/10.1016/j.chemgeo.2013.10.034>
- Newsome L, Morris K, Trivedi D, Bewsher A, Lloyd JR (2015) Biostimulation by Glycerol Phosphate to Precipitate Recalcitrant Uranium(IV) Phosphate. *Environmental Science and Technology*. 49(18):11070–11078. <https://doi.org/10.1021/acs.est.5b02042>
- Nilsson RH, Larsson KH, Taylor AFS, Bengtsson-Palme J, Jeppesen TS, Schigel D, Kennedy P, Picard K, Glöckner FO, Tedersoo L, Saar I, Kõljalg U, Abarenkov K. (2019) The UNITE database for molecular identification of fungi: Handling dark taxa and parallel taxonomic classifications. *Nucleic Acids Research*. 47(D1): D259–D264. <https://doi.org/10.1093/nar/gky1022>
- North NN, Dollhopf SL, Petrie L, Istok JD, Balkwill DL, Kostka JE (2004) Change in bacterial community structure during in situ biostimulation of subsurface sediment cocontaminated with uranium and nitrate. *Applied and Environmental Microbiology*. 70(8):4911–4920. <https://doi.org/10.1128/AEM.70.8.4911-4920.2004>
- Nothhaft DB, Templeton AS, Rhim JH, Wang DT, Labidi J, Miller HM, Boyd ES, Matter

- JM, Ono S, Young ED, Kopf SH, Kelemen PB, Conrad ME (2021) Geochemical, Biological, and Clumped Isotopologue Evidence for Substantial Microbial Methane Production Under Carbon Limitation in Serpentinites of the Samail Ophiolite, Oman. *Journal of Geophysical Research: Biogeosciences*. 126(10):e2020JG006025. <https://doi.org/10.1029/2020JG006025>
- Oh JJ, Kim JY, Kim YJ, Kim S, Kim GH (2021) Utilization of extracellular fungal melanin as an eco-friendly biosorbent for treatment of metal-contaminated effluents. *Chemosphere*. 272:129884. <https://doi.org/10.1016/j.chemosphere.2021.129884>
- Op De Beeck M, Lievens B, Busschaert P, Declerck S, Vangronsveld J, Colpaert JV (2014) Comparison and validation of some ITS primer pairs useful for fungal metabarcoding studies. *PLoS ONE*. 9(6):e97629. <https://doi.org/10.1371/journal.pone.0097629>
- Orlygsson J and Kristjansson JK (2014) The Family *Hydrogenophilaceae*. In: Rosenberg E, DeLong EF, Lory S, Stackebrandt E, Thompson F (eds) *The Prokaryotes*. Springer, Berlin, Heidelberg. https://doi.org/10.1007/978-3-642-30197-1_244
- Passarini MRZ, Ottoni JR, Dos Santos Costa PE, Hissa DC, Falcão RM, Melo VMM, Coutinho HD, Verde LCL (2022) Fungal community diversity of heavy metal contaminated soils revealed by metagenomics. *Archives of Microbiology*. 204(255):1–27. <https://doi.org/10.1007/s00203-022-02860-7>
- Paul M, Meyer J, Jenk U, Baacke D, Schramm A, Metschies T (2013) Mine Flooding and Water Management at Underground Uranium Mines two Decades after Decommissioning. *International Mine Water Assoc (IMWA) Conf. Reliable Mine Water Technology*, 1081–1087. Date of access: February 11, 2023. Retrieved from. <https://doi.org/10.13140/RG.2.1.2123.3682>
- Peng W, Li X, Lin M, Fan W (2020) Microbiological analysis of cadmium-contaminated sediments during biostabilization with indigenous sulfate-reducing bacteria. *Journal of Soils and Sediments*. 20:584–593. <https://doi.org/10.1007/s11368-019-02415-2>
- Phillips EJP, Landa ER, Lovley DR (1995) Remediation of uranium contaminated soils with bicarbonate extraction and microbial U(VI) reduction. *Journal of Industrial Microbiology*, 14(3–4):203–207. <https://doi.org/10.1007/BF01569928>
- Porsch K, Meier J, Kleinstaub S, Wendt-Potthoff K (2009) Importance of different physiological groups of iron reducing microorganisms in an acidic mining lake

remediation experiment. *Microbial Ecology*. 57(4):701–717. <https://doi.org/10.1007/s00248-009-9505-0>

Povedano-Priego C, Jroundi F, Lopez-Fernandez M, Morales-Hidalgo M, Martin-Sánchez I, Huertas FJ, Dopson M, Merroun ML (2022) Impact of anoxic conditions, uranium(VI) and organic phosphate substrate on the biogeochemical potential of the indigenous bacterial community of bentonite. *Applied Clay Science*. 216:106331. <https://doi.org/10.1016/j.clay.2021.106331>

Quast C, Pruesse E, Yilmaz P, Gerken J, Schweer T, Yarza P, Peplies J, Glöckner FO (2013) The SILVA ribosomal RNA gene database project: Improved data processing and web-based tools. *Nucleic Acids Research*, 41(D1):D590–D596. <https://doi.org/10.1093/nar/gks1219>

Rastogi G, Osman S, Kukkadapu R, Engelhard M, Vaishampayan PA, Andersen GL, and Sani RK (2010a) Microbial and Mineralogical Characterizations of Soils Collected from the Deep Biosphere of the Former Homestake Gold Mine, South Dakota. *Microbial Ecology*. 60(3):539–550. <https://doi.org/10.1007/s00248-010-9657-y>

Rastogi G, Osman S, Vaishampayan PA, Andersen GL, Stetler LD, Sani RK (2010b) Microbial diversity in uranium mining-impacted soils as revealed by high-density 16S microarray and clone library. *Microbial Ecology*. 59(1):94–108. <https://doi.org/10.1007/s00248-009-9598-5>

Rempfert KR, Miller HM, Bompard N, Nothhaft D, Matter JM, Kelemen P, Fierer N, Templeton AS (2017) Geological and geochemical controls on subsurface microbial life in the Samail Ophiolite, Oman. *Frontiers in Microbiology*. 8. <https://doi.org/10.3389/fmicb.2017.00056>

Sánchez-Castro I, Martínez-Rodríguez P, Abad MM, Descostes M, Merroun ML (2021) Uranium removal from complex mining waters by alginate beads doped with cells of *Stenotrophomonas* sp. Br8: Novel perspectives for metal bioremediation. *Journal of Environmental Management*. 296:113411. <https://doi.org/10.1016/j.jenvman.2021.113411>

Sánchez-Castro I, Martínez-Rodríguez P, Jroundi F, Solari PL, Descostes M, Merroun ML (2020) High-efficient microbial immobilization of solved U(VI) by the *Stenotrophomonas* strain Br8. *Water Research*. 183:116110. <https://doi.org/10.1016/j.watres.2020.116110>

- Sawyer DT (1964) Metal-Gluconate Complexes. *Chemical Reviews*. 64(6):633-643. <https://doi.org/10.1021/cr60232a003>
- Schaefer S, Steudtner R, Hübner R, Krawczyk-Bärsch E, Merroun ML (2021) Effect of Temperature and Cell Viability on Uranium Biomineralization by the Uranium Mine Isolate *Penicillium simplicissimum*. *Frontiers in Microbiology*. 12(802926). <https://doi.org/10.3389/fmicb.2021.802926>
- Schippers A, Hallmann R, Wentzien S, Sand W (1995) Microbial diversity in uranium mine waste heaps. *Applied and Environmental Microbiology*. 61(8):2930–2935. <https://doi.org/10.1128/aem.61.8.2930-2935.1995>
- Schuppan W and Hiller A (2012) Die Komplexlagerstätten Tellerhäuser und Hämmerlein - Uranbergbau und Zinnerkundung in der Grube Pöhla der SDAG Wismut. Sächsisches Landesamt für Umwelt, Landwirtschaft und Geologie (LfULG), Freiberg. Date of access: February 11, 2023. Retrieved from <https://slub.qucosa.de/id/qucosa%3A2741>
- Shen Z, Han J, Wang Y, Sahin O, Zhang Q (2013) The Contribution of ArsB to Arsenic Resistance in *Campylobacter jejuni*. *PLoS ONE*. 8(3):e58894. <https://doi.org/10.1371/journal.pone.0058894>
- Shuaib M, Azam N, Bahadur S, Romman M, Yu Q, Xuexiu C (2021) Variation and succession of microbial communities under the conditions of persistent heavy metal and their survival mechanism. *Microbial Pathogenesis*. 150:104713. <https://doi.org/10.1016/j.micpath.2020.104713>
- Steudtner R, Sachs S, Schmeide K, Brendler V, Bernhard G (2011) Ternary uranium(VI) carbonate humate complex studied by cryo-TRLFS. *Radiochimica Acta*. 99(11): 687–692. <https://doi.org/10.1524/ract.2011.1861>
- Thijs S, De Beeck MO, Beckers B, Truyens S, Stevens V, Van Hamme JD, Weyens N, Vangronsveld J (2017) Comparative evaluation of four bacteria-specific primer pairs for 16S rRNA gene surveys. *Frontiers in Microbiology*. 8(494):1–15. <https://doi.org/10.3389/fmicb.2017.00494>
- Tian R, Ning D, He Z, Zhang P, Spencer SJ, Gao S, Shi W, Wu L, Zhang Y, Yang Y, Adams BG, Rocha AM, Detienne BL, Lowe KA, Joyner DC, Klingeman DM, Arkin AP, Fields MW, Hazen TC, Stahl D A, Alm EJ, Zhou J (2020) Small and mighty: Adaptation of superphylum *Patescibacteria* to groundwater environment drives

- their genome simplicity. *Microbiome*. 8(51):1–15. <https://doi.org/10.1186/s40168-020-00825-w>
- Turick CE, Knox AS, Leverette CL, Kritzas YG (2008) In situ uranium stabilization by microbial metabolites. *Journal of Environmental Radioactivity*. 99(6):890–899. <https://doi.org/10.1016/j.jenvrad.2007.11.020>
- Umezawa K, Kojima H, Kato Y, Fukui M (2021) *Dissulfurispira thermophila* gen. nov., sp. nov., a thermophilic chemolithoautotroph growing by sulfur disproportionation, and proposal of novel taxa in the phylum *Nitrospirota* to reclassify the genus *Thermodesulfovibrio*. *Systematic and Applied Microbiology*. 44(2):126184. <https://doi.org/10.1016/j.syapm.2021.126184>
- Underwood JC, Akob DM, Lorah MM, Imbrigiotta TE, Harvey RW, Tiedeman RC (2022) Microbial community response to a bioaugmentation test to degrade trichloroethylene in a fractured rock aquifer, Trenton, N.J. *FEMS Microbiology Ecology*. 98(7):1–16. <https://doi.org/10.1093/femsec/fiac077>
- Văcar CL, Covaci E, Chakraborty S, Li B, Weindorf DC, Frențiu T, Pârvu M, Podar D (2021) Heavy metal-resistant filamentous fungi as potential mercury bioremediators. *Journal of Fungi*. 7(5):386. <https://doi.org/10.3390/jof7050386>
- Vulpus D, Geipel G, Baraniak L, Bernhard G (2006) Complex formation of neptunium(V) with 4-hydroxy-3-methoxybenzoic acid studied by time-resolved laser-induced fluorescence spectroscopy with ultra-short laser pulses. *Spectrochimica Acta Part A: Molecular and Biomolecular Spectroscopy*. 63(3):603-608. <https://doi.org/10.1016/j.saa.2005.06.007>
- Wang Z, Zachara JM, Yantasee W, Gassman PL, Liu C, Joly AG (2004) Cryogenic laser induced fluorescence characterization of U(VI) in Hanford vadose zone pore waters. *Environmental Science and Technology*. 38(21):5591–5597. <https://doi.org/10.1021/es049512u>
- WHO (2022) Guidelines for drinking-water quality: fourth edition incorporating the first and second addenda, Geneva: World Health Organization. 478-480. Date of access: February 20, 2023. Retrieved from <https://www.who.int/publications/i/item/9789240045064>
- Wilkins MJ, Livens FR, Vaughan DJ, Lloyd JR (2006) The impact of Fe(III)-reducing bacteria on uranium mobility. *Biogeochemistry*. 78(2):125–150. <https://doi.org/10.1007/s10533-006-9038-3>

[org/10.1007/s10533-005-3655-z](https://doi.org/10.1007/s10533-005-3655-z)

- Williams KH, Bargar JR, Lloyd JR, Lovley DR (2013) Bioremediation of uranium-contaminated groundwater: A systems approach to subsurface biogeochemistry. *Current Opinion in Biotechnology*. 24(3):489–497. <https://doi.org/10.1016/j.copbio.2012.10.008>
- WISMUT GmbH Brochure (2015) Date of access: February 20, 2022. Retrieved from <https://www.bmwk.de/Redaktion/EN/Publikationen/wismut-brochure.html>
- WISMUT GmbH Umweltbericht (2021) Date of access: October 3, 2023. Retrieved from <https://www.wismut.de/de/>
- Xu J, Veeramani H, Qafoku NP, Singh G, Riquelme MV, Pruden A, Kukkadapu RK, Gartman BN, Hochella MF (2017) Efficacy of acetate-amended biostimulation for uranium sequestration: Combined analysis of sediment/groundwater geochemistry and bacterial community structure. *Applied Geochemistry*. 78:172–185. <https://doi.org/10.1016/j.apgeochem.2016.12.024>
- Yabusaki SB, Fang Y, Long PE, Resch CT, Peacock AD, Komlos J, Jaffe PR, Morrison SJ, Dayvault RD, White DC, Anderson RT (2007) Uranium removal from groundwater via in situ biostimulation: Field-scale modeling of transport and biological processes. *Journal of Contaminant Hydrology*. 93(1–4): 216–235. <https://doi.org/10.1016/j.jconhyd.2007.02.005>
- You W, Peng W, Tian Z, Zheng M (2021) Uranium bioremediation with U(VI)-reducing bacteria. *Science of the Total Environment*. 798:149107. <https://doi.org/10.1016/j.scitotenv.2021.149107>
- Young D, Dollhofer V, Callaghan TM, Reitberger S, Lebuhn M, Benz JP (2018) Isolation, identification and characterization of lignocellulolytic aerobic and anaerobic fungi in one- and two-phase biogas plants. *Bioresource Technology*. 268: 470–479. <https://doi.org/10.1016/j.biortech.2018.07.103>
- Yu X, Dos Santos EC, White J, Salazar-Alvarez G, Pettersson LGM, Cornell A, Johnsson M (2021) Electrocatalytic Glycerol Oxidation with Concurrent Hydrogen Evolution Utilizing an Efficient MoO_x/Pt Catalyst. *Small*. 17:2104288. <https://doi.org/10.1002/sml.202104288>
- Zeng T, Li L, Mo G, Wang G, Liu H, Xie S (2019) Analysis of uranium removal capacity of anaerobic granular sludge bacterial communities under different initial pH

- conditions. *Environmental Science and Pollution Research*. 26(6):5613-5622. <https://doi.org/10.1007/s11356-018-4017-4>
- Zhang L, Li J, Lai JL, Yang X, Zhang Y, Luo XG (2022) Non-targeted metabolomics reveals the stress response of a cellulase-containing *penicillium* to uranium. *Journal of Environmental Sciences*. 120:9–17. <https://doi.org/10.1016/j.jes.2021.12.043>
- Zhang Z, Helms G, Clark SB, Tian G, Zanonato P, Rao L (2009) Complexation of Uranium(VI) by Gluconate in Acidic Solutions: a Thermodynamic Study with Structural Analysis. *Inorganic Chemistry*. 48:3814–3824. <https://doi.org/10.1021/ic8018925>
- Zhou C, Ontiveros-Valencia A, Cornette de Saint Cyr, L, Zevin AS, Carey SE, Krajmalnik-Brown R, Rittmann BE (2014) Uranium removal and microbial community in a H₂-based membrane biofilm reactor. *Water Research*. 64:255–264. <https://doi.org/10.1016/j.watres.2014.07.013>
- Zirnstein I, Arnold T, Krawczyk-Bärsch E, Jenk U, Bernhard G, Röske I. (2012) Eukaryotic life in biofilms formed in a uranium mine. *MicrobiologyOpen*. 1(2):83–94. <https://doi.org/10.1002/mbo3.17>

Supplementary

Table 1S. Alpha diversity index (Shannon) and richness (Chao1) of bacteria and fungi at genus level in water from the Schlema-Alberoda mine (R2; R4 and R5) and the Pöhla mine (P1; P2 and P5).

	Shannon	Chao1
Bacteria	P1	220
	P2	217
	P5	224
	R2	187
	R4	182
	R5	169
Fungi	P1	42
	P2	42
	P5	30
	R2	29
	R4	34
	R5	23

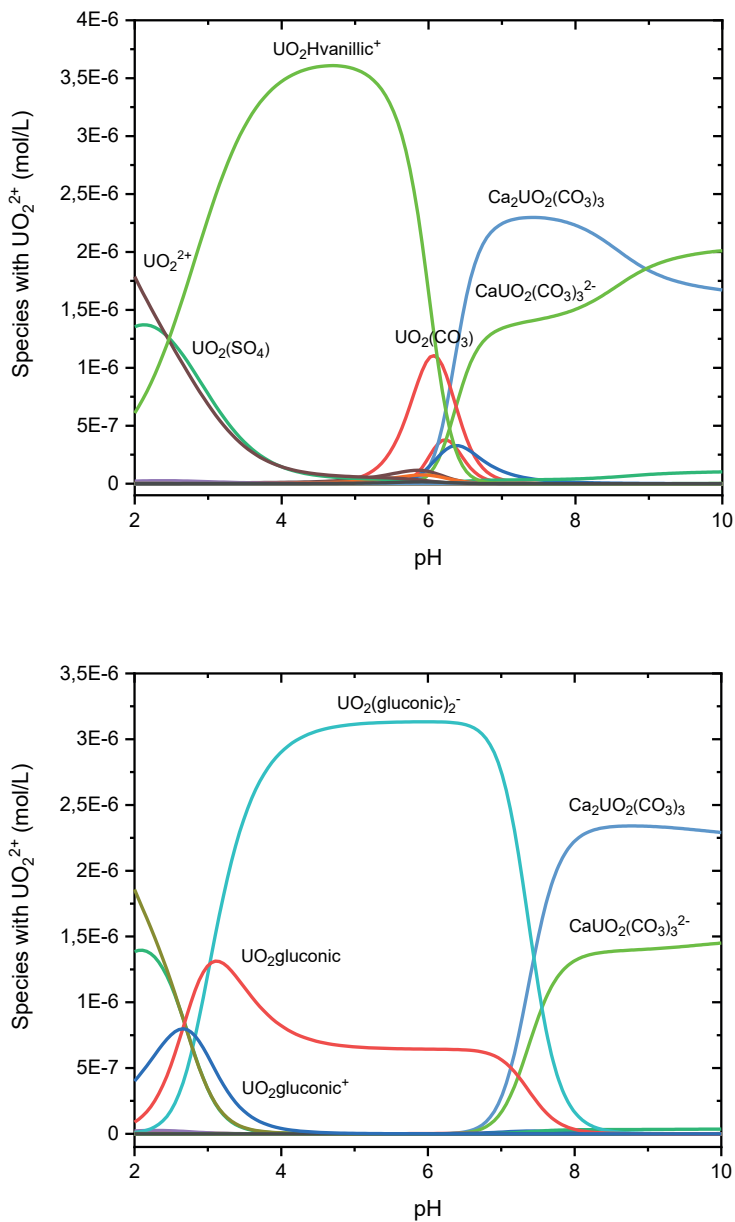


Fig. 1S: Thermodynamic speciation calculation of U(VI) with 10 mM vanillic acid and gluconic acid amended to sterile (autoclaved) Schlema-Alberoda mine water using the analogue database, data from the literature and the geochemical speciation code Geochemist's Workbench (version 17.0.1/Act2).

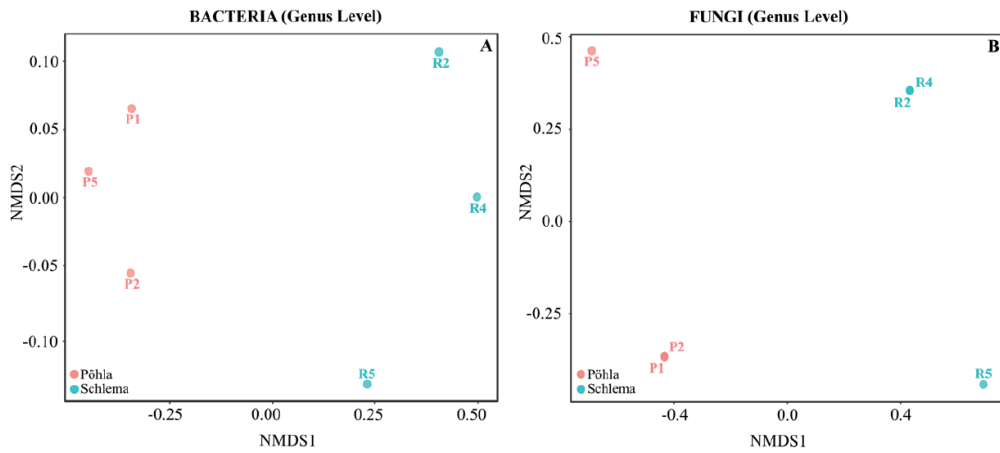


Fig. 2S. Bray–Curtis-based NMDS and PERMANOVA results of bacterial (A) and fungal (B) communities. Schlema-Alberoda (R2; R4; R5) and the Pöhla mine water (P1; P2; P5).

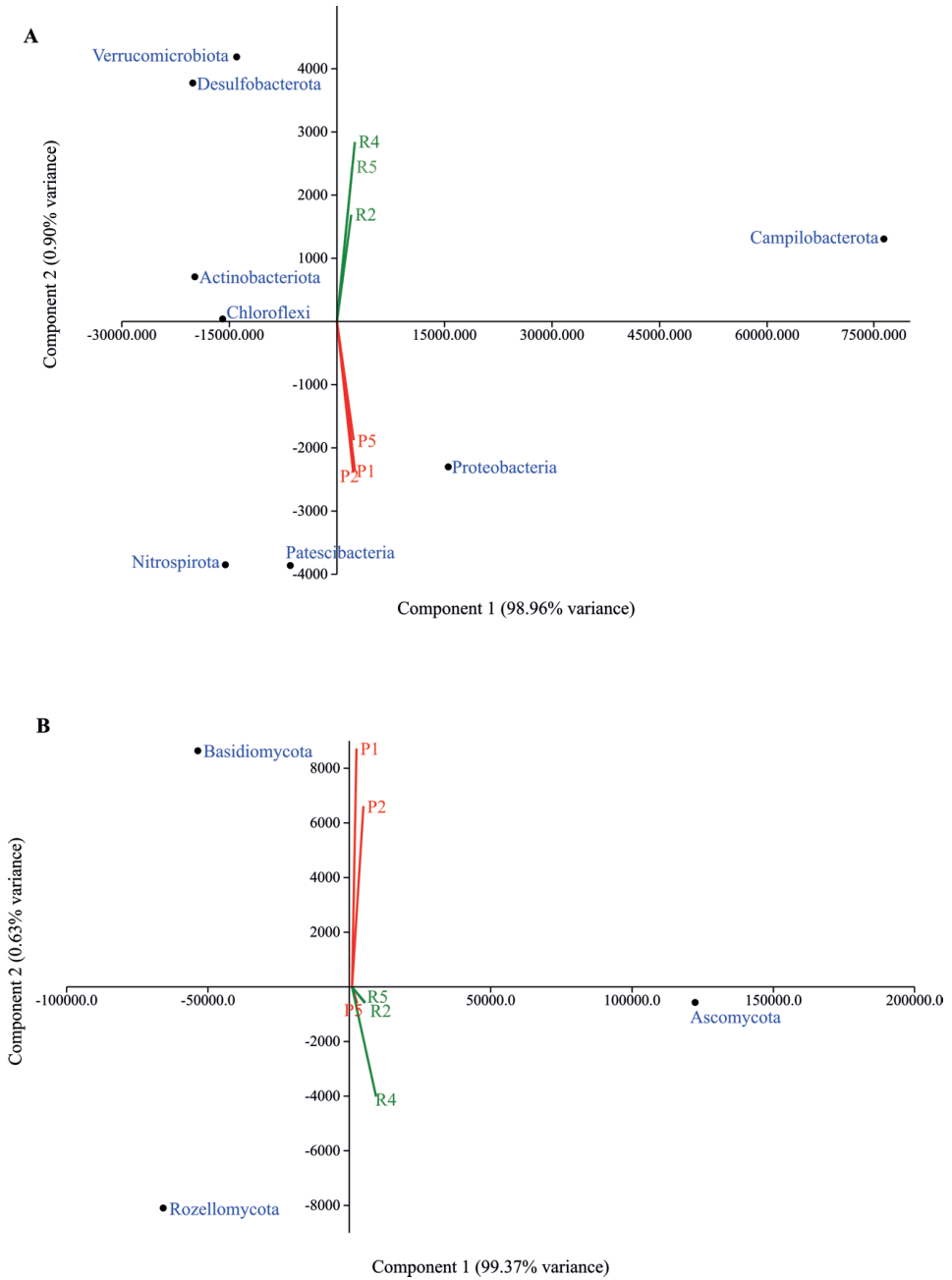
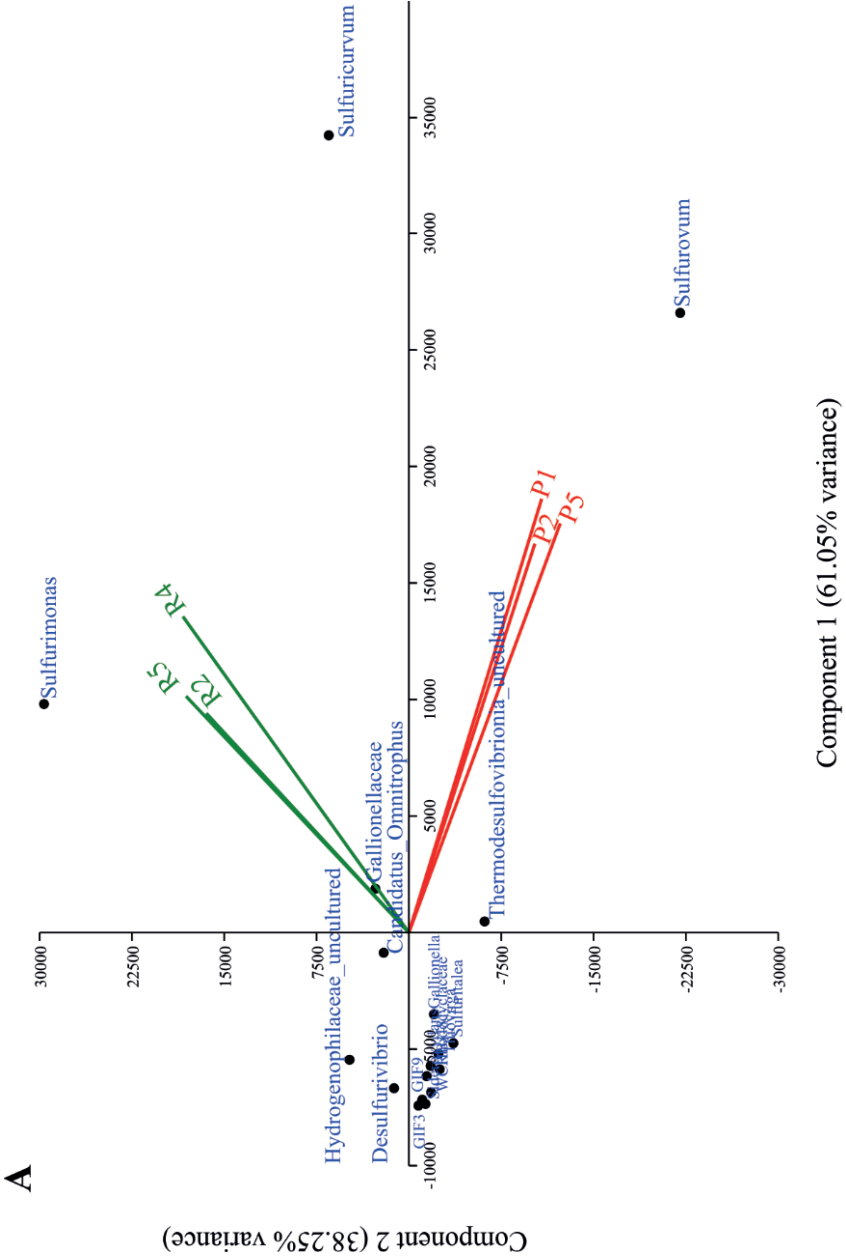


Fig. 3S. Principal component analysis (PCA) plot of bacterial (A) and fungal (B) communities at phylum level comparing the microbial community structure of the mine water from the Schlema-Alberoda (R2; R4; R5) and Pöhla mines (P1; P2; P5).

Fig. 4S. Principal component analysis (PCA) plot of bacterial (A) and fungal (B) communities at genus level comparing the microbial community structure of the mine water from the Schlema-Alberoda mine (R2; R4; R5) and the Pöhla mine (P1; P2; P5).



B

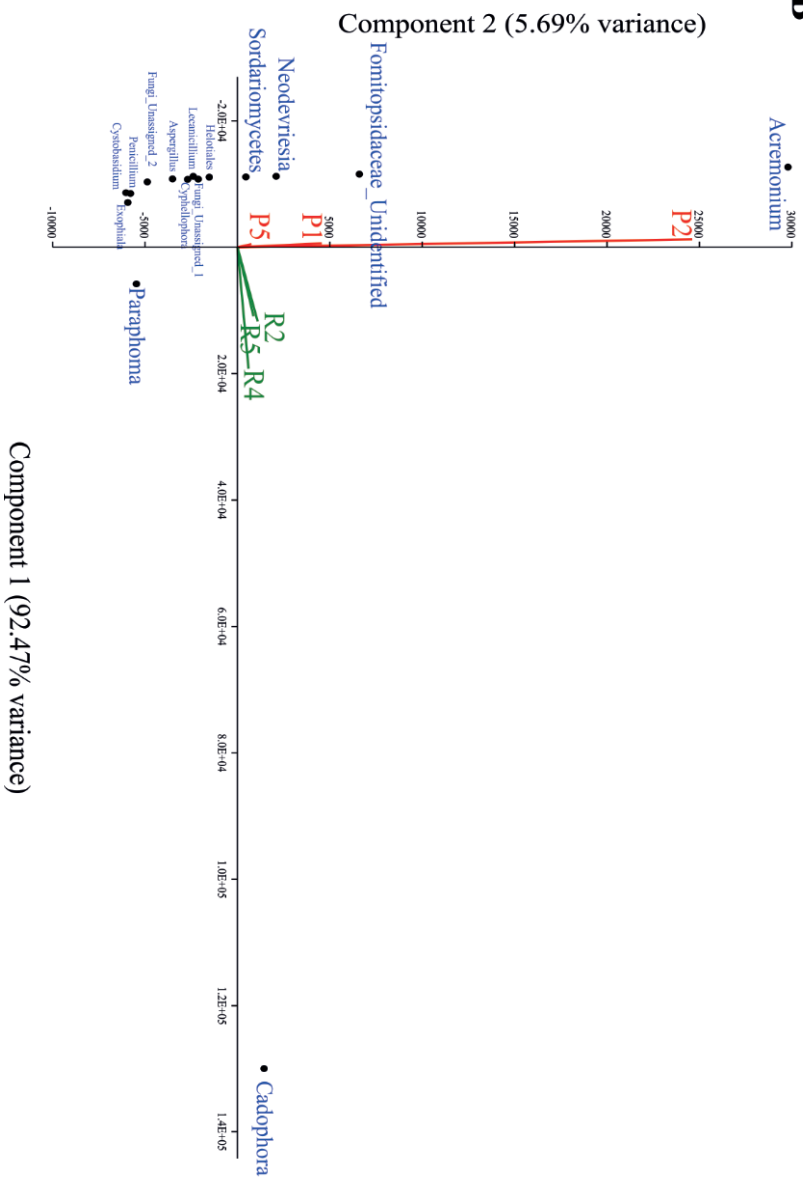




Photo by Tom Fisk

Chapter II:

Metatranscriptomics studies decipher key microbial metabolic pathways and their contribution to U(VI) reduction in mine waters

AUTHORS:

Antonio M. Newman-Portela ^{a,b,*}, Ting-Shyang Wei ^b, Evelyn Krawczyk-Bärsch ^b, Andrea Kassahun ^c, Thorsten Stumpf ^b, Mohamed L. Merroun ^a, Johannes Raff ^b.

^a Department of Microbiology, Faculty of Science, University of Granada, Spain.

^b Helmholtz-Zentrum Dresden-Rossendorf, Institute of Resource Ecology, Bautzner Landstraße 400, 01328 Dresden, Germany.

^c WISMUT GmbH, Chemnitz, Germany.

KEYWORDS: uranium, bacterial, next generation sequencing, RNA sequencing, gene expression

ABSTRACT

The chemical-based remediation of the former German U mines, Schlema-Alberoda and Pöhla (Wismut GmbH), decreased U to low residual levels (1.1 mg/l and 0.01 mg/l of U, respectively). Bioremediation based in the use of active microbial communities is considered as an innovative and promising method for the treatment of low U concentrations, such as in Schlema-Alberoda (1 mg/l), exceeding allowed limits in drinking (0.03 mg/l) and environmental waters (0.5 mg/l). U concentration and microbial diversity of the two mine waters did not differ between both sampling years, 2020 and 2021. In both years, the microbial community was dominated by the phyla Campilobacterota, Proteobacteria, and Patascibacteria, primarily involved in the biogeochemical cycles of C, S, and N, with potential for U reduction. Metatranscriptomic analyses were conducted on the basis of RNA sequencing to decipher key microbial metabolic pathways of the two mine waters. The results revealed the presence of a naturally active bacterial community with a comprehensive metabolic profile associated with carbohydrate degradation, oxidative phosphorylation, and S, N, and amino acids metabolisms, among other pathways, observed consistently across both mining sites. Stress adaptations (e.g., hydrogenase activity) of the microbial population were also evidenced. Furthermore, various genes related to key metabolic pathways involved in the sulphate reduction, such as assimilatory sulphate reduction (ASR) and dissimilatory sulphate reduction (DSR), showed strong regulation in Pöhla mine water in comparison to those in Schlema-Alberoda. In addition, genes involved in Fe reduction were only identified in Pöhla mine water.

The presented work highlights the presence of a potentially active microbial community in Pöhla, which could explain the lower U concentration (0.01 mg/l) in the mine water compared to that of Schlema-Alberoda (1 mg/l). The reduction of U(VI) could be attributed on the one hand to metal-reducing bacteria (e.g., *Geobacteraceae*). On the other hand, an abiotic

U(VI) reduction could have taken place by sulphide products formed during the sulphate reduction by sulphate-reducing bacteria (e.g., *Desulfobacca*).

1. Introduction

The Federal State of Saxony hosts two of the former main U mines in Germany (Wismut GmbH), Schlema-Alberoda and Pöhla. In both mines several tens of thousands of tons of U were mined in the second half of the 20th century. After the cessation of the mining activities, a legacy of U and other heavy metal contamination was left (WISMUT GmbH Brochure 2015; Newman-Portela et al. 2024). The remnants of radionuclides and other heavy metals at U mining sites could spread into the environment, leading to an increase in the contamination levels in soil and waters.

Since the closure of both mines, extensive monitoring has been carried out by the Wismut GmbH, and the implementation of physicochemical remediation methodologies through controlled flooding has been completed in both mines, with the processes respectively finished in 1995 (Pöhla) and 2008 (Schlema-Alberoda) (WISMUT GmbH Brochure 2015). The current concentration of U is 0.01 mg/l and 1 mg/l, respectively (Newman-Portela et al. 2024). To prevent the spread of the various mine water pollutants, Wismut GmbH operates mine water treatment plants at both flooded mines. However, traditional remediation technologies show a high implementation cost and are not effective for low U concentrations. An effective and promising method for tackling contaminated environments is the bioremediation. This innovative technology uses the potential of living organisms, such as bacteria, fungi and plants, to transform contaminants into less toxic forms.

Micro-organisms, such as bacteria, have the capacity to interact with U and other heavy metals through different mechanisms (Merroun and Selenska-Pobell 2008; Banala et al. 2021). Biomineralization and enzymatic transformation are the most commonly used strategies for U bioremediation. In particular, enzymatic reduction has been applied in the treatment of anoxic contaminated waters, altering the oxidation state of U, transforming it into a less soluble form and, therefore, less mobile and less toxic. For example, sulphate-reducing bacteria (SRB), such as *Desulfovibrio desulfuricans*, *Desulfovibrio vulgaris*, as well as iron-reducing bacteria (FeRB), such as *Geobacter sulfurreducens*, *Desulfotomaculum* sp., and *Desulfosporosinus*

sp. are able to transform the U oxidized form (U(VI)), which is soluble and bioavailable, into its reduced form (U(IV)), which is insoluble and less bioavailable (Lovley and Phillips 1992; Payne et al. 2002; Tang et al. 2021).

From the 2000s onwards, the use of DNA fragment sequencing studies based on the 16S rRNA gene was initiated to characterize the composition of microbial communities. Previous research in DNA-based microbial diversity analyses has confirmed the presence of a rich microbial diversity in both, Schlema-Alberoda and Pöhla mine water (Newman-Portela et al. 2024). The bacterial phyla *Campilobacterota* and *Proteobacteria* were identified in both mines, showing a high relative abundance compared to other microbial groups reported by other authors (Rastogi et al. 2010a, b; Zeng et al. in 2019; Lusa et al. 2019). The U(VI) reduction can occur through direct enzymatic activity, where bacteria utilize electrons released from organic substrates to convert the oxidized U(VI) into reduced U(IV). Additionally, there is the possibility of an indirect reduction, wherein bacteria first reduce the substrates to by-products (e.g., sulphide) that subsequently facilitate the reduction of U(VI) (You et al. 2021). Microbial community involved in the biogeochemical cycle of U, such as *Gallionella*, and *Sulfuricurvum* were identified in the mine water from Schlema-Alberoda and Pöhla (Chang 2005; Mondani et al. 2011). Additionally, bacterial genera previously reported for their roles in the biogeochemical cycles of S (e.g., *Sulfuritalea*), N (e.g., *Sulfuritalea*), and Fe (e.g., *Sideroxydans*) were also identified. Nevertheless, advances in sequencing technology have facilitated a more detailed and comprehensive analysis of the microbial community. Metatranscriptomics, based on mRNA sequences, has emerged as one of the main tools for understanding gene expression profiles and biological functions in different environments (Jroundi et al. 2023).

The aim of this study is to describe and explore the key metabolic pathways and activities related to biogeochemical cycles of S, N and C in the mine water from the two former U mines, Schlema-Alberoda and Pöhla. To achieve this objective, an analysis of different functional genes has been carried out using the RNA sequencing technique (RNA-Seq),

which constitutes the first metatranscriptomic analysis carried out in both mine waters. Additionally, using this data, the study seeks to determine whether the native micro-organisms present in the two mines could be involved in the difference in U concentrations observed in both sites. Finally, using the information obtained, the last aim is to optimize a future bioremediation strategy based on the bio-stimulation of the bacterial community involved in U reduction. Additional information is provided in Chapter III of this PhD thesis.

2. Materials and methods

2.1. Field site and mine water sampling description

Mine water samples were collected in July and September 2021 from the two flooded subsurface mine shafts Schlema-Alberoda and Pöhla (Wismut GmbH). A total of 50 L of mine water per mine was collected in an autoclaved canister under sterile conditions at an authorized sampling point in each mine. Sampling was carried out following the steps described in Newman-Portela et al. (2024). The water samples were transported to the laboratory at 4 °C. Upon arrival, water samples were prepared to perform DNA/RNA-based and physicochemical analyses. The samples were prepared as described below.

2.2. Determination of physicochemical parameters

To ascertain possible changes in the main physicochemical parameters between the water collected in 2020 (Newman-Portela et al. 2024) and the one collected in this study (2021), the water chemistry from both former U mines was characterized. The assessment of the key physicochemical parameters, specifically pH, redox potential (E_H), temperature, total organic carbon (TOC) and inorganic (TIC) carbon, dissolved organic carbon (DOC), total nitrogen (TN), cations (Na, K, Mg, Ca, Al, Si, P, Mn, Ba, Th, U) and anions (NO_2^- , NO_3^- , PO_4^{3-} , SO_4^{2-} , Cl^-) were carried out as described by Newman-Portela et al (2024). Prior to the determination of Fe and As the samples were treated by using nitric acid (HNO_3)/hydrogen peroxide (H_2O_2) digestions. To perform the geochemical analysis, an inductively

coupled plasma mass spectrometry (ICP-MS, ELAN9000, PerkinElmer, Germany), and high-performance ionic chromatography (HPIC, Dionex Integrion, Thermo Fisher Scientific, USA) were used. ICP-MS samples of each mine water were acidified using HNO_3 for cations analyses. TIC, TOC, DOC and TN were quantified by Multi N/C 2100S (Analytik Jena, Germany). All assays were done in triplicates. *In situ* measurement of mine water temperature was conducted using a standard thermometer. The pH and redox potential (E_{H}) were assessed *on site* by a pH meter (pH 3110, WTW, Germany) equipped with a BlueLine 16 pH microelectrode (Schott Instruments, Germany) and a micro redox electrode featuring a platinum ring (ORP electrode, Mettler-Toledo InLab, Spain), respectively.

2.3. Nucleic acids: sample preparation, extractions, amplification and sequencing

For RNA and DNA analysis, 800 mL of mine water was filtered separately through sterile membrane filters with pore sizes of 0.45 μm and 0.20 μm (Membrane Filter, MF-Millipore®, Germany). The filters for RNA extraction were promptly frozen using liquid nitrogen and stored at $-120\text{ }^\circ\text{C}$, while filters for DNA extractions were stored at $-20\text{ }^\circ\text{C}$. Both DNA and RNA extraction were conducted in three biological replicates.

2.3.1. DNA extraction and 16S rRNA sequencing

Each filter from above-mentioned was cut into four portions. Three of these portions were used for DNA extraction, while the fourth portion was stored $-20\text{ }^\circ\text{C}$ as backup. The DNA extraction was carried out using DNeasy PowerWater kit (QIAGEN, Germany) following the manufacturer's instructions. The quality and concentration of the extracted DNA were checked using agarose gel electrophoresis (0.75%) and the Qubit Fluorometer 4.0 (Thermo Fisher Scientific, USA) with the Qubit dsDNA HS Assay kit, respectively. The DNAs extracted from the three filter pieces were pooled together and considered as a biological replicate. The samples were amplified using Illumina barcoded 16S rRNA gene primers as previously described (Newman-Portela et al. 2024), with forward primer 341F (5'-CCTACGGGNGGCWGCAG-3') and the reverse primer 785R

(5'-GACTACHVGGGTATCTAATCC-3') targeting the hypervariable V3-V4 regions (Thijs et al. 2017). The 16S amplicon sequencing was carried out on Illumina MiSeq (300bp base-paired) platform at STAB-VIDA (Caparica, Portugal, <https://www.stabvida.com/es>).

2.3.2. RNA extraction and Metatranscriptome sequencing

Total RNA was extracted from each sample filter cut into four portions. The RNA extracted from the filter pieces was pooled and considered as a biological replicate. RNeasy PowerWater kit (QIAGEN, Germany) was used following the manufacturer's instructions and an on-column DNase digesting step was included. RNA concentrations were quantified fluorometrically via Qubit Fluorometer 4.0 (Thermo Fisher Scientific, USA) with the Qubit RNA HS Assay kit. RNA integrity number (RIN) was assessed using the Agilent 2100 Bioanalyzer (Agilent Technologies, Palo Alto, California) at the STAB-VIDA laboratories (STAB-VIDA, Portugal). The total RNA extracted from three biological replicates of mine water from Schlema-Alberoda (n=3) and Pöhla (n=3) were used for library construction (rRNA depletion) and metatranscriptome sequencing (STAB-VIDA, Portugal). The generated libraries were sequenced on a Illumina Novaseq platform (150 bp paired-end).

2.4. Community structure and gene analysis

2.4.1. 16S rRNA gene bacterial diversity analyses and biostatistics

16S rRNA gene amplicon sequencing was performed as previously described in Newman-Portela et al. (2024). Briefly, FastQC was used for the quality control of the raw DNA sequence data (Andrews 2010). Raw sequences were analysed by QIIME2 (Quantitative Insights into Microbial Ecology) (Caporaso et al. 2010; Bolyen et al. 2019) pipeline using DADA2 (Divisive Amplicon Denoising Algorithm 2). DADA2 were used to denoise the reads, including trimming and truncating low-quality regions, dereplicating the reads, filtering chimeras, inferring the amplicon sequence variants (ASVs) present and assigning taxonomy using a scikit-learn classifier pre-trained on SILVA (release 138 QIIME) for bacterial sequences with a clustering threshold of 97% similarity (Quast et al. 2013;

Callahan et al. 2016). ASVs containing at least 10 sequence reads were considered dominant in our analysis.

Alpha diversity was measured considering Chao1 metrics, Shannon index and Simpson index, using MicrobiomeAnalyst (v4.1.3) (<https://www.microbiomeanalyst.ca/> (accessed on 15 November 2023) (Fisher et al. 1943; Shannon 1948; Simpson 1949; Dhariwal et al. 2017). Beta diversity, similarity between taxa identities and their abundances per mine water sample were evaluated by permutational analysis of variance (PERMANOVA) using Bray-Curtis dissimilarities (Bray and Curtis 1957) and the result was visualised in a non-metric multidimensional scaling matrix (NMDS).

Additionally, bacterial taxa obtained from both mine waters were used for co-network analyses. Network analyses were performed in R using the “VEGAN” package (Oksanen et al. 2007). Only the strongest correlations ($\rho \geq 0.8$ and $\rho \leq -0.8$) were selected. For the construction and visualization of biological networks, the data were imported into Cytoscape software v.3.7.2 (Shannon et al. 2003).

2.4.2. Metatranscriptomic data processing and analysis

First, the Illumina adapters of forward and reverse reads, and the low-quality reads (QS<30) were removed using Cutadapt 4.2 (Martin 2011) and Trimmomatic v0.39 (Bolger et al. 2014), respectively. The SortMeRNA v2.1 (Kopylova et al. 2014) was then applied to filter remaining rRNA reads based on database constructed from LSU and SSU Silva 138.1 (Quast et al. 2013). Reads from all samples were assembled together to generate a single assembly using Trinity v2.14.0 (Grabherr et al. 2011). Functional genes of the assembled transcripts were predicted using Prodigal 2.6.3 (Hyatt et al. 2010). The read counts of each sample were estimated by mapping sequencing reads against the assembled transcripts using Bowtie2 2.5.1 (Langmead and Salzberg, 2012) and then quantified using featureCounts (Liao et al. 2014) under the Subread package 2.0.6. The generated count table was then applied to edgeR 4.0.15 (Robinson et al. 2010) for analysing differential gene expression (DGE) between microbial communities of

Pöhla and Schlema-Alberoda mine water with biological triplicates. Genes with fold change values of ≥ 2 , false-discovery-rate (FDR) values of ≤ 0.05 were designated DGE with significance.

The DGE of Pöhla and Schlema-Alberoda mine water were annotated against the KEGG Orthology database using GhostKOALA (Kanehisa et al. 2016a, b), and the completeness of each KEGG metabolic pathway was summarized using KEGG decoder (Graham et al. 2018). Then the overview of difference of significant KEGG metabolic pathways between Pöhla and Schlema-Alberoda communities was visualized by heatmap. The abundance of DGE (based on assigned KO, Table S6) involved in assimilatory and dissimilatory sulphate reduction was visualized using volcano plot in R. On the other hand, KEGG does not include iron reduction pathways; thus, FeGenie v1.2 (Garber et al. 2020) was applied to identify significantly expressed iron reduction genes in both mine water communities.

3. Results

3.1. Physicochemical parameters

The geochemical data from the current study demonstrate a notable similarity to the data reported in the prior year (Newman-Portela et al. 2024). This suggests a clear pattern of consistency, indicating stability in the geochemical parameters within the studied areas. Table 1 shows the measurements and the standard deviation of the physicochemical analyses conducted in the mine water of the Pöhla and Schlema-Alberoda. The results indicate a circumneutral pH (6.8 and 7.05) in the Pöhla and Schlema-Alberoda mine water, respectively. On the other hand, the E_H values ranged between -94 mV and $+89$ mV, evidencing reducing conditions in the Pöhla mine water. Furthermore, variability was observed in the electrical conductivity (EC) of the water, with values ranging from 0.485 mS/cm in the Pöhla mine water to 1.480 mS/cm in the Schlema-Alberoda mine water. Na and Ca are the predominant cations present in both, Pöhla and Schlema-Alberoda, mine waters. Their concentrations range between 21.9 mg/l and 101 mg/l for Na, and between 48.3 mg/l and 129 mg/l for Ca. Likewise, the concentrations of Mg, K and Mn are higher in Schlema-Alberoda compared

to Pöhla. They differ between 87.5 mg/l and 16 mg/l for Mg, 10 mg/l and 5.63 mg/l for K, 1.53 mg/l and 0.53 mg/l for Mn. The Fe concentrations measure 2.84 mg/l in Schlema-Alberoda and 4.75 mg/l in Pöhla. Regarding U concentration, the Schlema-Alberoda mine water (1.1 mg/l) is still two orders of magnitude higher compared to Pöhla (0.01 mg/l).

The SO_4^{2-} content in mine water ranged from 0.8 mg/l in Pöhla to 311 mg/l in Schlema-Alberoda. In the mine water of Schlema-Alberoda a higher concentration of TIC (99.8 mg/l) was observed, compared to the concentration measured in Pöhla (56.6 mg/l). However, in both mines, similar values for TOC and DOC were measured.

Table 1. Chemistry of the Schlema-Alberoda and Pöhla mine water.

	Schlema-Alberoda	Pöhla
Date	08.07.2021	08.09.2021
pH	7.05 ±0.1	6.8 ±0.1
E _H [mV]	+ 89 ±20	- 94 ±20
EC [mS/cm]	1.480	0.485
Temp. [°C]	25.4 ±1	18.6 ±1
Cations [mg/L]		
Na	101 ±1.40	21.9 ±0.44
Mg	85.7 ±1.23	16.0 ±0.32
Al	< 0.01	< 0.01
Si	7.26 ±0.09	10.5 ±0.23
K	10.3 ±0.04	5.63 ±0.09
Ca	129 ±1.53	48.3 ±0.55
Mn	1.53 ±0.01	0.15 ±0.004
Fe	2.84 ±0.02 *	4.75 ±0.02 *
As	1.17 ±0.03 *	1.83 ±0.03 *
Ba	0.03 ±0.001	1.70 ±0.024
Th	< 0.001	< 0.001
U	1.10 ±0.022	0.011 ±0.001
Anions [mg/L]		
Cl ⁻	48.5 ±1.465	3.57 ±0.122
NO ₂ ⁻	< 0.05	< 0.05
NO ₃ ⁻	0.378 ±0.006	0.302 ±0.005
PO ₄ ³⁻	< 0.05	< 0.05
SO ₄ ²⁻	311 ±7.744	0.811 ±0.01
[mg/L]		
TIC	99.8 ±0.319	56.6 ±0.685
TOC	5.3 ±0.089	5.17 ±0.057
DOC	5.0 ±0.067	5.0 ± n.d.
TN	< 0.1	0.26 ±0.007

TIC: total inorganic carbon; TOC: total organic carbon; TN: total nitrogen; EH: redox potential; EC: conductivity, Standard deviation with n=3; n.d. = not determined; * analysed by Wismut GmbH (ICP-analysis without centrifugation prior to acidification)

3.2. Bacterial Community

3.2.1. Alpha and beta diversity

Shannon, Chao1 and Simpson indices were used to determine alpha diversity (Table S1) within the microbial communities of both mine waters. The alpha diversity analysis revealed no significant differences, regardless of the index used ($p > 0.1$). In terms of species richness, the Chao1 estimator showed higher values associated with the Pöhla mine water samples (from 117 to 126) and lower values (from 74 to 88) associated with the Schlema-Alberoda mine water samples. As for the Shannon diversity index, the values obtained were higher in the Pöhla mine water (2.969 to 3.162) than in the Schlema-Alberoda mine water (2.313 to 2.518). Finally, through Simpson's index, the values found showed highly heterogeneous communities and no dominance of taxa (higher than 0.809). The values found are close to 1, and both communities can be considered heterogeneous. Although, a slightly more diverse bacterial community was observed in the Pöhla mine water samples than in the Schlema-Alberoda samples.

Beta diversity revealed no significant differences ($p > 0.1$) in the structure and abundance of the bacterial community at the genus level, as per PERMANOVA analysis (F: 114.37; R-squared: 0.96621; p : 0.1). Non-metric multidimensional scaling (NMDS) based on Bray-Curtis dissimilarity matrices visualized the variation in bacterial community composition with low stress (Stress: 0) among samples. However, NMDS revealed no clear correlations between the compared microbial communities (Fig. S1).

3.3. Variations in bacterial community composition

Most of the samples generated in the range of 71,260 to 85,250 raw sequencing reads, as detailed in Table S2, which is consistent with the expected result of around 100,000 sequencing reads. After taxonomic classification, a total of 190 ASVs were identified (Table S3), distributed in 40 phyla (Table S4). Within these phyla, 8 belonged to the Archaea domain (1.84%), while 32 were assigned to the Bacteria domain (98.10%). The remaining 0.06% were classified as "unassigned".

In the taxonomic analysis of the bacterial communities, it was observed that Campilobacterota (46.85%) and Proteobacteria (20.37%) were the most predominant bacterial phyla in both mine waters, followed by Patescibacteria (8.31%), Nitrospirota (6.05%), Verrucomicrobiota (4.55%), Chloroflexi (3.85%), Desulfobacterota (1.64%), Actinobacteriota (1.15%), Bacteroidota (1.13%), and Acetothermia (1.02%). Regarding the Archaea community, the predominant phylum was Nanoarchaeota (0.88%) (Fig. 1, Table S4). Uncultured delta proteobacterium Sva0485 and Planctomycetota were also identified with a relative abundance of ~1%.

The mine waters showed a strong presence of the genus *Sulfuricurvum*, with a mean relative abundance of 22.01% in Schlema-Alberoda and 12.18% in the Pöhla mine water (Fig. 2, Table S3). In particular, the Schlema-Alberoda mine water was characterised by a higher mean relative abundance than the Pöhla mine water for several bacterial genera, such as *Sulfurimonas* (30.98%), unidentified *Gallionellaceae* (15.01%), uncultured *Hydrogenophilaceae* (7.39%), *Desulfurivibrio* (2.49%), *Gallionella* (1.45%), *Flavobacterium* (1.79%), *Sideroxydans* (1.47%) and *Limnohabitans* (1.20%) (Fig. 2, Table S3).

In contrast, the Pöhla mine water was dominated by several bacterial genera with a higher mean relative abundance than Schlema-Alberoda, including *Sulfurovum* (28.43%), uncultured *Thermodesulfovibrionia* (10.54%), *Candidatus Omnitrophus* (5.58%), unidentified *Rhodocyclaceae* (4.37%), *Candidatus Moranbacteria* (3.39%), *Candidatus Magasanikbacteria* (2.36%), *Sulfuritalea* (2.19%), GIF9 (1.85%), *Acetothermia* (1.86%), GIF3 (1.36%), *Thiovirga* (1%), WCHB1-81 (1.29%), Sva0485 (1.32%), *Candidatus Woesebacteria* (1.28%) and *Parcubacteria* (1.11%) (Fig. 2, Table S3). Furthermore, the family *Geobacteraceae* and the genus *Desulfobacca* were exclusively identified in Pöhla mine water, with a relative abundance of less than 0.5%.

3.4. Co-occurrence networks

The exploration of co-occurrence networks is a useful method for determining the biological interactions occurring within microbial communities. Here, we have established a framework for generating co-occurrence networks

and comparing the relationships among bacterial groups at phylum level and key environmental parameters (U, Fe, and SO_4^{2-}), considering only strong correlations ($\rho > 0.8$ or $\rho < -0.8$). Figure 3 showed a total of 31 nodes (28 bacterial phyla, and 3 environmental parameters) and 345 edges between both mine waters. Positive correlations between nodes are shown in blue. Conversely, negative correlations are represented in pink.

A complex network with noteworthy interactions was obtained, mostly influenced by Dependientiae and Zixibacteria, which stand out for the number of connections with other groups. Furthermore, some bacterial phyla such as Acetothermia, Firmicutes, Actinobacteriota, Cyanobacteria, Bacteroidota, Planctomycetota, and Spirochaetota, along with archaeal phyla such as Iainarchaeota, Halobacterota, and Thermoplasmatota, emerged as key phyla, showing solid positive correlations with other groups in the community.

The main physicochemical factors showed a strong correlation with different bacterial groups. U and Fe were found to be positively correlated to Campilobacterota, Acidobacteriota, Cyanobacteria, Desulfobacterota, and Bacteroidota. On the other hand, Proteobacteria showed correlations with U, and SO_4^{2-} . Additionally, SO_4^{2-} was positively correlated with Acidobacteriota, Cyanobacteria, Desulfobacterota, and Bacteroidota. Furthermore, U was positively correlated with SO_4^{2-} , and Fe. In contrast, neither Dependientiae nor Zixibacteria showed positive correlations with any of the selected parameters.

Fig. 1. Barplot of the taxonomic distribution of bacterial diversity in the water samples from the Pöhla (P1; P5; P8) and Schlema-Alberoda mines (S1; S2; S6) at phylum level. Each sample comprises three replicates. Only the phyla identified in the three replicates with >0.5% relative abundance were included, while the remaining ones were included in “others”.

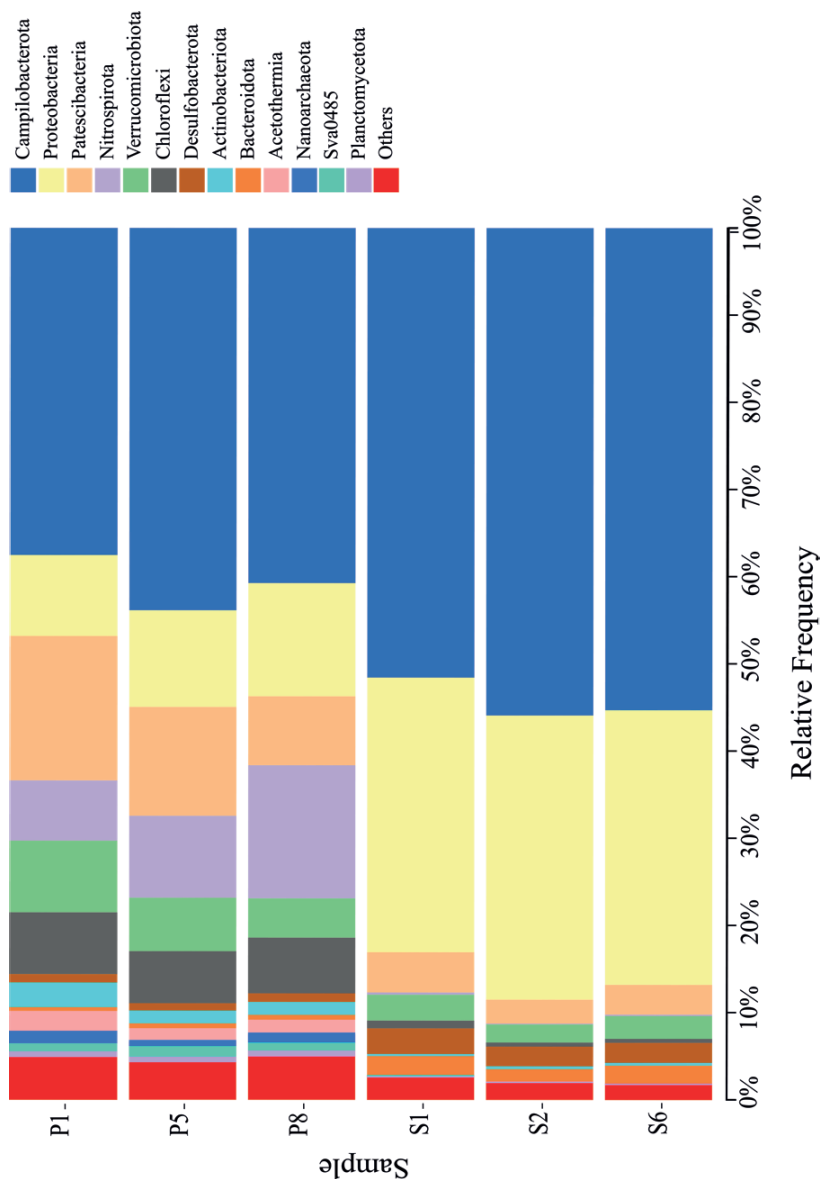
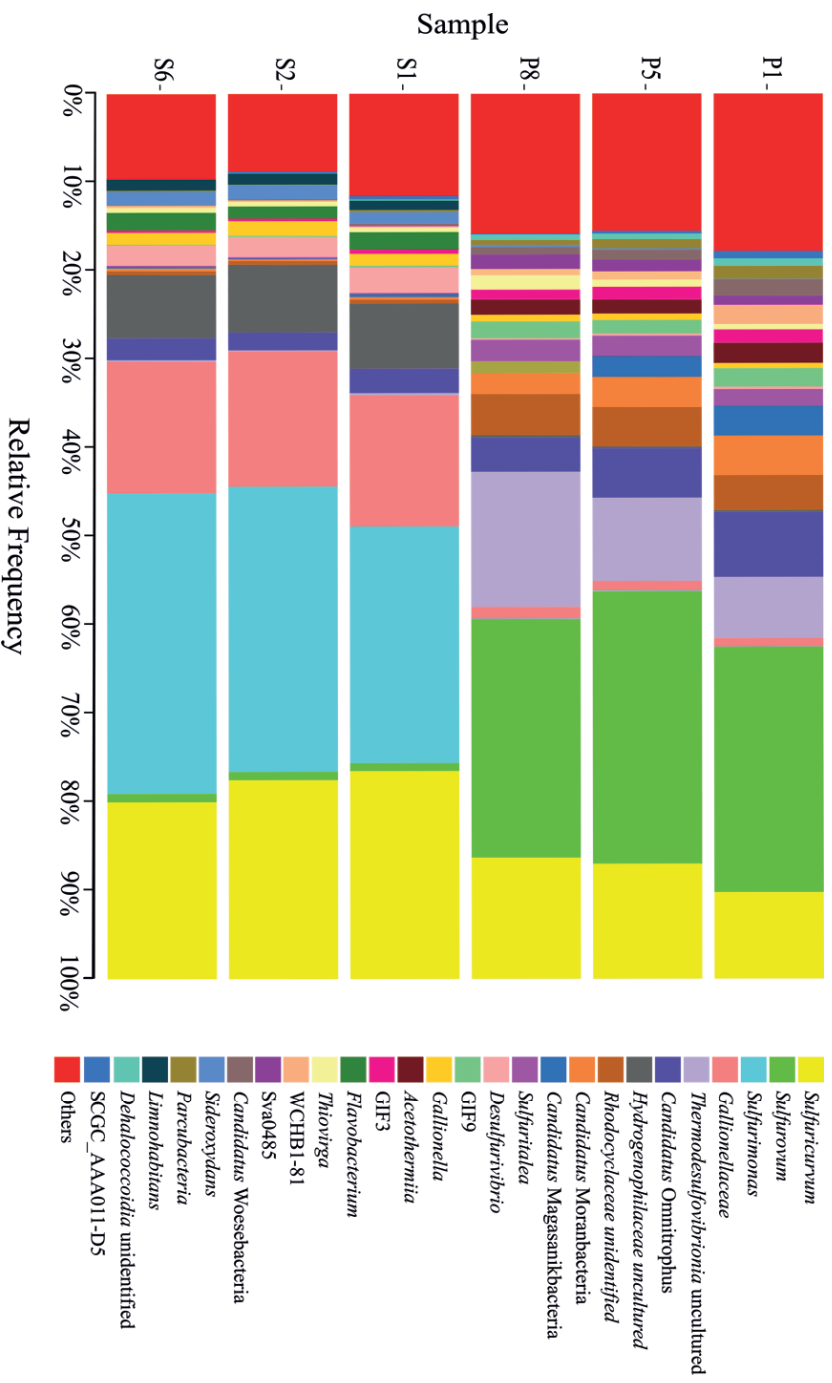


Fig. 2. Barplot of the taxonomic distribution of bacterial diversity in the water samples from the Pöhla (P1; P5; P8) and Schlemma-Alberoda mines (S1; S2; S6) at genus level. Each sample comprises three replicates. Only the genera identified in the three replicates with >0.5% relative abundance were included, while the remaining ones were included in “others”.



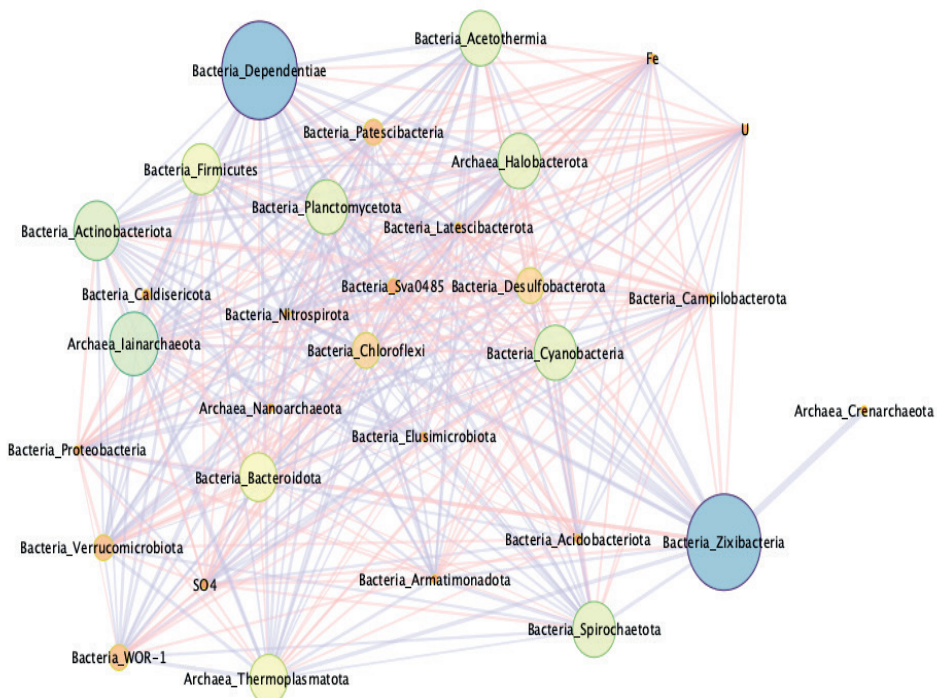


Fig. 3. Network analysis revealing co-occurrence patterns among bacterial taxa from Schlema-Alberoda, and Pöhla mine water, and the main physicochemical parameters (U, Fe, and SO_4^{2-}). Edges are coloured according to a positive correlation (in blue) and a negative correlation (in pink). Each connection represents strong correlations based on Pearson's correlation coefficient ($\rho \geq 0.8$ and $\rho \leq -0.8$). The size of the circle (node) is proportional to the number of correlations applying the betweenness centrality index.

3.5. Metatranscriptome sequencing

In total, the Illumina Novaseq platform generated 66 to 70 million reads (150 bp) for each of the 6 samples (Table S5). The comparison between the two mine waters revealed the differential expression of 202,391 genes, with 98,579 genes transcribed in the mine water of Pöhla, while 103,812 genes were significantly expressed in the mine water of Schlema-Alberoda (Fig. S2).

3.6. Functional profile of the microbial community in mine waters

A functional profile characterization has been carried out to explore potential metabolic pathways and adaptations of microbial populations in the mine waters of Schlema-Alberoda and Pöhla. A modified heatmap with the most 188

relevant metabolic pathways of Schlema-Alberoda and Pöhla is shown in Figures 4 and 5. Meanwhile, Figures S3 and S4 showed the total identified metabolic pathways of Schlema-Alberoda and Pöhla, respectively. The composition of these transcriptionally active genera detected in the mine water samples was very similar to that of the bacterial community previously reported by 16S rRNA gene sequencing analysis in this study and in the samples collected in 2020 (Newman-Portela et al. 2024).

Expression of functions related to “carbohydrate metabolism” and “energy production” such as glycolysis and tricarboxylic acid (TCA) cycle were detected in both samples and assigned to genera such as *Ferrigenium*, *Sulfuricurvum*, and *Sulfurimonas* in both mine water samples. Additionally, the potential for “carbon fixation” was primarily inferred through the Calvin-Benson-Bassham (CBB) and reverse tricarboxylic acid (rTCA) pathways and attributed to the genera *Sulfuritaela*, *Sulfuriferula*, *Thiothrix* and *Ferriphaselus*, among others. Noteworthy overexpression of the enzyme RuBisCo was observed in both Schlema-Alberoda and Pöhla, especially in *Sulfuritaela*, *Thiobacillus*, *Hydrogenophaga*, *Ferriphaselus*, and *Thiothrix*. Furthermore, pathways encoding for “amino acid (AA) metabolism”, such as glycine, histidine, and cysteine, among other amino acids, were observed to be highly active. Moderate expression levels of “anaplerotic genes” were identified in both mine waters, which are used to replenish TCA cycle intermediates.

Metabolic pathways associated with “flagellum biosynthesis” and “chemotaxis” were considered highly overexpressed in both mine waters. Genera such as *Methylobacter* and *Sulfurimonas*, among others, encode pathways for “flagellum production” and “chemotaxis” exhibiting higher activity in Schlema-Alberoda, and *Sulfuricurvum* showed high regulation in both pathways, in both Schlema-Alberoda and Pöhla mine waters.

3.6.1. Nitrogen and sulphur metabolism

The metabolic pathways involved in denitrification were also considered. A higher activity in the microbial community of the Schlema-Alberoda mine water was detected compared to that of the Pöhla mine water regarding the encoding of pathways related to nitrogen (N) metabolism. Dissimilatory

nitrate reduction pathways (to nitrite), nitrate oxidation, nitric oxide reduction, and nitrous-oxide reduction were present only in the Schlema-Alberoda mine water. Both Pöhla and Schlema-Alberoda mine waters showed expression profiles for nitrite reduction and N fixation.

In Schlema-Alberoda, nitrite reduction pathway was attributed to the genera *Sulfuritortus*, *Sulfuritaela*, *Dechloromonas*, *Sulfurimicrobium*, and *Sulfurimonas* (Fig. 4). In addition, dissimilatory nitrate reduction pathway was assigned to *Sulfuritortus*, *Thihalomonas*, *Sulfuricurvum*, and *Sulfurimonas*. Only genera *Sulfuritortus* and *Thihalomonas* were associated with nitrite oxidation. Additionally, nitrous oxide reduction was encoded by *Sulfurisoma*, *Shpaerotilus*, *Dechloromonas*, and *Sulfurimonas*. *Sideroxidans* was solely responsible for N fixation although the pathway is incomplete. Regarding Pöhla mine water, only genes associated with nitrite reduction and N fixation were detected, and attributed to *Dechloromonas* and *Sulfurimonas*, and *Sulfuricurvum*, respectively. *Dechloromonas*, *Sulfurimonas*, and *Gallionella* contributed to nitric oxide reduction.

Sulphur metabolism could play a significant role in U reduction, and notable expression profiles of various metabolic pathways, including genes involved in both sulphur oxidation and sulphate reduction, were observed in both mine waters. Reversible dissimilatory sulphate reduction was identified. These cover the complete reduction of sulphate to sulphide, as they encode enzymes responsible for sulphate reduction to sulphite. In Schlema-Alberoda, while the genera *Sideroxydans*, *Desulfurivibrio*, and *Thiothrix* cover both pathways, “dissimilatory sulphate < > APS”, and “dissimilatory sulphite < > APS”, *Sulfurisoma*, *Sulfuricurvum*, and *Sulfurimonas* encode only the “dissimilatory sulphate < > APS” pathway. In contrast, in Pöhla, the genera *Thiobacillus*, *Sulfuritaela*, *Sulfurisoma*, *Sideroxydans*, and *Desulfobacca* covered both pathways. *Sulfuritortus*, *Sulfuriferula*, *Sulfuricurvum*, *Sulfurovum* encoded only for the “dissimilatory sulfate < > APS” pathway. Likewise, *Thihalomonas*, and *Sulfurimicrobium* for the “dissimilatory sulfite < > APS” pathway.

High regulation for sulphide oxidation was observed in both mine waters. This could be a possible energy production pathway. *Caulobacter*,

Ferrigenium, *Methylobacter*, *Sulfuricurvum*, *Sulfurimonas*, *Sulfurisoma*, *Sulfuritalea*, *Sulfurovum*, and *Sideroxydans* encoded sulphide oxidation in both mines. Exclusively in Pöhla, genes encoding for sulphide oxidation were also expressed by genera like *Dechloromonas*, *Ferriphaselus*, *Gallionella*, *Methylococcus*, *Rhodoferrax*, and *Sulfuricaulis*. In the case of Schlemma-Alberoda, *Flavobacterium*, *Methylobacillus*, *Sulfuritortus*, *Thiobacillus*, *Thiohalomonas*, and *Thiothrix* encoded sulphide oxidation. Thiosulfate oxidation was also detected in both mine waters, but with highly incomplete pathway.

3.6.2. Heavy metals

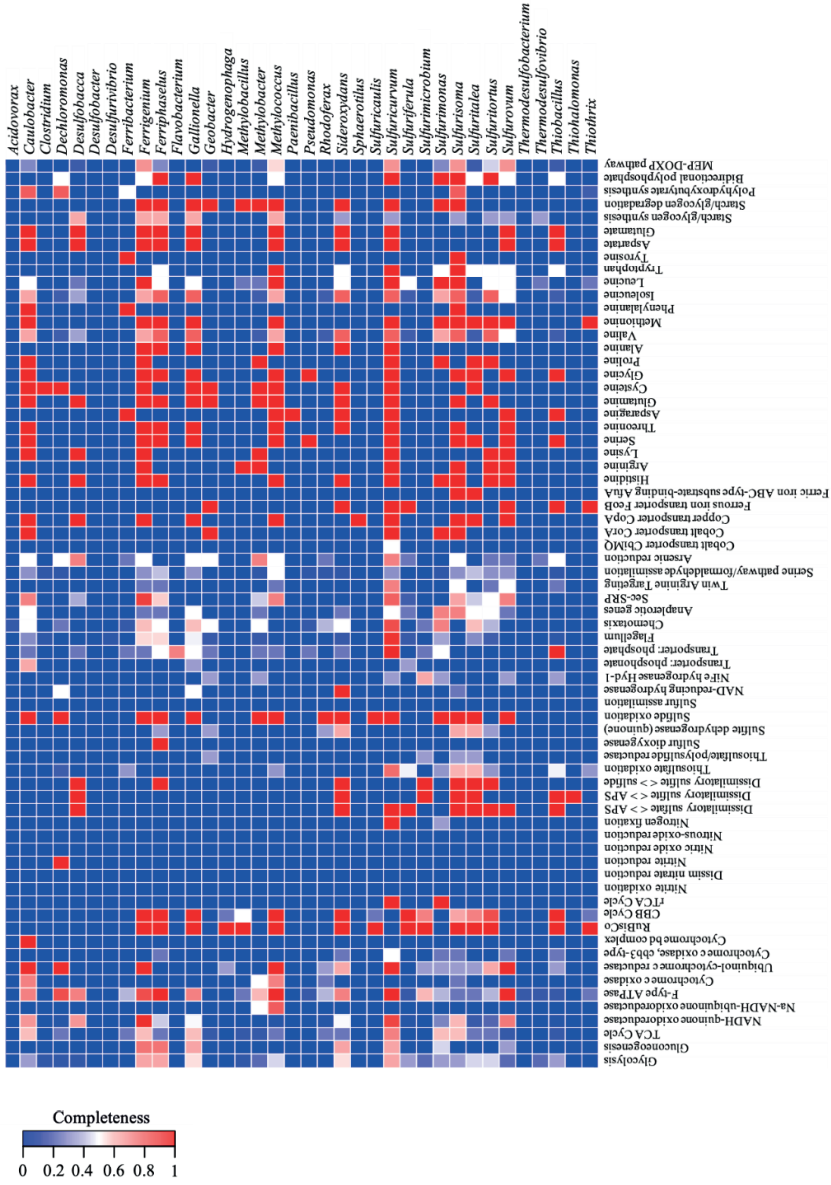
In addition to pathways related to N, S, and carbon metabolisms, the expression response to different types of stressful situations is detected. This is due to the challenging environment that the adverse conditions impose on the microbial community, such as the presence of heavy metals and radionuclides.

An increase in the expression of hydrogenase activity (e.g., NiFe-hydrogenase) was observed in both types of mine water. A wide variety of microbial groups use molecular hydrogen as electron donor to reduce contaminants, suggesting that hydrogenase activity could have promising applications in the bioremediation of heavy metals and radionuclides. Additionally, strong positive regulation of cytochromes was detected, especially cytochrome c oxidase and ubiquinol-cytochrome c reductase. The high expression of these cytochromes could be related to energy metabolism, especially those involved in electron transfer, such as type c cytochromes. “Oxidative phosphorylation” may occur through ATP synthase type F, ubiquinol-cytochrome c reductase, cytochrome c oxidase (type cbb3), and the cytochrome bd complex. Additionally, these cytochromes may play a significant role in U reduction (Rogiers et al. 2022). Our results showed the nearly complete expression of genes related to pathways for “arsenic reduction”. This implies the existence of a specific set of genes and proteins responsible for carrying out the biological transformation of As in both mine waters, suggesting a high potential microbial community to reduce As levels (Mohsin et al. 2023).

3.6.3. Transporters

Figures 4 and 5 show the expression of several genes coding for transporters, which are involved in the transport of cations, molecules, metabolites, nutrients, among others. A considerably high level of ionic transporters was observed, such as cobalt transporter (CbiMQ, CorA), copper transporter (CopA), iron transporters, and ATP-dependent ABC-type transporters (Ferric iron ABC-type substrate-binding AfuA). Additionally, high expression of phosphate transporters was identified.

Fig. 5. Summarized metabolic pathway heatmap of Pöhla. The heatmap represents metabolic pathway completeness based on the presence or absence of genes as determined by KEGG Decoder. Dark red (the colour scale is shown) represents a complete or highly complete pathway, while blue represents locations where a pathway is absent or highly incomplete.



3.7. Main genes expressed in sulphate and iron reduction in Schlema-Alberoda and Pöhla mine water

3.7.1. Key genes in sulphate reduction

Genes related to dissimilatory sulphate reduction (DSR) were identified in both mine water samples (Table S6 and Fig. 6). These genes include *sat* (sulphate adenylyltransferase (K00958)), *aprAB* (subunit A (K00394) and subunit B (K00395) of adenosine-5'-phosphosulfate reductase), and *dsrAB* (alpha subunit (K11180) and beta subunit (K11181) of dissimilatory sulphite reductase). The expression of the genes identified in assimilatory sulphate reduction (ASR) is shown in Figure 7. The following genes involved in ASR have been identified: *sat*, encoding sulphate adenylyltransferase (K00958); *cysJ* and *cysI*, encoding the alpha flavoprotein of sulphite reductase (NADPH) (K00380) and the beta component of the hemoprotein (K00381), respectively; *cysH*, encoding phosphoadenosine phospho sulphate reductase (K00390); *cysNC*, encoding the bifunctional enzyme CysN/CysC (K00955); *cysN* and *cysD*, encoding subunit 1 (K00956) and subunit 2 (K00957) of sulphate adenylyltransferase; *cysC*, encoding adenylylsulphate kinase (K00860); *sir*, encoding sulphite reductase (ferredoxin) (K00392); and *PAPSS*, encoding 3'-phosphoadenosine 5'-phosphosulfate synthase (K13811).

Our results showed higher expression for genes involved in DSR than ASR as shown in Figures 6 and 7. However, there is clearly higher expression in all genes encoding for DSR in Pöhla than in Schlema-Alberoda. Conversely, there is an opposite effect observed in genes encoding for ASR, with a higher expression in Schlema-Alberoda than in Pöhla. No expression for *PAPSS* and *sir* was observed in Pöhla. This suggests that the ASR pathway might be incomplete in Pöhla, as sulphite cannot be reduced to sulphide due to the absence of *sir*.

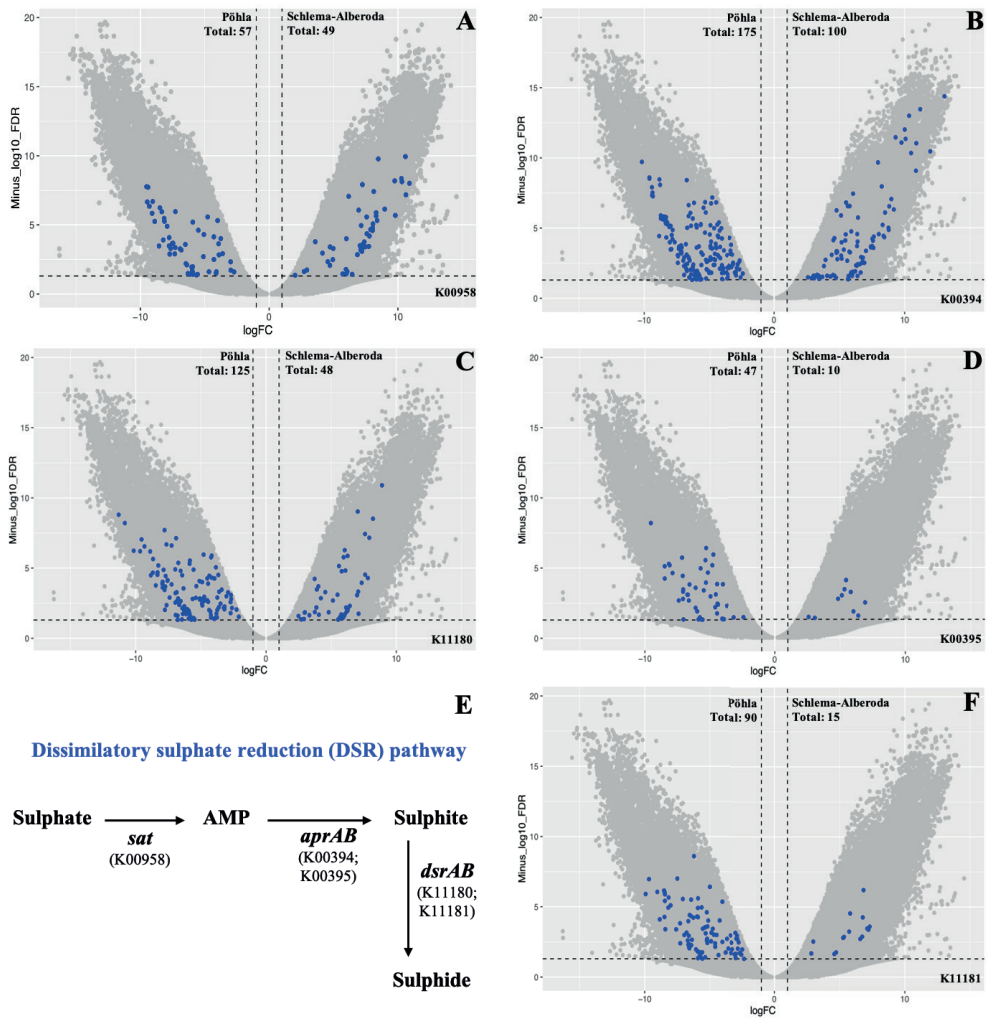


Fig. 6. Volcano plot of differentially expressed genes of dissimilatory sulphate reduction (DSR) in Pöhla mine water (left) and Schlema-Alberoda (right). A: *sat* (K00958); B: *aprA* (K00394); C: *aprAB* (K00395); D: *dsrA* (K11180); E: *dsrB* (K11181); F: DSR pathway.

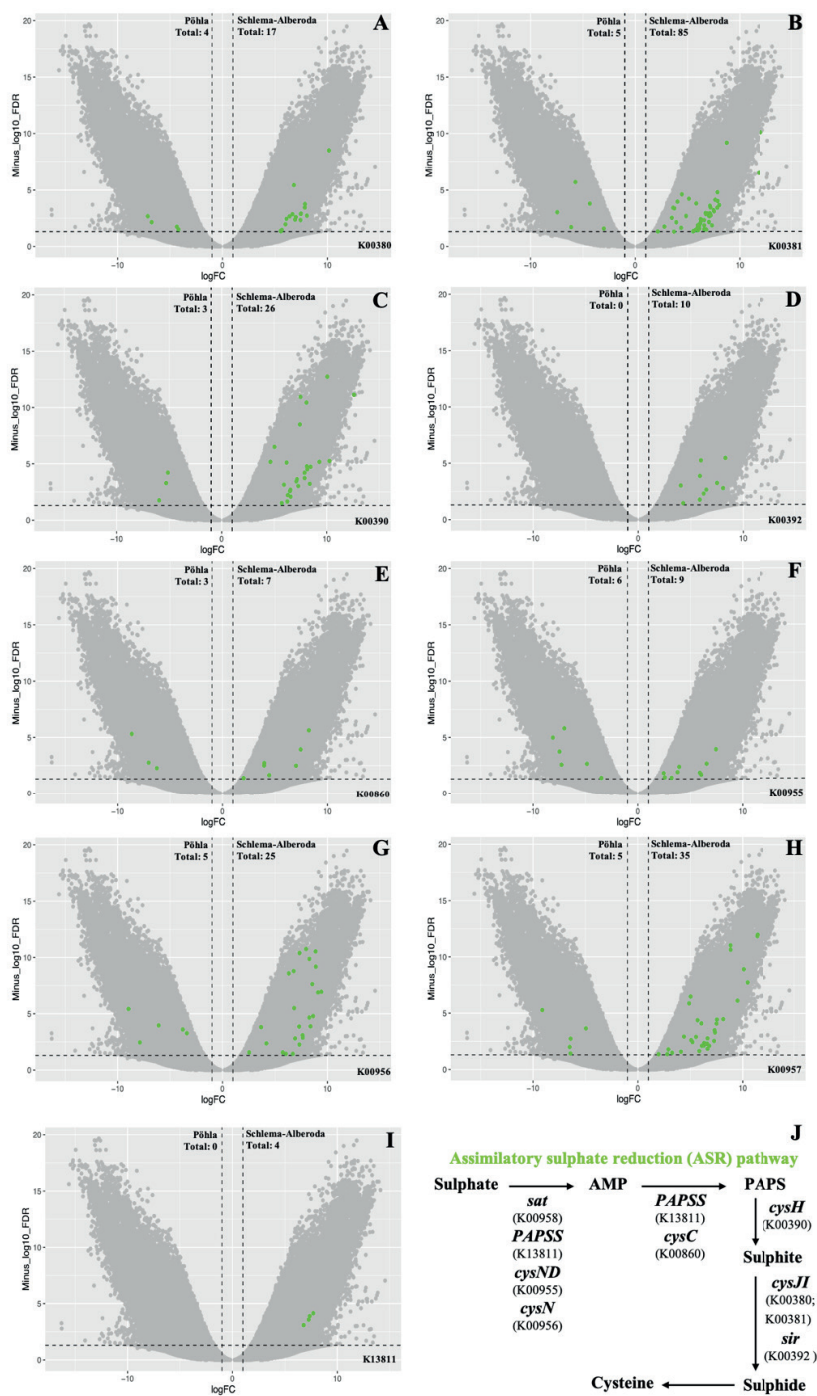


Fig. 7. Volcano plot of differentially expressed genes of assimilatory sulphate reduction (ASR) in Pöhla mine water (left) and Schlema-Alberoda (right). A: *cysJ* (K00380); B: *cysI* (K00381); C: *cysH* (K00390); D: *sir* (K00392); E: *cysC* (K00860); F: *cysND* (K00955); G: *cysN* (K00956); H: *cysD* (K00957); I: *PAPSS* (K13811); J: ASR pathway.

3.7.2. Key genes in Fe reduction

Different genes linked to Fe biogeochemical processes such Fe reduction, Fe oxidation, Fe storage and regulation were identified in the studied mine waters with different proportions. Regarding the genes associated with iron reduction, the findings from the identification of significantly expressed genes in both mine water communities indicated the presence of only two genes linked to dissimilatory iron reduction in Pöhla mine water (*omcS* (547981_1 and 237412_1)), while none were identified in Schlema-Alberoda mine water (Table S7). *OmcS* has been previously reported to play a significant role in electron transfer in biogeochemical redox cycles of elements like Fe and U and environmental bioremediation of metals and toxic organic compounds (Orellana et al. 2013). Additionally, a high expression of genes associated with Fe oxidation, Fe accumulation, and Fe regulation was observed in both mine waters (Table S7). However, a higher regulation was identified in Pöhla than in Schlema-Alberoda mine water sample.

4. Discussion

4.1. Physicochemical and microbiological characterisation of mine water samples

Successfully, the water samples from Schlema-Alberoda and Pöhla mine were previously characterized in terms of both geochemistry and the composition of the native microbial community (Newman-Portela et al. 2024). It was reported that the most prevalent bacterial phyla were Campilobacterota, Proteobacteria, and Patescibacteria. The present study aimed to investigate the effect of sampling time on the microbial activity in both mine waters, as well as on the microbial community composition considering the 2020 and 2021 sampling campaigns. However, no differences were observed in the bacterial community at the phylum level when comparing the sampling in 2020 and 2021. Also in 2021, Campilobacterota, Proteobacteria,

and Patescibacteria represented the dominant bacterial phyla in both mine waters, followed by Nitrospirota, Verrucomicrobiota, Chloroflexi, Actinobacteriota, and Desulfobacterota, among others. On the other hand, results obtained from co-occurrence network analysis provide insights into biological interactions within the microbial communities under study (e.g., Proteobacteria-U; Desulfobacterota-SO₄²⁻). The observed complex network reflects dynamic interconnections among various bacterial phyla and key environmental parameters, suggesting a highly interdependent community. For instance, the co-occurrence pattern among Campilobacterota, Acidobacteriota, Cyanobacteria, Desulfobacterota, and Bacteroidota may indicate sharing similar ecological niches, as they all could use Fe and U as electron acceptors, thus potentially competing from this view (Jiang and Hur 2012; Embree et al. 2014).

Regarding physicochemical parameters, the waters from Schlema-Alberoda and Pöhla mines kept a circumneutral pH (6.8 and 7.05). Additionally, Pöhla mine water showed a low E_H (-94 mV) compared to Schlema-Alberoda mine water (+89 mV). This reveals higher reducing conditions in Pöhla, which were not observed in Schlema-Alberoda. Physicochemical patterns often shape the structure and composition of the microbial community. Therefore, we further evaluated differences between the major microbial communities at the genus level in both mine waters, based on their environmental drivers (e.g., U, Fe, As, NO₃⁻, and SO₄²⁻). Bacteria involved in the N/S cycle (e.g., *Sulfuricurvum*, *Sulfurovum*, *Sulfurimonas*, *Sulfuritaela*, *Desulfurivibrio*) showed no considerable changes in relative abundance in comparison to the data of 2020 (Newman-Portela et al. 2024). These bacterial groups play a key role in U reduction (e.g., SRB such as *Desulfobacca*) and also in maintaining the stability of reduced U (e.g., nitrate-reducing bacteria (NRB) such as *Sulfuricurvum*, and sulphur-oxidizing bacteria (SOB) such as *Sulfurimonas*). No notable changes were observed in U and As concentrations. Conversely, changes in the concentration of Fe compared to the previous year were observed, possibly due to the sample preparation (Newman-Portela et al. 2024), as there were no changes in Fe concentration over the years according to data reported

by Wismut GmbH. In the present study, we found similar bacterial genera that were also identified in 2020. These were an unidentified genus of the family *Gallionellaceae*, unidentified genus of the family *Rhodocyclaceae*, *Gallionella*, and *Sideroxydans*.

4.2. Functional profile of the mine water microbial community

Schlema-Alberoda and Pöhla are two complex systems where the role of the microbial community could play an important function in the biogeochemical cycle of elements including U, Fe, and SO_4^{2-} (e.g., metal-reducing bacteria, and sulphate-reducing bacteria). Various metabolic pathways associated with carbohydrate degradation, oxidative phosphorylation, and S, N, and AA metabolisms, among others were shown in this study (Figures 4 and 5). Our results demonstrated the use of carbon in the metabolic dynamics of the bacterial community in both mine waters. *Sulfuritaela*, among others, possesses the complete set of genes for carbon fixation through the CBB cycle, including the gene encoding for RuBisCO (ribulose 1,5-bisphosphate carboxylase/oxygenase), a key enzyme in the CBB cycle catalysing CO_2 fixation. Additionally, the identification of the rTCA cycle in some microbes (*Sulfurimonas* and *Sulfuricurvum*) suggests that this pathway could be a probable mechanism of carbon incorporation. This suggests the possibility of autotrophic carbon assimilation in these micro-organisms.

Nitrate is a common co-contaminant in environments contaminated with U and can inhibit the reduction of U(VI). Microbe-mediated U reduction is usually limited under *in situ* conditions, often due to E_{H} , pH, limited electron donors, and the presence of competitive and energetically favourable terminal electron acceptors such as nitrate (Finneran et al. 2002). Low levels of nitrate were reported in the mine waters of Schlema-Alberoda and Pöhla (0.302 mg/l and 0.378 mg/l, respectively), probably due to microbial nitrate reduction by NRB. Nevertheless, the results showed a bacterial community in Pöhla where only *Dechloromonas* is positively related with nitrate reduction. In contrast, the bacterial community in Schlema-Alberoda samples may be capable of reducing/oxidizing nitrates/nitrites and also fixing N. Dissimilatory nitrate reduction to nitrite was found in various microbes (*Sulfuritortus*, *Thihalomonas* *Sulfuricurvum*,

and *Sulfurimonas*). Interestingly, nitrate reduction was found in both *Sulfurimonas* and *Sulfuricurvum*, and furthermore, both were found in higher relative abundance in Schlema-Alberoda (Newman-Portela et al. 2024). Both bacteria are able to oxidize reduced S compounds and using nitrate as a terminal electron acceptor (Lahme et al. 2019; Cron et al. 2019). Therefore, it is important to consider the dynamics between both cycles/metabolisms (N and S) as it may play a role in the stability of reduced U species by coupling nitrate reduction to the oxidation of S compounds and subsequently promoting the growth of metal-reducing micro-organisms such as SRB (e.g., *Desulfobacca*) (Chang 2005; Huang et al. 2021). Based on this, both SRB and NRB play a variety of important roles in mine water geochemistry, and their combined action promotes the reduction of U(VI) and stabilization of U(IV) species.

Likewise, it is important to consider a potential abiotic indirect reduction of U(VI). For example, the hydrogen sulphide resulting from sulphate reduction by SRB can abiotically reduce U(VI) to U(IV) or react with iron to form ferrous sulphide precipitates that may reduce U(VI) (Boonchayaanant et al. 2010; Hyun et al. 2014). In relation to the S cycle, the concentration of sulphate in the mine water of Schlema-Alberoda was notably higher, approximately two orders of magnitude than in Pöhla mine water. High activity was observed in various pathways of the S cycle in both, Schlema-Alberoda and Pöhla samples. There are two types of bacteria that use S: sulphur oxidizing bacteria (SOB), which use reduced compounds (e.g., H_2S) as electron donors, and the SRB, which use oxidized forms of S (e.g., SO_4^{2-}) as electron acceptors. SRB play a crucial role in U(VI) reduction, generating U(IV) species. These bacteria, by reducing sulphate to sulphide, can create a reducing environment that promotes U reduction, transforming soluble U(VI) into insoluble U(IV) (Lovley et al. 1993; Townsend et al. 2021). Our results showed positive regulation encompassing complete sulphate reduction (“dissimilatory sulphate \rightarrow APS” and “dissimilatory sulphite \rightarrow APS) involving several bacteria. In Pöhla, the genus *Desulfobacca* showed a low relative abundance (<0.5%) according to the 16S rRNA gene sequencing results. In addition, *Desulfobacca* was involved in the

sulphate reduction with a complete pathway in the Pöhla mine water. The concentration of U between both mine waters differs, being one hundred times higher in Schlema-Alberoda mine water than in Pöhla. This could be explained by the higher activity of SRB (e.g., *Desulfobacca*) as well as metal-reducing bacteria (e.g., *Geobacteraceae*), and the high reducing conditions in Pöhla mine water in comparison to the Schlema-Alberoda mine water.

It is important to highlight the diverse strategies used by the bacterial community in response to heavy metal stress. Bacteria use a variety of transporters (e.g., cobalt transporter (CbiMQ, CorA), copper transporter (CopA), iron transporters (Ferric iron ABC-type substrate-binding AfuA)) to regulate the presence of metal cations, which could help prevent the toxicity of elements such as U and other heavy metals by expelling them out from the intracellular space (Pinel-Cabello et al. 2021). Additionally, high levels of phosphate transporters were identified, indicating the necessity of phosphorus acquisition for the cell growth. Furthermore, the positive regulation of phosphate transporters could suggest the uptake and subsequent use of phosphate for U biomineralization as U detoxification mechanism (Pinel-Cabello et al. 2021).

Interestingly, expression of functions related to flagella and chemotaxis was observed, potentially providing cells an advantage by allowing propulsion via flagella and detection of surrounding chemotactic attractants, facilitating relocation to favourable micro-environments (Li et al. 2022). In response to heavy metals, hydrogen oxidizing bacteria (HOB) can use hydrogen as an electron donor to enzymatically reduce contaminants like U through hydrogenase activity. In our study, we report hydrogenase activity in members of the bacterial community from both mines (*Sulfurimonas* and *Sulfuricurvum*). These findings are consistent with other studies reporting hydrogenase expression in the presence of metals such as Ni, Pt, Pd, Ru, As, and Fe, as well as radionuclides like Tc and U (Woolfolk and Whiteley, 1962; Zadvorny et al. 2006; Marshall et al. 2008; Gao and Francis 2013; Teng et al. 2019). Therefore, hydrogenase activity would be involved in reducing these contaminants, decreasing thus their toxicity. Additionally,

strong positive regulation of cytochromes, such as cytochrome c oxidase and ubiquinol-cytochrome c reductase were detected. For instance, Lovley et al. (1993) reported that cellular extracts from the Hildenborough strain of *Desulfovibrio vulgaris*, containing hydrogenase and cytochrome c₃, reduced U(VI) to U(IV) using hydrogen as an electron source. Furthermore, in the absence of cytochrome c₃, a loss of U(VI) reduction capacity was observed in cellular extracts. Subsequently, Payne et al. (2002) confirmed that cytochrome c₃ was essential for U(VI) reduction in *D. vulgaris in vivo* when hydrogen was the electron donor using a mutant (mutant I2) lacking cytochrome c₃. This mutant showed deficient or no reduction of U(VI) when hydrogen was used as the electron donor. Interestingly, the *Geobacteraceae* family, identified with a very low relative abundance (<0.5%) exclusively in the Pöhla mine water, harbours dissimilatory metal-reducing microorganisms such as the genus *Geobacter* (Cologgi et al. 2014). *Geobacter* exhibited signs of complete or nearly complete metabolic pathways exclusively in Pöhla. This finding is noteworthy as other authors have reported an increase in *Geobacter* species detected within the *Geobacteraceae* family after biostimulation of U-contaminated waters. These organisms have been associated as the main bacteria responsible for U(VI) reduction in a U-contaminated aquifer located in Rifle, Colorado (Anderson et al. 2003). In addition, Schlema-Alberoda and Pöhla mine waters revealed expression of gene coding for As resistance pathways. However, a higher expression of As resistance genes was identified in Schlema-Alberoda. Shah and Damare (2020) reported that in the presence of As, ubiquinol-cytochrome C reductase, involved in energy metabolism in *Brevibacterium casei* #NIOB88, was positively regulated. This suggests that these enzymes could contribute to the microbial survival under As stress conditions. Likewise, both mine water samples showed a positive up-regulation of ubiquinol-cytochrome C reductase and arsenic resistance pathways in the bacterial genera *Ferrigenium*, *Sulfurisoma*, *Methylobacter*, and *Sulfuricurvum*.

4.3. Exploring gene expression patterns in sulphate and Fe reduction in mine waters

A more detailed analysis was conducted to identify functional enzymes related to the ASR and DSR pathways of SRB present in both mine waters. Such findings offer evidences of a microbial community involved in sulphate respiration. From the perspective of U bioremediation, studying the active SRB population could be valuable to design efficient U bioremediation strategies for the Schlema-Alberoda and Pöhla contaminated mine water as U-reducers are mainly sulphate and Fe reducers (Chang et al. 2001).

In the DSR pathway, the oxidation of organic compounds is coupled to sulphate reduction, producing sulphide as a metabolic by-product, thus generating energy. Meanwhile, the ASR pathway metabolizes sulphate into sulphide and subsequently into sulphur-containing amino acids such as cysteine (Kushkevych et al. 2020). These two pathways are crucial for sulphur transformation within the biogeochemical cycle of this element and have implications for microbial nutrition and environmental geochemistry. Our study indicated that all genes responsible for encoding enzymes involved in the DSR pathway are present in both mine water samples. In the DSR pathway (Fig. 6E), under anaerobic conditions, sulphate is initially converted to adenosine monophosphate (AMP) by sulphate adenylyltransferase (*sat*). Subsequently, AMP is reduced to sulphite by APS reductase (*aprAB*), and finally, through dissimilatory sulphite reductase (*dsrAB*), reduction to sulphide occurs (Zhang et al. 2019; Zhou et al. 2021). In contrast, the ASR pathway is more complex than the first pathway involving not only sulphate reduction to sulphide but also the biosynthesis of sulphur-containing amino acids like cysteine, and leads to no direct sulphide excretion (Longo et al. 2016). Zhou and co-authors (2021) reported that in the case of the ASR pathway, sulphate is first transformed into AMP, possibly by the action of *sat*, although the involvement of *PAPSS*, and *cysND* has also been described. Then, AMP is converted into 3'-phosphoadenosine-5'-phosphosulfate (PAPS), sulphite, and sulphide in steps catalysed by different enzymes including *PAPSS*, *cysC*, *cycH*, *cysJI*, and *sir* (Fig. 7). Finally, O-acetylserine sulfhydrylase catalyses the conversion of sulphide to cysteine (Kushkevych et al. 2020). In our study, no genes encoding for O-acetylserine sulfhydrylase were identified.

In both mine waters, higher expression of DSR pathway than ASR pathway was shown. Although, Pöhla mine water revealed higher expression of the DSR pathway than Schlema-Alberoda mine water (Fig. 6). Probably, this higher activity in the DSR pathway would be related to the anoxic conditions of the Pöhla mine water since under these conditions SRB preferentially utilize the DSR pathway for sulphate reduction (Dar et al. 2007). The sulphate concentration in Pöhla water is much lower than that measured in Schlema-Alberoda (0.8 mg/l and 311 mg/l, respectively). These results could be related to the high activity detected in the Pöhla samples for the DSR pathway. Sulphate adenylyltransferase (*Sat*) is an enzyme shared between the DSR and ASR pathways. Therefore, this could be an explanation for the similar *Sat* expression observed in both mine water samples (Fig. 7A). The ASR pathway was poorly identified in Pöhla, and the absence of *PAPSS* and *sir* genes was also identified. In contrast, this was not the case for Schlema-Alberoda, indicating that the bacteria present may be utilizing sulphate for other metabolic processes besides sulphate reduction. For example, sulphate could be preferentially used in cellular component biosynthesis.

OmcS was identified as one of the most prevalent multi-heme cytochromes, reported to be involved in the reduction of Fe(III) oxide (Qian et al. 2011). Likewise, it was suggested that OmcS, localized on the pili, facilitates the final stage of Fe(III) oxide reduction through conductive pili in *Geobacter* (Qian et al. 2011). Thus, OmcS facilitates electron transfer from the pili to Fe(III) oxide (Lovley et 2012). However, other bacterial genera such as *Shewanella* accelerate metal reduction by releasing compounds as flavin mononucleotide (FMN), which acts as an electron shuttles between the cell surface and Fe(III) oxides (Marsili et al. 2008; Covington et al. 2010; Qian et al. 2011). On the other hand, *Geothrix* release compounds of as yet unknown nature, although it is known to be a compound with characteristics similar to a water-soluble quinone, that can solubilize Fe(III) (Nevin and Lovley 2002).

In our results, *omcS* was the only identified gene involved in dissimilatory Fe reduction (Table S7), exclusively in the mine water of Pöhla. Although

some authors reported that U(VI) reduction is not exclusive to OmcS (Orellana et al. 2013), Qian and co-authors (2011) proved the reducing capacity of purified OmcS from a *G. sulfurreducens* mutant. They demonstrated the reduction of U(VI), Cr(VI), and Au(III) by this protein. The detection of *omcS*, possibly from *Geobacter* (*Geobacteraceae*), in the Pöhla sample can explain the lower concentration of U detected in this mine. In contrast, both mine waters exhibited high regulation for genes involved in Fe oxidation such as *cyc2*. All sequenced genomes of the known iron-oxidizing neutrophilic chemolithoautotrophic bacteria (FeOB) harbour homologues of *cyc2*, which encodes an iron-oxidizing outer membrane cytochrome (Cyc2) (Keffer et al. 2021). While *cyc2* appears to be the most widely distributed gene associated with Fe oxidation, other genes exclusively expressed in the Pöhla mine water could also be involved (*sulfocyanin* and *foxE*) (Table S7). Fe oxidizers were identified in both mine waters, including the genera *Sideroxydans* and *Gallionella*, as well as certain species of *Geobacter* (Garber et al. 2020). Furthermore, while Fe is an essential nutrient for almost all organisms, it poses problems due to its poor solubility and low availability. Therefore, one way to alleviate this problem is through the use of Fe storage genes (Andrews 1998, 2010) such as those identified that encode for ferritin-like domain (PF00210) in the Schlema-Alberoda and Pöhla mine waters (Table S7).

5. Conclusions

In summary, through a metatranscriptomic study, the key metabolic pathways and activities related to the S, N, and C cycles have been investigated for the first time in the former U mine waters of Schlema-Alberoda and Pöhla (Wismut GmbH). A complex scene has been observed in both mine waters, where the functional profile of the active microbial community has revealed the presence of diverse metabolic pathways, such as carbohydrate degradation and S and N metabolism. Notably, the genera *Sulfurimonas* and *Sulfuricurvum*, identified as dominant in both mine waters, showed positive regulation for nitrate reduction and oxidation of reduced S compounds. These activities could contribute to the stability of

reduced U. Our study showed a high regulation of two essential pathways in S metabolism, ASR and DSR, with implications in microbial nutrition and mine water geochemistry, being DSR the most active pathway. The high expression of genes encoding for the DSR pathway might be due to the preferred anoxic conditions for SRB in the Pöhla mine water. Since SRB preferentially utilize this pathway for sulphate reduction, the low sulphate concentration identified in Pöhla mine water could be explained. Additionally, a strong regulation of genes associated with Fe oxidation, storage, and regulation was observed, highlighting the role of FeRB in the Fe biogeochemical cycle. However, only two genes involved in Fe reduction were identified in the Pöhla mine water. These results suggest the presence of a microbial community (e.g., metal-reducing bacteria as *Geobacter*) in the Pöhla mine water, which could be involved in the process resulting in significant lower U concentration compared to Schlema-Alberoda mine water, as these bacteria have traditionally been described as excellent reducers of U. Additionally, we cannot disregard the possible abiotic indirect reduction resulting from hydrogen sulphides generated during sulphate reduction by SRB (e.g., *Desulfobacca*). Finally, this study provides valuable information about the microbial diversity and active microbial community, which could be used to design suitable bioremediation strategies based on the biostimulation of the native community of U-reducing microorganisms (e.g., *Geobacteraceae*) in the U contaminated mine waters.

6. References

- Anderson RT, Vrionis HA, Ortiz-Bernad I, Resch CT, Long PE, Dayvault R, Karp K, Marutzky S, Metzler DR, Peacock A, White DC, Lowe M, Lovley DR (2003) Stimulating the *in situ* activity of *Geobacter* species to remove uranium from the groundwater of a uranium-contaminated aquifer. *Applied and Environmental Microbiology*. 69(10):5884-5891. <https://doi.org/10.1128/AEM.69.10.5884-5891.2003>
- Andrews SC (1998) Iron storage in bacteria. *Advances in Microbial Physiology*. 40:281-351. [https://doi.org/10.1016/s0065-2911\(08\)60134-4](https://doi.org/10.1016/s0065-2911(08)60134-4)
- Andrews SC (2010) The Ferritin-like superfamily: Evolution of the biological iron storeman from a rubrerythrin-like ancestor. *Biochimica et Biophysica Acta*. 1800(8):691-705. <https://doi.org/10.1016/j.bbagen.2010.05.010>
- Banala UK, Das NPI, Toleti SR (2021) Microbial interactions with uranium: Towards an effective bioremediation approach. *Environmental Technology and Innovation*. 21:101254. <https://doi.org/10.1016/j.eti.2020.101254>
- Biswas R, Majhi AK, Sarka A (2019) The role of arsenate reducing bacteria for their prospective application in arsenic contaminated groundwater aquifer system. *Biocatalysis and Agricultural Biotechnology*. 20: 101218. <https://doi.org/10.1016/j.bcab.2019.101218>
- Boonchayaanant B, Gu B, Wang W, Ortiz ME, Criddle CS (2010) Can microbially-generated hydrogen sulfide account for the rates of U(VI) reduction by a sulfate-reducing bacterium?. *Biodegradation*. 21:81-95. <https://doi.org/10.1007/s10532-009-9283-x>
- Bolger AM, Lohse M, Usadel B (2014) Trimmomatic: a flexible trimmer for Illumina sequence data. *Bioinformatics*. 30(15):2114-2120. <https://doi.org/10.1093/bioinformatics/btu170>
- Bolyen E, Rideout JR, Dillon MR, Bokulich NA, Abnet CC, Al-Ghalith GA, Alexander H, Alm EJ, Arumugam M, Asnicar F, Bai Y, Bisanz JE, Bittinger K, Brejnrod A, Brislawn CJ, Brown CT, Callahan BJ, Caraballo-Rodríguez AM, Chase J, Cope EK, Da Silva R, Diener C, Dorrestein PC, Douglas GM, Durall DM, Duvall C, Edwardson CF, Ernst M, Estaki M, Fouquier J, Gauglitz JM, Gibbons SM, Gibson DL, Gonzalez A, Gorlick K, Guo J, Hillmann B, Holmes S, Holste H, Huttenhower C, Huttley GA, Janssen S, Jarmusch AK, Jiang L, Kaehler BD, Kang KB, Keefe CR, Keim P, Kelley ST, Knights D, Koester I, Kosciolk T, Kreps J, Langille MGI,

- Lee J, Ley R, Liu YX, Loftfield E, Lozupone C, Maher M, Marotz C, Martin BD, McDonald D, McIver LJ, Melnik AV, Metcalf JL, Morgan SC, Morton JT, Naimey AT, Navas-Molina JA, Nothias LF, Orchanian SB, Pearson T, Peoples SL, Petras D, Preuss ML, Pruesse E, Rasmussen LB, Rivers A, Robeson MS, Rosenthal P, Segata N, Shaffer M, Shiffer A, Sinha R, Song SJ, Spear JR, Swafford AD, Thompson LR, Torres PJ, Trinh P, Tripathi A, Turnbaugh PJ, Ul-Hasan S, Van der Hooft JJJ, Vargas F, Vázquez-Baeza Y, Vogtmann E, Von Hippel M, Walters W, Wan Y, Wang M, Warren J, Weber KC, Williamson CHD, Willis AD, Xu ZZ, Zaneveld JR, Zhang Y, Zhu Q, Knight R, Caporaso JG (2019) Reproducible, interactive, scalable and extensible microbiome data science using QIIME 2. *Nature Biotechnology*. 37(8):852–857. <https://doi.org/10.1038/s41587-019-0209-9>
- Bray JR and Curtis JT (1957) An Ordination of Upland Forest Communities of Southern Wisconsin. *Ecological Monographs*. 27:325-349. <http://dx.doi.org/10.2307/1942268>
- Callahan BJ, Mcmurdie PJ, Rosen MJ, Han WH, Johnson AJ, Holmes SP (2016) DADA2: High resolution sample inference from amplicon data. *Nature Methods*. 13(7):581–583. <http://dx.doi.org/10.1101/024034>
- Caporaso JG, Kuczynski J, Stombaugh J, Bittinger K, Bushman FD, Costello EK, Fierer N, Peña AG, Goodrich JK, Gordon JI, Huttley GA, Kelley ST, Knights D, Koenig JE, Ley RE, Lozupone C A, McDonald D, Muegge BD, Pirrung M, Reeder J, Sevinsky JR, Turnbaugh PJ, Walters WA, Widmann J, Yatsunencko T, Zaneveld J, Knight R (2010) QIIME allows analysis of high-throughput community sequencing data. *Nature Methods*. 7(5):335-336. <https://doi.org/10.1038/nmeth.f.303>
- Chang Y (2005) *In situ biostimulation of uranium reducing microorganisms at the Old Rifle UMTRA Site*. PhD diss., University of Tennessee. Date of access: February 11, 2023. Retrieved from http://trace.tennessee.edu/utk_graddiss/1895/
- Chang Y, Peacock AD, Long PE, Stephen JR, McKinley JP, Macnaughton SJ, Hussain AKMA, Saxton AM, White DC (2001) Diversity and characterization of sulfate-reducing bacteria in groundwater at uranium mill tailing site. *Applied and Environmental Microbiology*. 67(7):3149–3160. <https://doi.org/10.1128%2FAEM.67.7.3149-3160.2001>
- Chen D, Li Y, Zhao X, Shi M, Shi X, Zhao R, Zhu G (2023) Self-Standing Porous Aromatic Framework Electrodes for Efficient Electrochemical Uranium Extraction. *ACS Central Science*. 9(12):2326-2332. <https://doi.org/10.1021/acscentsci.3c01291>

- Covington ED, Gelbmann CB, Kotloski NJ, Gralnick JA (2010) An essential role for *UshA* in processing of extracellular flavin electron shuttles by *Shewanella oneidensis*. *Molecular Microbiology*. 78(2):519-532. <https://doi.org/10.1111/j.1365-2958.2010.07353.x>
- Cologgi DL, Speers AM, Bullard BA, Kelly SD, Reguera G (2014) Enhanced uranium immobilization and reduction by *Geobacter sulfurreducens* biofilms. *Applied and Environmental Microbiology*.80(21):6638-6646. <https://doi.org/10.1128/mbio.01074-21>
- Cron B, Henri P, Chan CS, Macalady JL, Cosmidis J (2019) Elemental Sulfur Formation by *Sulfuricurvum kujiense* Is Mediated by Extracellular Organic Compounds. *Frontiers in Microbiology*. 10:2710. <https://doi.org/10.3389/fmicb.2019.02710>
- Dar SA, Yao L, van Dongen U, Kuenen JG, Muyzer G (2007) Analysis of diversity and activity of sulfate-reducing bacterial communities in sulfidogenic bioreactors using 16S rRNA and *dsrB* genes as molecular markers. *Applied and Environmental Microbiology*. <https://doi.org/10.1128/aem.01875-06>
- Dhariwal A, Chong J, Habib S, King IL, Agellon LB, Xia J (2017) MicrobiomeAnalyst: A web-based tool for comprehensive statistical, visual and meta-analysis of microbiome data. *Nucleic Acids Research*. 45(W1):W180–W188. <https://doi.org/10.1093/nar/gkx295>
- Embree M, Qiu Y, Shieu W, Nagarajan H, O'Neil R, Lovley D, Zengler K (2014) The iron stimulon and fur regulon of *Geobacter sulfurreducens* and their role in energy metabolism. *Applied and Environmental Microbiology*. 80(9):2918-2927. <https://doi.org/10.1128%2FAEM.03916-13>
- Finneran KT, Housewright ME, Lovley DR (2002) Multiple influences of nitrate on uranium solubility during bioremediation of uranium-contaminated subsurface sediments. *Environmental Microbiology*. 4(9):510-516. <https://doi.org/10.1046/j.1462-2920.2002.00317.x>
- Fisher RA, Corbet AS, Williams CB (1943) The relation between the number of species and the number of individuals in a random sample of an animal population. *Journal of Animal Ecology*. 12:42–58. <https://doi.org/10.2307/1411>
- Gao W and Francis AJ (2013) Fermentation and hydrogen metabolism affect uranium reduction by *Clostridia*. *ISRN Biotechnology*. 2013:657160. <https://doi.org/10.4236/isrn.2013.20130657160>

[org/10.5402%2F2013%2F657160](https://doi.org/10.5402%2F2013%2F657160)

- Garber AI, Nealson KH, Okamoto A, McAllister SM, Chan CS, Barco RA, Merino N (2020) FeGenie: A Comprehensive Tool for the Identification of Iron Genes and Iron Gene Neighborhoods in Genome and Metagenome Assemblies. *Frontiers in Microbiology*. <https://doi.org/10.3389/fmicb.2020.00037>
- Grabherr MG, Haas BJ, Yassour M, Levin JZ, Thompson DA, Amit I, Adiconis X, Fan L, Raychowdhury R, Zeng Q, Chen Z, Mauceli E, Hacohen N, Gnirke A, Rhind N, di Palma F, Birren BW, Nusbaum C, Lindblad-Toh K, Friedman N, Regev A (2011) Full-length transcriptome assembly from RNA-Seq data without a reference genome. *Nature Biotechnology*. 29(7):644-652. <https://doi.org/10.1038%2Fnbt.1883>
- Graham ED, Heidelberg JF, Tully BJ (2018) Potential for primary productivity in a globally-distributed bacterial phototroph. *ISME Journal*. 12(7):1861-1866. <https://doi.org/10.1038/s41396-018-0091-3>
- Hu L, Wang Y, Ci M, Long Y (2023) Unravelling microbial drivers of the sulfate-reduction process inside landfill using metagenomics. *Chemosphere*. 313:137537. <https://doi.org/10.1016/j.chemosphere.2022.137537>
- Huang L, Bae HS, Young C, Pain AJ, Martin JB, Ogram A (2021) Campylobacterota dominate the microbial communities in a tropical karst subterranean estuary, with implications for cycling and export of nitrogen to coastal waters. *Environmental Microbiology*. 23(11):6749-6763. <https://doi.org/10.1111/1462-2920.15746>
- Hyun SP, Davis JA, Hayes KF (2014) Abiotic U(VI) reduction by aqueous sulfide. *Applied Geochemistry*. 50:7-10. <https://doi.org/10.1016/j.apgeochem.2014.07.021>
- Hyatt D, Chen GL, Locascio PF, Land ML, Larimer FW, Hauser LJ (2010) Prodigal: prokaryotic gene recognition and translation initiation site identification. *BMC Bioinformatics*. 11:119. <https://doi.org/10.1186/1471-2105-11-119>
- Ibáñez A, Garrido-Chamorro S, Coque JJR, Barreiro C (2023) From Genes to Bioleaching: Unraveling Sulfur Metabolism in *Acidithiobacillus* Genus. *Genes*. 14(9):1772. <https://doi.org/10.3390/genes14091772>
- Jiang S and Hur HG (2012) Effects of the anaerobic respiration of *Shewanella oneidensis* MR-1 on the stability of extracellular U(VI) nanofibers. *Microbes and Environments*. 28(3):312-315. <https://doi.org/10.1264/jsme2.me12149>

- Jroundi F, Povedano-Priego C, Pinel-Cabello M, Descostes M, Grizard P, Purevsan B, Merroun ML (2023) Evidence of microbial activity in a uranium roll-front deposit: Unlocking their potential role as bioenhancers of the ore genesis. *Science of the Total Environment*. 861:160636. <https://doi.org/10.1016/j.scitotenv.2022.160636>
- Kanehisa M, Sato Y, Kawashima M, Furumichi M, Tanabe M (2016a) KEGG as a reference resource for gene and protein annotation. *Nucleic Acids Research*. 44(D1):D457-462. <https://doi.org/10.1093/nar/gkv1070>
- Kanehisa M, Sato Y, Morishima K (2016b) BlastKOALA and GhostKOALA: KEGG Tools for Functional Characterization of Genome and Metagenome Sequences. *Journal of Molecular Biology*. 428(4):726-731. <https://doi.org/10.1016/j.jmb.2015.11.006>
- Keffer JL, McAllister SM, Garber AI, Hallahan BJ, Sutherland MC, Rozovsky S, Chan CS (2021) Iron Oxidation by a Fused Cytochrome-Porin Common to Diverse Iron-Oxidizing Bacteria. *12(4):e0107421*. <https://doi.org/10.1128/mbio.01074-21>
- Konrad R, Vergara-Barros P, Alcorta J, Alcamán-Arias ME, Levicán G, Ridley C, Díez B (2023) Distribution and Activity of Sulfur-Metabolizing Bacteria along the Temperature Gradient in Phototrophic Mats of the Chilean Hot Spring Porcelana. *Microorganisms*. 11(7):1803. <https://doi.org/10.3390/microorganisms11071803>
- Kopylova E, Noé L, Touzet H (2012) SortMeRNA: fast and accurate filtering of ribosomal RNAs in metatranscriptomic data. *Bioinformatics*. 28(24):3211-3217. <https://doi.org/10.1093/bioinformatics/bts611>
- Kucera M, Isserlin R, Arkhangorodsky A, Bader GD. AutoAnnotate: A Cytoscape app for summarizing networks with semantic annotations. *F1000Research*. 5:1717. <https://doi.org/10.12688/f1000research.9090.1>
- Kushkevych I, Cejnar J, Treml J, Dordević D, Kollar P, Vítězová M (2020) Recent Advances in Metabolic Pathways of Sulfate Reduction in Intestinal Bacteria. *Cells*. 9(3):698. <https://doi.org/10.3390/cells9030698>
- Lahme S, Enning D, Callbeck CM, Menendez Vega D, Curtis TP, Head IM, Hubert CRJ (2019) Metabolites of an Oil Field Sulfide-Oxidizing, Nitrate-Reducing *Sulfurimonas* sp. Cause Severe Corrosion. *Applied and Environmental Microbiology*. 85(3):e01891-18. <https://doi.org/10.1128/aem.01891-18>
- Langmead B and Salzberg SL (2012) Fast gapped-read alignment with Bowtie 2. *Nature Methods*. 9(4):357-359. <https://doi.org/10.1038/nmeth.1923>

- Li J, Liang Y, Miao Y, Wang D, Jia S, Liu CH (2020) Metagenomic insights into aniline effects on microbial community and biological sulfate reduction pathways during anaerobic treatment of high-sulfate wastewater. *Science of The Total Environment*. 742:140537. <https://doi.org/10.1016/j.scitotenv.2020.140537>
- Li L, Meng D, Yin H, Zhang T, Liu Y (2023) Genome-resolved metagenomics provides insights into the ecological roles of the keystone taxa in heavy-metal-contaminated soils. *Frontiers in Microbiology*. 14:1203164. <https://doi.org/10.3389/fmicb.2023.1203164>
- Li Q, Yang Y, Ma J, Sun J, Li G, Zhang R, Cui Z, Li T, Liu X (2023) Sulfur enhancement effects for uranium bioleaching in column reactors from a refractory uranium ore. *Frontiers in Microbiology*. 14:1107649. <https://doi.org/10.3389/fmicb.2023.1107649>
- Li X, Sun M, Zhang L, Finlay RD, Liu R, Lian B (2022) Widespread bacterial responses and their mechanism of bacterial metallogenic detoxification under high concentrations of heavy metals. *Ecotoxicology and Environmental Safety*. 246:114193. <https://doi.org/10.1016/j.ecoenv.2022.114193>
- Liao Y, Smyth GK, Shi W (2012) featureCounts: an efficient general purpose program for assigning sequence reads to genomic features. *Bioinformatics*. 30(7):923-930. <https://doi.org/10.1093/bioinformatics/btt656>
- Longo F, Motta S, Mauri P, Landini P, Rossi E. Interplay of the modified nucleotide phosphoadenosine 5'-phosphosulfate (PAPS) with global regulatory proteins in *Escherichia coli*: modulation of cyclic AMP (cAMP)-dependent gene expression and interaction with the HupA regulatory protein (2016) *Chemico-biological Interactions*. 259(Pt A):39-47. <https://doi.org/10.1016/j.cbi.2016.04.016>
- Lovley DR (2012) Long-range electron transport to Fe(III) oxide via pili with metallic-like conductivity. *Biochemical Society Transactions*. 40(6):1186-1190. <https://doi.org/10.1042/bst20120131>
- Lovley DR and Phillips EJ (1992) Reduction of Uranium by *Desulfovibrio desulfuricans*. *Applied and Environmental Microbiology*. 58(3):850-856. Retrieved from <https://journals.asm.org/doi/pdf/10.1128/aem.58.3.850-856.1992>
- Lovley DR, Widman PK, Woodward JC, Phillips EJ. Reduction of uranium by cytochrome c3 of *Desulfovibrio vulgaris* (1993) *Applied and Environmental Microbiology*. 59(11):3572-3576. <https://doi.org/10.1128/aem.59.11.3572-3576.1993>

- Lusa M, Knuutinen J, Lindgren M, Virkanen J, Bomberg M (2019) Microbial communities in a former pilot-scale uranium mine in Eastern Finland - Association with radium immobilization. *Science of The Total Environment*. 686:619-640. <https://doi.org/10.1016/j.scitotenv.2019.05.432>
- Marshall MJ, Plymale AE, Kennedy DW, Shi L, Wang Z, Reed SB, Dohnalkova AC, Simonson CJ, Liu C, Saffarini DA, Romine MF, Zachara JM, Beliaev AS, Fredrickson JK (2008) Hydrogenase- and outer membrane c-type cytochrome-facilitated reduction of technetium(VII) by *Shewanella oneidensis* MR-1. *Environmental Microbiology*. 10(1):125-136. <https://doi.org/10.1111/j.1462-2920.2007.01438.x>
- Marsili E, Baron DB, Shikhare ID, Coursolle D, Gralnick JA, Bond DR (2008) *Shewanella* secretes flavins that mediate extracellular electron transfer. *Proceedings of the National Academy of Sciences (Proceedings of the National Academy of Sciences of the United States of America)*. 105(10):3968-3973. <https://doi.org/10.1073/pnas.0710525105>
- Martin M (2011) Cutadapt Removes Adapter Sequences from High-Throughput Sequencing Reads. *EMBnet Journal*. 17:10-12. <https://doi.org/10.14806/ej.17.1.200>
- Merroun ML and Selenska-Pobell S (2008) Bacterial interactions with uranium: An environmental perspective. *Journal of Contaminant Hydrology*. 102(3-4): 285-295. <https://doi.org/10.1016/j.jconhyd.2008.09.019>
- Mo S, Yan B, Gao T, Li J, Kashif M, Song J, Bai L, Yu D, Liao J, Jiang C (2023) Sulfur metabolism in subtropical marine mangrove sediments fundamentally differs from other habitats as revealed by SMDB. *Scientific Reports*. 13(1):8126. <https://doi.org/10.1038/s41598-023-34995-y>
- Mohsin H, Shafique M, Zaid M, Rehman Y. (2023) Microbial biochemical pathways of arsenic biotransformation and their application for bioremediation. *Folia Microbiologica*. 68(4):507-535. <https://doi.org/10.1007/s12223-023-01068-6>
- Negm S, Greenberg A, Larracunte AM, Sproul JS (2021) RepeatProfiler: A pipeline for visualization and comparative analysis of repetitive DNA profiles. *Molecular Ecology Resources*. 21(3):969-981. <https://doi.org/10.1111/1755-0998.13305>
- Nevin KP, Lovley DR. Mechanisms for accessing insoluble Fe(III) oxide during dissimilatory Fe(III) reduction by *Geothrix fermentans*. *Applied and Environmental Microbiology*. 68(5):2294-2299. <https://doi.org/10.1128/AEM.68.5.2294-2299.2002>

- Newman-Portela AM, Krawczyk-Bärsch E, Lopez-Fernandez M, Bok F, Kassahun A, Drobot B, Steudtner R, Stumpf T, Raff J, Merroun ML (2024) Biostimulation of indigenous microbes for uranium bioremediation in former U mine water: multidisciplinary approach assessment. *Environmental Science and Pollution Research*. 31(5):7227-7245. <https://doi.org/10.1007/s11356-023-31530-4>
- Oksanen J, Simpson GL, Blanchet FG, Kindt R, Legendre P, Minchin PR, O'Hara RB, Solymos P, Stevens MHH, Szoecs E, Wagner H, Barbour M, Bedward M, Bolker B, Borcard D, Carvalho G, Chirico M, De Caceres M, Durand S, Evangelista HBA, FitzJohn R, Friendly M, Furneaux B, Hannigan G, Hill MO, Lahti L, McGlinn D, Ouellette MH, Cunha ER, Smith T, Stier A, Ter Braak CJF, Weedon J. (2007) Community Ecology Package - Vegan: Community Ecology Package. R Package 1.8–8. Date of access: March 01, 2024. Retrieved from <https://cran.r-project.org/web/packages/vegan/vegan.pdf>
- Orellana R, Leavitt JJ, Comolli LR, Csencsits R, Janot N, Flanagan KA, Gray AS, Leang C, Izallalen M, Mester T, Lovley DR (2013) U(VI) reduction by diverse outer surface c-type cytochromes of *Geobacter sulfurreducens*. *Applied and Environmental Microbiology*. 79(20):6369-6374. <https://doi.org/10.1128%2FAEM.02551-13>
- Payne RB, Gentry DM, Rapp-Giles BJ, Casalot L, Wall JD (2002) Uranium reduction by *Desulfovibrio desulfuricans* strain G20 and a cytochrome c3 mutant. *Applied and Environmental Microbiology*. 68(6):3129-3132. <https://doi.org/10.1128%2FAEM.68.6.3129-3132.2002>
- Pinel-Cabello M, Jroundi F, López-Fernández M, Geffers R, Jarek M, Jauregui R, Link A, Vilchez-Vargas R, Merroun ML (2021) Multisystem combined uranium resistance mechanisms and bioremediation potential of *Stenotrophomonas bentonitica* BII-R7: Transcriptomics and microscopic study. *Journal of Hazardous Materials*. 403:123858. <https://doi.org/10.1016/j.jhazmat.2020.123858>
- Qian X, Mester T, Morgado L, Arakawa T, Sharma ML, Inoue K, Joseph C, Salgueiro CA, Maroney MJ, Lovley DR. (2011) Biochemical characterization of purified OmcS, a c-type cytochrome required for insoluble Fe(III) reduction in *Geobacter sulfurreducens*. *Biochimica et Biophysica Acta*. 1807(4):404-12. <https://doi.org/10.1016/j.bbabi.2011.01.003>
- Quast C, Pruesse E, Yilmaz P, Gerken J, Schweer T, Yarza P, Peplies J, Glöckner FO (2013) The SILVA ribosomal RNA gene database project: improved data processing and web-based tools. *Nucleic Acids Research*. 41:D590-6. <https://doi.org/10.1093/nar/nks121>

[org/10.1093%2Fnar%2Fgks1219](https://doi.org/10.1093%2Fnar%2Fgks1219)

Raggi L, García-Guevara F, Godoy-Lozano EE, Martínez-Santana A, Escobar-Zepeda A, Gutierrez-Rios RM, Loza A, Merino E, Sanchez-Flores A, Licea-Navarro A, Pardo-Lopez L, Segovia L, Juarez K (2020) Metagenomic Profiling and Microbial Metabolic Potential of Perdido Fold Belt (NW) and Campeche Knolls (SE) in the Gulf of Mexico. *Frontiers in Microbiology*. 11:1825. <https://doi.org/10.3389%2Ffmicb.2020.01825>

Rastogi G, Osman S, Kukkadapu R, Engelhard M, Vaishampayan PA, Andersen GL, and Sani RK (2010a) Microbial and Mineralogical Characterizations of Soils Collected from the Deep Biosphere of the Former Homestake Gold Mine, South Dakota. *Microbial Ecology*. 60(3):539–550. <https://doi.org/10.1007/s00248-010-9657-y>

Rastogi G, Osman S, Vaishampayan PA, Andersen GL, Stetler LD, Sani RK (2010b) Microbial diversity in uranium mining-impacted soils as revealed by high-density 16S microarray and clone library. *Microbial Ecology*. 59(1):94–108. <https://doi.org/10.1007/s00248-009-9598-5>

Robinson MD, McCarthy DJ, Smyth GK (2010) edgeR: a Bioconductor package for differential expression analysis of digital gene expression data. *Bioinformatics*. 26(1):139-40. <https://doi.org/10.1093/bioinformatics/btp616>

Rogiers T, Van Houdt R, Williamson A, Leys N, Boon N, Mijnenonckx K (2022) Molecular Mechanisms Underlying Bacterial Uranium Resistance. *Frontiers in Microbiology*. 13:822197. <https://doi.org/10.3389%2Ffmicb.2022.822197>

Romão CV, Pereira IA, Xavier AV, LeGall J, Teixeira M (1997) Characterization of the [NiFe] hydrogenase from the sulfate reducer *Desulfovibrio vulgaris* Hildenborough. *Biochemical and Biophysical Research Communications*. 240(1):75-9. <https://doi.org/10.1006/bbrc.1997.7598>

Shah S, Damare S (2020) Cellular response of *Brevibacterium casei* #NIOSBA88 to arsenic and chromium-a proteomic approach. *Brazilian Journal of Microbiology*. 51(4):1885-1895. <https://doi.org/10.1007%2Fs42770-020-00353-7>

Shannon CE (1948) A mathematical theory of communication. *The Bell System Technical Journal*. 27(3):379–423. <https://doi.org/10.1002/j.1538-7305.1948.tb01338.x>

Shannon P, Markiel A, Ozier O, Baliga NS, Wang JT, Ramage D, Amin N, Schwikowski B, Ideker T (2003) Cytoscape: a software environment for integrated models of

- biomolecular interaction networks. *Genome Research*. 13(11):2498-504. <https://doi.org/10.1101/gr.1239303>
- Simpson E (1949) Measurement of Diversity. *Nature*. 163:688. <https://doi.org/10.1038/163688a0>
- Su G, Kuchinsky A, Morris JH, States DJ, Meng F (2010) GLay: community structure analysis of biological networks. *Bioinformatics*. 26(24):3135-3137. <https://doi.org/10.1093/bioinformatics/btq596>
- Sugio T, Iwahori K, Takeuchi K, Negishi A, Maeda T, Kamimura K (2001) Cytochrome c oxidase purified from a mercury-resistant strain of *Acidithiobacillus ferrooxidans* volatilizes mercury. *Journal of Bioscience and Bioengineering*. 92(1):44-49. [https://doi.org/10.1016/S1389-1723\(01\)80197-3](https://doi.org/10.1016/S1389-1723(01)80197-3)
- Teng Y, Xu Y, Wang X, Christie P (2019) Function of Biohydrogen Metabolism and Related Microbial Communities in Environmental Bioremediation. *Frontiers in Microbiology*. 10:106. <https://doi.org/10.3389/fmicb.2019.00106>
- Thijs S, De Beeck MO, Beckers B, Truyens S, Stevens V, Van Hamme JD, Weyens N, Vangronsveld J (2017) Comparative evaluation of four bacteria-specific primer pairs for 16S rRNA gene surveys. *Frontiers in Microbiology*. 8(494):1–15. <https://doi.org/10.3389/fmicb.2017.00494>
- Townsend LT, Kuipers G, Lloyd JR, Natrajan LS, Boothman C, Mosselmans JFW, Shaw S, Morris K (2021) Biogenic Sulfidation of U(VI) and Ferrihydrite Mediated by Sulfate-Reducing Bacteria at Elevated pH. *ACS Earth and Space Chemistry*. 5(11):3075-3086. <https://doi.org/10.1021/acsearthspacechem.1c00126>
- Tuovinen H, Pelkonen M, Lempinen J, Pohjolainen E, Read D, Solatie D, Lehto J (2018) Behaviour of Metals during Bioheap Leaching at the Talvivaara Mine, Finland. *Geosciences*. 8(2):66. <https://doi.org/10.3390/geosciences8020066>
- WISMUT GmbH Brochure (2015) Date of access: March 01, 2024. Retrieved from <https://www.bmwk.de/Redaktion/EN/Publikationen/wismut-brochure.html>
- Woolfolk CA, Whiteley HR (1962) Reduction of inorganic compounds with molecular hydrogen by *Micrococcus lactilyticus*. I. Stoichiometry with compounds of arsenic, selenium, tellurium, transition and other elements. *Journal of Bacteriology*. 84(4):647-658. <https://doi.org/10.1128/jb.84.4.647-658.1962>

- You W, Peng W, Tian Z, Zheng M (2021) Uranium bioremediation with U(VI)-reducing bacteria. *Science of the Total Environment*. 798:149107. <https://doi.org/10.1016/j.scitotenv.2021.149107>
- Zadvorny OA, Zorin NA, Gogotov IN (2006) Transformation of metals and metal ions by hydrogenases from phototrophic bacteria. *Archives of Microbiology*. 184(5):279-85. <https://doi.org/10.1007/s00203-005-0040-1>
- Zeng T, Li L, Mo G, Wang G, Liu H, Xie S (2019) Analysis of uranium removal capacity of anaerobic granular sludge bacterial communities under different initial pH conditions. *Environmental Science and Pollution Research*. 26(6):5613-5622. <https://doi.org/10.1007/s11356-018-4017-4>
- Zhang L, Song C, Xu Y, Shi Y, Liu X (2022) Isolation, characterization and S₂--oxidation metabolic pathway of a sulfur-oxidizing strain from a black-odor river in Beijing. *Water Supply*. 22(4):3729–3743. <https://doi.org/10.2166/ws.2022.011>
- Zhang SY, Xiao X, Chen SC, Zhu YG, Sun GX, Konstantinidis KT (2021) High Arsenic Levels Increase Activity Rather than Diversity or Abundance of Arsenic Metabolism Genes in Paddy Soils. *Applied and Environmental Microbiology*. 87(20):e0138321. <https://doi.org/10.1128/aem.01383-21>
- Zhang X, Zhang L, Zhang L, Ji Z, Shao Y, Zhou H, Bao Y, Qu Y, Liu L (2019) Comparison of rhizosphere bacterial communities of reed and Suaeda in Shuangtaizi River Estuary, Northeast China. *Marine Pollution Bulletin*. 140:171-178. <https://doi.org/10.1016/j.marpolbul.2019.01.041>
- Zhou L, Ou P, Zhao B, Zhang W, Yu K, Xie K, Zhuang WQ (2021) Assimilatory and dissimilatory sulfate reduction in the bacterial diversity of biofoulant from a full-scale biofilm-membrane bioreactor for textile wastewater treatment. *Science of The Total Environment*. 772:145464. <https://doi.org/10.1016/j.scitotenv.2021.145464>

Supplementary material

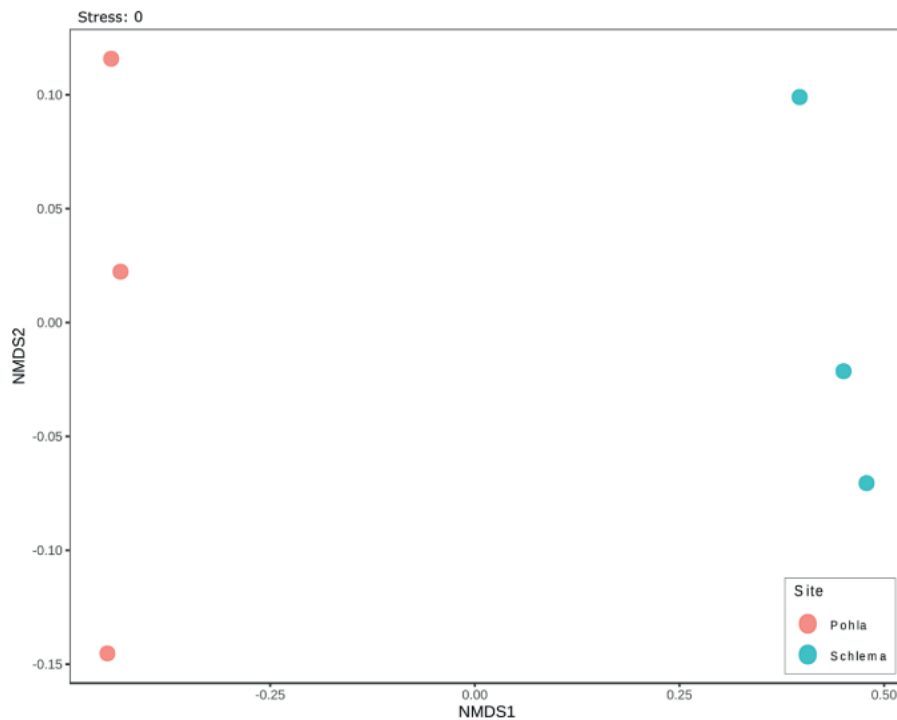


Fig. S1. Bray–Curtis-based NMDS and PERMANOVA results of bacterial communities. Schlema-Alberoda (S1; S2; S6) and the Pöhla mine water (P1; P5; P8).

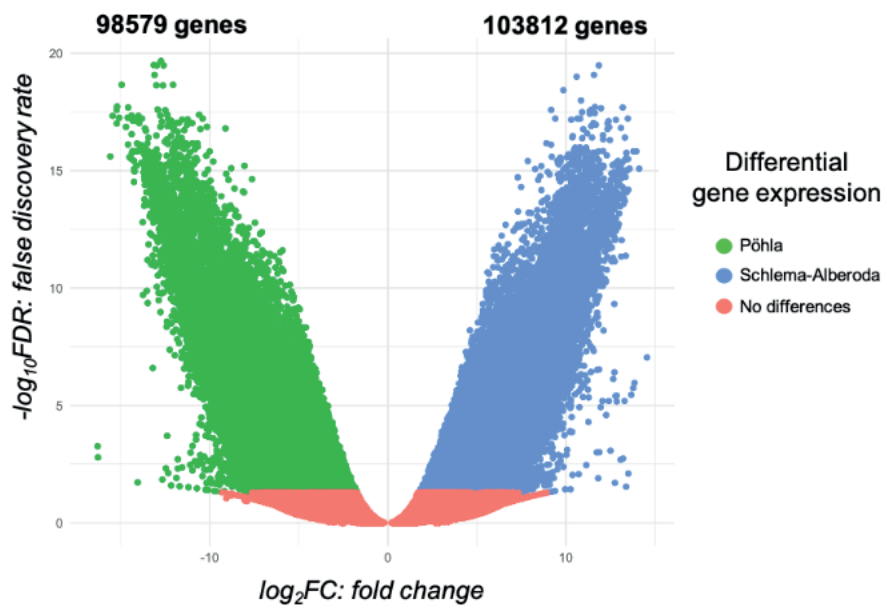


Fig. S2. Volcano plot of differential gene expression (fold change (FC) ≥ 2 and false discovery rate (FDR) ≤ 0.05) between Pöhla (green) and Schlema-Alberoda (blue) mine water.

Fig. S3. Complete metabolic pathway heat map of Schlemma-Alberoda. The heat map represents metabolic pathway completeness based on the presence or absence of genes as determined by KEGG Decoder. Dark red (the colour scale is shown) represents a complete or highly complete pathway, while white represents locations where a pathway is absent or highly incomplete.

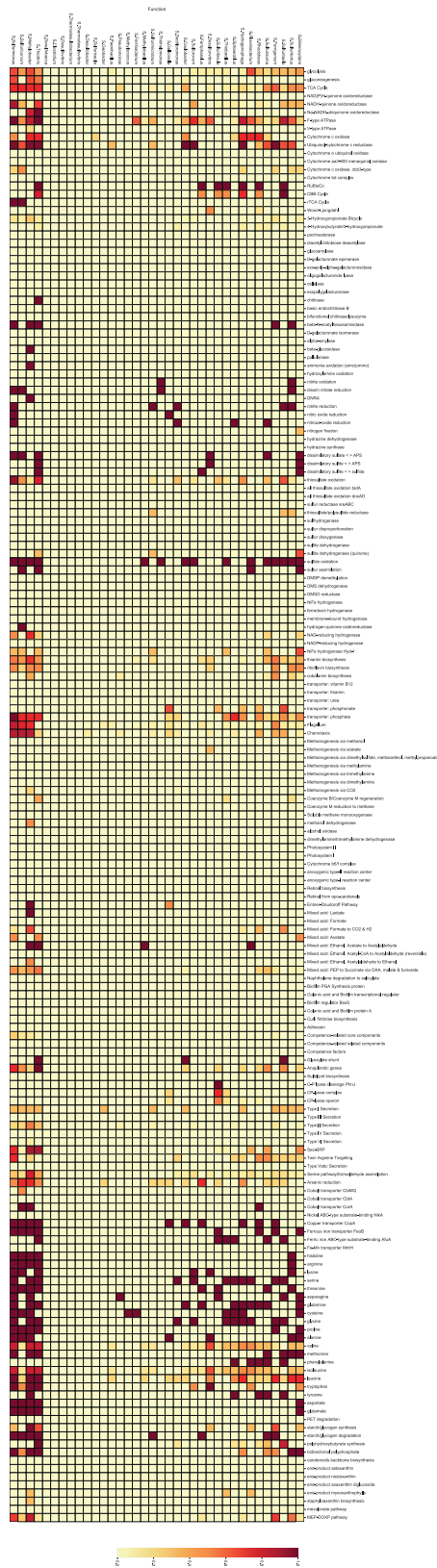


Table S1. Alpha diversity index (Shannon and Simpson) and richness (Chao1) of bacteria at genus level in water from the Schlema-Alberoda mine (S1; S2; S6)) and the Pöhla mine (P1; P5; P8).

		Shannon	Simpson	Chao1
Bacteria	P1	3.162	0.892	117
	P5	2.960	0.868	126
	P8	2.969	0.878	122
	S1	2.518	0.840	88
	S2	2.275	0.809	74
	S6	2.313	0.810	80

Table S2. Quality assessment of raw DNA-seq data.

Sample	Number of reads	Mean read length [b]
S1	79 364	300
S4	78 862	300
S6	75 936	300
P1	71 260	300
P5	85 250	300
P8	82 516	300

Table S3. Genera relative abundance of the bacterial and archaeal communities of the water samples from the Pöhla (P1; P5; P8) and Schlema-Alberoda mines (S1; S2; S6).

	Relative abundance (%)						
	Total	P1	P5	P8	S1	S4	S6
<i>Sulfuricurvum</i>	16.64	9.81	13.02	13.72	23.51	22.50	20.01
<i>Sulfurovum</i>	16.25	27.68	30.74	26.89	0.88	0.88	0.91
<i>Sulfurimonas</i>	13.78	0.04	0.07	0.08	26.72	32.23	33.99
<i>Gallionellaceae</i>	7.30	0.96	1.12	1.34	14.83	15.33	14.87
<i>Thermodesulfovibrionia_uncultured</i>	6.05	6.92	9.41	15.28	0.26	0.10	0.17
<i>Candidatus_Omnitrophus</i>	4.10	7.35	5.56	3.83	2.73	1.99	2.46
<i>Hydrogenophilaceae_uncultured</i>	3.41	0.19	0.21	0.28	7.37	7.66	7.14
<i>Rhodocyclaceae</i>	2.64	3.96	4.47	4.67	0.46	0.43	0.44
<i>Candidatus_Moranbacteria</i>	1.96	4.45	3.38	2.34	0.27	0.18	0.29
<i>Candidatus_Magasanikbacteria</i>	1.37	3.35	2.36	1.36	0.34	0.11	0.16
<i>Sulfuritalea</i>	1.29	1.89	2.29	2.40	0.11	0.14	0.15
<i>Desulfurivibrio</i>	1.24	0.29	0.24	0.18	2.92	2.27	2.28
GIF9	1.08	2.09	1.56	1.92	0.17	0.13	0.11
<i>Gallionella</i>	1.03	0.58	0.71	0.74	1.34	1.67	1.35
<i>Acetothermia</i>	1.02	2.29	1.57	1.72	0.00	0.00	0.00
GIF3	0.91	1.51	1.46	1.12	0.49	0.29	0.26
<i>Thiovirga</i>	0.79	0.60	0.80	1.61	0.46	0.48	0.53
<i>Flavobacterium</i>	0.79	0.00	0.00	0.00	1.97	1.38	2.00
WCHB1-81	0.78	2.18	0.95	0.72	0.20	0.20	0.25
Sva0485	0.76	1.03	1.31	1.63	0.08	0.00	0.00
<i>Candidatus_Woesebacteria</i>	0.75	1.86	1.13	0.85	0.22	0.12	0.08
<i>Sideroxydans</i>	0.74	0.06	0.16	0.24	1.31	1.59	1.52
<i>Parcubacteria</i>	0.67	1.47	1.26	0.61	0.22	0.07	0.12
<i>Limnohabitans</i>	0.53	0.00	0.00	0.00	1.08	1.26	1.27
<i>Dehalococcoidia</i>	0.51	1.06	0.88	0.76	0.04	0.03	0.00
SCGC_AAA011-D5	0.51	0.71	0.44	0.25	0.78	0.60	0.32
<i>Candidatus_Yanofskybacteria</i>	0.45	0.92	0.89	0.57	0.05	0.00	0.00
JGI_0000069-P22/JGI_0000069-P22	0.39	0.00	0.00	0.00	1.07	0.59	0.99
<i>Brevundimonas</i>	0.39	0.00	0.00	0.00	0.90	0.90	0.84
<i>Anaerolineaceae_uncultured</i>	0.36	0.52	0.43	0.90	0.06	0.00	0.06
<i>Methylobacter</i>	0.33	0.00	0.09	0.10	0.76	0.58	0.64
<i>Parcubacteria</i>	0.32	0.75	0.64	0.28	0.07	0.02	0.03
<i>Gracilibacteria</i>	0.31	0.66	0.56	0.48	0.00	0.00	0.00
Unassigned	0.29	0.33	0.26	0.35	0.36	0.20	0.18
<i>Berkelbacteria</i>	0.28	0.60	0.35	0.22	0.16	0.18	0.14
<i>Candidatus_Uhrbacteria</i>	0.27	0.27	0.17	0.14	0.45	0.33	0.36
<i>Thiothrix</i>	0.27	0.00	0.02	0.06	0.69	0.49	0.53
<i>Rhodocyclaceae_uncultured</i>	0.25	0.00	0.05	0.11	0.52	0.48	0.46
<i>Methanomassiliicoccales_uncultured</i>	0.23	0.48	0.38	0.37	0.05	0.00	0.00
Pir4_lineage	0.22	0.36	0.25	0.17	0.18	0.21	0.15
<i>Candidatus_Kerfeldbacteria</i>	0.22	0.49	0.25	0.10	0.12	0.21	0.14
<i>Methylophilaceae</i>	0.21	0.46	0.38	0.28	0.00	0.00	0.00
<i>Woesearchaeales</i>	0.20	0.49	0.38	0.18	0.10	0.00	0.00
<i>Zixibacteria</i>	0.20	0.24	0.24	0.49	0.03	0.00	0.06
<i>Candidatus_Colwellbacteria</i>	0.19	0.35	0.39	0.17	0.00	0.07	0.10

<i>Pelolinea</i>	0.18	0.39	0.34	0.26	0.00	0.00	0.00
<i>Candidatus_Methanoperedens</i>	0.17	0.38	0.23	0.29	0.00	0.00	0.00
RBG-13-46-9	0.16	0.35	0.33	0.22	0.00	0.00	0.00
MSBL5	0.16	0.26	0.26	0.35	0.00	0.00	0.00
<i>Ferriphaseilus</i>	0.16	0.21	0.24	0.40	0.00	0.00	0.00
Pla4_lineage	0.15	0.14	0.24	0.41	0.00	0.00	0.00
<i>Candidatus_Peribacteria</i>	0.15	0.38	0.21	0.19	0.03	0.03	0.00
<i>Woesearchaeales</i>	0.15	0.30	0.17	0.13	0.08	0.05	0.14
<i>Methylotenera</i>	0.15	0.00	0.05	0.05	0.34	0.26	0.29
<i>Arcobacteraceae_uncultured</i>	0.15	0.00	0.00	0.00	0.36	0.29	0.33
BSV26	0.14	0.25	0.25	0.24	0.00	0.00	0.00
<i>Desulfobacca</i>	0.14	0.24	0.17	0.29	0.03	0.00	0.03
<i>Lainarchaeales</i>	0.13	0.30	0.23	0.16	0.00	0.00	0.00
<i>Lentisphaeria</i>	0.13	0.38	0.17	0.17	0.00	0.00	0.00
<i>Desulfatiglang</i>	0.12	0.24	0.29	0.12	0.00	0.00	0.00
<i>Chthonomonadales</i>	0.12	0.16	0.19	0.29	0.00	0.00	0.00
<i>Actinomarinales_uncultured</i>	0.12	0.17	0.15	0.23	0.00	0.05	0.05
<i>Latescibacteraceae</i>	0.11	0.14	0.17	0.26	0.00	0.00	0.00
<i>Methanomassiliicoccaceae_uncultured</i>	0.11	0.17	0.16	0.27	0.00	0.00	0.00
WOR-1	0.11	0.27	0.12	0.14	0.06	0.00	0.08
<i>Dehalococcoidales_uncultured</i>	0.10	0.20	0.17	0.16	0.00	0.00	0.00
<i>Dehalococcoidia_661239</i>	0.10	0.23	0.16	0.09	0.07	0.02	0.00
<i>Bacteroidetes_vadinHA17</i>	0.10	0.06	0.15	0.29	0.02	0.00	0.00
<i>Chlamydiales</i>	0.10	0.11	0.12	0.03	0.15	0.07	0.12
B29	0.10	0.16	0.07	0.29	0.00	0.00	0.00
WWE3	0.10	0.19	0.07	0.10	0.10	0.05	0.08
<i>Methylomonadaceae</i>	0.10	0.02	0.02	0.05	0.25	0.16	0.17
<i>Babeliales</i>	0.09	0.19	0.16	0.15	0.00	0.00	0.00
SG8-4	0.09	0.17	0.12	0.09	0.10	0.00	0.05
<i>Caulobacter</i>	0.09	0.04	0.05	0.05	0.22	0.14	0.08
<i>Bathyarchaeia</i>	0.09	0.11	0.00	0.29	0.09	0.00	0.03
<i>Candidatus_Iainarchaeum</i>	0.08	0.17	0.17	0.09	0.00	0.00	0.00
<i>Gaiellales_uncultured</i>	0.08	0.16	0.15	0.14	0.00	0.00	0.00
FW22	0.08	0.16	0.11	0.15	0.00	0.00	0.00
<i>Firmicutes</i>	0.08	0.10	0.07	0.08	0.12	0.05	0.03
<i>Candidatus_Vogelbacteria</i>	0.08	0.07	0.04	0.04	0.13	0.12	0.08
<i>Candidatus_Peregrinibacteria</i>	0.08	0.00	0.00	0.00	0.25	0.10	0.18
WCHB1-02	0.07	0.21	0.17	0.00	0.00	0.00	0.00
OPB41	0.07	0.09	0.12	0.16	0.00	0.00	0.00
<i>Ruminiclostridium</i>	0.07	0.11	0.12	0.14	0.00	0.00	0.00
Sh765B-TzT-20	0.07	0.15	0.12	0.10	0.00	0.00	0.00
<i>Aminicenantales</i>	0.07	0.04	0.03	0.02	0.09	0.14	0.12
<i>Gastranaerophilales</i>	0.07	0.00	0.02	0.03	0.16	0.12	0.13
ABY1	0.07	0.07	0.02	0.00	0.15	0.11	0.12
<i>Comamonadaceae_Curvibacter</i>	0.07	0.00	0.00	0.00	0.11	0.17	0.21
<i>Sedimenticolaceae_uncultured</i>	0.07	0.00	0.00	0.00	0.14	0.20	0.14
<i>Candidatus_Staskawiczbacteria</i>	0.06	0.12	0.13	0.08	0.00	0.00	0.00
MBNT15	0.06	0.10	0.10	0.10	0.00	0.00	0.00
<i>Jorgensenbacteria</i>	0.06	0.10	0.07	0.06	0.04	0.00	0.05
<i>Spirochaetaceae_uncultured</i>	0.06	0.14	0.07	0.11	0.00	0.00	0.00
<i>Candidatus_Liptonbacteria</i>	0.06	0.00	0.00	0.00	0.17	0.15	0.11
<i>Methylomonas</i>	0.06	0.00	0.00	0.00	0.15	0.13	0.13

JGI-0000079-D21	0.06	0.00	0.00	0.00	0.18	0.22	0.00
Unassigned	0.06	0.00	0.00	0.00	0.00	0.12	0.29
D8A-2	0.05	0.09	0.13	0.07	0.00	0.00	0.00
<i>Candidatus_Komeilibacteria</i>	0.05	0.14	0.13	0.00	0.04	0.00	0.00
<i>Candidatus_Nomurabacteria</i>	0.05	0.00	0.09	0.09	0.13	0.00	0.00
<i>Saccharimonadales</i>	0.05	0.13	0.09	0.06	0.00	0.00	0.00
<i>Qipengyuania</i>	0.05	0.10	0.08	0.07	0.00	0.00	0.00
<i>Sphingomonas</i>	0.05	0.10	0.07	0.11	0.00	0.00	0.00
DTU014	0.05	0.11	0.07	0.08	0.00	0.00	0.00
<i>Methanolinea</i>	0.05	0.08	0.06	0.15	0.00	0.00	0.00
JG30-KF-CM66	0.05	0.06	0.05	0.14	0.00	0.00	0.00
<i>Syntrophus</i>	0.05	0.05	0.00	0.22	0.00	0.00	0.00
<i>Syntrophales</i>	0.04	0.11	0.09	0.00	0.00	0.00	0.00
NKB15	0.04	0.07	0.08	0.07	0.00	0.00	0.00
<i>Methylococcus</i>	0.04	0.00	0.07	0.12	0.00	0.00	0.00
<i>Candidatus_Falkowbacteria</i>	0.04	0.06	0.07	0.07	0.00	0.00	0.00
BSV40	0.04	0.09	0.07	0.05	0.04	0.00	0.00
Lineage_IV	0.04	0.15	0.05	0.02	0.00	0.00	0.00
<i>Methylomonadaceae_uncultured</i>	0.04	0.00	0.04	0.04	0.11	0.03	0.05
MB-A2-108	0.04	0.08	0.04	0.12	0.00	0.00	0.00
FS118-23B-02	0.04	0.12	0.03	0.07	0.00	0.00	0.00
<i>Candidatus_Azambacteria</i>	0.04	0.00	0.00	0.00	0.13	0.08	0.08
<i>Candidatus_Paceibacter</i>	0.04	0.00	0.00	0.00	0.11	0.11	0.06
<i>Sulfuricellaceae</i>	0.04	0.00	0.00	0.00	0.09	0.11	0.09
<i>Omnitrophales</i>	0.03	0.05	0.07	0.03	0.00	0.00	0.03
<i>Hungateiclostridiaceae</i>	0.03	0.05	0.05	0.07	0.00	0.00	0.00
cvE6	0.03	0.06	0.05	0.04	0.00	0.00	0.00
SPG12-343-353-B75	0.03	0.08	0.05	0.04	0.00	0.00	0.00
<i>Thermincola</i>	0.03	0.08	0.05	0.04	0.00	0.00	0.00
<i>Kazania</i>	0.03	0.09	0.05	0.03	0.02	0.00	0.00
<i>Candidatus_Pacebacteria</i>	0.03	0.00	0.04	0.00	0.10	0.02	0.03
CPla-3_termite_group	0.03	0.04	0.04	0.06	0.00	0.00	0.00
DG-56	0.03	0.05	0.04	0.09	0.00	0.00	0.00
TTA-B15	0.03	0.04	0.03	0.03	0.00	0.08	0.00
<i>Bacteriovorax</i>	0.03	0.00	0.00	0.00	0.06	0.09	0.07
<i>Chloroplast</i>	0.03	0.00	0.00	0.00	0.05	0.08	0.10
<i>Hirschia</i>	0.03	0.00	0.00	0.00	0.11	0.05	0.06
<i>Hydrogenophaga</i>	0.03	0.00	0.00	0.00	0.06	0.05	0.10
<i>Aenigmarchaeales</i>	0.03	0.03	0.00	0.00	0.07	0.03	0.05
<i>Desulfosarcinaceae_uncultured</i>	0.03	0.05	0.00	0.11	0.00	0.00	0.00
<i>Microgenomatia</i>	0.02	0.03	0.06	0.00	0.00	0.00	0.00
SR-FBR-L83	0.02	0.05	0.06	0.00	0.00	0.00	0.00
<i>Geobacteraceae</i>	0.02	0.00	0.05	0.03	0.00	0.00	0.00
<i>Methanobacterium</i>	0.02	0.03	0.05	0.04	0.00	0.00	0.00
TA06	0.02	0.00	0.04	0.05	0.00	0.00	0.00
<i>Alphaproteobacteria_uncultured</i>	0.02	0.08	0.04	0.03	0.00	0.00	0.00
CPR2	0.02	0.00	0.03	0.06	0.00	0.00	0.00
<i>Terrimicrobium</i>	0.02	0.00	0.03	0.07	0.00	0.00	0.00
GW2011_GWC1_47_15	0.02	0.05	0.03	0.04	0.00	0.00	0.00
SAR202_clade	0.02	0.03	0.02	0.04	0.00	0.00	0.00
<i>Methylacidiphilaceae_uncultured</i>	0.02	0.07	0.02	0.04	0.00	0.00	0.00
<i>Patescibacteria</i>	0.02	0.04	0.01	0.00	0.07	0.00	0.03

CG1-02-32-21	0.02	0.00	0.00	0.00	0.06	0.05	0.02
<i>Terrimonas</i>	0.02	0.00	0.00	0.00	0.05	0.06	0.03
<i>Sulfurimonadaceae</i>	0.02	0.00	0.00	0.00	0.10	0.00	0.06
vadinBA26	0.02	0.00	0.00	0.12	0.00	0.00	0.00
<i>Candidatus_Buchananbacteria</i>	0.02	0.00	0.00	0.00	0.07	0.00	0.05
<i>Candidatus_Kaiserbacteria</i>	0.02	0.00	0.00	0.00	0.05	0.05	0.06
<i>Asticcacaulis</i>	0.02	0.00	0.00	0.00	0.04	0.03	0.06
<i>Rhizobium</i>	0.02	0.00	0.00	0.00	0.00	0.10	0.06
<i>Rhodobacter</i>	0.02	0.00	0.00	0.00	0.00	0.05	0.10
WPS-2	0.02	0.05	0.00	0.03	0.04	0.03	0.00
<i>Methanoregula</i>	0.02	0.10	0.00	0.03	0.00	0.00	0.00
<i>Rhizomicrobium</i>	0.01	0.00	0.05	0.00	0.00	0.00	0.00
<i>Lentimicrobiaceae</i>	0.01	0.00	0.04	0.00	0.03	0.00	0.00
<i>Pirellulaceae_uncultured</i>	0.01	0.00	0.04	0.02	0.00	0.00	0.00
<i>Campylobacterales_uncultured</i>	0.01	0.00	0.03	0.05	0.00	0.00	0.00
WD2101_soil_group	0.01	0.00	0.03	0.03	0.00	0.00	0.00
<i>Candidatus_Obscuribacter</i>	0.01	0.02	0.03	0.00	0.00	0.00	0.00
WCHB1-41	0.01	0.03	0.03	0.00	0.00	0.00	0.00
<i>Chloroflexi</i>	0.01	0.00	0.02	0.03	0.00	0.00	0.00
Clostridia_vadinBB60_group	0.01	0.00	0.02	0.03	0.00	0.00	0.00
<i>Azospirillum</i>	0.01	0.00	0.02	0.02	0.00	0.00	0.00
<i>Methyloglobulus</i>	0.01	0.03	0.02	0.02	0.00	0.00	0.00
Bacteriap25	0.01	0.04	0.02	0.00	0.00	0.00	0.00
Methanofastidiosales_uncultured	0.01	0.00	0.00	0.00	0.06	0.00	0.03
GOUTB8	0.01	0.00	0.00	0.05	0.00	0.00	0.00
Frankiales_Sporichthyaceae	0.01	0.00	0.00	0.00	0.03	0.05	0.00
IheB3-7	0.01	0.00	0.00	0.00	0.06	0.00	0.03
SBR1031	0.01	0.00	0.00	0.00	0.07	0.00	0.03
<i>Desulfobulbales_uncultured</i>	0.01	0.00	0.00	0.04	0.00	0.00	0.00
<i>Marinimicrobia_(SAR406_clade)</i>	0.01	0.00	0.00	0.00	0.03	0.03	0.00
<i>Myxococcota</i>	0.01	0.00	0.00	0.00	0.03	0.02	0.01
<i>Candidatus_Jacksonbacteria</i>	0.01	0.00	0.00	0.00	0.00	0.04	0.03
GWA2-38-13b	0.01	0.00	0.00	0.00	0.04	0.00	0.03
<i>Beijerinckiaceae</i>	0.01	0.00	0.00	0.08	0.00	0.00	0.00
<i>Beggiatoaceae_uncultured</i>	0.01	0.00	0.00	0.00	0.00	0.00	0.07
<i>Comamonadaceae</i>	0.01	0.00	0.00	0.00	0.03	0.05	0.00
<i>Ottowia</i>	0.01	0.00	0.00	0.00	0.00	0.00	0.08
<i>Rhodoferax</i>	0.01	0.00	0.00	0.04	0.00	0.00	0.00
<i>Methylobacillus</i>	0.01	0.00	0.00	0.04	0.00	0.00	0.00
<i>Methylophilaceae_uncultured</i>	0.01	0.00	0.00	0.00	0.00	0.03	0.06
PRD18C08	0.01	0.00	0.00	0.00	0.08	0.00	0.00

Table S4. Phyla relative abundance of the bacterial and archaeal communities of the water samples from the Pöhla (P1; P5; P8) and Schlema-Alberoda mines (S1; S2; S6).

	Relative abundance (%)						
	Total	P1	P5	P8	S1	S4	S6
Bacteria_Campilobacterota	46.85	37.52	43.86	40.74	51.57	55.91	55.30
Bacteria_Proteobacteria	20.37	9.28	11.07	12.96	31.47	32.57	31.48
Bacteria_Patescibacteria	8.31	16.56	12.48	7.91	4.63	2.75	3.41
Bacteria_Nitrospirota	6.05	6.92	9.41	15.28	0.26	0.10	0.17
Bacteria_Verrucomicrobiota	4.55	8.21	6.11	4.49	2.95	2.06	2.61
Bacteria_Chloroflexi	3.85	7.08	5.97	6.39	0.90	0.47	0.46
Bacteria_Desulfobacterota	1.64	0.98	0.85	1.00	2.96	2.27	2.30
Bacteria_Actinobacteriota	1.15	2.80	1.44	1.45	0.22	0.30	0.30
Bacteria_Bacteroidota	1.13	0.44	0.57	0.57	2.18	1.44	2.06
Bacteria_Acetothermia	1.02	2.29	1.57	1.72	0.00	0.00	0.00
Archaea_Nanoarchaeota	0.88	1.55	1.02	0.60	0.96	0.65	0.46
Bacteria_Sva0485	0.76	1.03	1.31	1.63	0.08	0.00	0.00
Bacteria_Planctomycetota	0.52	0.72	0.72	0.79	0.28	0.21	0.20
Archaea_Thermoplasmatota	0.34	0.66	0.54	0.64	0.05	0.00	0.00
Bacteria_Firmicutes	0.32	0.54	0.52	0.50	0.12	0.05	0.03
Archaea_Halobacterota	0.24	0.56	0.29	0.47	0.00	0.00	0.00
Archaea_Iainarchaeota	0.20	0.47	0.40	0.25	0.00	0.00	0.00
Bacteria_Zixibacteria	0.20	0.24	0.24	0.49	0.03	0.00	0.06
Bacteria_Armatimonadota	0.15	0.21	0.23	0.38	0.00	0.00	0.00
Bacteria_WOR-1	0.11	0.27	0.12	0.14	0.06	0.00	0.08
Bacteria_Cyanobacteria	0.11	0.02	0.05	0.03	0.21	0.20	0.24
Bacteria_Latescibacterota	0.11	0.14	0.17	0.26	0.00	0.00	0.00
Bacteria_Caldisericota	0.10	0.24	0.19	0.03	0.00	0.08	0.00
Archaea_Crenarchaeota	0.09	0.11	0.00	0.29	0.09	0.00	0.03
Bacteria_Dependentiae	0.09	0.19	0.16	0.15	0.00	0.00	0.00
Bacteria_Acidobacteriota	0.08	0.04	0.03	0.07	0.09	0.14	0.12
Unassigned	0.06	0.00	0.00	0.00	0.00	0.12	0.29
Bacteria_Synergistota	0.06	0.00	0.00	0.00	0.18	0.22	0.00
Bacteria_MBNT15	0.06	0.10	0.10	0.10	0.00	0.00	0.00
Bacteria_Spirochaetota	0.06	0.14	0.07	0.11	0.00	0.00	0.00
Bacteria_NKB15	0.04	0.07	0.08	0.07	0.00	0.00	0.00
Bacteria_Elusimicrobiota	0.04	0.15	0.05	0.02	0.00	0.00	0.00
Archaea_Euryarchaeota	0.04	0.03	0.05	0.04	0.06	0.00	0.03
Bacteria_Bdellovibrionota	0.03	0.00	0.00	0.00	0.06	0.09	0.07
Archaea_Aenigmarchaeota	0.03	0.03	0.00	0.00	0.07	0.03	0.05
Bacteria_WPS-2	0.02	0.05	0.00	0.03	0.04	0.03	0.00
Bacteria_Myxococcota	0.02	0.04	0.02	0.00	0.03	0.02	0.01
Archaea_Micrarchaeota	0.02	0.00	0.00	0.00	0.06	0.05	0.02
Bacteria_TA06	0.02	0.00	0.04	0.05	0.00	0.00	0.00
Bacteria_Marinimicrobia (SAR406)	0.01	0.00	0.00	0.00	0.03	0.03	0.00

Table S5. Quality assessment of raw RNA-seq data.

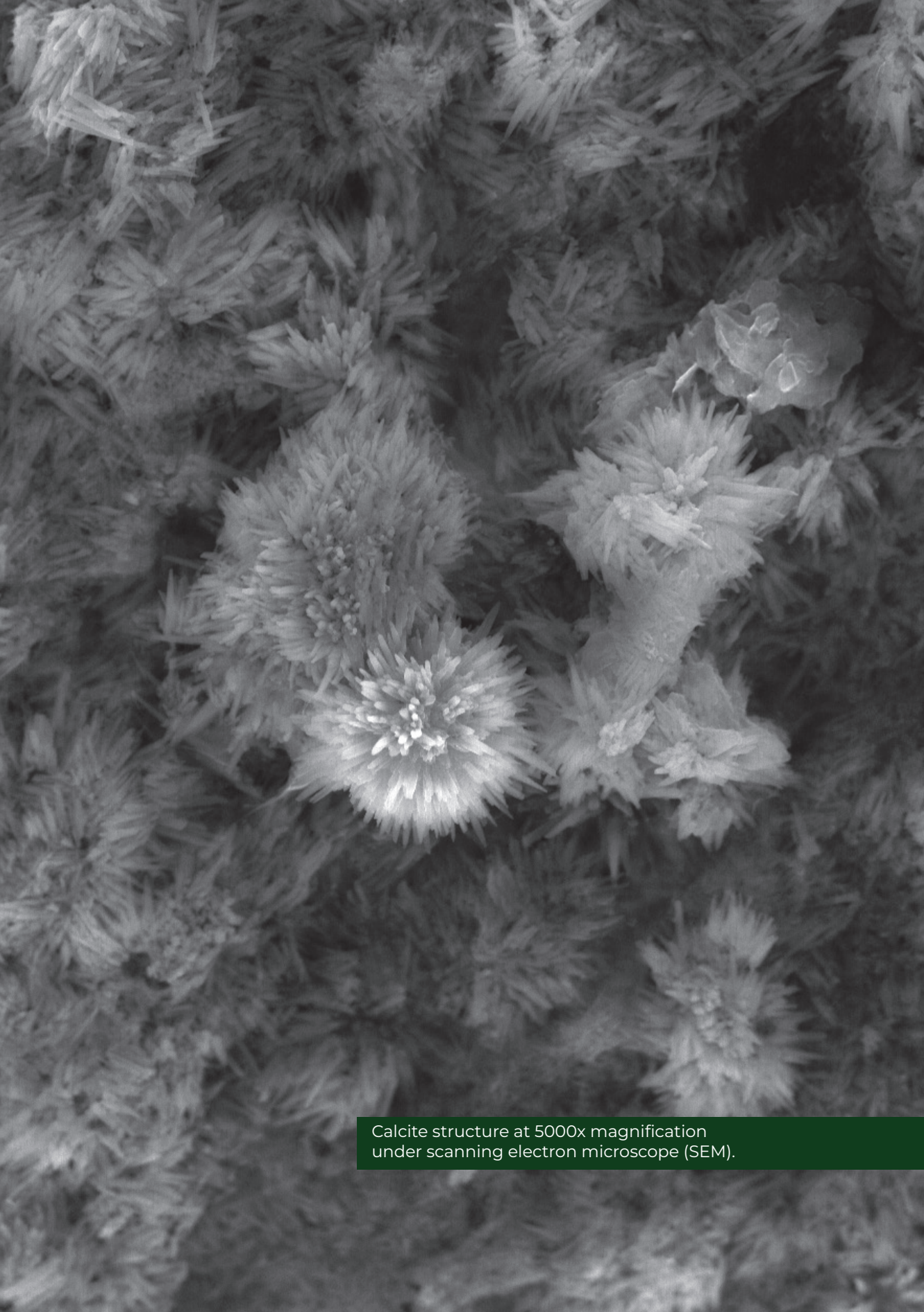
Sample	Number of bases [Mbp]	Number of reads	Mean read length [bp]
S1	14316	66 812 164	150
S4	18690	68 531 042	150
S6	14230	66 409 588	150
P1	11539	69 238 128	150
P5	11744	70 468 276	150
P8	11511	69 066 338	150

Table S6. Genes involved in assimilatory and dissimilatory of sulphate reduction by KO.

Module M00569	Dissimilatory sulfate reduction (DSR)	Gene	Gene No. in Pöhla	Gene No. in Schlema- Alberoda
KO	K00958	<i>sat</i>	57	49
	K00394	<i>aprA</i>	175	100
	K00395	<i>aprB</i>	47	10
	K11180	<i>dsrA</i>	125	48
	K11181	<i>dsrB</i>	90	15
Module M00176	Assimilatory sulfate reduction (ASR)			
KO	K13811	<i>PAPSS</i>	0	4
	K00958	<i>sat</i>	57	49
	K00860	<i>cysC</i>	3	7
	K00955	<i>cysNC</i>	6	9
	K00957	<i>cysD</i>	5	35
	K00956	<i>cysN</i>	5	25
	K00390	<i>cysH</i>	3	26
	K05907	<i>apr</i>	0	0
	K00380	<i>cysJ</i>	4	17
	K00381	<i>cysI</i>	5	85
	K00392	<i>sir</i>	0	10

Table S7. Genes involved in the biological iron cycle in both mine waters by FeGenie v1.2

Category	Gene	Gene No. in Pöhla	Gene No. in Schlema-Alberoda
Fe-oxidation	<i>sulfocyanin</i>	1	0
	<i>foxE</i>	2	0
	<i>cyc2</i>	29	17
Fe-storage	<i>ferritin</i>	86	55
Fe-reduction	<i>omcS</i>	2	0
Fe-regulation	<i>dtxR</i>	10	4
	<i>pvdS</i>	34	27
	<i>fur</i>	63	36
	<i>fecR</i>	40	48
	<i>fecR</i>	0	1
	<i>pchR</i>	7	7
	<i>yqjI // yqjH</i>	13	6



Calcite structure at 5000x magnification under scanning electron microscope (SEM).

Chapter III:

New insight into U(IV) and U(V) formation by glycerol-based stimulation of indigenous U reducing bacteria in U mine water: multidisciplinary approach characterization

AUTHORS:

Antonio M. Newman-Portela ^{a,b,*}, Kristina O. Kvashnina ^{b,d}, Elena Bazarkina ^{b,d}, André Rossberg ^{b,d}, Frank Bok ^b, Andrea Kassahun ^c, Björn Drobot ^b, Thorsten Stumpf ^b, Johannes Raff ^b, Mohamed L. Merroun ^a, Evelyn Krawczyk-Bärsch ^b.

^a Department of Microbiology, Faculty of Science, University of Granada, Spain.

^b Helmholtz-Zentrum Dresden-Rossendorf, Institute of Resource Ecology, Bautzner Landstraße 400, 01328 Dresden, Germany.

^c WISMUT GmbH, Chemnitz, Germany.

^d Rossendorf Beamline (BM20-ROBL), European Synchrotron Radiation Facility, Grenoble, France.

KEYWORDS: pentavalent uranium; tetravalent uranium; mine water; bacteria; bioremediation; nanoparticles.

ABSTRACT

The ability of the native microbial community from the water of the Schlema-Alberoda mine (Wismut GmbH, Germany) to reduce U(VI) based on the use of glycerol as electron donor was investigated with the aim of improving the bioremediation strategy for U-contaminated mine water. The multidisciplinary approach combining analytical (Inductively Coupled Plasma Mass Spectrometry, High-Performance Ion Chromatography, thermodynamic calculation) and spectroscopic methods (High-Energy-Resolution Fluorescence-Detected X-ray Absorption Near-Edge Structure, Extended X-Ray Absorption Fine Structure, Ultraviolet-visible spectroscopy) clearly showed the reduction of the initial U(VI) to U(V) and U(IV) in the microcosms, amended with glycerol. The formation of U(IV) and U(V) nanoparticles (NPs) was confirmed through microscopic methods (High-Angle Annular Dark-Field Scanning Transmission Electron Microscopy) due to the microbial reduction of U(VI). The results indicate that glycerol is an effective stimulant in promoting the enzymatic reduction of soluble U(VI) to U(IV) in the form of uraninite NPs and U(V) as FeUO_4 NPs on the bacterial surface. This is the first report describing the formation of biogenic FeU(V)O_4 NPs in low U contaminated environmental samples

1. Introduction

Uranium (U) is a naturally occurring radionuclide distributed in the Earth's crust, water and living organisms (Chen et al. 2021). For decades, Eastern Germany was affected by intense U mining activity that left a large legacy of contaminated environments. Schlema-Alberoda mine (Saxony, Germany) was a major U producer at that time and after its cessation in the 1990s, conventional remediation strategies based on controlled flooding and subsequent U water treatment were started. As a result, U(VI) concentration decreased to 1 mg/l, which exceeds the maximum U(VI) concentration in drinking water (0.03 mg/l) established by WHO (Ansoborlo et al. 2015; WHO 2022) and maximum discharge limits into the aquatic environment in Saxony (Wismut GmbH Umweltbericht 2021). Thus, the used conventional remediation technologies do not meet the set water quality regulatory standard for beneficial reuse of the U mine water for different purposes (e.g., irrigation, especially in water-stressed regions) within the concept of circular economy (Annandale et al. 2017). Therefore, over the past three decades, bioremediation has emerged as a promising method to support and outperform chemical treatments due to its cost-effectiveness and environmental sustainability (Sánchez-Castro et al. 2021; Banala et al. 2021). The effectiveness of U bioremediation relies on biogeochemical processes that control its speciation, mobility, and thus bioavailability. The main strategies for U bioremediation involve U phosphate biomineralization under oxic conditions (Martínez-Rodríguez et al. 2023), and enzymatic reduction, also known as bioreduction under anoxic conditions (Lakaniemi et al. 2019). Williams et al. (2013) reported bioreduction based on the stimulation of U-reducing bacteria could be considered as an efficient method for U removal. In both, laboratory and field scale studies, several electron donors have been used to promote the growth and activity of U-reducing bacteria, encompassing acetate (Anderson et al. 2003; Istok et al. 2004; Marshall et al. 2009), lactate (Finneran et al. 2002; Shelobolina et al. 2008), ethanol (Wu et al. 2006, 2007; Shelobolina et al. 2008), hydrogen (Junier et al. 2010; Liu et al. 2002; Marshall et al. 2009) and glycerol (Madden et al. 2007; Newsome et al. 2015). These

bacterial strains couple the oxidation of electron donors with the reduction of U(VI) to U(IV). The hexa- and tetravalent U forms prevail stable under oxidizing and strongly reducing conditions, respectively (Smedley and Kinniburgh 2023). Under oxic conditions, U(VI) is soluble as a uranyl ion (UO_2^{2+}) and readily forms complexes with carbonates, among others, providing a remarkable mobility (Bernhard et al. 1998; Newman-Portela et al. 2023). In contrast, U(IV), under reducing conditions, is insoluble and less mobile, thus potentially less bioavailable. The reduction of U(VI) to U(IV) by microbes produces an insoluble precipitate of U, often associated to crystalline uraninite (UO_2) (Newsome et al. 2014). However, with the improvement of spectroscopic and microscopic techniques, other phases such as amorphous mononuclear U(IV) or U(IV) bound to organic ligand have been identified (Lakaniemi et al. 2019). It is well known that biogenic U(IV) phases are very susceptible to re-oxidation and remobilization. Therefore, for the successful application of long-term U bio-stabilization, it is crucial to understand the structure, composition, and stabilities of U(IV) phases. In addition to U(IV), recent studies have reported the presence of U(V) during the reduction of U(VI) to U(IV) (*Desulfosporosinus hippei* DSM 8344^T, Hilpmann et al. 2023). U(V) is typically considered as an unstable and transient state, but previous studies have demonstrated its stabilization under aqueous conditions through the use of a polydentate aminocarboxylate ligand (Faizova et al. 2018). Additionally, U(V) phases have been found to exhibit increased stability when incorporated into mineral lattices alongside iron-containing phases (Collins and Rosso 2017; Roberts et al. 2017). Vettese et al. (2020) and Crean et al. (2020) have also identified stable U(V) species. Vettese et al. (2020) identified U(V) species after 120.5 hours as a result of the reduction of U(VI) carried out by *Shewanella oneidensis* MR1. Conversely, Crean et al. (2020) reported the stability of FeUO_4 particles in the medium term (>25 years) under ambient conditions. These few reports shed some light into the impact of pure cultures of some bacterial strains on the presence and stability of U(V) species as result of U(VI) reduction. However, the environmental impact of U(V) and its long-term stability need to be addressed in the context

of U mine water bioremediation-based experiments through stimulation of U-reducing bacteria.

In a previous work, the geochemical and microbiological characterization of the studied mine water and the screening of most suitable electron donor (glycerol) for the stimulation of U-reducers, were conducted (Newman-Portela et al. 2024). The present work is focused on the process understanding as well as the design and optimization of a U mine water bioremediation strategy, through stimulation of U-reducers by amendment of glycerol. The formation of U(IV) and even U(V) was investigated using a multidisciplinary approach of spectroscopy and microscopy. Various spectroscopic techniques, such as Ultraviolet-Visible Spectroscopy (UV/Vis), Powder X-Ray Diffraction (PXRD), High-Energy-Resolution Fluorescence-Detected X-ray Absorption Near-Edge Structure (HERFD/XANES) and Extended X-Ray Absorption Fine Structure (EXAFS) as well as microscopic techniques, such as High-Angle Annular Dark-Field Scanning Transmission Electron Microscopy (HAADF-STEM), Scanning Electron Microscopy in combination with Energy-Dispersive X-Ray Spectroscopy (SEM/EDXS) provided insights into the structure of biogenic U(V) and U(IV) species and their long-term stability.

2. Materials and methods

2.1. Mine water collection and storage

During a sampling campaign in June 2022, a 50 L autoclaved canister was used to collect fresh mine water from the Wismut GmbH Schlema-Alberoda mine (Newman-Portela et al. 2024). The samples were taken from the inlet of the mine water treatment plant receiving continuous pumped water from the mine. To prevent the collection of wastewaters, a proper purging of the sampling pipes and tap was performed. This step was essential to accurately keep the chemical and microbiological composition of the mine water. Physical parameters like pH and redox potential (E_H) were measured *in situ*. The mine water sample was transported at 4 °C to the laboratory for its immediate use in the preparation of the U reduction microcosm experiments.

2.2. Stimulation of U reducing bacteria in U mine water microcosm experiments

In order to assess the bioremediation potential of the indigenous U-reducing microbial community of the Schlema-Alberoda mine water, a series of anoxic microcosms were elaborated. Two-litre serum bottles were filled with freshly collected water and supplemented with glycerol (10 mM). Glycerol (ROTIPURAN, Germany) was selected as the most suitable electron donor for the U-reducers (Newman-Portela et al. 2024). To evaluate the significant involvement of biological processes in the U reduction, control microcosms were performed at the same time. In a set of microcosms, unamended mine water was used as a control (SAC), while in another set of control microcosms, mine water was sterilized (autoclaved) and amended with glycerol (ASA+G). The microcosms were incubated for 130 days at 28 ± 2 °C in the dark.

2.3. Physio-chemical monitoring of microcosms

The main parameters of the mine water (e.g., pH, E_H , the concentration of U, Fe, As and SO_4^{2-}) were monitored during the biostimulation experiment at weekly intervals. The pH of the mine water was measured using a pH meter 3110 (WTW, Germany), equipped with a BlueLine 16 pH microelectrode from Schott Instruments (Germany). To determine the E_H values, a micro redox electrode featuring a platinum ring (ORP electrode, Mettler-Toledo InLab, Spain) was utilized. At the beginning and at the end of the biostimulation experiment, a total analysis of the dissolved cations (Na, K, Mg, Ca, Al, Si, P, Mn, Fe, As, Ba, Th, U) and anions (NO_2^- , NO_3^- , PO_4^{3-} , SO_4^{2-} , Cl^-) were performed by Inductively Coupled Plasma Mass Spectrometry (ICP-MS, ELAN 9000, PerkinElmer, Germany) and High-Performance Ion Chromatography (HPIC, Dionex Integrion, Thermo Fisher Scientific, USA), respectively. Prior to analysis by ICP-MS, the samples were acidified using nitric acid (HNO_3). Total inorganic/organic carbon (TIC/TOC), dissolved organic carbon (DOC) and total nitrogen were also quantified (Multi N/C 2100S, Analytik Jena, Germany).

2.4. Thermodynamic calculation

The analytical data, which were obtained at the end of the biostimulation experiment, were used to calculate the predominance fields of the possible U species. A Pourbaix diagram was generated utilizing the geochemical speciation code Geochemist's Workbench, version 17.0.1/Act2. The thermodynamic database utilized for this calculation was the ThermoChimie database Version 10.a (Giffaut et al. 2014; Grivé et al. 2015).

2.5. U solid phase characterization

During the biostimulation experiment, distinct black precipitates were formed at the bottom of the microcosms. The black precipitates were sampled at different times according to different U concentrations (U removal rate) in the supernatant of the microcosms. Thus, samples of the black precipitates were obtained when the U concentration in the supernatant had decreased by 20%, 60% and 90%, respectively based on the monitoring data. They were collected by centrifuging the mine water microcosm at 4,020 x g for 15 minutes (Hettich EBA 21, Germany) while maintaining anoxic conditions. Subsequently, the samples were prepared within a glovebox for UV/Vis spectroscopy and for HERFD-XANES and EXAFS measurements as well as for HAADF-STEM analysis.

Additionally, in order to assess the stability of the reduced U(VI) products against oxidizing factors, the black precipitate of the microcosm, characterized by 90% decrease of the U concentration in the supernatant, was prepared in a glovebox. It remained afterwards under oxidizing conditions for 4 weeks until it was measured by HERFD-XANES and HAADF-STEM.

2.5.1. Ultraviolet–visible (UV/Vis) spectroscopy

In order to obtain evidence of U(IV) presence and formation, UV/Vis spectrophotometric analyses were carried out using the Cary 5G UV/VIS-NIR spectrophotometer (Varian, U.S.). A spectral range between 350 and 750 nm was performed with a minimum step width of 0.1 nm. For sample preparation, we used the methodology described by Hilpmann et al. (2023) with modifications. For each measurement, 2 grams of black precipitate

was dissolved in 3 mL of 5 M HCl under stirring at 120 rpm for 45 minutes. Subsequently, it was centrifuged at room temperature at $10,000 \times g$ (Eppendorf 5415, Germany) for 15 minutes and transferred to a quartz glass cuvette. An aquo ion U(IV) solution of 100 μM in 5 M HCl was used as the reference spectrum. The data processing and visualization was carried out using Matlab. An implementation of a rolling ball algorithm (Drobot et al. 2020; Vogel et al. 2021) was used to remove the intense background originating from organic and inorganic substances in the precipitate.

2.5.2. HERFD-XANES and EXAFS spectroscopy

The oxidation state and local coordination of U in the black precipitates was determined using HERFD-XANES and EXAFS. The measurements were carried out at the BM20 Rossendorf beamline (ROBL) (Scheinost et al. 2021) of the European Synchrotron Radiation Facility (ESRF) in Grenoble (France), where the storage ring was operated in the multi-bunch filling mode at 6 GeV with a 200 mA current.

For HERFD-XANES and EXAFS measurements, the black precipitates of the microcosms, which were characterized by a different decrease of the U concentration in the supernatant (20%, 60%, 90%), were prepared inside a glovebox. The samples for HERFD-XANES measurements were placed as wet pastes inside special holders with round recess of 1 mm depth. The holders were single-confined with a Kapton foil of 13-micron thickness. For EXAFS measurements, we transferred the black precipitate as wet paste into a 3 mm thick polyethylene holder, which was double-confined between with 13 μm Kapton tape and polyethylene. Subsequently, the HERFD-XANES and EXAFS samples were immediately frozen in liquid N_2 , transported to the beamline at the ESRF in the frozen state and measured under cryo-conditions.

We performed HERFD-XANES measurements at the M_4 -edge (Kvashnina et al. 2013), and fluorescence EXAFS measurements at the U L_3 -edge (Lee et al. 1981). HERFD spectra were recorded using a Johann-type X-ray emission spectrometer in a vertical Rowland geometry (Kvashnina and Scheinost 2016) equipped with a silicon drift X-ray detector (©Ketec). The incident energy was selected using a Si(111) double-crystal monochromator.

Two Si mirrors before and after the monochromator were used to collimate the beam and reject higher harmonics. The incident energy was calibrated using HERFD spectra of reference compound, i.e., the maximum energy position of U HERFD-XANES was set at 3725 eV (U M_4 -edge, UO_2 reference). The beam size was estimated to be ~ 30 μm (vertically) by ~ 2 mm (horizontally). The X-ray emission spectrometer was equipped with five crystal analyzers with a 1 m bending radius, Si(220) for HERFD measurements U M_4 -edge (3728 eV). The spectrometer was tuned to the maximum of the U M_β emission line (3339.8 eV). The corresponding Bragg angles was 75. A helium gas-filled bag was placed to fill the optical path sample-crystal analyzers-detector to reduce the absorption of the fluorescence signal by air. The energy resolution was estimated to be ~ 1 eV. The HERFD-XANES U M_4 edge spectra were recorded with 0.2 eV step and the counting time of 3 seconds per point. Each individual spectrum was ~ 6 min of duration for U. To increase signal-to-noise ratio, 4-10 spectra per sample were collected and averaged.

In the case of U L_3 edge EXAFS measurements the white X-ray beam was monochromatized by using a Si(111) double crystal monochromator in channel cut mode, while two Rh-coated coated mirrors reduced the higher harmonics. For each sample the fluorescence signal of the $L\alpha_{1,2}$ line was accumulated by using a 18-element Ge-detector and the K edge absorption spectrum of a Y metal foil was measured simultaneously for energy calibration. The incident photon flux and the absorption of the Y metal foil was measured by using gas-filled ionization chambers. Per sample 6-9 energy scans were accumulated and averaged in order to receive a sufficient high signal-to-noise ratio as needed for further data analysis. The samples were measured under cryogenic conditions by using a closed cycle He-cryostat. For the calculation of the photoelectron wave vector (k) the ionization potential at the U L_3 edge was arbitrarily set to 17.185 keV. We used the EXAFSPAK software for data processing, including energy calibration, averaging of multiple sample scans, X-ray absorption background correction, EXAFS signal isolation, and structural model fitting (George 1995). The *ab-initio* scattering code FEFF8.20 (Ankudinov et al.

2002) was used for calculating theoretical amplitude and phase scattering functions, while liebigite (Mereiter 1982) and uraninite (Wyckoff 1963) served as structural models. Assuming the presence of coexisting U(IV), U(V), and U(VI) species, we applied the iterative target factor analysis (ITFA) method (Rossberg et al. 2003) for the mathematical decomposition of the spectral mixtures into pure U component spectra and their fractions in the data.

2.5.3. Powder X-ray diffraction (PXRD)

The X-ray diffraction diffractogram of the collected black precipitate were recorded using a MiniFlex 600 Powder X-ray diffractometer (Rigaku, Tokyo, Japan) equipped with a Cu K α X-ray source (40 keV/15 mA operation for X-ray generation) and the D/teX Ultra 1D silicon strip detector in the Bragg–Brentano θ – 2θ geometry at a scanning speed of 2 degrees per min. The sample was collected from the microcosm in which the U concentration had decreased by 90% in the supernatant. The peak position was determined with PDXL 2 program. The sample was completely dried inside an anoxic glovebox and subsequently ground to obtain a fine powder. During the measurements, hermetically sealed low-background sample holders covered with Kapton tape were used.

2.5.4. Transmission and scanning electron microscopy

The crystallographic/structural analysis and cellular localization of U reduction products were examined using High-Angle Annular Dark-Field Scanning Transmission Electron Microscopy (HAADF-STEM FEI TITAN G2 80-300, University of Granada, Spain) equipped with Energy-Dispersive X-Ray Spectroscopy (EDXS), Selected Area Electron Diffraction (SAED), and Fast Fourier Transform (FFT).

Sample preparation for HAADF-STEM was conducted at the Biological Sample Preparation Laboratory located in the “*Centro de Instrumentación Científica*” at the University of Granada. The black precipitate, which was collected from a microcosm with a U decrease of 90% in the supernatant, was fixed with a 2.5% glutaraldehyde solution in a 10% PBS buffer. Subsequently, the sample was embedded in resin (Epon 812). To obtain

ultra-thin sections (75 - 80 nm), a diamond knife on a ultramicrotome (Reichert Ultracut S, Germany) was used. The sections were placed on copper grids and coated with carbon. The samples were examined at an acceleration voltage of 200 kV under standard operating conditions with liquid nitrogen anti-contamination placed.

Additionally, a Hitachi S-4800 high-resolution scanning electron microscope (SEM) with a voltage of 5-30 kV was used in combination with an energy-dispersive X-ray spectroscopy (EDXS) microanalysis system to characterize the black precipitate. For sample preparation, the black precipitate was placed on the carbon-coated surface of the specimen holder in an anoxic chamber. The sample was maintained under anoxic conditions until completely dried. Subsequently, the sample was transferred for observation in a vacuum chamber without any further preparation step. Furthermore, a sample was prepared at the beginning of the experiment to study the natural colloidal particles of the system bearing metals such as U, Fe, and As using SEM/EDXS. A volume of 50 mL of the water sample was filtered using a pressure filter holder (Sartorius, Fisher Scientific) with a 50 nm pore size membrane (Isopore™ Membrane Filters Typ VMTP) and a pressure of 4 bar. From the filter membrane, a section was cut and placed onto the carbon-coated surface of the specimen holder and vapourised with gold (Au). The sample was directly analysed by SEM/EDXS.

3. Results

3.1. Physico-chemical monitoring of the mine water microcosms

In biostimulation experiments, 10 mM glycerol was amended to Schlemma-Alberoda mine water in microcosms under anaerobic conditions. The monitoring of the main physico-chemical parameters (pH, E_H , concentrations of U, Fe, As and SO_4^{2-}) of the microcosms was carried out for 130 days. In addition, a series of control microcosms were set up for comparison. In the microcosms, which were supplemented with glycerol, the formation of a black precipitate at the bottom of the bottles were visually observed during the experiment (Fig. 1S). The formation of a black precipitate probably indicates the biological reduction of soluble hexavalent U(VI) through the

stimulation of glycerol oxidizers.

The physico-chemical parameters of the mine water (pH, E_H , and the concentrations of U, Fe, As and SO_4^{2-}) in the different microcosms was characterized. Data of the water chemistry in the microcosm during the experiment analysed by ICP-MS and HPIC are shown in Table S1 and in Figure 1. In addition, the full chemical composition of the mine water at the end of the experiment is shown in Table S2 of the supplementary material. At the beginning of the biostimulation experiment, a pH of 7.5 and an E_H of +398 mV was recorded. As time progressed, the pH exhibited fluctuations, reaching a maximum value of 8 during the first 20 days. Afterwards, the pH of the mine water decreased and stabilized close to the initial value of 7.5. In contrast, the E_H showed a strong decrease during the experiment from $+398 \pm 20$ mV to -114 ± 20 mV at the end of the experiment after 130 days (Fig. S2 and Table S2). In contrast, slight decrease in E_H was observed in the control microcosms (Table S2).

As shown in Figure 1, the addition of glycerol to the microcosm resulted in a remarkable decrease in the U(VI) concentration from 1 to 0.04 mg/l (decrease by 96%) at the end of the experiment, whereby only a slight decrease was observed during the first 20 days (about 5-10%). A strong decrease could only be detected after 40 days. Minor changes were also observed in the control microcosms, where the final U(VI) concentration were 0.75 mg/l in the SAC microcosm and 0.64 mg/l in the ASA+G microcosm. The concentrations of Fe, SO_4^{2-} , and As experienced substantial decreases of approximately 98%, 68%, and 44%, respectively.

The analysis of the dissolved cations and anions at the end of the experiment (Table S2), show a decrease in Ca concentration of about 33%, 50% and 59% in the experimental and the control microcosms, respectively. NO_2^- and NO_3^- concentrations were initially and finally extremely low (<0.5 mg/l). The initial measurements of dissolved organic carbon (DOC) and total organic carbon (TOC) were low (1.89 and 1.79 mg/l, respectively), but notably increased by two orders of magnitude by the end of the experiment. Total inorganic carbon (TIC) levels were high, both at the beginning and end, with a higher concentration specifically observed at the experiment's

end. In the SAC control group, TOC and TIC levels were comparable, but there was a slightly more pronounced change in DOC levels. In contrast, in the ASA+G control group, TIC levels showed minor fluctuations, but TOC and DOC values increased by up to 3 orders of magnitude compared to the original Schlema-Alberoda mine water (SA). Total nitrogen (TN) remained below the detection limit throughout the experiment.

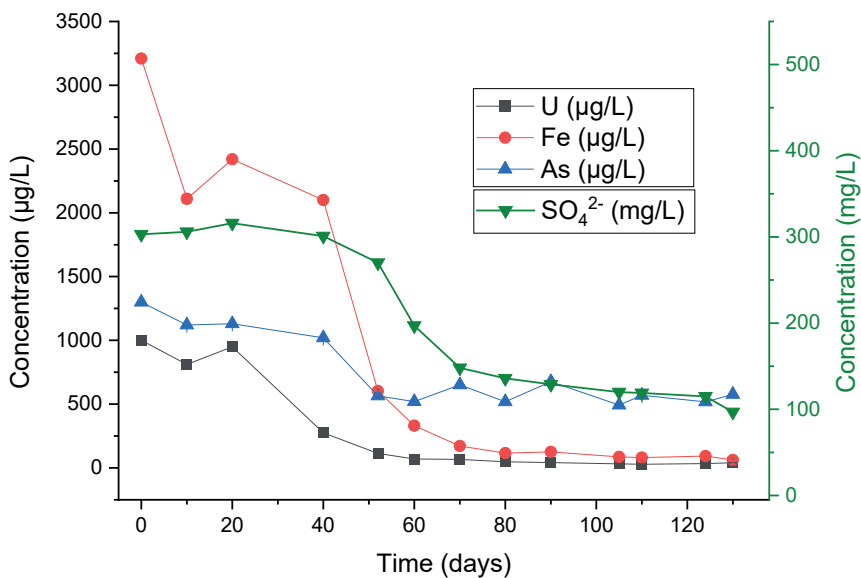


Fig. 1. Monitoring of Fe, As and U(VI) concentration in µg/l and SO₄²⁻ in mg/l in microcosm experiments using 10 mM glycerol as electron donor for 130 days. The error bar represents one standard deviation of 3 replicates. Errors are so small that the error bars are not visible.

3.2. Thermodynamic calculation

The obtained physico-chemical data during the reduction experiment were used to calculate the predominance fields of potential U species under the experimental conditions at different incubation time up to 130 days (Fig. 2). The Pourbaix diagram was calculated using the geochemical speciation code Geochemist's Workbench, version 17.0.1/Act2. The thermodynamic database used was the ThermoChimie Version 10.a database (Giffaut et al. 2014; Grivé et al. 2015). The results predict the aqueous Ca₂UO₂(CO₃)₃ species as the main species in the Schlema-Alberoda mine water at the beginning of the experiment. Due to the biostimulation of the indigenous bacteria and the resulting decrease of the E_H, the reduction of hexavalent U to tetravalent U and the formation of the solid U(IV) species uraninite is predicted after 40-50 days.

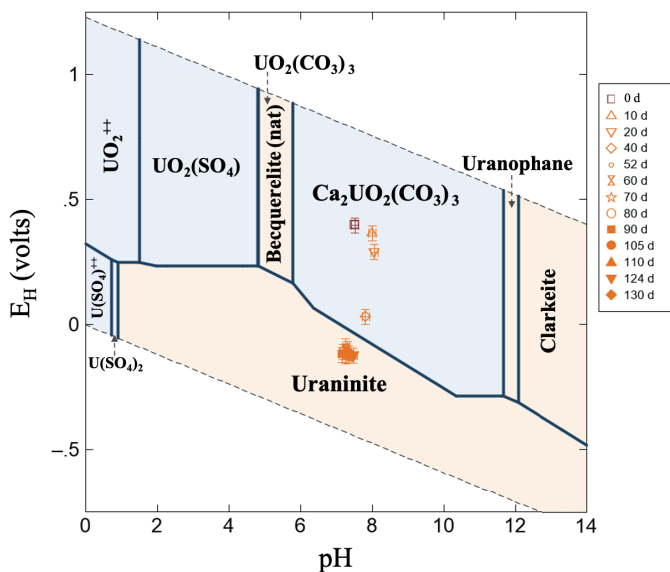


Fig. 2. Pourbaix diagram for the Schlemma-Alberoda mine water microcosms after thermodynamic calculation using Geochemist's Workbench Version 17.0.1/Act2 geochemical speciation code and analytical data.

3.3. Characterization of the black precipitate

3.3.1. UV/Visible analysis

UV/VIS spectroscopy was used to monitor the presence of U(IV) in the microcosm experiments. Figure 3 shows the UV/VIS absorption spectra obtained from the black precipitates, which were taken at different times, determined by different U concentrations in the supernatant of the microcosms, when the U concentration in the supernatant had decreased by 20%, 60% and 90% based on the monitoring data. The samples were dissolved in prior to the measurements in 5 M HCl.

No visible UV/VIS absorption bands were identified in the black precipitates of the microcosm, in which U had decreased by 20% in the supernatant. However, three UV/VIS absorption bands (560, 652 and 676 nm) slightly shifted to the right, distinctive for U(IV) (Tutschku et al. 2003; Gao and Francis 2008; Hilpmann et al. 2023), were recorded in the spectra of the black precipitates, which are characterized by 60% and 90% U decrease in

the supernatants. In addition, the amplitude of the three absorption bands increases with the decrease of U. The appearance and increase of this latter band could be attributed to the binding of U(IV) with chloride, probably due to the high concentration of HCl for the sample preparation (Tutschku et al. 2003).

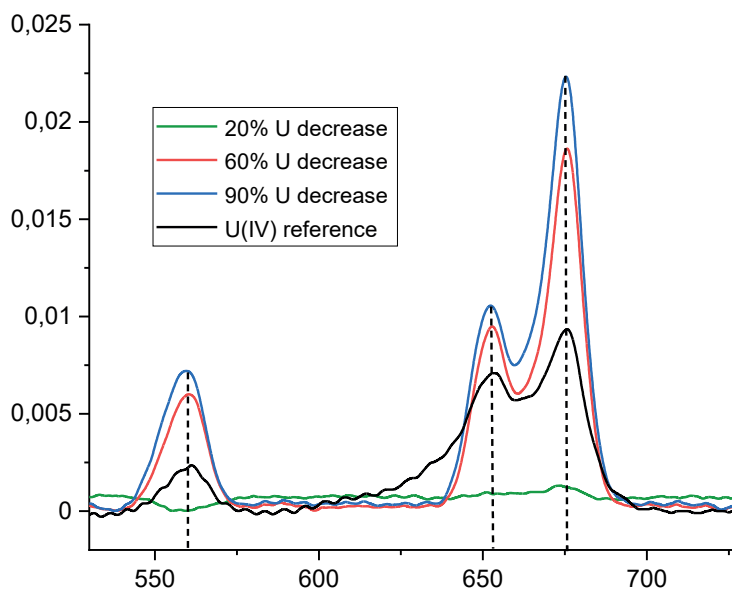


Fig. 3. UV/VIS spectra of the black precipitates, obtained from microcosms with 20%, 60% and 90% U decrease in the supernatants in comparison with the normalized reference spectrum of aquo ion U(IV) in HCl. The samples were dissolved in 5 M HCl prior to the measurements.

3.3.2. Powder X-ray diffraction (PXRD)

The black precipitate, which was collected at the end of the experiment from a microcosm with 90% decrease of the U concentration in the supernatant, was analysed by PXRD. The PXRD patterns obtained show the main peaks characteristic of calcite (COD-1600112) at 2θ values of 31.55° , 35.97° , 39.43° , 43.16° , 48.58° , 58.27° (Fig. S4).

However, the PXRD pattern of the measured sample (Fig. S4) did not show any diffraction pattern associated with U(IV). This is probably due to the low concentration of the radionuclide, the detection limit of the technique,

and/or the amorphous appearance of biogenic U(IV). Additionally, the lack of crystallinity could also be ascribed to the nanometric size of the formed U(IV) particles.

3.3.3. HERFD-XANES and EXAFS spectroscopy analysis

Using the highly sensitive techniques of HERFD-XANES at the U M_4 -edge and EXAFS at the U L_3 -edge the speciation and oxidation states of U in the black precipitates were determined.

In order to comprehend the reduction process, we studied the black precipitates of the microcosms that were characterized after 20%, 60%, and 90% decrease of the U concentration in the supernatant.

Fig. 4 shows the HERFD-XANES spectra of the samples in comparison with the reference spectra of U(IV), U(V) and U(VI). The hexavalent U M_4 HERFD reference shows three features (marked in green) (Kvashnina and Butorin 2022). The spectra of the sample with the lowest 20% decrease of U in the supernatant is broad and demonstrate the presence of U(VI), i.e. it has the first feature at ~ 3727 eV, which are characteristic of U(VI) reference compound (Fig. 4A). In addition, the spectrum also has a characteristic feature of the U(IV) reference at ~ 3725 eV that confirms the presence of U(IV) in the black precipitate. A similar result is shown by the spectrum of the sample collected after 60% of U decrease in the supernatant. Here, the first feature of U(VI) is less pronounced. In contrast the spectral feature of U(IV) is more pronounced (Fig. 4B). Contrary to this, after 90% of U decrease, the spectrum of the corresponding supernatant of the microcosm clearly shows no features of U(VI). Indeed, the U(IV) is the dominant oxidation state (Fig. 4C). Furthermore, this HERFD spectrum shows a shoulder at ~ 3726.5 eV, which can be assigned to the pentavalent oxidation states of U. To quantify the contributions of U(IV), U(V), and U(VI), we applied the iterative transformation factor analysis (ITFA) (Rossberg et al. 2003). As references, we used spectra of UO_2 for U(IV), uranyl (VI) for U(VI), and U(V) was taken as uranate in $UMoO_5$, as published by Pan et al. (2020). The summarized results from ITFA are shown in the barplot of Figure 4 (E) and demonstrate that the oxidation state (V) of U is present

already from early stages in the reduction process. To our knowledge, this is the first time such high proportions of pentavalent U are identified in environmental samples. The proportion of this oxidation state increases together with that of U(IV), with approximately 30% for pentavalent U and approximately 70% for tetravalent U identified in the most reduced sample, collected after 90% of U removal.

The HERFD-XANES spectra of the sample prepared outside of the glovebox and subsequently exposed to oxidizing conditions for 4 weeks, demonstrate predominance of U(VI), with contributions of both U(V), and to a less U(IV) (Fig. 4D). The data summarized in the bar graph of the ITFA (Fig. 4E) indicate that the tetravalent oxidation state (IV) decreases down to 7%. In contrast, surprisingly, the contribution of U(V) increased to 53%, while that of U(VI) reached 40%.

To the best of our knowledge, this proportion of U(V) is the highest ever recorded in environmental samples under oxidizing conditions, demonstrating the stabilization of U(V) by indigenous micro-organisms in the environment.

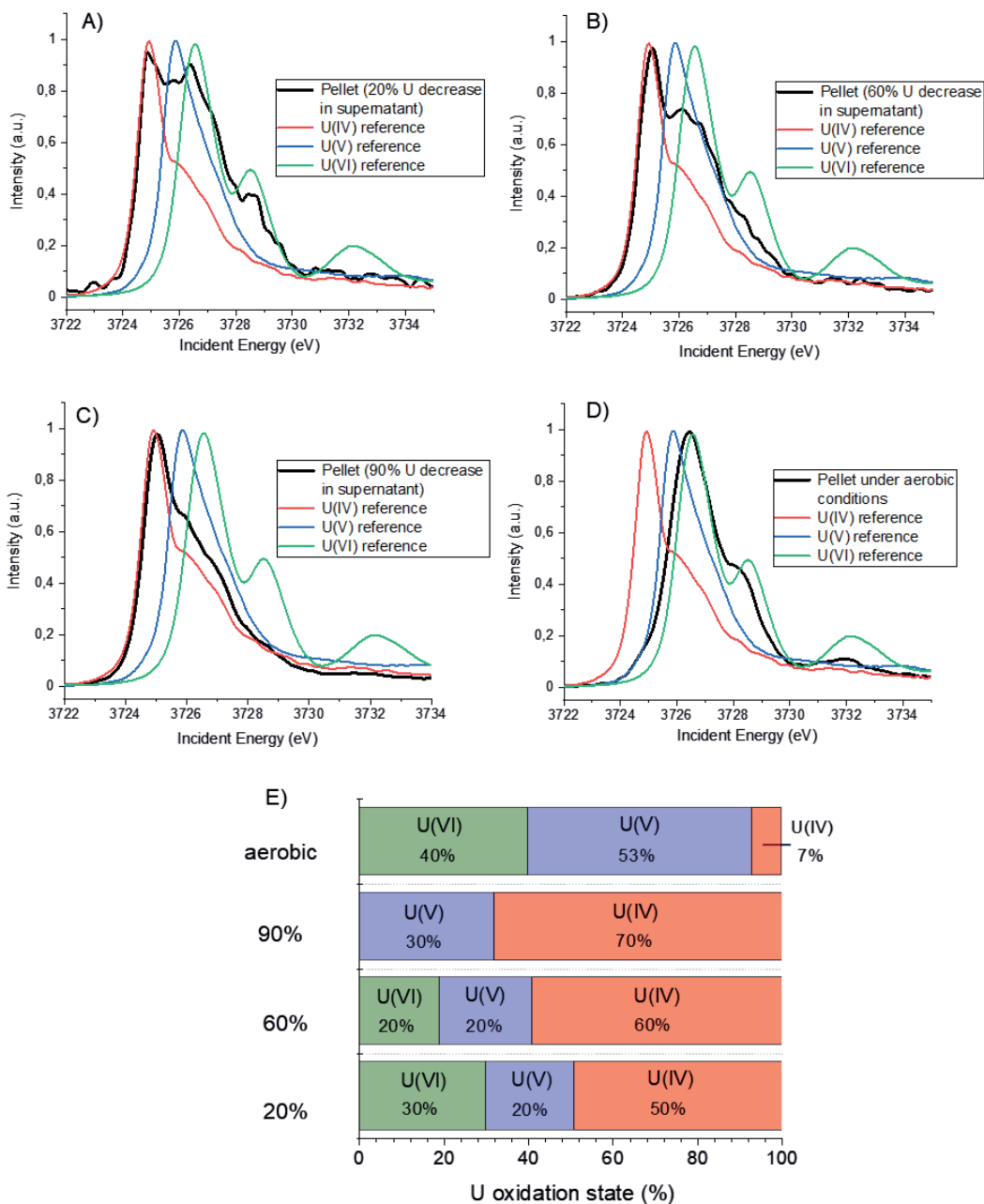


Fig. 4. A-C: HERFD-XANES spectra at the $U M_4$ -edge, recorded from the black precipitates at different decreases of the U concentration in the supernatant of the microcosms (20%, 60%, 90%) compared with U reference spectra: U(IV) as UO_2 , U(V) as $UMoO_5$ and U(VI) as UO_2^{2+} . D: HERFD-XANES spectra at the $U M_4$ -edge, recorded from the sample exposed to oxidizing conditions during 4 weeks. E: Corresponding fractions of U(VI), U(V), and U(IV) as determined by ITFA analysis. Estimated error of the ITFA analysis: 2 %.

The initial evaluation of the U L₃-edge k³-weighted EXAFS spectra and their corresponding Fourier transforms (FT), which were recorded on the black precipitates from the microcosms (black), clearly reveal progressive changes in U speciation (Fig. 5). The O_{axial(ax)} FT peak of U(VI), which is located at 1.43 Å (Fig. 5, peak 1), decreases strongly as the U concentration in the supernatant of the microcosms decreases by 20%, 60% and 90%. Furthermore, the peak at 3.64 Å (Fig. 5, peak 2) stemming from a U-U interaction exhibits a progressive increase in amplitude simultaneously with the decrease of the U concentration. Two spectral components were identified by ITFA analysis which reproduce the spectral mixtures very well. In order to identify the chemical origin of the components we applied target factor analysis (TFA) as described in Hilpmann et al. (2023). TFA enables the search for reference compounds in a spectral database whose spectra would enable a reproduction of the measured spectral mixtures by their linear combination. The database contains 81 spectra of various organic and inorganic U-reference compounds in U oxidation states of IV, V and VI. The TFA identified best matching references are colloidal uraninite phases (U(IV)), solid and aqueous U(VI)- and U(V)-carbonates like Na₄UO₂(CO₃)₃, UO₂(CO₃)₃⁴⁻, and electrochemically synthesized UO₂(CO₃)₃⁵⁻, respectively.

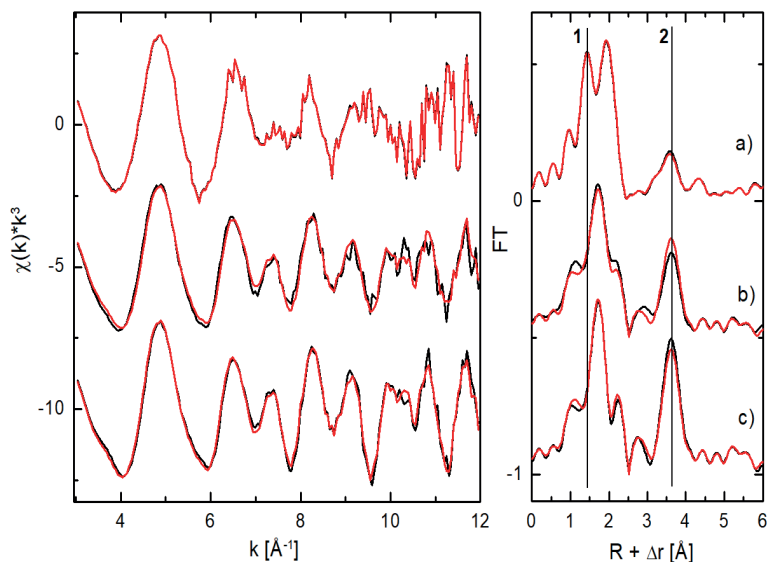


Fig. 5. U L_3 -edge k^3 -weighted EXAFS spectra (left) and corresponding Fourier-transforms (FT, right) from the black precipitates of the Schlema-Alberoda mine water microcosms (10 mM glycerol, anaerobic conditions) at different decrease rates of the U concentration in the supernatants of the microcosms: 20% (a), 60% (b), 90% (c) all in black and ITFA reproductions (red).

Prior to the shell fit of the pure U-species their spectra were isolated from the spectral mixtures by application of the ITFA method as described in Hilpmann et al. (2023). For the application of the isolation procedure we assumed that one spectral component represents a pure uraninite-like phase and that the other component does not contain an U-U interaction, hence we minimized for one of the components the amplitude of the U peak located at 3.64 \AA (Fig. 5, peak 2).

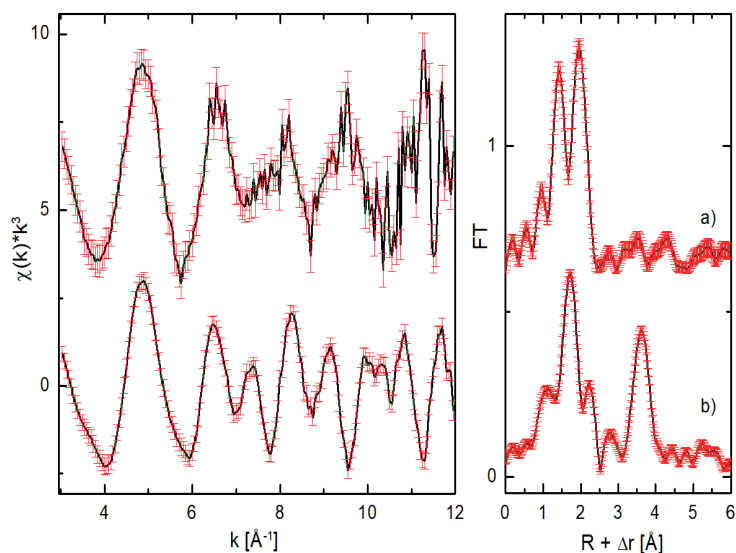


Fig. 6. U L_3 -edge k^3 -weighted EXAFS spectra (left) and corresponding Fourier-transforms (FT, right) of the ITFA isolated U species (black) with estimated standard deviations (red). U(V/VI) species a), uraninite-like phase b).

In the case of the ITFA isolated spectrum a) (Fig. 6) the U signal at 3.64 \AA is substantially minimized, hence no U(IV) contamination is expected for this spectrum, while the isolated spectrum b) (Fig. 6) is in good accordance with the measured spectrum (Fig. 5 c)). The shell fit EXAFS structural parameter gained for the isolated spectra of the two U-species and for the best matching U-references are listed in Table 1, while the fits are shown in Fig. 7.

Table 1. Shell fit EXAFS structural parameter for the ITFA isolated U species, the reference compounds $\text{Na}_4\text{UO}_2(\text{CO}_3)_3$, $\text{UO}_2(\text{CO}_3)_3^{4-}$, $\text{UO}_2(\text{CO}_3)_3^{5-}$ and for colloidal uraninite together with average radial distances (R) from literature.

<i>Path</i>	<i>CN</i>	<i>R/Å</i>	<i>DW/Å²</i>	<i>dE0/eV</i>
<i>U(V/VI) species, S₀ = 0.6</i>				
<i>O_{ax}</i>	2.0 ^f	1.848(8)	0.0060(9)	6.9(9)
<i>MS U-O_{ax(1)}-O_{ax(2)}</i>	2.0/	3.696/	0.0120/	6.9/
<i>O_{eq}</i>	6.4(9)	2.454(7)	0.006(1)	6.9/
<i>C</i>	3.2/	2.95(5)	0.013(8)	6.9/
<i>Na₄UO₂(CO₃)₃, S₀ = 0.9</i>				
<i>O_{ax}</i>	2.0 ^f	1.823(2), 1.83[1]	0.0015(2)	3.7(4)
<i>MS U-O_{ax(1)}-O_{ax(2)}</i>	2.0/	3.646/	0.0030/	3.7/
<i>O_{eq}</i>	6.0 ^f	2.406(3), 2.40[1]	0.0057(3)	3.7/
<i>C</i>	3.0/	2.883(9), 2.90[1]	0.004 ^f	3.7/
<i>UO₂(CO₃)₃⁴⁻, S₀ = 0.9</i>				
<i>O_{ax}</i>	2.0 ^f	1.799(2), 1.80[2]	0.0016(2)	3.6(5)
<i>MS U-O_{ax(1)}-O_{ax(2)}</i>	2.0/	3.598/	0.0032/	3.6/
<i>O_{eq}</i>	6.0 ^f	2.444(4), 2.44[2]	0.0066(3)	3.6/
<i>C</i>	3.0/	2.907(9), 2.90[2]	0.004 ^f	3.6/
<i>UO₂(CO₃)₃⁵⁻, S₀ = 0.9</i>				
<i>O_{ax}</i>	2.0 ^f	1.858(4), 1.91 [3]	0.0060(4)	3.9(5)
<i>MS U-O_{ax(1)}-O_{ax(2)}</i>	2.0/	3.716/	0.0120/	3.9/
<i>O_{eq}</i>	6.0 ^f	2.479(5), 2.50 [3]	0.0090(4)	3.9/
<i>C</i>	3.0/	2.926(8), 2.93 [3]	0.004 ^f	3.9/
<i>Uraninite-like species, S₀ = 1</i>				
<i>O</i>	8.3(6)	2.326(6), 2.35[4], 2.36[5]	0.016(1)	-9.9(7)
<i>U</i>	3.9(5)	3.838(5), 3.84[4], 3.86[5]	0.0065(8)	-9.9/

<i>Colloidal uraninite</i> §, $S_0 = 1$				
O	6.4(4)	2.315(4) [6]	0.0121(8)	-8.7(5)
U	4.5(4)	3.839(3) [6]	0.0053(5)	-8.7/

Fitted k-range $3.00 \text{ \AA}^{-1} - 11.95 \text{ \AA}^{-1}$. CN = coordination number, R = radial distance, DW = Debye-Waller factor, dE0 = shift in energy threshold, S_0 = amplitude reduction factor, f = fixed parameter, / = linked parameter. Estimated standard deviations of the variable parameter in parenthesis. Spectrum of $\text{UO}_2(\text{CO}_3)_3^{4-}$ (#) and colloidal uraninite (§) taken from [2] and [6] but fitted in the shorter k-range of $3.00 \text{ \AA}^{-1} - 11.95 \text{ \AA}^{-1}$.

[1] Ondrus et al. (2003); [2] Rossberg et al. (2009); [3] Ikeda et al. (2007); [4] Schofield (2008); [5] Sharp et al. (2009); [6] Veeramani et al. (2013).

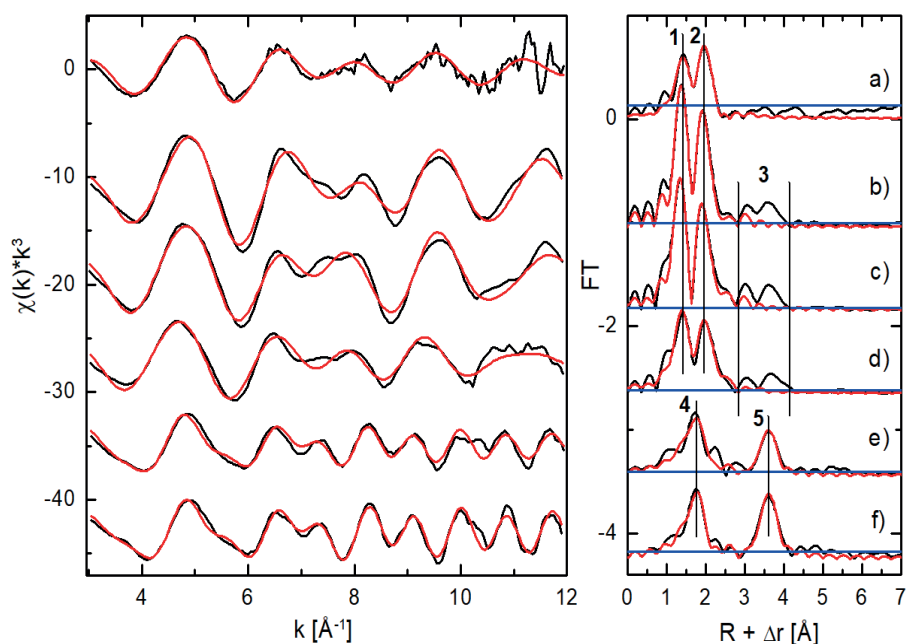


Fig. 7. U L_{3} -edge k^3 -weighted EXAFS spectra (left) and corresponding Fourier-transforms (FT, right) of the ITFA isolated U species (a, e) and the best matching reference compounds $\text{Na}_4\text{UO}_2(\text{CO}_3)_3$ (b), $\text{UO}_2(\text{CO}_3)_3^{4-}$ (c), $\text{UO}_2(\text{CO}_3)_3^{5-}$ (d), and colloidal uraninite (f) (black) with shell fit (red). Peaks are O_{ax} (1), O_{eq} (2), MS paths related with $\text{U-O}_{\text{eq}}-\text{O}_{\text{ax}}$ and $\text{U-C-O}_{\text{dist}}$ in the R-range (3), O coordinated to U(IV) (4), U-U interaction (5). Level of experimental error conservatively estimated as the FT maximum in the range $6 \text{ \AA} - 25 \text{ \AA}$ (blue line).

Despite of other multiple scattering (MS) paths we considered besides the single scattering paths only the MS path along the uranyl unit ($\text{U-O}_{\text{ax}(1)}-\text{O}_{\text{ax}(2)}$). In the case of the U(V/VI) species the amplitude reduction factors (S_0) were estimated by assuming a coordination number (CN) of six equatorial O atoms. Since for this species and the relevant references S_0 variate between 0.6 - 0.9 (Table 1) the error in the determination of the CN is expected to be relatively high so that reliable conclusions from inspecting CN's are not admitted. The reason of this uncertainty could be a wrong assumption made for the CN's and/or measuring effects like self-absorption and thickness effects caused by inhomogeneities of the bacterial sample material. However, the inspection of the radial distances is more conclusive since the error in their determination is relatively low ($\pm 0.02 \text{ \AA}$). In consideration of the radial distances gained by the shell fit the following observations can be drawn:

The uranyl-species shows a relatively high R_{Oax} of 1.85 \AA which is in a closer agreement with the R_{Oax} of 1.86 \AA measured for the U(V)-species $\text{UO}_2(\text{CO}_3)_3^{5-}$ than with the R_{Oax} of 1.82 \AA and 1.80 \AA measured for the U(VI)-species $\text{Na}_4\text{UO}_2(\text{CO}_3)_3$ and $\text{UO}_2(\text{CO}_3)_3^{4-}$, respectively. Since in general R_{Oax} of U(V) compounds is assumed to be higher than R_{Oax} of structural complementary U(VI) compounds we can assume that U(V) is present at high supernatant U-concentrations (Fig. 5, sample a)), but we cannot exclude the presence of U(VI) because also U(VI)-references were found by TFA. However, in all TFA identified references U interacts with carbonato groups, hence a mixture of uranyl-carbonato complexes with U in the oxidation states V and VI is most probable. Further evidence for the presence of carbonato-complexes is given by the long R_{Oeq} distance of 2.45 \AA which is in line with the distance of 2.44 \AA and 2.48 \AA measured for the aqueous carbonato complexes $\text{UO}_2(\text{CO}_3)_3^{4-}$ and $\text{UO}_2(\text{CO}_3)_3^{5-}$, respectively, in which the carbonato groups are bidentate coordinated to U(VI) and U(V). A bidentate binding mode of carboxylic groups is reflected by the presence of the FT-features in the R-interval $2.84 \text{ \AA} - 4.12 \text{ \AA}$ (Fig. 7) originating from strong MS paths connected with the linearly arranged C and distal (dist) O

atoms ($\text{U-C-O}_{\text{dist}}$) as clearly visible in the case of the reference compounds. The uranyl species does not show these MS FT features, which might be masked through the rather high level of the experimental error (Fig. 7 a). However, the relatively long R_{Oax} of 1.85 Å and R_{Oeq} of 2.45 Å, the fitted C atoms at 2.95 Å, which are also observed for the references at $R_{\text{C}} = 2.88 \text{ Å} - 2.93 \text{ Å}$, and the TFA identified references hints univocally to the presence of carbonato groups which are bidentately bound to U(VI) and U(V).

In the case of the uraninite-like species $R_{\text{O}} = 2.33 \text{ Å}$ and $R_{\text{U}} = 3.84 \text{ Å}$ agree within the common error in determination of radial distances ($\pm 0.02 \text{ Å}$) with the distances measured for the colloidal uraninite reference ($R_{\text{O}} = 2.32 \text{ Å}$ and $R_{\text{U}} = 3.84 \text{ Å}$), while the CN_{U} are within the error of their standard deviation equal for both. Consequently, we can conclude that at low supernatant U concentrations in the microcosms the biogenic formed species corresponds structurally to uraninite.

3.3.4. HAADF-STEM and SEM analysis

A combination of HAADF-STEM/EDXS and SEM/EDXS was used to investigate the cellular location, structure and physico-chemical properties of the U(VI) reduction products, aiming to elucidate the U(VI) bioreduction process by the native biostimulated microbial community.

In Figure 8 (A-B), HAADF-STEM micrographs of a thin section of a bacterial cell from the black precipitate show electron-dense accumulations at the cell surface, which has been also observed in several cells (data not shown). Elemental distribution maps (Fig. 8 (E-H)) and spectra generated by EDXS (Fig. 8 (C-D)) revealed that the accumulates on the cell surface were composed of U, Fe, and S. Furthermore, a distinct element distribution within the cell surface electron dense accumulations was observed, with Fe and S being mainly distributed in the inner part, while U was predominantly present in the outer part of the accumulations. However, U was also detected in the inner part of the accumulations.

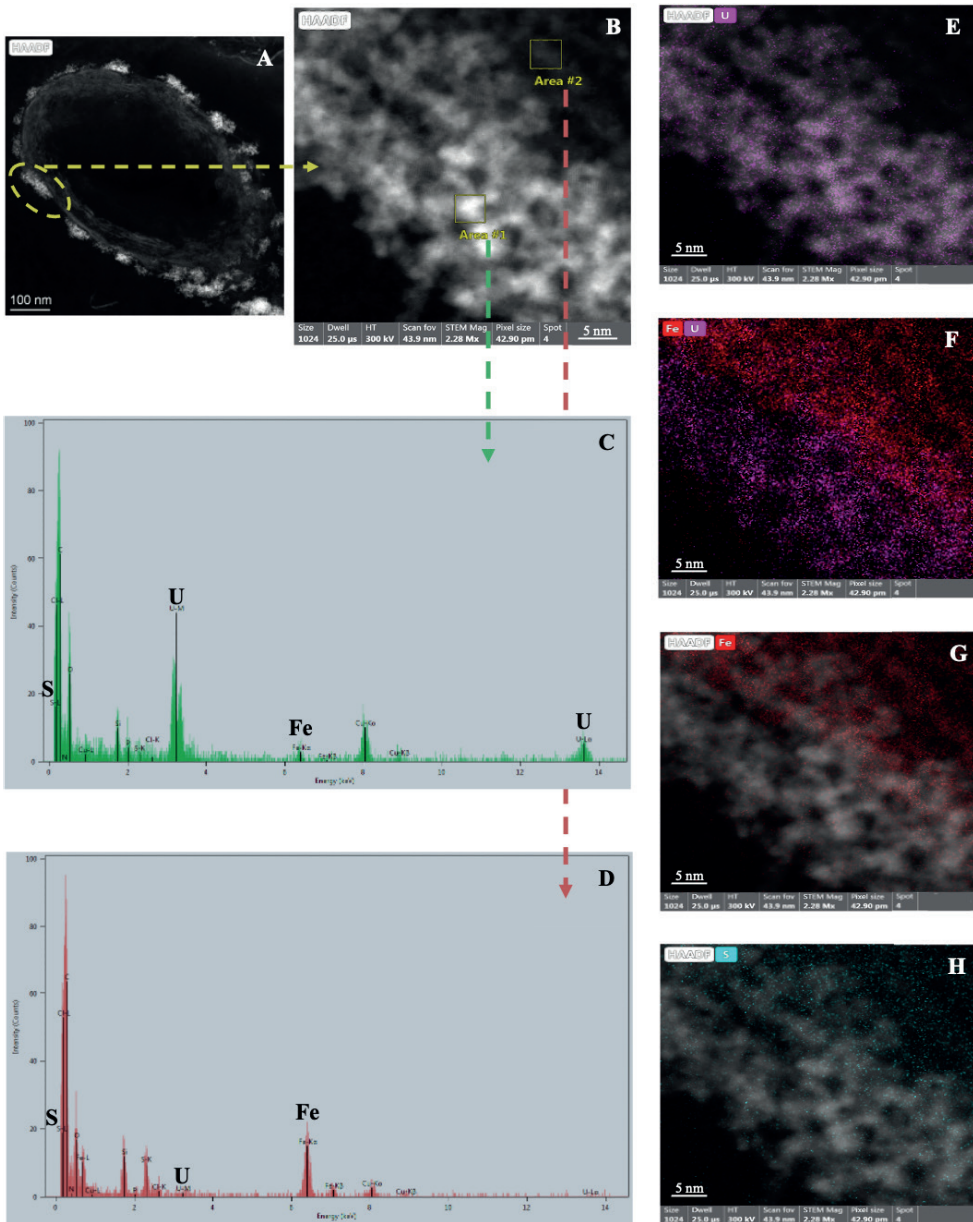


Fig. 8. HAADF-STEM micrographs of a thin section of the collected black precipitate showing electron-dense accumulations produced during incubation and induced by biostimulation of the native micro-organisms community by glycerol (A-B). EDXS spectra (C-D) and elemental distribution maps (E-H) showing their elemental composition of U, Fe and S.

The integration of HAADF-STEM techniques, including SAED and HRTEM, was utilized to confirm the presence of U nanoparticles (UNPs) with an approximate size of 2-5 nm in these accumulations (Fig. 9).

The SAED patterns of selected UNPs indicate their amorphous nature and did not exhibit crystallization pattern (Fig. 9 (A-C)). The lack of crystallinity in the biogenic UNPs has been previously reported by Bhattacharyya et al. (2017). The lack of crystallinity may be attributed to the fact that these particles form as such small crystalline entities that they cannot produce diffraction patterns. Nevertheless, HRTEM show that distinct lattice spacings of 0.273 and 0.315 nm, possibly corresponding to crystallographic planes of uraninite, have been identified according to the American Mineralogist crystal structure database (<http://rruff.geo.arizona.edu>) (Fig. 9 (D-E)). Additionally, other lattice spacings notably different in value, such as 0.308 nm, 0.338 nm primarily, and 0.298 nm to a lesser extent, were observed (Fig. 9 (D-E)). These d-spacings could correspond to crystallographic planes of uranyl iron oxide (FeUO_4), as indicated by the American Mineralogist crystal structure database (<http://rruff.geo.arizona.edu>). To the best of our knowledge, this is the first report of FeUO_4 NPs in environmental samples associated with native microbial communities. These NPs were predominantly identified on the inner surface of the accumulations. Conversely, uraninite NPs were mainly located on the outer surface of the accumulations. In addition, very few d-spacings of 0.271 and 0.242 nm were identified, which did not correspond to uraninite or FeUO_4 NPs. These distances were attributed to the crystal faces $\{200\}$ and $\{210\}$ of pyrite, respectively.

To determine the accuracy of the obtained spacing distances, a total of 219 NPs were measured in 3 different cells, and the corresponding proportions were calculated. The values obtained were 53% for FeUO_4 NPs, 42% for uraninite NPs, and 5% for pyrite NPs.

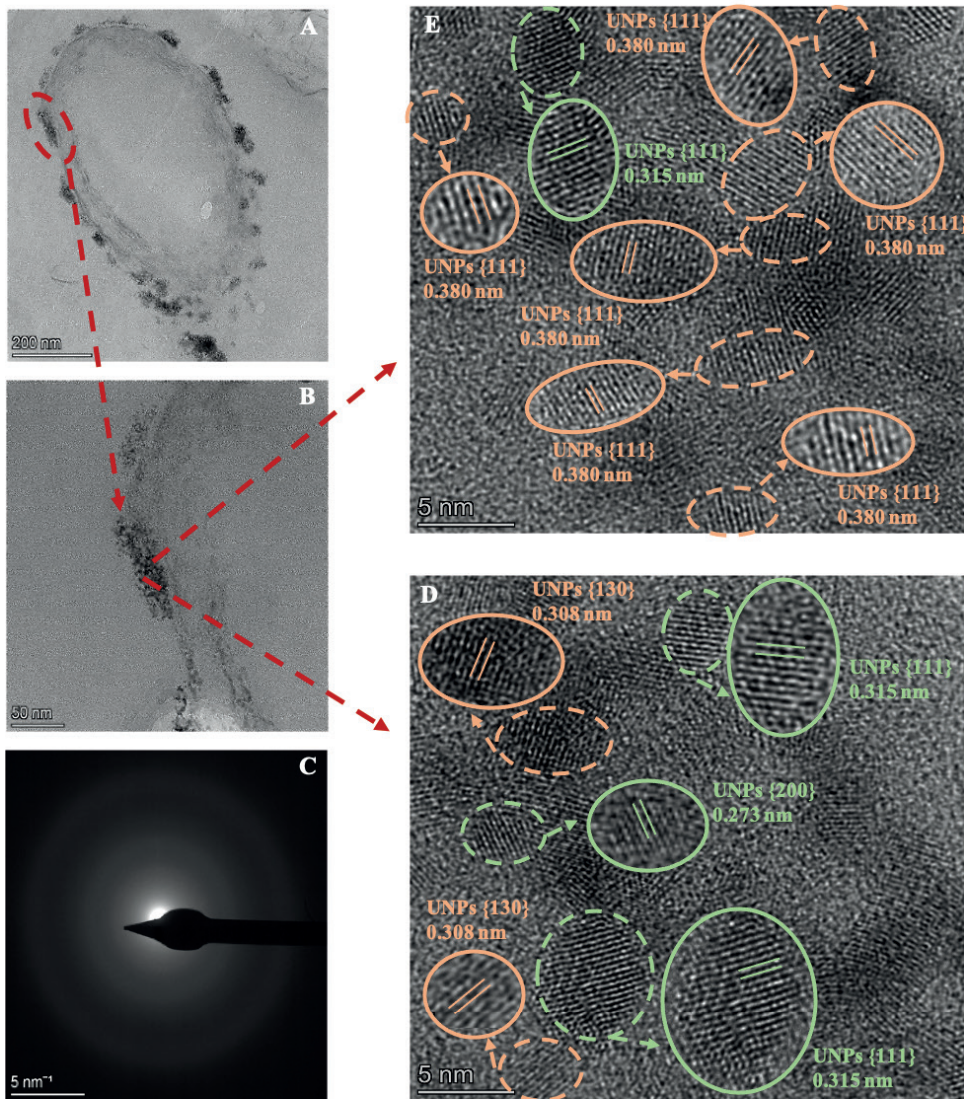


Fig. 9. HAADF-STEM micrograph of UNPs from the collected black precipitate showing electron-dense clusters formed during incubation, induced by biostimulation of the native micro-organism community by glycerol (A-B). Enlarged SAED pattern (C) and HRTEM image (D and E) corresponding to the interior of the accumulation, are showing several UNPs, which are crippled. Lines drawn in the magnified circles, indicate lattice spacings which correspond to crystallographic planes. Uraninite NPs in red and FeUO_4 NPs in green.

The images obtained by SEM provided further information about the black precipitate. Figure 10 (A) shows the formation of rosette-like calcite structures predominantly. Additionally, other structures were found to a lesser extent, exhibiting a cubic conformation. The rosette-like calcite structures were analysed using EDXS, generating a spectrum where Ca, as expected, was identified along with U, Fe, and S (Fig. 10 (B)). When the calcite structure was observed at a magnification of x250k with BSE coupling, the observation of NPs, possibly UNPs, on the surface of the calcite crystal became possible (Fig.10 (D-G)).

The SEM micrographs obtained for colloid identification demonstrate the aggregation of colloidal particles. Furthermore, EDXS confirmed the presence of Fe and As as major constituents, as shown in Figure S3.

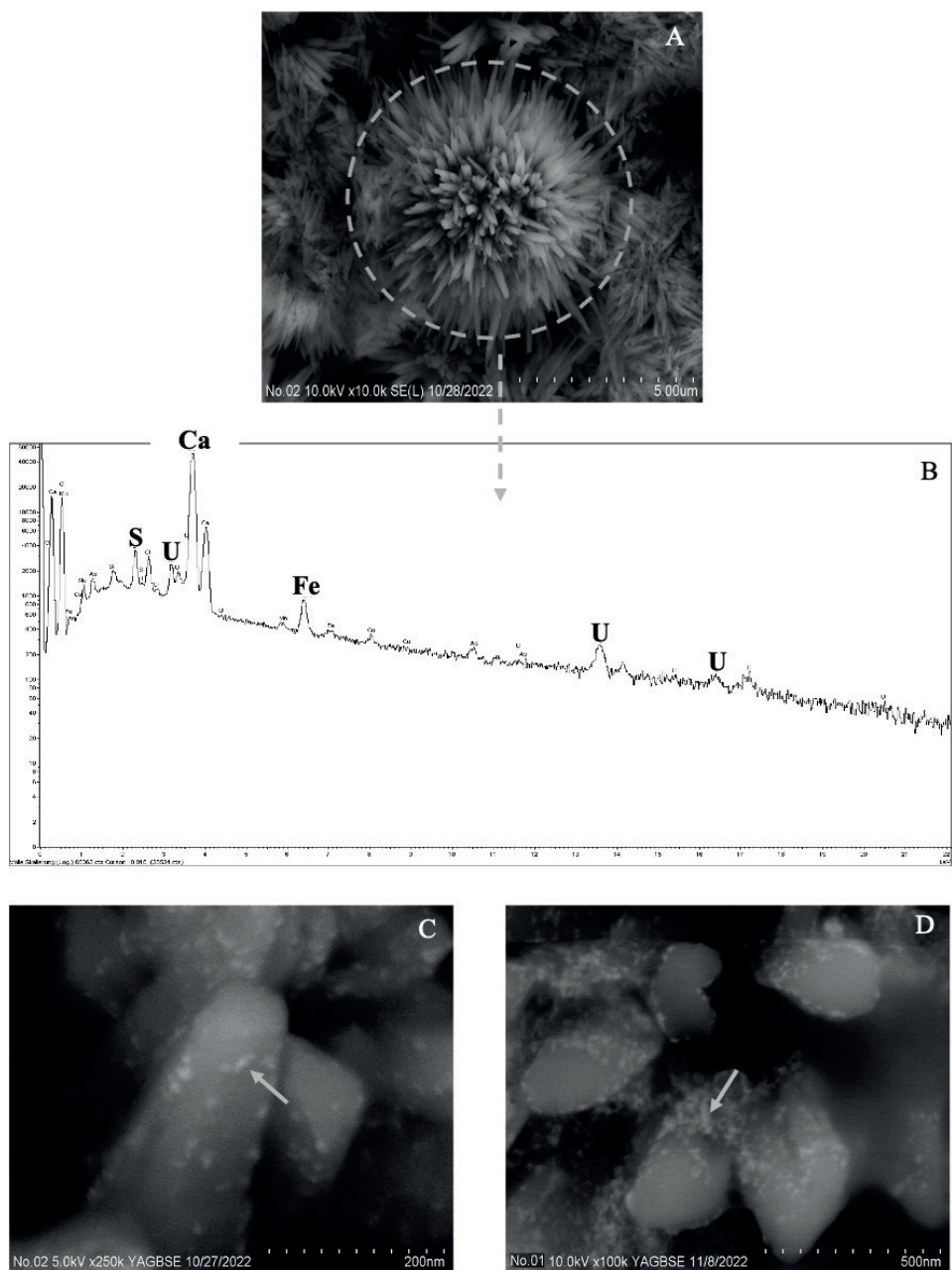


Fig. 10. SEM image (SE) of the black precipitate at the end of the kinetic experiment showing a calcite rosette (C) formed during the experiment. EDXS spectra (B) indicates the elemental composition of Ca, U, Fe and S of a calcite rosette. UNPs (arrow) were detected on the crystals' surfaces (F, G) by BSE detector.

4. Discussion

4.1. Geochemistry and kinetics of U reduction in mine water microcosms

A glycerol-amended, U-contaminated mine water microcosm was set to assess the potential of U-reducing native microbial communities in removing and bioremediating low U concentrations (1 mg/l) under anoxic conditions. Understanding the impact of microbes in the biogeochemical cycling of U is crucial for predicting its chemical speciation and mobility and assessing its toxicity, which may help to design efficient bioremediation strategies. However, the mobility of U is also controlled by abiotic parameters such as pH, E_H , and dissolved ions. In the present study, the first probable evidence of soluble U(VI) reduction to U(IV) in the Schlema-Alberoda mine water was observed (Fig. S1) due to the formation of a black precipitation. Possibly this occurred due to the activity of U-reducers including sulphate-reducing bacteria (SRB), which reduce SO_4^{2-} to sulphide. Previous studies support this finding (Hua et al. 2006; Cason et al. 2012).

Figure 1, Figure S2 and Table S1 show the changes in physico-chemical parameters in the microcosm during 130 days. At the end of the experiment, no considerable pH change was observed in the microcosm. However, the E_H exhibited a remarkable downward trend in values, ranging from +398 to -114 mV (Fig. S2), indicating the stimulation of microbial activity (oxidation of glycerol, reduction of sulphate) leading to the formation of reducing conditions favouring U(VI) reduction in the altered microcosm.

Nitrate, ferric ion and sulphate are final electron acceptors with a higher thermodynamic preference for microbes than U. These oxidants should be priorly consumed before U reduction occurs in the microcosm (Finneran et al. 2002). In the experiment, low nitrate levels were observed (Table S1). The presence of NO_3^- may pose a challenge in the bioremediation of U contaminated environments, as it might re-oxidize the reduced U (Safonov et al. 2018). However, in our case, this would not be an issue, considering the low observed values. Similarly, after 52 days, a decrease of 81% and 64% for Fe and As, respectively, was observed. Iron reducing

bacteria (e.g., family *Rhodocyclaceae*) identified in the U mine water could play a major role in the reduction of Fe(III) and formation of Fe(II) under anoxic conditions. The decrease of the As and Fe levels is associated with a reduction of U concentration of 72% and 90% after 40 and 52 days, respectively. When reducing conditions were reached, the concentrations of SO_4^{2-} decreased by 68% at the end of the experiment, while Fe and U decreased by 98% and 96%, respectively (Fig. 1). The reduced values of Fe and SO_4^{2-} could be mainly attributed to the role played by iron-reducing bacteria (FeRB) and SRB, both closely related to the reduction of soluble U(VI) (Lovley et al. 1993; Wilkins et al. 2006; You et al. 2021).

The addition of glycerol lead to an increase in the concentrations of total inorganic/organic carbon (TIC/TOC) and dissolved organic carbon (DOC), with a considerable increase of two orders of magnitude in TOC and DOC (Table S2). This increase is due to the stimulation of the growth of bacteria involved in the biogeochemical cycles of U and other elements like S and Fe providing an abundant source of nutrients and energy for their metabolism. On the other hand, the substantial increase in TIC concentration could have an indirect impact on the bacterial community, influencing and/or maintaining circumneutral pH stability.

4.2. Characterization of the black precipitate: linking spectroscopic and microscopic methodologies

Thermodynamic models play a crucial role in the analysis of the impact of abiotic and biotic processes in U biogeochemical cycle, allowing the study of the distribution and stability of chemical species in aqueous solutions as function of E_{H} and pH values. Through the Pourbaix diagram (Fig. 2), the theoretical U chemical speciation of U at the end of the experiment was predicted in great detail, indicating its reduction and the potential formation of uraninite as the main reduction product.

The formation of biogenic uraninite was corroborated with experimental evidence obtained through UV/Vis spectroscopy and EXAFS, which provided tangible evidence of U reduction. In Figure 3, characteristic peaks of U(IV) can be observed in the UV/Vis spectrum for the samples at different reduction rates, with a slight redshift. It is important to mention

that the difference in the peak amplitudes at 650 nm and 675 nm, compared to other previously reported spectra (Tutschku et al. 2003; Hilpmann et al. 2023), could be explained by the use of a high concentration of HCl during sample preparation, as reported by Tutschku et al. 2003. On the other hand, Gao and Francis (2008) reported that the 560 nm absorption band resulted from biogenic U(IV) species due to the microbial reduction of U(VI). Additionally, an increase in the intensity of the U(IV) UV/Vis spectrum was observed as the U concentration in the supernatant of the microcosms decreased.

A combination of HERFD-XANES spectrum analysis and ITFA evaluation was used to estimate the approximate proportion of different U oxidation states in black precipitates subjected to the different decrease of U in the supernatant of the microcosms. In Figure 4, the HERFD-XANES spectra and a barplot showing the relative percentage of each oxidation state in each sample with a different decrease of the U concentration in the supernatant (20%, 60%, 90%). The results obtained revealed that in all three analysed samples, U(IV) was the dominant oxidation state compared to the others (U(VI) and U(V)). Additionally, the fractions of U(VI) decreased in the black precipitates as the U concentrations in the supernatants decreased. These results are in agreement with those reported by other authors on the prevalence of U(IV) as the dominant oxidation state during microbial U(VI) reduction (Schofield et al. 2008; Newsome et al. 2014; Hilpmann et al. 2023). However, the surprising finding was the identification of U(V) in all samples with a proportion ranging from 21% to 32% depending on the decrease of the U concentration. This suggests that the products of microbial reduction of U(VI) are not limited exclusively to U(IV) but could also include U(V) phases. Complementarily, the analysis of the EXAFS spectra of the black precipitates, subjected to the different decrease of U, clearly revealed the reduction of soluble U(VI) and the formation of uraninite and U(VI)/U(V)-carbonates. The isolation of the pure U-species from the spectral mixtures by ITFA analysis resulted in the identification of two spectral components. The chemical origin of these components identified by TFA revealed colloidal uraninite phases as one of the best

matching references in the samples, which were characterized by a high decrease of U in the supernatant. In addition, a U species was identified, which could be assigned to U(VI)/U(V)-carbonates. Due to the radial distances, which were gained by the shell fit, we can assume the existence of a U(V)-carbonato complex. However, U(VI)-carbonato complexes cannot be excluded, especially not in the samples with a low decrease of U in the supernatant. The formation of a U(V)-carbonate complex has also been confirmed by microscopic studies, as can be seen in Figure 8C+D, where EDXS in combination with BSE allowed the identification of UNPs on the surface of the calcite crystals.

Further methods were used to identify uraninite in the black precipitates. PXRD studies were unfortunately not successful, since a crystalline phase corresponding mainly to calcite was dominantly identified (Fig. 8A). These findings align with the microscopic characterization using SEM, where calcite rosette structures were observed. The precipitation of calcium carbonate, such as calcite, induced by anaerobic micro-organisms has been widely documented, as well as the encrustation of NPs, primarily with a negative charge and, to a lesser extent, with a positive charge, as it grows on the crystal surface (Suzuki et al. 2016; Skuce et al. 2017).

Furthermore, the HAADF-STEM technique was used to investigate the structure and physical properties of the reduced U products. Figure 6 shows element distribution maps and the spectra generated by EDXS, revealing the presence of localized electron-dense clusters dispersed around the cell. These clusters exhibit characteristic enrichments primarily in U, as well as Fe and S. These localized accumulations are of particular interest, as other researchers have reported the distribution of reduced U around the cell surface in bacteria such as *Geobacter sulfurreducens*, *Shewanella oneidensis* MR-1, and *Thermus scotoductus*, among others (Marshall et al. 2006; Cason et al. 2012; Orellana et al. 2013).

The formation of uraninite NPs was confirmed by HRTEM, where d-spacings of 0.273 and 0.315 nm corresponding to the crystallographic planes of uraninite were identified, based on the crystal structure database of the American Mineralogist (<http://rruff.geo.arizona.edu>). Although clear

signs of crystallinity were not observed via SAED, it is highly possible that the nanoscale size of these structures justifies this lack of evidence. The formation of uraninite is commonly reported in the literature (Ulrich et al. 2008; Schofield et al. 2008; Sharp et al. 2009). However, other authors have reported the formation of different types of U(IV) biominerals in U(VI) reduction processes (Bernier-Latmani et al. 2010; Newsome et al. 2015). In addition to uraninite NPs, other lattice spacings that did not match those reported for uraninite were identified. These d-spacings were correlated with FeUO_4 according to the American Mineralogist database (<http://rruff.geo.arizona.edu>), a metal monouranate first reported by Bacmann and Bertaut 1967. The presence of stable U(V) in the FeUO_4 structure has been confirmed, although it is true that various possible combinations based on the oxidation states of Fe and U can be adopted, potentially accommodating U(VI), U(V), or U(IV) in its structure (Guo et al. 2016). However, Collins and Rosso (2017) reported that the crystal structure of FeUO_4 with U(V)-Fe(III) pairing is substantially more thermodynamically stable than the U(VI)-Fe(II) pairing. Luo et al. (2022), based on their PXRD results, reported the microbial reduction of U(VI) producing both UO_2 and FeUO_4 , referring to the latter in its oxidation state as U(VI). Based on the results obtained from HERFD-XANES, where high proportions of U(V) were reported, we suggest that the monouranate FeUO_4 identified in our samples is primarily composed of U(V). If so, it would be the first time that FeUO_4 originating directly and/or indirectly from biotic processes by a microbial community has been reported. Likewise, possibly due to the action of SRBs producing sulphide, pyrite NPs (iron disulphide) were identified based on the obtained d-spacing and comparison with the American Mineralogist database (<http://rruff.geo.arizona.edu>). Nevertheless, these pyrite NPs were found in a smaller proportion compared to uraninite and FeUO_4 NPs. Our findings were not limited to the identification of a few NPs; rather, to ensure a more representative analysis, we meticulously counted a total of 219 nanoparticles from three distinct cells in various samples. The results revealed a wide distribution, with FeUO_4 NPs constituting 53%, uraninite NPs comprising 42%, and pyrite NPs making up 5% of the total count.

To the best of our knowledge, this is the first study reporting the formation of U(V) species as result of U(VI) reduction within a mine water microcosm at environmental relevant conditions for U bioremediation purpose. The very limited available literature primarily focuses on the U(VI) reduction to U(V) under controlled laboratory conditions, utilizing pure microbial cultures such as FeOB (Vettese et al. 2020; Renshaw et al. 2005) and SRB (Hilpmann et al. 2023). These studies suggest one electron transfer as a mechanism for the U(VI) to U(V) reduction process, followed by a disproportionation towards U(VI) and/or U(IV) due to the instability of U(V).

4.3. Long-term environmental implications and future perspectives for U(IV) and U(V)

As a bioremediation strategy, microbial enzymatic reduction is an excellent complementary and/or alternative to traditional remediation technologies. However, several factors should be considered after reduction process that could affect the re-oxidation of the reduced products which in turn reduce their long-term stability. In our case, U(IV), in the form of biogenic uraninite, can be easily re-oxidized by various factors such as changes in pH, E_H , increased nitrate concentration, or exposure to molecular oxygen, among others. Additionally, the UNPs could be of concern because they are exhibiting great mobility in groundwater as colloids and can be easily re-oxidized, as observed with uraninite NPs (Suzuki et al. 2016). Therefore, characterizing the long-term stability of U reduced products in presence of oxidant agents like O_2 is of great help in optimizing this strategy. In the present study, HERFD-XANES combined with ITFA analysis was used to assess the stability of U reduction products in presence of O_2 by determining the proportions of U(VI), U(V) and U(IV) from a sample that showed over 90% reduction of U(VI) in the supernatant of the microcosms. Prior to the HERFD-XANES measurements, the black precipitate was exposed to O_2 for 4 weeks. The results obtained (Fig. 4D) showed clear evidence of re-oxidation of U(IV) to U(VI). This is not surprising as biogenic uraninite tends to easily re-oxidize in the presence of various oxidizing factors such as oxygen. In an attempt to enhance the stability and longevity of

the reduced U(IV), Glycerol-P has been used as an electron donor, which provides reducing conditions and is capable of forming a U(IV) phosphate biomineral that is considerably more resistant to oxidative remobilization (Newsome et al. 2015). Conversely, values of 53% were also identified for U(V). This could indicate the stability of pentavalent U in our system in the presence of oxygen and represents the first reported instance of such prolonged stability of pentavalent U in environmental samples mediated by micro-organisms. U(V) is well-known for its relative instability due to the disproportionation between U(IV) and U(VI), as reported by various authors (Renshaw et al. 2005; Arnold et al. 2009). However, Crean et al. (2020) reported the stability of FeUO_4 particles in the medium term (>25 years) under oxic and variable humidity conditions. Similarly, immobilizing the reduced U(IV) product on the crystal surface could provide higher stability and, primarily, reduce the mobility of UNPs (Suzuki et al. 2016).

5. Conclusions

In summary, this study investigated the microbial reduction of U in microcosms of water contaminated with a low concentration of U (1 mg/l) by stimulating the native microbial community with glycerol as electron donor.

The results showed evidence of U(VI) reduction to U(IV) due to the activity of U-reducing micro-organisms through glycerol oxidation. Spectroscopic and microscopic analysis confirmed the formation of different reduced products of U(VI), as well as the formation of mineral phase such as calcite and pyrite.

The reduced U products were mainly identified in tetra- and pentavalent oxidation states. U(IV) was associated with biogenic uraninite, and U(V) were detected as U(V)-carbonato complex and as a metallic monouranate (FeUO_4). The reduced products were presented as nanometric particles on calcite crystals and around the bacterial surface, where U(V) as FeUO_4 was identified for the first time. Additionally, the study determined unusual stability of U(V) for four weeks exposed to molecular oxygen oxidation, which had not been previously reported in biogenic environmental samples.

Overall, this work is part of a multidisciplinary and complex project, providing valuable information about the microbial reduction of U(VI) directly in environmental samples and the formation of U(V) species. These findings can serve as a guide for future research seeking to optimize bioremediation strategies and address challenges related to the long-term stability of reduced U products. Understanding these processes is essential for designing effective bioremediation strategies and addressing U contamination in affected environments.

6. References

- Anderson RT, Vrionis HA, Ortiz-Bernad I, Resch CT, Long PE, Dayvault R, Karp K, Marutzky S, Metzler DR, Peacock A, White DC, Lowe M, and Lovley, DR (2003) Stimulating the *In Situ* Activity of *Geobacter* Species to Remove Uranium from the Groundwater of a Uranium-Contaminated Aquifer. *Applied and Environmental Microbiology*. 69(10):5884–5891. <https://doi.org/10.1128/AEM.69.10.5884-5891.2003>
- Ankudinov AL, Bouldin C, Rehr JJ, Sims J, Hung H (2002) Parallel calculation of electron multiple scattering using Lanczos algorithms, *Phys. Rev. B* 65, 104107 (2002). <http://doi.org/10.1103/PhysRevB.65.104107>
- Annandale J, Burgess J, Tanner P (2017) Where there's muck there's brass: irrigated agriculture with mine impacted waters. *International Mine Water Assoc (IMWA) Conf. Mine Water and Circular Economy*. 915–922. Date of access: February 02, 2022. Retrieved from http://www.mwen.info/docs/imwa_2017/IMWA2017_Annandale_915.pdf
- Ansoborlo E, Lebaron-Jacobs L, Prat O (2015) Uranium in drinking-water: A unique case of guideline value increases and discrepancies between chemical and radiochemical guidelines. *Environment International*. 77:1–4. <https://doi.org/10.1016/j.envint.2014.12.011>
- Arnold PL, Jason BL, Dipti P (2009) Pentavalent Uranyl Complexes. *Coordination Chemistry Reviews*. 253(15–16):1973–1978. <https://doi.org/10.1016/j.ccr.2009.03.014>.
- Bacmann M, Bertaut EF, Blaise A, Chevalier R, Roult G (1969) Magnetic Structures and Properties of UFeO₄. *Journal of Applied Physics*. 40(3): 1131–1132. <https://doi.org/10.1063/1.1657561>.
- Bacmann M and Bertaut EF (1967) Structure Du Nouveau Composé UFeO₄. *Bulletin de La Société Française de Minéralogie et de Cristallographie*. 90(2):257–58. <https://doi.org/10.3406/bulmi.1967.6108>.
- Bader M, Rossberg A, Steudtner R, Drobot B, Großmann K, Schmidt M, Musat N, Stumpf

- T, Ikeda-Ohno A, Cherkouk A (2018) Impact of Haloarchaea on Speciation of Uranium - A Multispectroscopic Approach. *Environmental Science and Technology* 52(21):12895–12904. <https://doi.org/10.1021/acs.est.8b02667>.
- Banala UK, Das NPI, Toleti SR (2021) Microbial interactions with uranium: Towards an effective bioremediation approach. *Environmental Technology and Innovation*. 21:101254. <https://doi.org/10.1016/j.eti.2020.101254>
- Bernhard G, Geipel G, Brendler V, Nitsche H (1998) Uranium speciation in waters of different uranium mining areas. *Journal of Alloys and Compounds*. 271–273: 201–205. [https://doi.org/10.1016/S0925-8388\(98\)00054-1](https://doi.org/10.1016/S0925-8388(98)00054-1)
- Bernier-Latmani R, Veeramani H, Dalla Vecchia E, Junier P, Lezama-Pacheco JS, Suvorova EI, Sharp JO, Wigginton NS, Bargar JR (2010) Non-Uraninite Products of Microbial U(VI) Reduction. *Environmental Science and Technology*. 44(24):9456–9462. <https://doi.org/10.1021/es101675a>.
- Bhattacharyya A, Campbell KM, Kelly SD, Roebbert Y, Weyer S, Bernier-Latmani R, Borch T (2017) Biogenic Non-Crystalline U (IV) Revealed as Major Component in Uranium Ore Deposits. *Nature Communications*. 8(IV):1–8. <https://doi.org/10.1038/ncomms15538>.
- Cason ED, Piater LA, Heerden EV (2012) Reduction of U(VI) by the Deep Subsurface Bacterium, *Thermus Scotoductus* SA-01, and the Involvement of the ABC Transporter Protein. *Chemosphere*. 86(6): 572–577. <https://doi.org/10.1016/j.chemosphere.2011.10.006>.
- Chen L, Liu, J, Zhang W, Zhou J, Luo D, Li Z (2021) Uranium (U) source, speciation, uptake, toxicity and bioremediation strategies in soil-plant system: A review. *Journal of Hazardous Materials*. 413:125319. <https://doi.org/10.1016/j.jhazmat.2021.125319>
- Collins RN and Rosso KM (2017) Mechanisms and Rates of U(VI) Reduction by Fe(II) in Homogeneous Aqueous Solution and the Role of U(V) Disproportionation. *Journal of Physical Chemistry A*. 121(35): 6603–6613. <https://doi.org/10.1021/acs.jpca.7b05965>.
- Crean DE, Stennett MC, Livens FR, Grolimund D, Borca CN, Hyatt NC (2020) Multimodal

- X-ray microanalysis of a UFeO_4 : evidence for the environmental stability of ternary U(V) oxides from depleted uranium munitions testing. *Environ. Sci. Process Impacts*. 22(7): 1577–1585. <https://doi.org/10.1039/d0em00243g>
- Drobot B, Vogel M, Steudtner R, Rossberg A, Foerstendorf H (2020) Implementation of a ‘Rolling Ball’ algorithm for spectroscopy. HZDR - Institute of Resource Ecology - Annual Report 2020, 27. Retrieved from: <https://www.hzdr.de/publications/PublDoc-17382.pdf>
- Faizova R, Scopelliti R, Chauvin AS, Mazzanti M (2018) Synthesis and Characterization of a Water Stable Uranyl(V) Complex. *Journal of the American Chemical Society*. 140(42):13554–13557. <https://doi.org/10.1021/jacs.8b07885>.
- Finneran KT, Anderson RT, Nevin KP, Lovley DR (2002) Potential for bioremediation of uranium-contaminated aquifers with microbial U(VI) reduction. *Soil and Sediment Contamination*. 11(3):339–357. <https://doi.org/10.1080/20025891106781>
- Gao W and Francis AJ (2008) Reduction of Uranium(VI) to Uranium(IV) by *Clostridia*. *Applied and Environmental Microbiology*. 74(14):4580–4584. <https://doi.org/10.1128/AEM.00239-08>.
- George GN and Pickering IJ (1995) EXAFSPAK: A Suite of Computer Programs for Analysis of X-Ray Absorption Spectra. Stanford Synchrotron Radiation Laboratory. https://scholar.google.com/scholar_lookup?title=EXAFSPAK%3A%20A%20Suite%20of%20Computer%20Programs%20for%20Analysis%20of%20X-Ray%20Absorption%20Spectra.&publication_year=1993&author=G.N.%20George&author=I.J.%20Pickering
- Giffaut E, Grivé M, Blanc P, Vieillard P, Colàs E, Gailhanou H, Gaboreau S, Marty N, Madé B, Duro L (2014) Andra thermodynamic database for performance assessment: ThermoChimie. *Applied Geochemistry*. 49:225–236. doi.org/10.1016/j.apgeochem.2014.05.007
- Grivé M, Duro L, Colàs E, Giffaut E (2015) Thermodynamic data selection applied to radionuclides and chemotoxic elements: an overview of the ThermoChimie-TDB. *Applied Geochemistry*. 55:85-94. doi.org/10.1016/j.apgeochem.2014.12.017

- Guo X, Tiferet E, Qi L, Solomon JM, Lanzirotti A, Newville M, Engelhard MH, Kukkadapu RK, Wu D, Ilton ES, Asta M, Sutton SR, Xu H, Navrotsky A (2016) U(v) in Metal Uranates: A Combined Experimental and Theoretical Study of MgUO₄, CrUO₄, and FeUO₄. Dalton Transactions. 45(11): 4622–4632. <https://doi.org/10.1039/c6dt00066e>.
- Hilpmann S, Rossberg A, Steudtner R, Drobot B, Hübner R, Bok F, Prieur D, Bauters S, Kvashnina KO, Stumpf T, Cherkouk, A (2023) Presence of Uranium(V) during Uranium(VI) Reduction by *Desulfosporosinus Hippei* DSM 8344T. Science of the Total Environment. 875:162593. <https://doi.org/10.1016/j.scitotenv.2023.162593>.
- Hua B, Xu H, Terry J, Deng B (2006) Kinetics of Uranium(VI) Reduction by Hydrogen Sulfide in Anoxic Aqueous Systems. Environmental Science and Technology. 40(15):4666–4671. <https://doi.org/10.1021/es051804n>.
- Ikeda A, Hennig C, Tsushima S, Takao K, Ikeda Y, Scheinost AC, Bernhard G (2007) Comparative Study of Uranyl(VI) and -(V) Carbonato Complexes in an Aqueous Solution. Inorganic Chemistry 46 (10):4212-4219. <https://doi.org/10.1021/ic070051y>.
- Istok JD, Senko JM, Krumholz LR, Watson D, Bogle MA, Peacock A, Chang YJ, White DC (2004) In Situ Bioreduction of Technetium and Uranium in a Nitrate-Contaminated Aquifer. Environmental Science and Technology. 38(2):468–475. <https://doi.org/10.1021/es034639p>
- Junier P, Suvorova EI, Bernier-Latmani R (2010) Effect of Competing Electron Acceptors on the Reduction of U(VI) by *Desulfotomaculum reducens*. Geomicrobiology Journal. 27(5):435–443. <https://doi.org/10.1080/01490450903480293>.
- Kvashnina KO, Butorin SM, Martin P, Glatzel P (2013) Chemical State of Complex Uranium Oxides. Physical Review Letters. 111(25):1–5. <https://doi.org/10.1103/PhysRevLett.111.253002>.
- Kvashnina KO, Kvashnin YO, Butorin SM (2014) Role of Resonant Inelastic X-Ray Scattering in High-Resolution Core-Level Spectroscopy of Actinide Materials. Journal of Electron Spectroscopy and Related Phenomena. 194:27–36. <https://doi.org/10.1016/j.elspec.2014.01.016>.

- Kvashnina KO and Scheinost AC (2016) A Johann-Type X-Ray Emission Spectrometer at the Rossendorf Beamline. *Journal of Synchrotron Radiation*. 23(3):836–841. <https://doi.org/10.1107/S1600577516004483>.
- Kvashnina KO and Butorin SM (2022) High-Energy Resolution X-Ray Spectroscopy at Actinide $M_{4,5}$ and Ligand K Edges: What We Know, What We Want to Know, and What We Can Know. *Chemical Communications*. 58(3):327–342. <https://doi.org/10.1039/d1cc04851a>.
- Lakaniemi AM, Douglas GB, Kaksonen AH (2019) Engineering and Kinetic Aspects of Bacterial Uranium Reduction for the Remediation of Uranium Contaminated Environments. *Journal of Hazardous Materials*. 371:198–212. <https://doi.org/10.1016/j.jhazmat.2019.02.074>.
- Lee PA, Citrin PH, Eisenberger P, Kincaid BM (1981) Extended X-Ray Absorption Fine Structure Its Strengths and Limitations as a Structural Tool. *Reviews of Modern Physics*. 53(4):769–806. <https://doi.org/10.1103/RevModPhys.53.769>.
- Lovley DR, Roden EE, Phillips EJP, Woodward JC (1993) Enzymatic Iron and Uranium Reduction by Sulfate-Reducing Bacteria. *Marine Geology*. 113(1–2):41–53. [https://doi.org/10.1016/0025-3227\(93\)90148-O](https://doi.org/10.1016/0025-3227(93)90148-O).
- Luo C, Zhang T, Yuan Z, Fu Z, Lv S, Huang C, Hu B, Zhu Y, Zheng B (2022) Removal of Hexavalent Uranium [U(VI)] by Magnetite in the Presence of Metal-Reducing Bacteria from Rice Soil. *Environmental Technology and Innovation*. 28:102616. <https://doi.org/10.1016/j.eti.2022.102616>.
- Madden AS, Smith AC, Balkwill DL, Fagan LA, Phelps TJ (2007) Microbial uranium immobilization independent of nitrate reduction. *Environmental Microbiology*. 9(9):2321–2330. <https://doi.org/10.1111/j.1462-2920.2007.01347.x>
- Marshall MJ, Beliaev AS, Dohnalkova AC, Kennedy DW, Shi L, Wang Z, Boyanov MI, Lai B, Kemner KM, McLean JS, Reed SB, Culley DE, Bailey VL, Simonson CJ, Saffarini DA, Romine MF, Zachara JM, Fredrickson JK (2006) C-Type Cytochrome-Dependent Formation of U(IV) Nanoparticles by *Shewanella Oneidensis*. *PLoS Biology*. 4(8):1324–1333. <https://doi.org/10.1371/journal.pbio.0040268>.

Marshall MJ, Dohnalkova AC, Kennedy DW, Plymale AE, Thomas SH, Löffler FE, Sanford RA, Zachara JM, Fredrickson JK, Beliaev AS (2009) Electron Donor-Dependent Radionuclide Reduction and Nanoparticle Formation by *Anaeromyxobacter Dehalogenans* Strain 2CP-C. *Environmental Microbiology*. 11(2):534–43. <https://doi.org/10.1111/j.1462-2920.2008.01795.x>.

Martínez-Rodríguez P, Sánchez-Castro I, Ojeda JJ, Abad MM, Descostes M, Merroun ML (2023) Effect of different phosphate sources on uranium biomineralization by the *Microbacterium* sp. Be9 strain: A multidisciplinary approach study. *Frontiers in Microbiology*. 13:1092184. <https://doi.org/10.3389/fmicb.2022.1092184>

Mereiter K (1982) The crystal structure of liebigite, $\text{Ca}_2\text{UO}_2(\text{CO}_3)^3 \cdot 11\text{H}_2\text{O}$. *Tschermaks Mineralogische und Petrographische Mitteilungen* 30:277-288.

Newman-Portela AM, Krawczyk-Bärsch E, Lopez-Fernandez M, Bok F, Kassahun A, Drobot B, Stuedtner, R, Stumpf T, Raff J, Merroun ML (2023). Biostimulation of indigenous microbes for uranium bioremediation in former U mine water: multidisciplinary approach assessment. *Environmental Science and Pollution Research*. <https://doi.org/10.1007/s11356-023-31530-4>.

Newsome L, Morris K, Lloyd JR (2014) The biogeochemistry and bioremediation of uranium and other priority radionuclides. *Chemical Geology*. 363:164–184. <https://doi.org/10.1016/j.chemgeo.2013.10.034>

Newsome L, Morris K, Trivedi D, Bewsher A, Lloyd JR (2015) Biostimulation by Glycerol Phosphate to Precipitate Recalcitrant Uranium(IV) Phosphate. *Environmental Science and Technology*. 49(18):11070–11078. <https://doi.org/10.1021/acs.est.5b02042>

Ondrus P, Skála R, Veselovsky F, Sejkora J, Vitti C (2003) Cejkaite, the triclinic polymorph of $\text{Na}_4(\text{UO}_2)(\text{CO}_3)_3$ - a new mineral from Jáchymov, Czech Republic. *American Mineralogist* 88 (4):686-693.

Orellana R, Leavitt JJ, Comolli LR, Csencsits R, Janot N, Flanagan KA, Gray AS, Leang C, Izallalen M, Mester T, Lovley DR (2013) U(VI) Reduction by Diverse Outer Surface c-Type Cytochromes of *Geobacter Sulfurreducens*. *Applied and Environmental Microbiology*. 79(20):6369–6374. <https://doi.org/10.1128/AEM.02551-13>.

- Pan Z, Bártová B, LaGrange T, Butorin SM, Hyatt NC, Stennett MC, Kvashnina KO, Bernier-Latmani R (2020) Nanoscale Mechanism of UO_2 Formation through Uranium Reduction by Magnetite. *Nature Communications*. 11(1):1–12. <https://doi.org/10.1038/s41467-020-17795-0>.
- Renshaw JC, Butchins LJC, Livens FR, May I, Charnock JM, Lloyd JR (2005) Bioreduction of Uranium: Environmental Implications of a Pentavalent Intermediate. *Environmental Science and Technology*. 39(15):5657–5660. <https://doi.org/10.1021/es048232b>.
- Roberts HE, Morris K, Law GTW, Mosselmans JFW, Bots P, Kvashnina KO, Shaw S (2017) Uranium(V) Incorporation Mechanisms and Stability in Fe(II)/Fe(III) (Oxyhydr)Oxides. *Environmental Science and Technology Letters*. 4(10):421–426. <https://doi.org/10.1021/acs.estlett.7b00348>.
- Rossberg A, Reich T, Bernhard G (2003) Complexation of Uranium(VI) with Protocatechuic Acid-Application of Iterative Transformation Factor Analysis to EXAFS Spectroscopy. *Analytical and Bioanalytical Chemistry*. 376(5):631–38. <https://doi.org/10.1007/s00216-003-1963-5>.
- Rossberg A, Ulrich KU, Weiss S, Tsushima S, Hiemstra T, Scheinost AC (2009) Identification of Uranyl Surface Complexes on Ferrihydrite: Advanced EXAFS Data Analysis and CD-MUSIC Modeling. *Environmental Science & Technology* 43 (5): 1400-1406. <https://doi.org/10.1021/es801727w>.
- Safonov AV, Babich TL, Sokolova DS, Grouzdev DS, Tourova TP, Poltareus AB, Zakharova EV, Merkel AY, Novikov AP and Nazina TN (2018) Microbial Community and in situ Bioremediation of Groundwater by Nitrate Removal in the Zone of a Radioactive Waste Surface Repository. *Frontiers in Microbiol.* 9:1985. doi: 10.3389/fmicb.2018.01985
- Sánchez-Castro I, Martínez-Rodríguez P, Abad MM, Descostes M, Merroun ML (2021) Uranium Removal from Complex Mining Waters by Alginate Beads Doped with Cells of *Stenotrophomonas* Sp. Br8: Novel Perspectives for Metal Bioremediation. *Journal of Environmental Management*. 296:1–10. <https://doi.org/10.1016/j.jenvman.2021.113411>.

- Scheinost AC, Claussner J, Exner J, Feig M, Findeisen S, Hennig C, Kvashnina KO, Naudet D, Prieur D, Rossberg A, Schmidt M, Qiu C, Colomp P, Cohen, C, Dettona E, Dyadkin V, Stumpf T (2021) ROBL-II at ESRF: A Synchrotron Toolbox for Actinide Research. *Journal of Synchrotron Radiation*. 28:333–349. <https://doi.org/10.1107/S1600577520014265>.
- Schofield EJ, Veeramani H, Sharp JO, Suvorova E, Bernier-Latmani R, Mehta A, Stahlman J, Webb S, Clark D, Conradson S, Ilton ES, Bargar JR (2008) Structure of Biogenic Uraninite Produced by *Shewanella Oneidensis* Strain MR-1. *Environmental Science and Technology*. 42(21):7898–7904. <https://doi.org/10.1021/es800579g>.
- Sharp JO, Schofield EJ, Veeramani H, Suvorova EI, Kennedy DW, Marshall MJ, Mehta A, Bargar JR Bernier-Latmani R (2009) Structural Similarities between Biogenic Uraninites Produced by Phylogenetically and Metabolically Diverse Bacteria. *Environmental Science and Technology*. 43(21):8295–8301. <https://doi.org/10.1021/es901281e>.
- Shelobolina ES, Vrionis HA, Findlay RH, Lovley DR (2008) *Geobacter Uraniireducens* Sp. Nov., Isolated from Subsurface Sediment Undergoing Uranium Bioremediation. *International Journal of Systematic and Evolutionary Microbiology*. 58(5):1075–78. <https://doi.org/10.1099/ijs.0.65377-0>.
- Skuce RL, Tobler DJ, MacLaren I, Lee MR, Phoenix VR (2017) Immobilization of Nanoparticles by Occlusion into Microbial Calcite. *Chemical Geology*. 453:72–79. <https://doi.org/10.1016/j.chemgeo.2017.02.005>.
- Smedley PL and Kinniburgh DG (2023) Uranium in Natural Waters and the Environment: Distribution, Speciation and Impact. *Applied Geochemistry*. 148:105534. <https://doi.org/10.1016/j.apgeochem.2022.105534>.
- Suzuki Y, Mukai H, Ishimura T, Yokoyama TD, Sakata S, Hirata T, Iwatsuki T, Mizuno T (2016) Formation and Geological Sequestration of Uranium Nanoparticles in Deep Granitic Aquifer. *Scientific Reports* 6:2–7. <https://doi.org/10.1038/srep22701>.
- Suzuki Y, Kelly SD, Kemner KM, Banfield JF (2002) Nanometre-Size Products of Uranium Bioreduction. *Nature*. 419(6903):134–134. <https://doi.org/10.1038/419134a>.

- Tutschku J, Hennig C, Geipel G, Bernhard G (2004) UV-Vis Measurements of Uranium (VI) and Uranium (IV) in Concentrated Chloride Solution Prepared with the Electrochemical Cell. FZR – IRC Annual Report, 12. Retrieved from: https://inis.iaea.org/collection/NCLCollectionStore/_Public/36/055/36055540.pdf
- Ulrich KU, Singh A, Schofield EJ, Bargar JR, Veeramani H, Sharp JO, Bernier-Latmani R, Giammar DE. (2008) Dissolution of Biogenic and Synthetic UO₂ under Varied Reducing Conditions. *Environmental Science and Technology*. 42(15):5600–5606. <https://doi.org/10.1021/es800647u>.
- Veeramani H, Scheinost AC, Monsegue N, Qafoku NP, Kukkadapu R, Newville M, Lanzirotti A, Pruden A, Murayama M, Hochella MF (2013) Abiotic Reductive Immobilization of U(VI) by Biogenic Mackinawite. *Environ. Sci. Technol.* 2013, 47, 2361–2369. <https://doi.org/10.1021/es304025x>.
- Vettese GF, Morris K, Natrajan LS, Shaw S, Vitova T, Galanzew J, Jones DL, Lloyd JR (2020) Multiple Lines of Evidence Identify U(V) as a Key Intermediate during U(VI) Reduction by *Shewanella Oneidensis* MR1. *Environmental Science and Technology*. 54(4):2268–76. <https://doi.org/10.1021/acs.est.9b05285>.
- Vogel M, Steudtner R, Fankhänel T, Raff J, Drobot B (2021) Spatially Resolved Eu(III) Environments by Chemical Microscopy. *Analyst*. 146(22):6741–45. <https://doi.org/10.1039/d1an01449h>.
- WHO (2022) Guidelines for drinking-water quality: fourth edition incorporating the first and second addenda, Geneva: World Health Organization. 478-480. Date of access: February 20, 2023. Retrieved from <https://www.who.int/publications/i/item/9789240045064>
- Wilkins MJ, Livens FR, Vaughan DJ, Lloyd JR (2006) The impact of Fe(III)-reducing bacteria on uranium mobility. *Biogeochemistry*. 78(2):125–150. <https://doi.org/10.1007/s10533-005-3655-z>
- Williams KH, Bargar JR, Lloyd JR, Lovley DR (2013) Bioremediation of uranium-contaminated groundwater: A systems approach to subsurface biogeochemistry. *Current Opinion in Biotechnology*. 24(3):489–497. <https://doi.org/10.1016/j.copbio.2012.10.008>

WISMUT GmbH Umweltbericht (2021) Date of access: October 3, 2023. Retrieved from <https://www.wismut.de/de/>

Wu WM, Carley J, Luo J, Ginder-Vogel MA, Cardenas E, Leigh MB, Hwang C, Kelly SD, Ruan C, Wu L, Nostrand JV, Gentry T, Lowe K, Carroll S, Luo W, Fields MW, Gu B, Watson D, Kemner KM, Marsh T, Tiedje J, Zhou J, Fendorf S, Kitanidis PK, Jardine PM, Criddle CS (2007) In Situ Bioreduction of Uranium (VI) to Submicromolar Levels and Reoxidation by Dissolved Oxygen.” *Environmental Science and Technology*. 41(16):5716–5723. <https://doi.org/10.1021/es062657b>.

Wu, WM, Carley J, Gentry T, Ginder-Vogel MA, Fienen M, Mehlhorn T, Yan H, Carroll S, Pace MN, Nyman J, Luo J, Gentile ME, Fields MW, Hickey RF, Gu B, Watson D, Cirpka OA, Zhou J, Fendorf J, Kitanidis PK, Jardine PM, Criddle CS (2006) Pilot-Scale in Situ Bioremediation of Uranium in a Highly Contaminated Aquifer. 2. Reduction of U(VI) and Geochemical Control of U(VI) Bioavailability. *Environmental Science and Technology*. 40(12):3986–3995. <https://doi.org/10.1021/es051960u>.

Wyckoff, RWG (1963) *Crystal Structures*. Band 1, 2. Auflage:239–444.

You W, Peng W, Tian Z, Zheng M (2021) Uranium bioremediation with U(VI)-reducing bacteria. *Science of the Total Environment*. 798:149107. <https://doi.org/10.1016/j.scitotenv.2021.149107>

Supplementary material

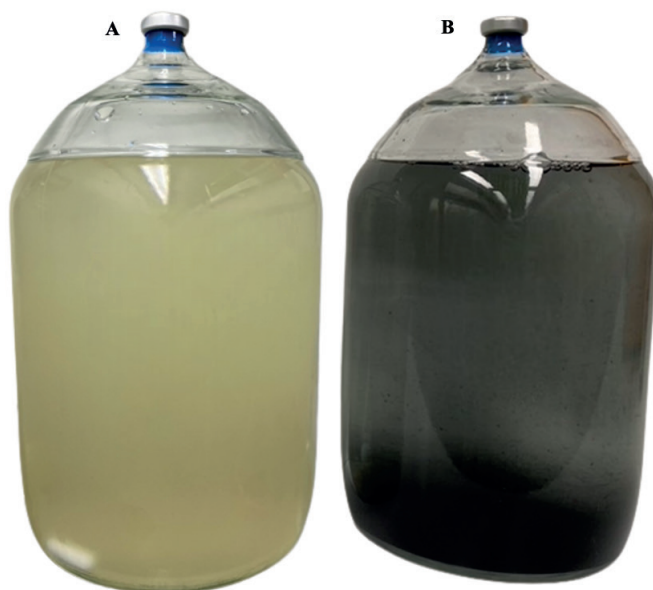


Figure S1. Colour transition during the U(VI) reduction process in the microcosms at the beginning of the experiment (A) and at the end (B).

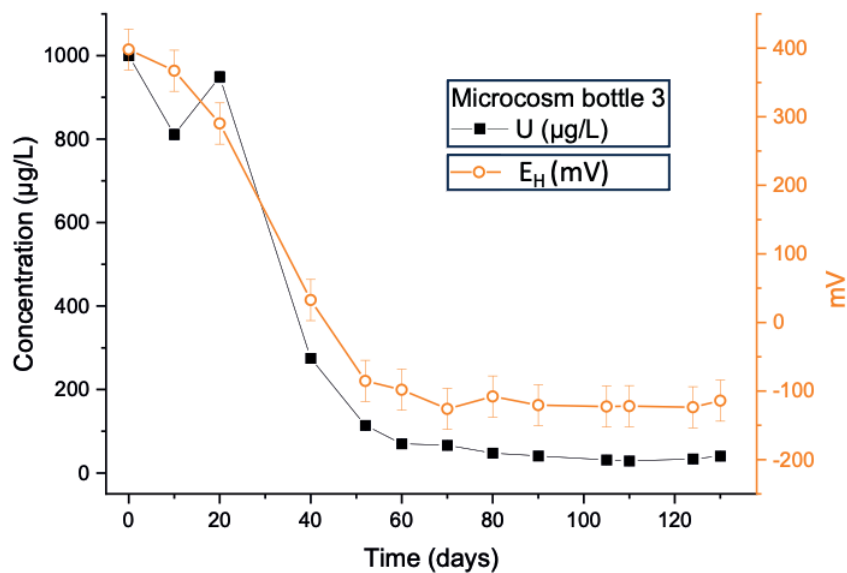


Fig. S2. Monitoring of U(VI) concentration in $\mu\text{g/l}$ and E_H (mV) in a microcosm experiment using 10 mM glycerol as electron donor for 130 days.

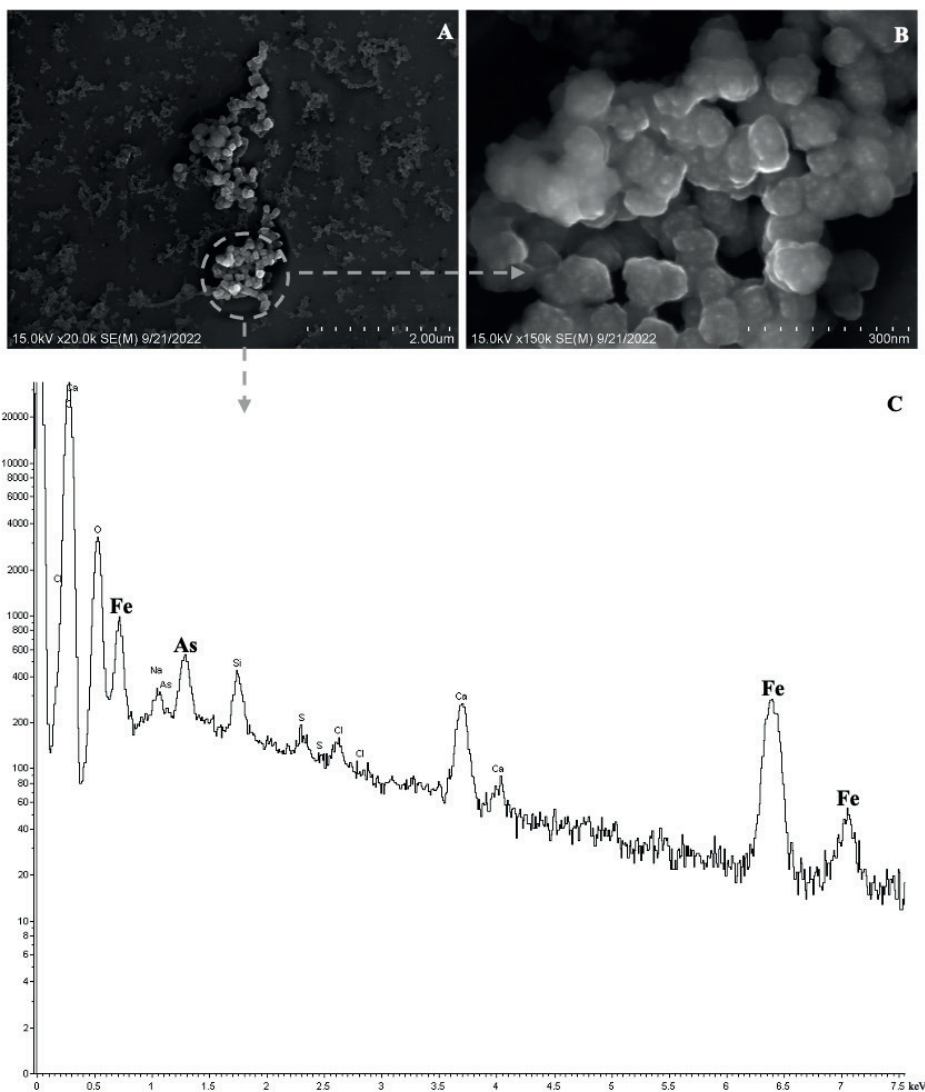


Fig. S3. SEM image of a portion of the filter after Pressure Filtration of the mine water, showing colloidal aggrupation (A, B). The EDXS spectrum (C) indicates the elemental composition, primarily consisting of Fe and As.

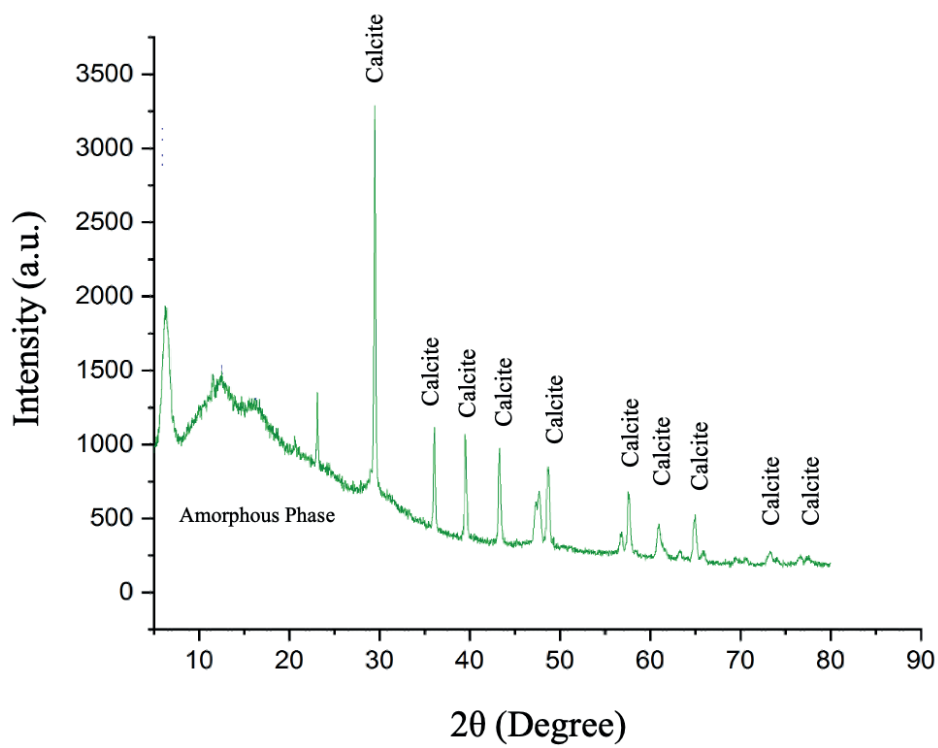


Fig. S4. PXRD pattern demonstrates calcite in the back precipitate.

Table S1. Chemistry of the mine water during the monitoring of the U(VI)-reduction experiment.

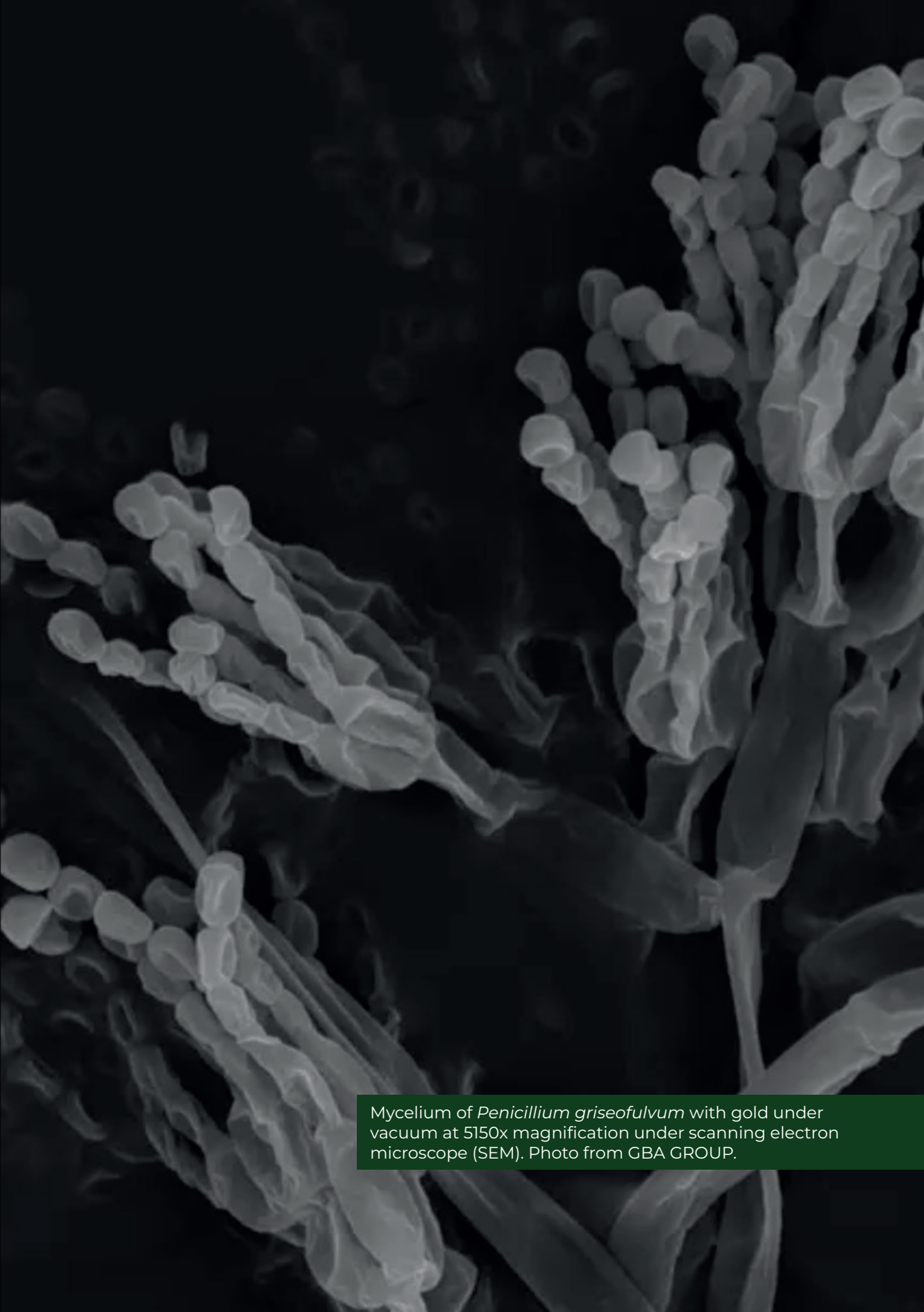
Time (days)	0	10	20	40	52	60	70	80	90	105	110	124	130
E_H [mV]	398	367	290.9	32.7	-85.2	-98.1	-126	-108	-120.6	-122.5	-122	-123.6	-114
pH	7.5	8.0	8.1	7.8	7.3	7.3	7.3	7.2	7.2	7.3	7.4	7.5	7.4
Cations													
[mg/L]													
Fe	3.21	2.11	2.42	2.10	0.60	0.33	0.17	0.12	0.13	0.09	0.08	0.09	0.06
As	1.3	1.12	1.13	1.02	0.57	0.52	0.65	0.52	0.68	0.49	0.57	0.52	0.58
U	1.00	0.81	0.95	0.28	0.11	0.07	0.07	0.05	0.04	0.03	0.03	0.03	0.04
Anions [mg/L]													
SO_4^{2-}	303	306	316	301	270	197	148	136	129	120	119	115	96.8

E_H : Redox potential.

Table S2. Physico-chemical characterization of Schlema-Alberoda mine water in July 2022 (SA) and at the end of the microcosm experiments after 130 days (SA+G, SAC, ASA+G).

	SA	SA+G	SAC	ASA+G
pH	7.5 ±0.1	7.4 ±0.1	7.4 ±0.1	7.7 ±0.1
E _H [mV]	398 ±0.1	-114 ±0.1	68 ±30	135 ±30
Temp. (°C)	25.5 ±1	28 ±1	28 ±1	28 ±1
Cations [mg/L]				
Na	89.3 ±0.2	90.03 ±1.57	84.3 ±0.5	85.66 ±1.39
Mg	54.2 ±0.5	51.13 ±1.57	45.3 ±1	47.87 ±0.76
Al	< 0.001	< 0.001	< 0.01	< 0.01
Si	7.5 ±0.1	9.01 ±0.26	8.3 ±0.1	8.94 ±0.16
P	< 0.01	< 0.1	< 0.1	< 0.1
K	9.3 ±0.05	10.22 ±0.02	10.1 ±0.16	9.97 ±0.22
Ca	122 ±0.6	81.53 ±2.1	58.9 ±1.1	48.93 ±1.03
Mn	1.4 ±0.05	1.19 ±0.002	0.12 ±0	0.12 ±0.002
Fe	3.21 ±0.02 *	0.17 ±0.1	2.2 ±0.1	0.33 ±0.02
As	1.3 ±0.02 *	0.97 ±0.04	1.4 ±0.005	0.78 ±0.04
Ba	0.03	0.03	0.03	0.02
Th	< 0.001	< 0.001	< 0.001	< 0.001
U	1.0 ±0.01	0.05 ±0.01	0.75 ±0.005	0.64 ±0.02
Anions [mg/L]				
Cl ⁻	51.6 ±0.25	< 0.05	50.3 ±0.1	48.1 ±0.1
NO ₂ ⁻	< 0.5	< 0.05	< 0.05	< 0.05
NO ₃ ⁻	0.1 ±0.01	< 0.05	< 0.05	< 0.05
PO ₄ ³⁻	< 0.5	< 0.05	< 0.05	< 0.05
SO ₄ ²⁻	302.0 ±1.0	94.6 ±1.0	289.5 ±3.5	291.7 ±1.0
[mg/L]				
TIC	56.8 ± 1.1	75.6 ±1.3	68.4 ±0.4	64.9 ±0.5
TOC	1.9 ±0.1	280.2 ±0.8	3.1 ±0.27	451.4 ±1.1
DOC	1.8 ±0.17	285.3 ±0.8	9.33 ±1.07	463.1 ±0.9
TN	< 0.1	< 0.5	< 0.5	< 0.5

SA: Schlema-Alberoda mine water during sampling; SA+G: Schlema-Alberoda mine water + 10 mM glycerol; SAC: Schlema-Alberoda mine water after 130 days; ASA+G: sterilized (autoclaved) Schlema-Alberoda mine water + 10 mM glycerol; E_H: Redox potential; Temp: Temperature; TIC: total inorganic carbon. TOC: total organic carbon, TN: total nitrogen; standard deviation with n=3; * analysed by Wismut GmbH (ICP analysis without centrifugation prior to acidification).



Mycelium of *Penicillium griseofulvum* with gold under vacuum at 5150x magnification under scanning electron microscope (SEM). Photo from GBA GROUP.

Chapter IV:

Exploring the fungal community in U-contaminated mine waters: a strategic approach for the mycoremediation of metalloid and radionuclide-contaminated environments

AUTHORS:

Antonio M. Newman-Portela ^{a,b,*}, Esther Peula Ruiz ^a, Cristina Povedano-Priego ^a, Evelyn Krawczyk-Bärsch ^b, Inés Martín Sánchez ^a, Andrea Kassahun ^c, Thorsten Stumpf ^b, Johannes Raff ^b, Mohamed L. Merroun ^a

^a Department of Microbiology, Faculty of Science, University of Granada, Granada, Spain.

^b Helmholtz-Zentrum Dresden-Rossendorf, Institute of Resource Ecology, Bautzner Landstraße 400, 01328 Dresden, Germany.

^c WISMUT GmbH, Chemnitz, Germany.

KEYWORDS: mine water, uranium, selenium, nanoparticles, fungi, mycoremediation.

ABSTRACT:

Anthropogenic activities such as metal mining and processing can lead to a considerable input of heavy metals and radionuclides into the environment. Looking toward the negative effects of such contamination, an efficient approach to remediation of the affected areas is needed. Bioremediation using metal-tolerant fungi is considered a promising and cost-effective approach. The aim of this study was to isolate, identify, and biochemically characterize indigenous fungi from mine waters of two former U mines in Germany (Schlema-Alberoda and Pöhla, Wismut GmbH) and to screen for those with potential for heavy metal and radionuclide bioremediation. 14 fungal strains belonging to the genera *Cadophora*, *Acremonium*, *Aspergillus*, *Penicillium*, *Cladosporium*, *Trichoderma*, and *Schizophyllum* were isolated. Most of the fungal isolates exhibited high lignocellulolytic enzymes and phosphatase activity stimulating the growth and activity of bacteria involved in U reduction and biomineralization in the mine waters. The bioremediation potential was assessed using isolates from the genera *Cadophora*, *Aspergillus*, and *Penicillium*, which were exposed to U, while *Schizophyllum*, *Trichoderma*, *Cladosporium*, and *Acremonium* were exposed to Se. Field Emission Scanning Electron Microscopy (FESEM) indicate the probable U(VI) phosphate biomineralization by *C. malorum* mediated by phosphatase activity. Both *T. harzianum* and *Acremonium* sp. demonstrated significant ability to reduce Se(IV) to Se(0) nanostructures, with reduction rates of 69.20% and 95.90%, respectively. The biogenic Se(0) nanostructures exhibited high stability and lower toxicity as they presented trigonal and monoclinic structure as was demonstrated by high-resolution transmission electron microscope (HRTEM), high-angle annular dark-field detector coupled (HAADF) with an energy-dispersive X-ray spectroscopy (EDXS), and selected area electron diffraction (SAED). Our findings suggest that isolates from contaminated habitats have potential applications in heavy metal and radionuclide bioremediation.

1. Introduction

Uranium (U), widely used since its discovery in the late 18th century for colouring glass and ceramics, has been associated with different applications in both military and civilian industries (Schulz 2023). The mobility and toxicity of U in the environment depend upon its oxidation state, being +VI and +IV the most commonly distributed in the environment. The higher toxicity is associated with hexavalent U (U(VI)) compared to tetravalent U (U(IV)), mainly due to differences in their ability to form water-soluble species, thereby increasing their bioavailability (Maher et al. 2013). Over time, the extraction and processing of U have generated a considerable amount of waste that could pose risks to the environment and public health. Additionally, U fission products, such as Selenium 79 (^{79}Se), are noteworthy (Aguerre and Frechou, 2006). Nuclear activities focused on energy production generate ^{79}Se , another relevant radionuclide (Aguerre and Frechou, 2006). The chemical toxicity of Se is also associated with its oxidation state, with Se oxyanions, such as selenate [Se(VI)] and selenite [Se(IV)], being the most toxic forms due to their high solubility and mobility, causing adverse effects in the environment (Ruiz-Fresneda et al. 2018; Siddharthan et al. 2023). On the other hand, elemental Se [Se(0)] and selenides [Se(-II)] are less soluble and immobile, thus exhibiting low toxicity in terrestrial and aquatic environments.

Traditionally, the management of contaminated environments has been addressed through the use of conventional remediation technologies, focusing on physical, chemical, or combined approaches (such as electrocoagulation, ion exchange, membrane separation, adsorption, and chemical reduction) (Akash et al. 2022; Cheng et al 2022; Ullah et al. 2023). However, these conventional methodologies are costly, complex and inefficient for low metal concentrations, representing a significant barrier to their implementation (Coelho et al. 2020a; Zhu and Chen 2009). In response to these challenges, bioremediation emerges as a highly promising strategy for rehabilitating environments contaminated by heavy metals and radionuclides due to its effectiveness and economic savings. In addition

to cost reduction, bioremediation offers greater ease of implementation and effectiveness for Se and low U concentrations (Sabuda et al. 2020; Sanchez-Castro et al. 2021; Newman-Portela et al. 2024).

Bioremediation aims to restore contaminated soils and waters through biological processes involving bacteria, fungi, algae, and/or plants (Yaashikaa et al. 2022; Martínez-Rodríguez et al. 2023). The use of fungi in bioremediation, known as mycoremediation, offers different advantages compared to the application of other micro-organisms or plants (Mumtaz et al. 2013; Kumar et al. 2021). Although research efforts in the past decade have primarily focused on studying bacteria for heavy metals and radionuclides remediation, fungi demonstrate greater tolerance to high contamination levels compared to algae, archaea, and bacteria (Mumtaz et al. 2013; Liang et al. 2019; Ruiz-Fresneda et al. 2023; Povedano-Priego et al. 2024).

Fungi are widely distributed in nature and harbour high diversity, with only 148,000 species identified to date and an estimated ~90% of fungi yet undiscovered (Cheek et al. 2020). These micro-organisms have developed adaptive mechanisms that enable them to thrive in contaminated environments by high concentrations of heavy metals and radionuclides. The interaction between fungi and U can occur through processes such as biosorption, intracellular accumulation, or mineralization (Bayramoğlu et al. 2006; Gargarello et al. 2008; Liang et al. 2015; Lusa and Bomberg 2021; Povedano-Priego et al. 2024). In the case of Se, the main mechanisms mainly involve Se biotransformations which include enzymatic reduction and biovolatilization. Enzymatic reduction of Se lead to the formation of Se(0) nanoparticles (NPs) with different morphology, size and allotropes (Ruiz-Fresneda et al. 2024). In the case of biovolatilization, different volatile biogenic Se species are generated (Siddharthan et al. 2023). Newman-Portela and co-authors (2024) reported the structure and composition of fungal community in the water of two former U mines, Schlemma-Alberoda and Pöhla using culture-independent methods based on next generation sequencing (NGS). The water sample from the Pöhla mine showed notable fungal diversity and richness, with *Acremonium* as the

dominant genus, followed by an unidentified genus of the *Fomitopsidaceae* family, *Lecanicillium*, and to a lesser extent, *Aspergillus*. In contrast, in Schlema-Alberoda, the fungal community exhibited less diverse and strongly dominated by the genus *Cadophora*. Moreover, *Penicillium* sp. was present but with a lower relative abundance in both mine waters. In the mine water of Schlema-Alberoda and Pöhla, other genera were identified with a relative abundance of less than 1%. Among them, *Cladosporium* sp., *Trichoderma* sp., and *Schizophyllum* sp. were found, although these specific details were not reported in the publication.

In this study, culture-dependent methods were used to isolate and identify fungal strains in the U mine water from Schlema-Alberoda and Pöhla. The fungal isolates were molecularly identified and successfully some of the dominant genera were isolated from the mine water of both U mines, according to Newman-Portela and co-authors (2024). Additionally, to assess the potential of the native fungal community for U remediation, the enzymatic activity of isolated fungi and the interaction of some isolated fungal with U were studied. The fungi selected for the fungus-U interaction were those identified with potential for U bioremediation based on the literature, such as *Penicillium* sp. and *Aspergillus* sp., along with *Cadophora* sp., a fungal isolate that was highly represented in the mine water with the highest U concentration, Schlema-Alberoda (1 mg/l). One of the most relevant processes is the phosphate biomineralization of U(VI) by fungi at U-contaminated sites through phosphatase activity, generating orthophosphates from organic phosphate substrate (e.g., glycerol-2-phosphate (G2P)) (Povedano-Priego et al. 2024). Fungi could use glycerol as a carbon source and fungal phosphatase activity could form different uranyl-phosphate precipitates through a phosphatase-mediated process. Furthermore, this study assesses the immobilization of Se by fungi isolated from both former Saxon mines. Se, a metalloid with significant environmental impact due to its high toxicity to living organisms, was investigated in its interaction with fungi using Se(IV) as an inactive analogue of ⁷⁹Se.

2. Materials and methods

2.1. Mine water sample collection

In August and September 2020, 3 L of mine water were collected in various sterile glass bottles from the former U mines, Schlema-Alberoda and Pöhla, respectively. The sampling was carried out simultaneously in time and using the methodology described by Newman-Portela et al. (2024). The mine water samples were transported to the laboratory at a temperature of 4 °C and then stored at the same conditions until processing.

2.2. Isolation of fungal strains from mine water samples

The collected fresh mine water was filtered through sterile membrane filters of 0.45 µm and 0.20 µm pore sizes (Membrane Filter, MF-Millipore®, Germany). Three biological replicates were analysed for each mine water sample. Each filter was aseptically cut into four equal pieces, and each piece was placed on Potato Dextrose Agar (PDA) solid culture plates (Biolife, Italy). The PDA composition included potato extract (5 g), glucose (20 g), and agar (17 g), prepared according to the manufacturer's instructions. The samples were incubated at 25 ± 2 °C for 7 days.

After the incubation period, fungal mycelium from various strains could be observed emerging from the filter pieces inoculated on PDA. For isolation, 5 mm diameter agar discs were taken from the initial PDA plates containing the filter, using a Transfertube™ (Spectrum Laboratories, California). The agar discs containing the mycelium were inoculated into fresh PDA medium and incubated for 5 days at 25 ± 2 °C. This process was repeated until pure colonies were obtained. Plates with pure colonies were sealed with parafilm and stored at 4 °C. Finally, the isolated fungal strain's collection is preserved on PDA and malt extract agar (Biolife, Italy). The composition of the malt extract agar is listed as follows: maltose (12.5 g/l), dextrin (2.5 g/l), glycerol (1 g/l), peptocomplex (2.6 g/l) and agar (17 g/l)

2.3. Morphological characterization of the fungal isolates

In order to taxonomically classify the different isolated fungi, a morphological identification based on both macroscopic and microscopic observation was used. Macroscopic observation allowed us to identify the

different fungi through a visual examination of the isolates over a period of one to two weeks. For microscopic analysis, samples of a small portion of the mycelium were prepared through a simple staining with lactophenol blue solution (Sigma-Aldrich, U.S.) and observed using an optical microscope Dialux22 (Leitz, Germany). The digital images were captured using a connected Olympus camera (Olympus, Japan).

2.4. Molecular identification of cultured fungal isolates

2.4.1. DNA extraction

Fungi were cultivated in sterile tubes with 3 mL of malt extract broth (Biolife, Italy) at a temperature of 28 °C and an agitation speed of 170 rpm for 3 days. Subsequently, 0.05 g of mycelium was collected and stored at -20 °C until the DNA extraction. Total fungal DNA extraction for each isolated colony was carried out following the protocol described by Martín-Platero et al. 2007, modified as reported in Povedano-Priego et al. 2024. The quality and concentration of the samples were assessed through 0.75% agarose gel electrophoresis and the Qubit dsDNA BR Assay kit on the Qubit Fluorometer 4.0 (Thermo Fisher Scientific, USA), respectively.

2.4.2. PCR amplification and Sanger sequencing

A set of common primers, ITS-1 (5'-*TCCGTAGGTGAACCTGCGG*-3'), forward primer and ITS-4 (5'-*TCCTCCGCTTATTGATATGC*-3'), reverse primer were used to yield fragments of ~600-base pair (bp) long of the ITS region. PCR reactions were mixed in a total volume of 25 µL containing 15 ng of DNA, 8 mM dNTPs, 2.5 mM MgCl₂, 1X PCR Buffer, 15 µM of each primer and 5 U/µL of Horse-Power-Taq DNA polymerase (Canvax Biotech, Spain), and conducted in a Mastercycler® Nexus Thermocycler (Eppendorf, Germany) with an initial denaturation step for 2 minutes at 94 °C was followed by 30 cycles of denaturation at 94 °C for 40 seconds, annealing at 54 °C for 40 seconds and extension at 72 °C for 40 seconds, with a final extension at 72 °C for 5 minutes. The amplified fragments were visualized by electrophoresis in 1% agarose gel stained with RedSafe (iNtRON Biotechnology, Korea) using a gel documentation system InGenius3 (Syngene, India). DNA amplicons concentrations were

evaluated by the Qubit dsDNA BR Assay kit on the Qubit Fluorometer 4.0 (Thermo Fisher Scientific, USA).

PCR products purified by Clean-Easy™ PCR Purification Kit (Canvax, Spain) were sequenced by Sanger sequencing at the *Instituto de Parasitología y Biomedicina López Neyra* (IPBLN) Genomics Facility (CSIC, Granada, Spain).

2.4.3. Data analysis

Sequences were assembled, edited and aligned with BioEdit (version 7.09) (Hall 1999). Sequences obtained were compared with the NCBI GenBank accessions using BLAST to identify the isolated strains.

2.5. Extracellular enzymes characterisation

2.5.1. Cellulase activity

The solid carboxymethylcellulose (CMC) medium was used to study the cellulase activity of the isolated fungi. The CMC composition consisted in carboxymethylcellulose (10 g/l), yeast extract (2.5 g/l), peptone (2.5 g/l), ammonium sulphate (0.5 g/l), calcium chloride (0.5 g/l), monobasic potassium phosphate (0.5 g/l), dibasic potassium phosphate (0.1 g/l) and agar (20 g/l). The inoculated CMC medium was incubated at 28 ± 2 °C for 5-6 days.

To assess the presence of cellulase activity, the surface of the solid culture plates was covered with an iodine solution. The presence of a transparent halo around the colony indicates a positive result.

2.5.2. Lignin peroxidase activity

The study of lignin peroxidase (LiP) activity was conducted using the agar-malt medium amended with sawdust. The medium composition is as follows: malt extract (20 g/l), sieved sawdust (4 g/l), guaiacol (1 mL/l), agar (20 g/l), and the pH was adjusted to 5.5. The inoculated culture medium was incubated at 28 ± 2 °C for 4 weeks. A positive result is indicated by the formation of a brown-red halo around the colony. Guaiacol is initially colourless, but in the presence of the LiP, it oxidizes, exhibiting a brown-red colour.

2.5.3. Laccase activity

The laccase activity was evaluated by inoculating isolated fungi in the Kirk solid medium (Kirk et al. 1986) with minor modifications by the amendment of ABTS (2,2'-azino-bis(3-ethylbenzothiazoline-6-sulphonic acid)). The formulation of the medium is as follows: Glucose (10 g/l), KH_2PO_4 (2 g/l), $\text{MgSO}_4 \cdot 7 \text{H}_2\text{O}$ (0.5 g/l), $\text{CaCl}_2 \cdot 2 \text{H}_2\text{O}$ (0.1 g/l), ammonium tartrate (0.2 g/l), ABTS (0.2 g/l), and agar (20 g/l). Finally, the pH was adjusted to 5.5. The inoculated solid culture medium was incubated at $28 \pm 2 \text{ }^\circ\text{C}$ in darkness until greenish-blue halos were observed. The appearance of the halo indicates a positive result, as it is due to the presence of ABTS⁺, produced after the oxidation of ABTS by laccase.

2.5.4. Amylase activity

To determine the amylase activity, isolated fungi were inoculated in starch agar solid medium, whose composition is as follows: yeast extract (3 g/l), peptone (5 g/l), starch (10 g/l), and agar (20 g/l). The inoculated solid medium was incubated at $28 \pm 2 \text{ }^\circ\text{C}$ for 5-6 days.

A positive result is observed after staining the starch agar solid medium with lugol solution and subsequently removing the excess. The presence of a transparent halo around the fungal colony due to starch hydrolysis indicates a positive result.

2.5.5. API ZYM test

The *API*® 20 *ZYM* test (BioMérieux, France) is a semi-quantitative test designed to evaluate the activity of nineteen hydrolytic enzymes. To prepare fungal isolates for the *API*® *ZYM* test, strains were initially cultivated in 3 mL of malt extract broth (Biolife, Italy). The samples were incubated at $28 \pm 2 \text{ }^\circ\text{C}$ for 5 days. Subsequently, the samples were centrifuged at $4,020 \times g$ for 5 minutes to obtain a clear supernatant which was further analysed. Media without the tested isolates was used as a control. *API*® *ZYM* tests were performed following the manufacturer's instructions by placing 65 μl of the supernatant at the appropriate points on the test strip. Strips were incubated for 4.5 h at $37 \text{ }^\circ\text{C}$. Reading was done visually, and the colour reactions recorded according to the manufacturer's instructions, by using

the API ZYM colour scale (ranging from 0 to 5). Based on the quantity of substrate metabolized, the classification is as follows: 0 corresponds to a negative reaction, 1 signifies up to 5 nmol, 2 represents 6 to 10 nmol, 3 indicates 11 to 20 nmol, 4 denotes 21 to 30 nmol, and 5 signifies 31 to 40 nmol or more. Therefore, 1 to 5 are considered as positive reactions.

2.6. U interactions with fungal isolates

Glass Erlenmeyer flasks were used to study the interaction of fungal isolates with U in abiotic and biotic treatments. All the treatments consisted in 15 mL of Schlemma-Alberoda mine water amended with 10 mM glycerol 2-phosphate (G2P) as an organic phosphate source. A 1 mM uranyl acetate stock solution in 0.1 M sodium perchlorate was added using sterilized 0.22 μm pore-size membrane filters to each flask to obtain a final U concentration of 0.05 mM and 0.1 mM, respectively. For biotic treatments, the fungal strains *C. malorum* (H1), *A. sydowii* (H5), and *P. polonicum* (H16) were grown aerobically in malt extract broth (Biolife, Italy) for 7 days at 28 ± 2 °C. Then the fungal biomass was recovered by centrifugation (5000 x g for 10 minutes) and washed twice in saline solution to remove all the culture media. Biotic controls without U, and abiotic controls were performed. A total of 12 treatments were settled up: AC (abiotic control), AC-U1 (abiotic control with 0.05 mM U), AC-U2 (abiotic control with 0.1 mM U), H1 (*Cadophora* H1), H1-U1 (*Cadophora* H1 with 0.05 mM U), H1-U2 (*Cadophora* H1 with 0.1 mM U), H5 (*Aspergillus* H5), H5-U1 (*Aspergillus* H5 with 0.05 mM U), H5-U2 (*Aspergillus* H5 with 0.1 mM U), H16 (*Penicillium* H16), H16-U1 (*Penicillium* H16 with 0.05 mM U), H16-U2 (*Penicillium* H16 with 0.1 mM U). All the flasks were incubated aerobically under room temperature and shaken (140 rpm) for 7 days.

After incubation, 1 mL of each treatment was added to 1.5 mL tubes and centrifuged at 14.000 x g for 5 minutes. This step was performed three times to obtain the pellets for microscopy analyses. Samples were observed using High Resolution Scanning Electron Microscopy (HRSEM). The analysis was performed in a Field Emission Scanning Electron Microscopy (FESEM) equipped with SE, SE-inLens, BSE detectors (Zeiss SMT) coupled to Energy Dispersive X-ray (EDXS) microanalysis.

2.7. Fungal Se tolerance and interaction studies

2.7.1. Minimum inhibitory concentration (MIC) and tolerance index (TI) for Se

PDA medium was used for the fungal Se tolerance studies. The appropriate amounts of sodium selenite ($\text{Na}_2\text{O}_3\text{Se}$, 1M) stock solutions were added to the molten PDA to achieve the required concentrations (0 mM, 0.25 mM, 0.5 mM, 1 mM, 2 mM, 4 mM, 8 mM, 16 mM, 32 mM). The resulting medium was poured into Petri plates after gentle shaking. Non-amended PDA medium was used as a control. Petri plates were inoculated by placing 6 mm mycelial discs from selected fungal isolates onto the agar surface and were incubated at 28 ± 2 °C for 14 days. All assays were conducted in triplicate. The determination of the Minimum Inhibitory Concentration (MIC) involves determining the lowest metal concentration that trigger complete inhibition of visible fungal growth. In our study, the MIC was determined as the concentration at which there was no observed increase in the initial size of the mycelial disc (Ruiz-Fresneda et al. 2024).

The tolerance index (TI) was determined using images from the same plates used in MIC experiments for the analysis of fungal growth area over a 14-day period (Ruiz-Fresneda et al. 2024). This parameter is commonly calculated as the ratio between the growth area of fungi exposed to the metal and the growth area of fungi without metal exposure during the same period (Liaquat et al. 2020). The fungal colony area was measured using ImageJ (<http://imagej.nih.gov/ij>), based on equation ⁽¹⁾. The evaluation criteria for the tolerance index (TI) were applied, establishing that values between 0.00 and 0.20 represent very low metal tolerance since 0.21 and 0.40 values represent low tolerance, values between 0.41 and 0.60 indicate moderate metal tolerance, values between 0.61 and 0.80 suggest high metal tolerance, values between 0.80 and 0.99 signify very high metal tolerance, and values of 1.00 or higher reflect extremely high metal tolerance (Joo and Hussein, 2012; Oladipo et al. 2018; Ruiz-Fresneda et al. 2024).

⁽¹⁾TI = fungal growth area in the presence of metal (mm) ÷ fungal growth in the absence of metal (mm).

2.7.2. Assessing Se(IV) reduction by selected fungi: ICP-MS and HRTEM

The isolated strains *S. commune*, *C. cladosporioides*, *T. harzianum*, and *Acremonium* sp. were selected to assess their potential in Se remediation. A potato dextrose broth (PDB) (Biolife, Italy) was prepared, enriched with Se(IV) at three final concentrations of 0.25 mM, 0.5 mM, and 1 mM, using an initial stock solution of sodium selenite ($\text{Na}_2\text{O}_3\text{Se}$). Additionally, a biotic control was prepared for each studied fungus, consisting of non-Se-enriched and inoculated PDB medium, and an abiotic control for each tested Se concentration, composed of Se-enriched but non-inoculated PDB medium. Finally, 60 mL of Se-enriched PDB medium were dispensed, and the fungal strains were individually inoculated, exposing them to each of the previously mentioned concentrations. These samples were incubated at 28 ± 2 °C with agitation (140 rpm) for one month. Samples were named as: H10) *S. commune*; H2) *C. cladosporioides*; H7) *T. harzianum*; H8) *Acremonium* sp.; J) 0.25 mM sodium selenite; K) 0.50 mM sodium selenite; L) 1 mM sodium selenite; B) biotic control, and AB) abiotic control.

The rate of selenite [Se(IV)] reduction to elemental selenium [Se(0)] was determined after one month. Samples with the highest concentration of Se, 1 mM, were tested. To achieve this, the residual concentration of Se(IV) in the culture medium was measured using inductively coupled plasma mass spectrometry (ICP-MS) with a NexION 300D system (PerkinElmer, U.S.) after acidification with nitric acid (HNO_3).

For the microscopy analysis, mycelium from the PDB supplemented with a 1 mM Se concentration was collected in 1.5 ml tubes and centrifuged at $14,000 \times g$ for 5 minutes. The mycelium was processed for transmission electron microscopy (TEM) analysis following the method described in Merroun et al. 2005. Samples were observed using the Thermo Fisher Scientific TALOS F200X high-resolution transmission electron microscope and the high-angle annular dark-field (HAADF) detector coupled with an energy-dispersive X-ray spectroscopy (EDXS) Super X microanalysis system. Samples of *T. harzianum* and *Acremonium* sp. were selected for ICP-MS and TEM studies based on the fact that they showed the highest

tolerance to Se.

3. Results

3.1. Isolated fungal strains from mine water

3.1.1. Macroscopic and microscopic morphological identification

In this work, a total of 14 fungi strains were isolated from the mine waters of the Schlema-Alberoda and Pöhla mine. Initially, they were classified using morphological characteristics (macroscopic/microscopic including colony colour, pigmentation, as well as hyphal and spore morphology (Fig. 1 and 2). All isolates were identified at the genus level (Table 1) through macroscopic and microscopic observation, while we could not identify the fungal strain labelled as H10 due to a lack of spore formation. All morphologically identified fungal isolates and the unidentified isolate were selected for molecular identification.

In Figure 1 and 2, most representative morphological characteristics of the isolates are presented. For example, the strains from the genus *Penicillium* (e.g., H3, H4, H6, H12, and H16) was distinguished by their brush-shaped conidiophore or “penicillus” and the colonies presented a green coloration of different shades. *Aspergillus* (e.g., H5 and H17) showed a growth of a black and white cottony colony, and in others dark blue which changed to dark green over time due to abundant sporulation. In addition, the characteristic spherical structure or “aspergillate head” formed by the conidiophore was observed. In turn, the genus *Acremonium* (e.g., H8) was characterised by slow growth and the colonies showed a white-pinkish-orange colour. Hyphae are thin and simple. Conidiophores were globose and weakly branched. The spores had a pinhead shape. In the case of *Cladosporium* (e.g., H2, H9, and H15), olive-green colour and a velvety aerial mycelium were observed. The reverse side was black. The spores were elongated and cylindrical, resembling an acorn. On the other hand, *Trichoderma* (e.g., H7) showed septate solitary or grouped hyphae in the shape of a bottle with small and oval conidia were observed. Spores appeared as rod-shaped clubs and showed rapid growth. *Cadophora* (e.g., H1) was characterised by brown-black, septate mycelium and spores adopted an oval or ellipsoidal

shape. The isolated H10 had a white cottony mycelium and a hyphal lattice was observed at the microscope. No signs of sporulation were observed at any time.

Table 1. Identification of fungal isolates, based on morphological characterization, obtained from Schlema-Alberoda and Pöhla mine water.

Isolate	Code	Mine	Isolate	Code	Mine
<i>Cadophora</i> sp.	H1	Schlema-Alberoda	<i>Acremonium</i> sp.	H8	Pöhla
<i>Trichoderma</i> sp.	H7	Schlema-Alberoda	//	H10	Pöhla
<i>Penicillium</i> sp.	H4	Schlema-Alberoda	<i>Aspergillus</i> sp.	H5	Pöhla
<i>Penicillium</i> sp.	H6	Schlema-Alberoda	<i>Aspergillus</i> sp.	H17	Pöhla
<i>Cladosporium</i> sp.	H2	Schlema-Alberoda	<i>Penicillium</i> sp.	H3	Pöhla
<i>Cladosporium</i> sp.	H9	Schlema-Alberoda	<i>Penicillium</i> sp.	H12	Pöhla
<i>Cladosporium</i> sp.	H15	Schlema-Alberoda	<i>Penicillium</i> sp.	H16	Pöhla

//": no identified.

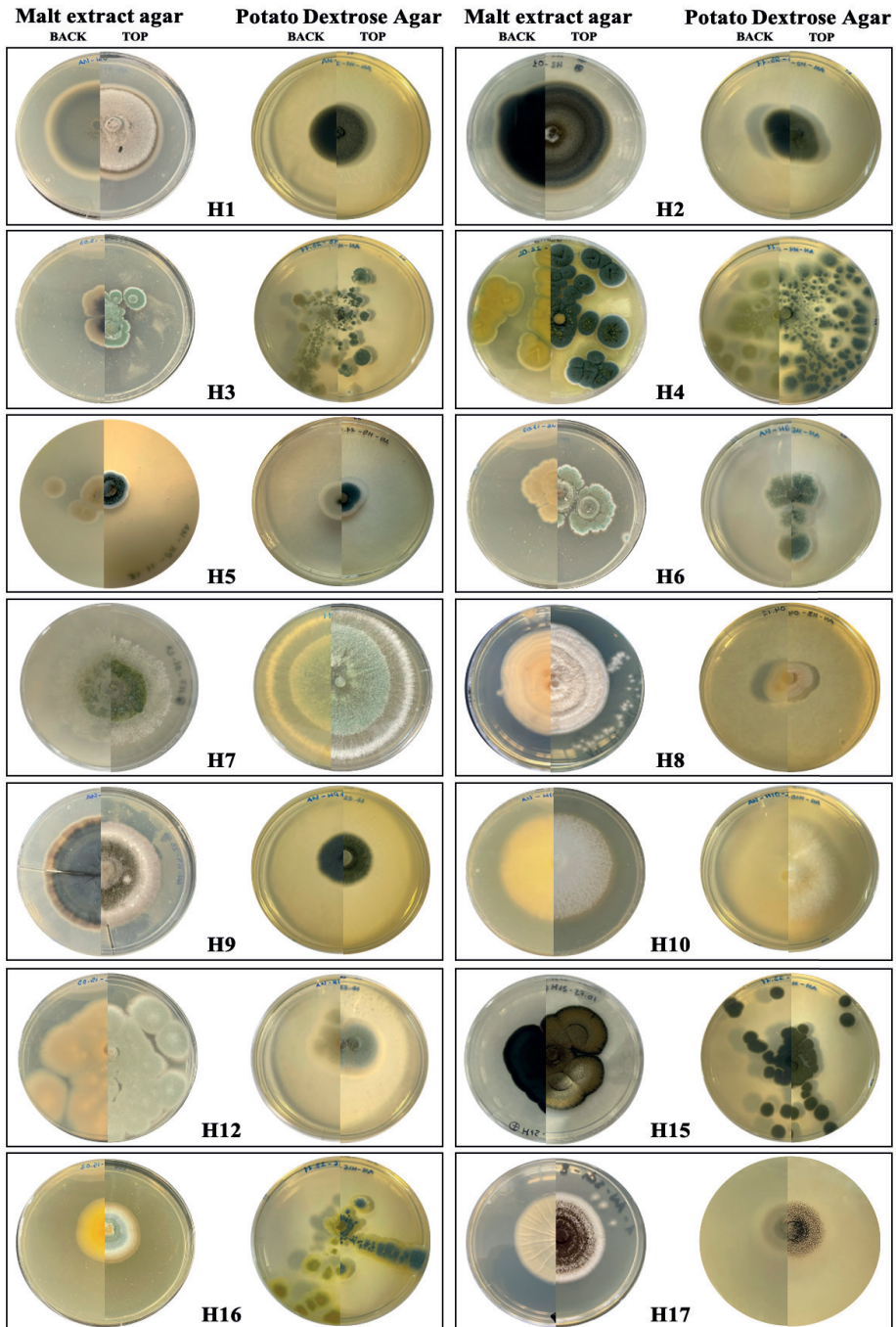


Fig. 1. Macroscopic characteristics of the isolated fungal strains from the mine waters of Schlemma-Alberoda and Pöhl. Back of the plate (substrate mycelium) in the left and top of the plate (aerial mycelium) in the right.

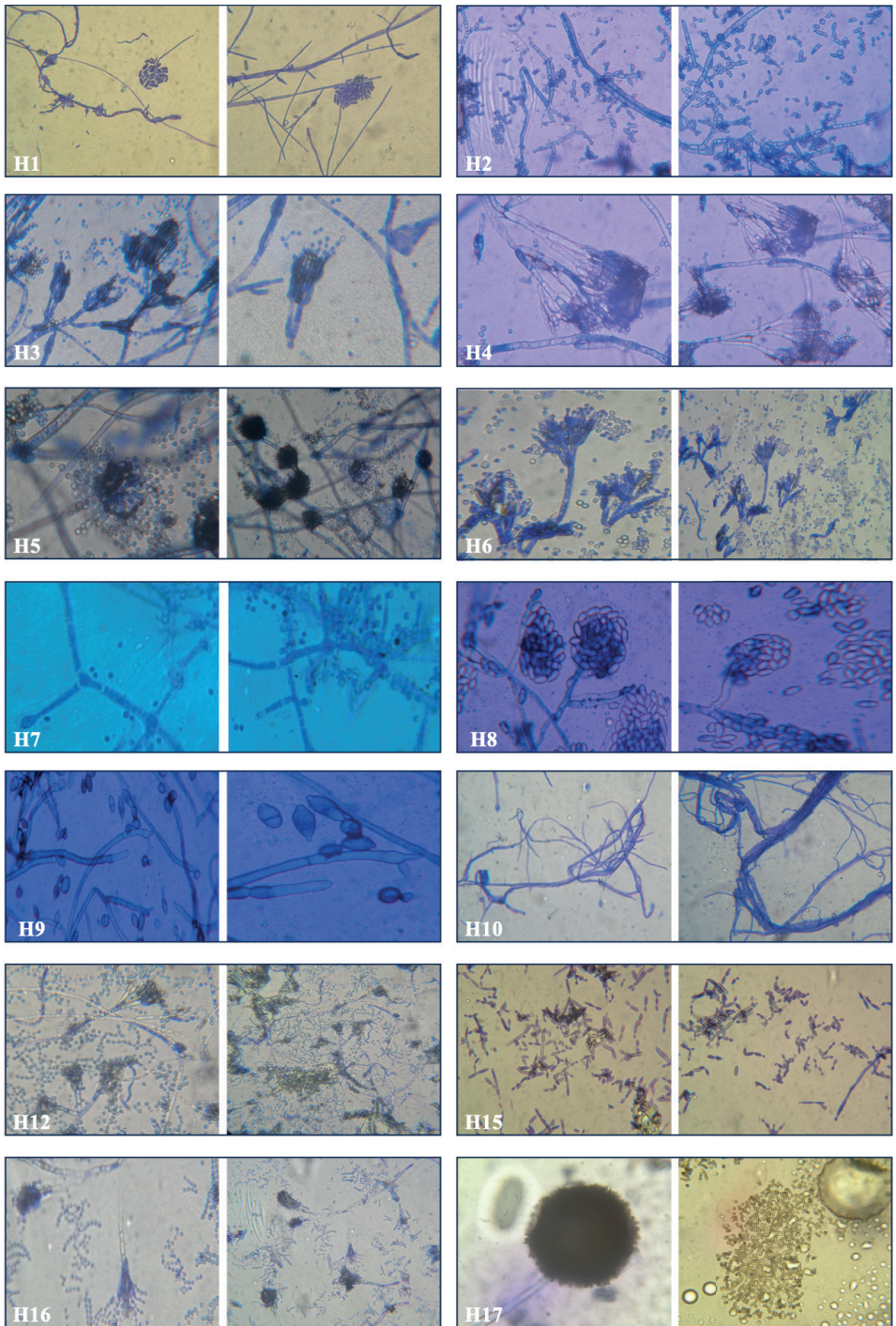


Fig. 2. Microscopic characteristics (magnification x60) of the isolated fungal strains from the mine waters of Schlema-Alberoda and Pöhla.

3.1.2. Molecular identification of the isolated fungi

Table 2 shows the fungi isolated from the mine waters samples of the Schlema-Alberoda and Pöhla mine. Most of the isolated strains showed a phylogenetic similarity ranging from 98% to 100% with related fungi recorded in the database. Molecular identification was achieved to species level for ten of the fourteen isolates and the rest to genus level. The results obtained are consistent with the taxonomic genus assignment based on the morphological characterization of the isolated colonies (see section 3.1.1). This molecular identification approach proves to be particularly effective, especially working with *Penicillium* sp. and *Cladosporium* sp., where the isolated species had similar macro- and microscopic characteristics.

The isolated species belong to four classes as the following: Eurotiomycetes (*Aspergillus* and *Penicillium*), Dothideomycetes (*Cladosporium*), Sordariomycetes (*Trichoderma*, *Acremonium*, *Cadophora*) and Agaricomycetes (*Schizophyllum*). *Schizophyllum commune* (H10) was successfully molecularly identified.

Penicillium was the most frequently isolated genus with 35.71%, followed by *Cladosporium* (21.43%) and *Aspergillus* (14.29%). According to the BLAST search, isolates H3, H4, H6, H12, and H16 were determined to be *Penicillium*. Among them, three exhibited a 100% similarity percentage, matching with the species *P. magnielliptisporum*, *P. mexicanum*, and *P. polonicum*. Three species of *Cladosporium* were identified, assigned to H2, H9, and H15. Isolates H2 and H15 were classified as *C. cladosporioides* (with a 98.36% similarity) and *C. limoniforme* (with a 99.60% similarity), respectively. There were two *Aspergillus* species, H5 and H17, which were assigned to the genera *A. sydowii* (with a 99.80% similarity) and *A. niger* (with a XX% similarity).

Trichoderma sp., *Acremonium* sp., *Cadophora* sp., and *Schizophyllum* sp. each represented 7.14%. *Trichoderma* sp., *Cadophora* sp., and *Schizophyllum* sp. were identified as *Trichoderma harzianum*, *Cadophora malorum*, and *Schizophyllum commune*, with similarity percentages of 98.66%, 99.46%, and 98.37%, respectively. In the case of *Acremonium* (H8), it could only be classified at the genus level as *Acremonium* sp.

(with a 99.21% similarity). *T. harzianum*, *C. malorum*, and *S. commune* were exclusively isolated from the water of the Schlema-Alberoda mine. Conversely, *Aspergillus*, *Acremonium* sp. and *S. commune* were found only in the water of the Pöhla mine. However, the genus *Penicillium* sp. was present in both mines.

Table 2. Fungal isolated strain identification, based on BLAST comparison in GenBank, obtained from Schlema-Alberoda (S) and Pöhla mine (P) water (ND, not determined)

Code	Isolate	Place	Query Cover	Per. Ident.	Acc. Len
H1	<i>Cadophora malorum</i>	S	100%	99.46%	811
H2	<i>Cladosporium cladosporioides</i>	S	100%	98.36%	554
H3	<i>Penicillium magnielliptisporum</i>	P	99%	100%	612
H4	<i>Penicillium</i> sp.	S	100%	100%	576
H5	<i>Aspergillus sydowii</i>	P	99%	99.80%	538
H6	<i>Penicillium mexicanum</i>	S	99%	100%	588
H7	<i>Trichoderma harzianum</i>	S	100%	98.66%	681
H8	<i>Acremonium</i> sp.	P	97%	99.21%	508
H9	<i>Cladosporium</i> sp.	S	98%	100%	590
H10	<i>Schizophyllum commune</i>	P	100	98.37%	734
H12	<i>Penicillium</i> sp.	P	98%	99.80%	605
H15	<i>Cladosporium limoniforme</i>	S	100%	99.60%	844
H16	<i>Penicillium polonicum</i>	P	100%	100%	612
H17	<i>Aspergillus niger</i>	P	100%	99.46%	593

3.2. Enzymatic activity characterization

The isolated fungal strains were assessed for different enzymatic activities including cellulase, amylase, laccase and LiP, using different culture medium. These analyses are needed for the screening of fungi involved in the degradation of complex organic carbon substrates, such as cellulose and starch, for radionuclide and heavy metals bioremediation purposes.

The results shown in Table 2 indicate that most of the isolates (92.86%), demonstrate amylase activity. In addition, cellulase (71.43%) and laccase

(57.14%) activities dominated compared to LiP activity (2.85%). *C. malorum*, *S. commune* and *A. niger* showed positive results for all four enzymatic activities tested on solid medium. Moreover, *Acremonium* sp. also showed LiP activity. Only the H12 isolate (*Penicillium* sp.) exhibited growth, but no enzymatic activity was detected.

The extracellular enzymatic activity profile of fungal strains using the API ZYM test is reported in Table 3. Among the isolated strains, *Acremonium* sp., *P. polonium*, and *A. niger* were characterized by the highest number of active hydrolytic enzymes, followed by *C. malorum* and *C. cladosporioides*. All isolates exhibited acid phosphatase, alkaline phosphatase, and naphthol-AS-BI-phosphohydrolase activity, except for *P. mexicanum* and *Penicillium* sp. H4, which tested negative for naphthol-AS-BI-phosphohydrolase and alkaline phosphatase, respectively. Cystine arylamidase activity was exclusively detected in the *C. malorum* isolate, while *C. cladosporioides* stood out as the only isolate exhibiting α -mannosidase and α -fucosidase activities. *S. commune* was the only one with α -chymotrypsin activity.

Table 3. Fungal extracellular enzyme production.

Code	Isolate	Enzyme activity			
		Cellulase	Amylase	Laccase	Lignin peroxidase
H1	<i>Cadophora malorum</i>	+	+	+	+
H2	<i>Cladosporium cladosporioides</i>	+	+	+	-
H3	<i>Penicillium magnielliptisporum</i>	+	+	+	-
H4	<i>Penicillium</i> sp.	+	+	-	-
H5	<i>Aspergillus sydowii</i>	-	+	-	-
H6	<i>Penicillium mexicanum</i>	+	+	-	-
H7	<i>Trichoderma harzianum</i>	+	+	-	-
H8	<i>Acremonium</i> sp.	-	+	+	+
H9	<i>Cladosporium</i> sp.	+	+	+	-
H10	<i>Schizophyllum commune</i>	+	+	+	+
H12	<i>Penicillium</i> sp.	-	-	-	-
H15	<i>Cladosporium limoniforme</i>	+	+	+	-
H16	<i>Penicillium polonicum</i>	-	+	-	-
H17	<i>Aspergillus niger</i>	+	+	+	+

"+": evidence of enzymatic activity, "-": no evidence of enzymatic activity.

Table 4. Activity of fungal extracellular enzyme isolated from Schlema-Alberoda (S) and Pöhla (P) mine water.

Isolate	Enzyme activity ^{*,**}																			
	1	2	3	4	5	6	7	8	9	10	11	12	13	14	15	16	17	18	19	20
Control ^{***}	0	0	0	0	0	0	0	0	0	0	0	0	0	0	0	0	0	0	0	0
H1 <i>C. malorum</i>	0	1	3	1	0	0	1	0	0	1	3	0	0	0	0	0	1	2	0	0
H2 <i>C. cladosporioides</i>	0	1	1	1	0	0	0	0	0	3	3	0	0	0	0	0	0	3	1	1
H3 <i>P. magnelliipsporium</i>	0	2	0	1	0	0	0	0	0	2	3	0	0	0	0	0	2	5	0	0
H4 <i>Penicillium</i> sp.	0	0	1	1	0	1	0	0	0	2	3	0	0	0	1	3	2	0	0	0
H5 <i>A. sydowii</i>	0	2	1	0	0	0	0	0	0	5	4	2	0	0	0	0	4	1	0	0
H6 <i>P. mexicanum</i>	0	1	1	1	0	0	0	0	0	2	0	1	0	0	0	0	1	0	0	0
H7 <i>T. harzianum</i>	0	1	1	1	0	0	0	0	0	5	3	2	0	0	0	0	3	0	0	0
H8 <i>Acromonium</i> sp.	0	1	1	0	0	1	0	0	1	0	5	5	0	0	0	1	5	1	1	0
H9 <i>Cladosporium</i> sp.	0	1	3	2	0	1	0	0	0	1	2	0	0	0	0	0	0	0	0	0
H10 <i>S. commune</i>	0	1	1	2	0	1	2	0	0	1	5	5	0	2	0	0	4	2	0	0
H12 <i>Penicillium</i> sp.	0	1	1	1	0	0	0	0	0	3	2	0	0	0	0	0	1	0	0	0
H15 <i>C. limoniforme</i>	0	1	2	1	0	1	0	0	0	4	3	0	0	0	0	4	2	0	0	0
H16 <i>P. polonicum</i>	0	1	1	1	1	0	0	0	0	5	5	0	0	0	1	2	1	1	1	0
H17 <i>A. niger</i>	0	3	1	1	0	2	0	0	0	5	5	4	0	0	3	1	5	0	0	0

*Enzymes: 1) control 2) alkaline phosphatase, 3) esterase (C4), 4) esterase lipase (C8), 5) lipase (C14), 6) leucine arylamidase, 7) valine arylamidase, 8) cystine arylamidase, 9) trypsin, 10) α -chymotrypsin, 11) acid phosphatase, 12) naphthol-as-bi-phosphohydrolase, 13) α -galactosidase, 14) β -galactosidase, 15) β -glucuronidase, 16) α -glucosidase, 17) β -glucosidase, 18) N-acetyl- β -glucosaminidase, 19) α -mannosidase, 20) α -fucosidase. **0 – no activity, 1–5 – activity increases with colour intensity (1 low activity, 5 high activity). ***control: malt extract broth.

3.3. Fungal insights into the interaction with U

HRSEM was employed to investigate the cellular localization of U complexes and the interaction mechanisms of U with the fungi *C. malorum* (H1), *A. sydowii* (H5), and *P. polonicum* (H16). This approach is a useful tool for assessing the U bioremediation potential of the selected isolated strains based on the U phosphate biomineralization. The interaction of the three strains (H1, H5, and H16) was examined under two different U concentrations, 0.05 mM and 0.1 mM, with untreated Schlema-Alberoda mine water as a control.

Figure 5S shows the set of experiments and the changes observed during 7 days of incubation. No changes were recorded in the abiotic (AC, AC1-U1, and AC-U2) and biotic (H1, H5, and H16) controls. All fungi exhibited growth in the presence of the radionuclide. The most notable changes were observed in the interaction of U with *C. malorum* (H1). Darkening of the *C. malorum* (H1) mycelium and extracellular medium was evident. Additionally, a slight darkening in the mycelium of *P. polonicum* (H16) was observed. In contrast, no changes were detected in *A. sydowii* (H5).

HRSEM analysis were conducted for all U-treated samples, but in Figure 5, only the data where the radionuclide was detected is presented. In the 0.05 mM U treatment, HRSEM images and EDXS spectra revealed the presence of electron-dense precipitates, possibly U-phosphates, exclusively in the presence of *C. malorum* (Fig. 5 (A and C)). In contrast, when analysing the sample with 0.1 mM U, electron-dense accumulations were observed in all micrographs (Fig. 5 (B, E, and F)), and the corresponding EDXS spectra identified both U and P. In addition to U and P, the EDXS spectra confirmed the presence of Ca, with the highest intensity peaks identified in the EDXS spectrum of *C. malorum* (Fig. 5 (D)). Ultimately, remarkable peaks of calcium (Ca) were identified in all samples, and in the *P. polonicum* H16 experiment, structures were identified whose primary composition consisted of Ca and carbon C, as showed in Figure 6S.

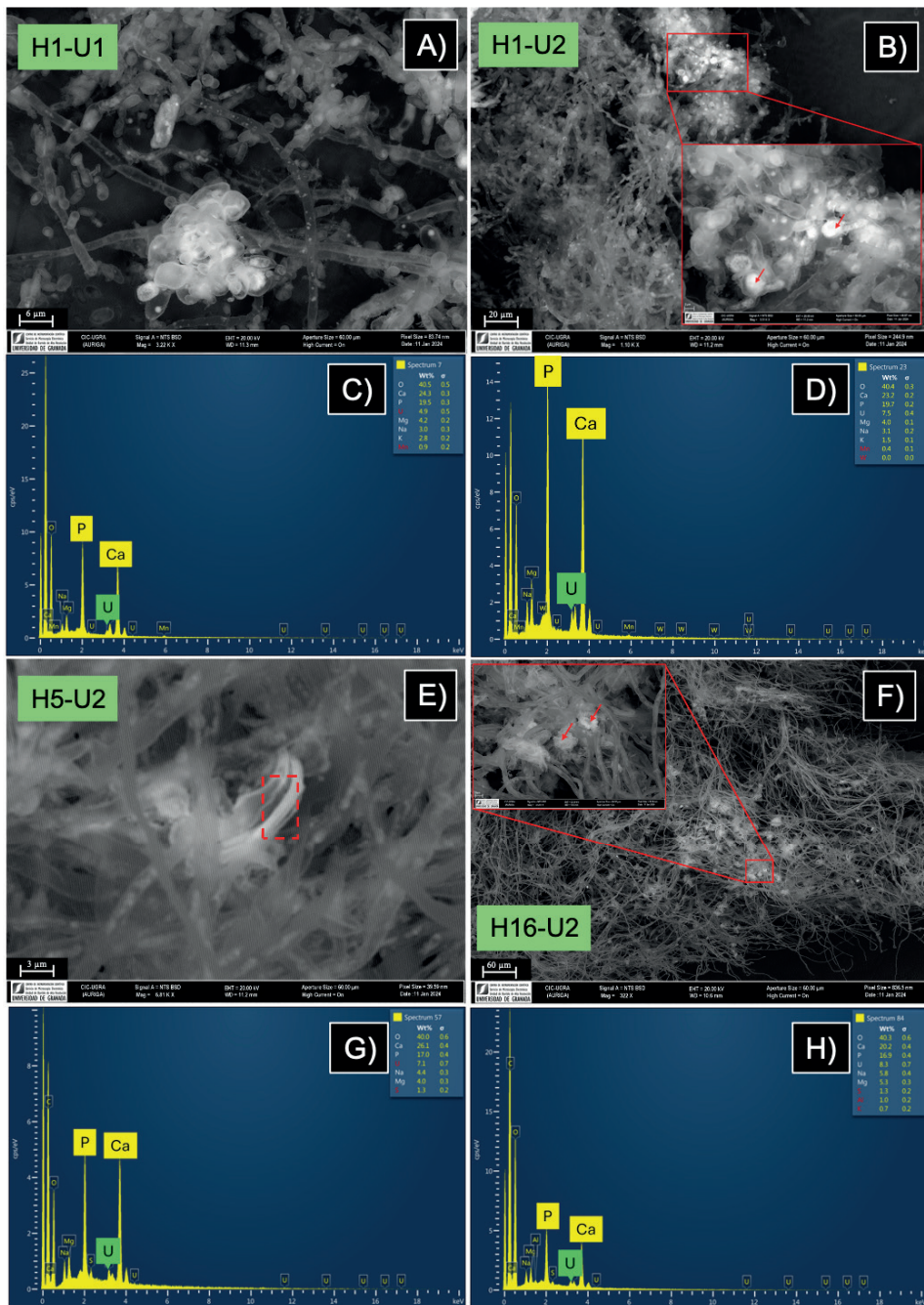


Fig 5. HRSEM image showing electron-dense U accumulations in fungal mycelium after 7 days of U incubation (0.05 mM) in sample U1(A) and 0.1 mM in sample U2(B, E and F). EDXS spectra confirm the composition of U and P in the electron-dense accumulations (C, D, G and F).

3.4. Fungi and Se interaction

3.4.1. MIC and TI results

To determine the low metalloids concentrations that inhibit the visible growth of isolated fungal species, MIC assays were conducted. MIC values suggested the level of tolerance against individual metals of the isolates and allowed for the evaluation of the potential of the isolated strain for bioremediation of Se. The Se(IV) MIC for the fungal strains studied is shown in Table 1S. 42.68% of the isolates exhibited a MIC higher than 32 mM of Se, while 21.43% presented a MIC of 8 mM of Se. Additionally, 14.26% showed a MIC of 4 mM of Se, and 7.14% of the isolates showed a MIC of 16 mM, 2 mM, and 1 mM. Isolates *C. malorum* (H1), *Penicillium* sp. (H4), *A. sydowii* (H5), *T. harzianum* (H7), *Acremonium* sp. (H8), and *Penicillium* sp. (H12) were able to tolerate the highest concentrations of Se, with respective MIC values of >32 mM. Others such as *C. cladosporioides* (H2), *P. mexicanum* (H6), *S. commune* (H10), and *A. niger* (H17) could tolerate high concentrations of Se, with respective MIC values of >16, 8, 8, and 8 mM.

In various fungal isolates, a colour alteration was observed in response to the presence of Se in the medium. For example, *A. sydowii* (H5), *S. commune* (H10), and *Penicillium* sp. (H12) in PDA enriched with Se(IV), the fungal mycelium changed to a red-orange colour. This colour change was probably due Se(IV) reduction to Se(0).

The TI, calculated as the ratio of the growth area of the fungi exposed to the metal to their respective control, was determined based on the concentrations obtained through MIC assays. The results indicated that *Acremonium* sp. (H8) was the strain with the highest TI values (0.66, 0.45, 0.42, 0.26, 0.26, 0.25, 0.25, and 0.26, respectively for 0.25, 0.5, 1, 2, 4, 8, 16, and 32 mM of Se(IV)). Tolerance index to Se(IV) was exhibited in the order of *Acremonium* sp. (H8) > *C. malorum* (H1) > *Penicillium* sp. (H12) > *T. harzianum* (H7) > *A. sydowii* (H5) > *Penicillium* sp. (H4) > *C. cladosporioides* (H2) > *C. limoniforme* (H15) > *P. mexicanum* (H6) > *A. niger* (H17) > *S. commune* (H10) > *Cladosporium* sp. (H9) > *P.*

magnielliptisporum (H3) > *P. polonicum* (H16). TI values obtained agree with their MIC results.

3.4.2. Fungi and Se interaction experiment: ICP-MS and HRTEM analyses

The reduction of selenite [Se(IV)] to elemental selenium [Se(0)] was evidenced by the appearance of an orange-red or red colour in the mycelium and/or in the culture medium (Ruiz-Fresneda et al. 2018; 2024). In Figure 2S, changes in the colour of the mycelium can be observed, with intense red colour in *T. harzianum* (Figure 2S, H7) and orange-red colour in the case of *Acremonium* sp. (Figure 2S, H8). Additionally, in *Acremonium* sp. an extracellular reduction can be observed due to a change in the colour of the culture medium. In the case of *S. commune*, (Figure 3S, H10) a low reduction of Se in the mycelium can be observed. In contrast, hardly any growth or evidence of Se reduction was observed in *C. cladosporioides* (Figure 3S, H9). No changes were observed in abiotic controls (data not shown).

ICP-MS analysis showed that biomass of *T. harzianum* and *Acremonium* sp. contacted with 1 mM Se(IV) for 1 month exhibited high Se reduction of about 69.20% and 95.90%, respectively. Visual evaluation of the colour changes, characterised by a change to red and/or orange-red in the samples, indicated a significant reduction rate of Se(IV) to Se(0) in the mycelium of *T. harzianum* (69.20%) and, similarly, both in the mycelium and extracellularly in the case of *Acremonium* sp. (95.90%). While no Se reduction was observed for *C. cladosporioides*, the mycelium of *S. commune* exhibited low Se reduction rate.

High-resolution transmission electron microscopy was used to determine the cellular localization and structural characteristics of the reduced Se(IV) products. Samples of *T. harzianum* and *Acremonium* sp. amended with 1 mM of Se were analysed. After one month of incubation (Fig. 3 and 4), several empty spaces were observed in the cell micrographs of the samples due to sample preparation (Fig. 4S). However, it was possible to detect some SeNPs in both the *T. harzianum* and *Acremonium* sp. samples. Using the HAADF-STEM system, ultra-thin sections were observed where NPs

were identified as electron-dense particles in the extracellular space (Fig. 3 (A) and 4 (A)). Their presence inside the cells is not ruled out based on the empty spaces that have been located.

Element distribution maps (Fig. 3 (B-D) and 4 (B-D)) and EDXS spectra (Fig. 3 (E) and 4(E)) also indicated the presence of NPs constituted by Se (SeNPs) in addition to sulphur (S).

The combination of the HAADF-STEM, SAED and HRTEM confirmed the crystalline structure of the SeNPs (Fig. 3 (F-M) and 4 (F-M)). Patterns obtained from SAED analysis revealed the crystalline nature of the nanostructures (Fig. 3 (K and M) and 4 (K and M)). The HRTEM image of the nanoparticles formed in both fungi shows two different lattice spacings of 0.37 and 0.29 nm (Fig. 3 (J and L) and 4 (J and L)) according to the American Mineralogist Crystal Structure Database (<http://rruff.geo.arizona.edu/AMS/amcsd.phpamcsd.php>). Specifically, 0.29 nm is close to the 0.3 nm d-spacing, which may correspond to planes (1 0 1) of trigonal Se (t-Se) and (2 2 1) of monoclinical (m-Se), among other planes. The other d-spacings obtained (0.37 nm) match that of 0.37 nm and may also correspond to the plane (1 0 0) of t-Se and different planes of m-Se.

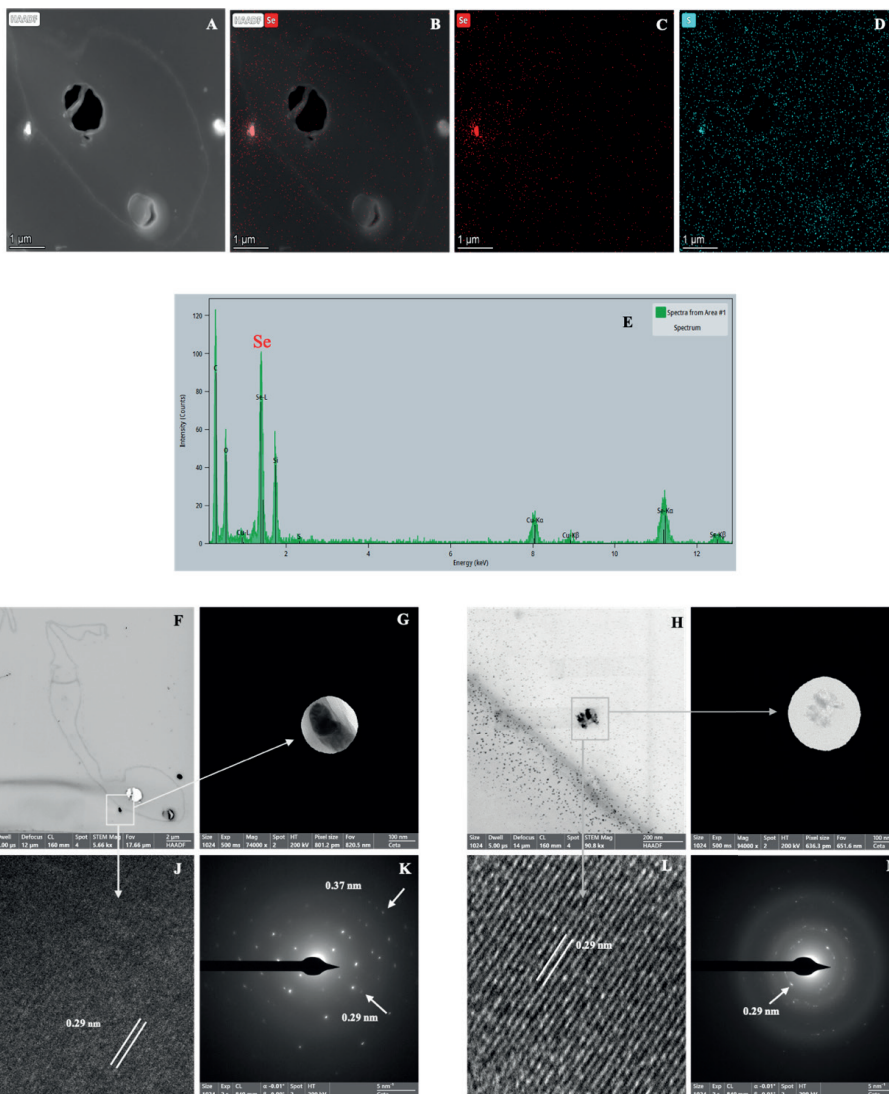


Fig 3. Thin-section micrographs showing SeNPs produced by *T. harzianum* after 1 month of incubation. Element distribution maps and EDXS spectrum displaying their elemental composition Se and S (B-E). HRTEM images derived from a single nanostructure (J and L). SAED pattern (K and M).

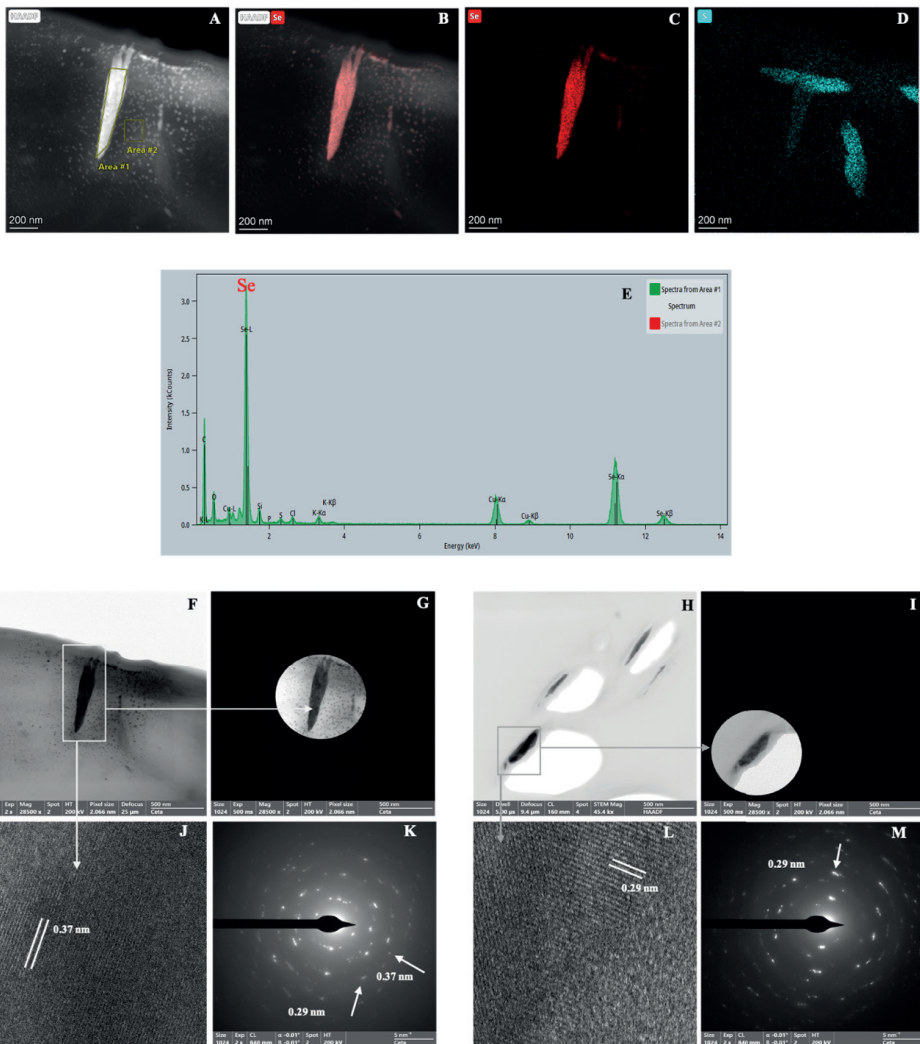


Fig 4. Thin-section micrographs showing SeNPs produced by *Acromonium* sp. after 1 month of incubation. Element distribution maps and EDXS spectrum displaying their elemental composition Se and S (B-E). HRTEM images derived from a single nanostructure (J and L). SAED pattern (K and M).

4. Discussion

It is well known that fungi exhibit higher adaptation than bacteria to environments contaminated with heavy metals and/or radionuclides (e.g., U) (Mumtaz et al. 2013). The diverse metabolic and physiological capabilities of fungi have a significant impact on contaminants, limiting their bioavailability and thereby reducing toxicity. Therefore, environments contaminated with U and other heavy metals present promising habitats for the identification and isolation of species with a great potential for effective bioremediation of U and/or other heavy metals, considering the adaptation mechanisms developed under specific conditions and their viability in natural environments. However, research attention has primarily focused on the role of bacteria, especially those capable of sulphate (SBR) or iron (FeRB) reduction, coupled with U(VI) reduction, to remediate U-contaminated environments under anoxic conditions over the past decades (Lovley et al. 1991; Phillips et al. 1995; Newsome et al. 2014; Hilpmann et al. 2023).

4.1. Isolated fungal community: taxonomic characterization

In this study, culture-dependent techniques were used to isolate a total of fourteen fungal strains, which were identified through a combination of ITS sequencing and morphological characterization-based techniques. Fourteen colonies were identified at the genus level, and of these, ten could be classified at the species level. The isolated fungi belong to the genera *Cadophora*, *Acremonium*, *Aspergillus*, *Penicillium*, *Cladosporium*, *Trichoderma*, and *Schizophyllum*. These taxonomic data are consistent with those obtained previously through next-generation sequencing (NGS) of the internal transcribed spacer (ITS) described in the chapter 2 of the thesis (Newman-Portela et al. 2024).

Our previous study indicated that the water from the Schlema-Alberoda mine was strongly dominated by the presence of *Cadophora* (Newman-Portela et al. 2024). Successfully, we isolated a fungal strain of *C. malorum* from the water of this mine. *C. malorum* has previously shown tolerance to high levels of Cu, as well as moderate levels of Hg and Zn, as reported by Văcar et al. (2021). It is noteworthy that Staudenrausch and co-authors (2005) had previously reported the presence of *Phialophora finlandia*

(now *C. Finlandia*; Harrington and McNew 2003) as member of the fungal community in a U-mining heap in Ronneburg (Thuringia, Germany). Subsequently, the genus *Penicillium* was the most abundant, with a total of five different fungal strains isolated (H3, H4, H6, H12, and H16). The widely distribution of the *Penicillium* genus is attributed to its metabolic versatility, allowing it to colonize different substrates. It is commonly observed in U-contaminated environments such as water and sediments, as well as in bentonite microcosms supplemented with U (Coelho et al. 2020b; Schaefer et al. 2021; Povedano-Priego et al. 2024). Previous research has highlighted the effectiveness of *Penicillium* species in interacting with U and other heavy metals. For example, the fungal isolate *P. piscarium* from the Osamu Utsumi U mine (Minas Gerais, Brazil) demonstrated the ability to remove over 90% of U through biosorption. Similarly, Schaefer and co-authors (2021) reported a U removal up to 80% through U biomineralization in the form of U phosphate after 48 hours, by *P. simplicissimum* KS1, an isolate from the former U mine of Königstein (Saxony, Germany). Regarding heavy metals, the fungal strain *P. polonicum*, also isolated in our study, demonstrated the ability to immobilize Pb(II) in the cell wall, precipitate it as pyromorphite, within the cell (Xu et al. 2020). Interestingly, isolates of *Schizophyllum*, *Cladosporium*, and *Trichoderma* were previously identified in the water of the Schlema-Alberoda mine (Newman-Portela et al. 2024). *S. commune* showed a high capacity for U sorption and accumulation both intracellularly and at the cell wall (Günther et al. 2014). *Cladosporium* sp. strain F1 was able to remove between 77.5% and 99.6% of U, depending on pH, through U-phosphate adsorption (Lee et al. 2021). Similarly, the same strain showed a biosorption capacity of 98.9% of Pb-P at pH 7 (Lee et al. 2023). In our work, we isolated three different strains of *Cladosporium*, including *C. cladosporioides* which has been reported to tolerate various metals (Cu, Co, Zn, Fe, Mn, Au, Ni, Ag, and Zn) and heavy metals (Cd, Cr, and Pb) (Pethkar et al. 2021; Dusengemungu et al. 2022). On the other hand, the genus *Trichoderma* is widely used as bioinoculants in agriculture, but its potential in heavy metal and radionuclide bioremediation has been extensively explored in recent years. Zhang and

co-authors (2020) reported the tolerance of *T. brevicompactum* to Cu, Cr, Cd, and Zn ranging from 150 to 200 mg/l and Pb up to 1600 mg/l. Likewise, *T. harzianum*, a strain also isolated in this study, showed high tolerance to metals Cd, Pb, and Cu, according to Mohammadian and co-authors (2017), and a maximum U biosorption capacity of 612 mg/g according to the data reported by Akhtar and co-authors (2007).

As for the water from the Pöhla mine, the genus *Acremonium* and some species of the genus *Aspergillus* (H5 and H17) were isolated, representing 29.66% and 3.11% of the fungal community, respectively, according to our previous publication. *Acremonium* sp., exhibited high resistance to metals (e.g., Zn, Fe, Cu, Al, and Pb), and U sorption ability (Ma and et al. 2014). *Acremonium* sp. sorbs between 44.4% and 81.4% of U, and after long years of storage, retains its biosorption capacity, although the activity is slightly lower, ranging from 23.5% to 65.8% (Bekmukhamedova and Mamiyev 2023). In addition, dead dry biomass of *Acremonium* sp. reported maximum sorption capacities of 162 mg/g (Gargarello et al. 2008). Regarding *Aspergillus*, Bekmukhamedova and Mamiyev (2023) also reported the U biosorption capacity of *A. niger*, ranging from 33.9% to 49.6%, and after a long time, between 24.2% and 42.8%. Additionally, the pre-treated dry biomass of *A. niger* was capable of removing 98.43% of U through the sorption of the radionuclide (Sana et al. 2015).

4.2. Characterization of extracellular enzyme activity by fungi isolated from U-contaminated mine water

The characterization of extracellular enzyme production by fungi is crucial for the design of mycoremediation strategy. In this study, various enzymatic activities, such as cellulase, amylase, laccase, and LiP, were analysed using different culture media. Additionally, a total of 18 enzymatic activities were identified through the API ZYM test, with alkaline phosphatase, acid phosphatase and naphthol-AS-BI-phosphohydrolase being potentially relevant for U bioremediation.

Enzymatic activities like cellulase, amylase, laccase, and LiP have been extensively explored within different industrial sectors, including pharmaceuticals, food, beverages, detergents, fuels, pulp and paper

(Dhevagi et al. 2021). Fungi producing these enzymes exhibit higher potential for bioremediation. This is attributed to their crucial role as primary degraders of complex organic carbon sources in contaminated and oligotrophic environments (Andlar et al. 2018). As a result of their activity, monosaccharides are generated, which are not only further metabolized by these fungi but are also used as energy and C source for the growth of other microorganisms, such as bacteria.

The walls of the former Schlema-Alberoda and Pöhla mines are covered with wood, mainly coniferous. During the mining period, microbial degradation of wood was observed, and the subsequent mine flooding accelerated the decomposition of lignocellulosic biomass mediated by fungi, releasing molecules such as sugars, saccharic acids, vanillin and organic acids (Baraniak et al. 2002; Newman-Portela et al. 2024). The bacterial community could use these carbon sources for growth or even as electron donors, promoting the reduction of soluble U (e.g., SRB and FeRB).

Enzymatic characterization of isolated fungi showed that the majority of strains had activity for the degradation of organic carbon source, such as starch (92.86% of isolates). The fungi's ability to degrade raw materials containing lignocellulose is attributed to a highly efficient enzymatic system, including laccase, LiP, and cellulase. The laccase and LiP activities are responsible for modifying and degrading lignin protecting cellulose (Andlar et al. 2018). Subsequently, the liberated cellulose is hydrolysed by cellulases, releasing valuable end products (e.g., glucose) (Krause et al. 2020). Some fungi can simultaneously hydrolyse lignin and cellulose (Sanchez 2009). The decomposition of lignocellulosic biomass is primarily attributed to basidiomycetes (e.g., *Schizophyllum* sp.), although ascomycetes (e.g., *Aspergillus* sp. or *Trichoderma* sp.) are also capable (Sanchez 2009, Krause et al. 2020). In our study, the 71.43% of the isolates displayed cellulase activity. However, the fungi showing laccase and LiP activities are not so frequently represented with 57.14% and 2.85%, respectively.

Our results suggest potential candidates such as *C. malorum*, *S. commune*, and *A. niger*, as they tested positive for each of the aforementioned

enzymatic activities. Therefore, compared to the rest of the isolates, these microorganisms may exhibit a higher capacity to thrive in oligotrophic environments contaminated with U. Additionally, as previously reported, they have the capability to interact with the radionuclide, reducing its toxicity. In the context of U bioremediation, a crucial role in U biomineralization lies in the enzymatic activity of phosphatase. Microbial phosphatase leads to the degradation of organic phosphates and subsequent release of inorganic phosphates for U biomineralization as U-phosphates (Martínez-Rodríguez et al. 2023). Regarding phosphatases, all isolates showed, to a greater or lesser extent, alkaline/acid phosphatase activity, and, except for *P. mexicanum* and *Penicillium* sp. H4, naphthol-AS-BI-phosphohydrolase and alkaline phosphatase activity, respectively. Overall, fungal isolates exhibited higher activity of acid phosphatase and naphthol-AS-BI-phosphohydrolase than that of alkaline phosphatase. This finding could confirm the potential of these isolates to be used as promoters of U-phosphate biomineralization mediated by fungal phosphatase enzymatic activity.

4.3. U and Se fungal interactions

Mycoremediation is emerging as an alternative option to conventional approaches for the removal heavy metals, and radionuclides, increasing interest due to its straightforward implementation. In this study, we investigated the interaction of various fungal isolates from two former U mines with U and Se.

An effective strategy for the mycoremediation of this radionuclide involves the biomineralization of U(VI) phosphates. In our study, we investigated the interaction of *C. malorum*, *A. sydowii*, and *P. polonicum* with U. To date, and to the best of our knowledge, this is the first report documenting the interaction of these isolate fungi with U. HRSEM characterization of fungal biomass amended with uranyl acetate to achieve a final U concentration of 0.05 mM and 0.1 mM, respectively, show electron-dense accumulations whose composition, confirmed by EDXS analysis, indicates the presence of U and P, possibly forming U-phosphate association. To the best of our understanding, the previously identified phosphatase activity

(see section 3.2) may lead to the degradation of organic phosphates and subsequent release of inorganic phosphates, forming U-phosphates. In our study, precipitates of U-phosphates were associated with fungal biomass and their cellular localization was not determined due to the nature of the microscopic (HRSEM) technique used. U-phosphates deposited on the cell wall could indicate a passive biosorption process where functional groups bind to U ions (Povedano-Priego et al. 2024). Intracellularly located precipitates could form due to the active uptake of U(VI) and its precipitation with intracellular orthophosphates (Yang et al. 2012). Thus, we have demonstrated that fungal isolates *C. malorum*, *A. sydowii*, and *P. polonicum* can precipitate U-phosphate biominerals when amended with an organic source of P. The results shed more light on the potential roles of fungi in the biogeochemistry of U and P, as well as the application of these mechanisms for the recovery or bioremediation of the radionuclide.

Finally, HRSEM results and EDXS spectra showed high peaks of calcium (Ca) in all samples. Ca biomineralization has been previously reported in fungi, typically as calcium oxalates (Gadd 2007). HRSEM-EDXS analyses of U interaction experiments with *P. polonicum* reported structures whose composition was mainly defined by Ca and C. According to Newman-Portela et al. (2024), the mine water of Schlemma-Alberoda has a high concentration of Ca and carbonates, so we cannot rule out that fungi induce the mineralization of calcium carbonates (e.g., calcite) during the experiment. Environments rich in Ca and carbonates pose a stress factor for fungi due to subsequent osmotic pressure and Ca cytotoxicity. The formation of Ca-oxalates has been suggested as a means to immobilize excess Ca. While this process is well-documented for bacteria, it remains a hypothesis concerning fungi (Bindschedler et al. 2016). On the other hand, calcium carbonates are an important and relatively soluble mineral phase that can affect the transport of U, although our results did not report any such interaction with U.

Despite Se being a metalloid, its high concentration can be toxic, affecting membrane integrity, spore germination, and the activity of antioxidant enzymes (Li et al. 2023). The toxicity of Se to fungi is clearly showed in

our MIC and TI assays. Our results reported *Acremonium* sp. as one of the isolates with the highest MIC to Se (>32 mM). Conversely, another strain of *Acremonium* sp., isolated by Ruiz-Fresneda and co-authors (2024), exhibited a much lower MIC (0.5 mM). This implies that our isolate reported a MIC nearly two orders of magnitude higher. Furthermore, different strains within the same genus (e.g., *Penicillium*, *Aspergillus*, and *Cladosporium*) were identified, all showing varying values of tolerance to Se. Thus, the MIC value suggests that the level of tolerance against Se (and probable against any other metal) depends on the type of fungal strain. For instance, five fungal strains of an equivalent genus (*Penicillium*) displayed a marked difference in Se tolerance level, which can be attributed to different strategies or mechanisms of tolerance exhibited by the diverse fungi. In this work, three out of the four strains overcome the toxicity of Se(IV) through reduction, evidenced by the formation of a characteristic red precipitate. Our results indicate that isolates *S. commune*, *T. harzianum*, and *Acremonium* sp. are able to reduce the soluble, mobile and toxic Se specie (Se(IV) to Se(0), with *T. harzianum* and *Acremonium* sp. reporting the best results. While *C. cladosporioides* showed no evidence of Se reduction in our study. However, Singh et al. 2015 reported Se reduction by *Cladosporium* sp.

This study also assessed the potential of *T. harzianum* and *Acremonium* sp. strains to produce Se(0) nanostructures as a result of Se reduction. In nature, there are amorphous (*a* - Se) and crystalline allotropes of elemental Se (including monoclinic (*m* - Se) and trigonal (*t* - Se) Se). Different microorganisms can transform amorphous varieties into crystalline ones, which are more stable, making them of great interest for the bioremediation of Se-contaminated environments (Ruiz-Fresneda et al. 2024, Liang et al. 2019).

The allotropic structure of SeNPs was determined using SAED and HRTEM, revealing crystalline Se(0) with d-spacings of 0.29 and 0.37 nm in the SeNPs samples from *Acremonium* sp. and *T. harzianum*. Rosenfeld et al. (2017) reported that most SeNPs were amorphous, except for those synthesized by the *Acremonium strictum*, which were crystalline with spacings of 0.37

nm, consistent with our findings. On the other hand, *Trichoderma* species have the potential to be used for synthesizing nanoparticles on a large scale through the use of an environmentally friendly production process (Tomah et al. 2023; Liang et al. 2019). Nandini et al. (2017) successfully reported the biogenic synthesis of SeNPs by six species belonging to the *Trichoderma* genus, including *T. harzianum*.

Our measured d-spacings could correspond to the (1 0 0) and (1 0 1) planes of *t* - Se, respectively. However, the d-spacings of 0.29 and 0.37 nm could correspond to different crystal planes of both *m* - Se and *t* - Se, necessitating the use of other techniques, such as X-ray diffraction (XRD), for a more precise determination of the crystal structure (Ruiz-Fresneda et al. 2023).

5. Conclusions

In this study, we have characterized the fungal diversity using culture-dependent techniques and explored the bioremediation potential of U and Se by isolated fungal strains from two former U mine waters, Schlema-Alberoda and Pöhla. The fungal population composition mostly aligns with previous studies characterizing fungal communities using NGS of the ITS. A total of 14 strains belonging to the genera *Cadophora*, *Acremonium*, *Aspergillus*, *Penicillium*, *Cladosporium*, *Trichoderma*, and *Schizophyllum* were isolated and identified. Furthermore, the fungal isolates exhibit a variety of enzymatic activities for lignocellulosic biomass degradation (e.g., lignin peroxidase, cellulase, and laccase) and phosphate metabolism (e.g., alkaline phosphatase, acid phosphatase, and naphthol-AS-BI-phosphohydrolase) relevant for U biomineralization such as uranyl-phosphate. These biochemical data will help to screen for fungal isolates with heavy metal/radionuclide bioremediation potential in oligotrophic environments. Thus, the bioremediation potential of *C. malorum*, *A. sydowii*, and *P. polonicum* against U and of *S. commune*, *C. cladosporioides*, *T. harzianum*, and *Acremonium* sp. against Se was evaluated. The most significant results against U were observed in *C. malorum*, the dominant strain isolated from U-contaminated water in the Schlema-Alberoda mine, where U phosphate biomineralization in the presence of U (0.05 mM and

0.1 mM) was observed. The fungal phosphatase activity studied may have mediated the formation of these uranyl-phosphates. In the case of Se, *T. harzianum* and *Acremonium* sp., showed extremely high tolerance to Se(IV) (MIC>32 mM). Both strains demonstrated the ability to reduce Se(IV) to Se(0), and through techniques such as HAADF-STEM, SAED, and HRTEM, the formation of highly stable and less toxic crystalline nanostructures with two different lattice spacings of 0.37 and 0.29 nm, possibly corresponding to t-Se and/or m-Se planes, was confirmed. Lastly, further research is still needed to enhance fungal bioremediation activity and expand the process for industrial applications and other heavy metals and radionuclides. Currently, less than 10% of the total fungal diversity worldwide has been identified for its relevance in biotechnological applications, suggesting ample opportunities for future research and discoveries in the bioremediation field.

6. References

- Aguerre S and Frechou C (2006) Development of a Radiochemical Separation for Selenium with the Aim of Measuring Its Isotope 79 in Low and Intermediate Nuclear Wastes by ICP-MS. *Talanta*. 69(3): 565–571. <https://doi.org/10.1016/j.talanta.2005.10.028>
- Akash S, Sivaprakash B, Raja VCV, Rajamohan N (2022) Remediation Techniques for Uranium Removal from Polluted Environment – Review on Methods, Mechanism and Toxicology. *Environmental Pollution*. 302:119068. <https://doi.org/10.1016/j.envpol.2022.119068>
- Akhtar K, Akhtar MV, Khalid AM (2007) Removal and Recovery of Uranium from Aqueous Solutions by *Trichoderma Harzianum*. *Water Research*. 41(6):1366–1378. <https://doi.org/10.1016/j.watres.2006.12.009>
- Andlar M, Rezić T, Marđetko N, Kracher D, Ludwig R, Šantek B (2018) Lignocellulose degradation: An overview of fungi and fungal enzymes involved in lignocellulose degradation. *Engineering in Life Sciences*. 18(11):768-778. <https://doi.org/10.1002%2Felsc.201800039>
- Baraniak L, Bernhard G, Nitsche H (2002) Influence of hydrothermal wood degradation products on the uranium adsorption onto metamorphic rocks and sediments. *Journal of Radioanalytical and Nuclear Chemistry*. 253(2):185–190. <https://doi.org/10.1023/A:1019657503952>
- Bayramoğlu G, Çelik G, Arica MY (2006) Studies on accumulation of uranium by fungus *Lentinus sajor-caju*. *Journal of Hazardous Materials*. 136(2):345-353. <https://doi.org/10.1016/j.jhazmat.2005.12.027>
- Bekmukhamedova NK, Mamiyev MS (2023) Biosorbent ability of metals by microorganisms from the collection fund after long-term storage. *IOP Conference Series: Earth and Environmental Science*. 1142:012110. Date of access: February 11, 2024. Retrieved from <https://iopscience.iop.org/article/10.1088/1755-1315/1142/1/012110/pdf>
- Bindschedler S, Cailleau G, Verrecchia E (2016) Role of Fungi in the Biomineralization of Calcite. *Minerals*. 6(2):1–19. <https://doi.org/10.3390/min6020041>
- Cheek M, Lughadha EN, Kirk P, Lindon H, Carretero J, Looney B, Douglas B, Haelewaters D, Gaya E, Llewellyn T, Ainsworth AM, Gafforov Y, Hyde K, Crous P, Hughes M, Walker BE, Forzza RC, Wong KM, Niskanen T (2020) *New Scientific Discoveries:*

Plants and Fungi. *Plants People Planet*. 2:371–579. <https://doi.org/10.1002/ppp3.10148>

Cheng C, Luyao C, Kexin G, Jingxi X, Yangzhen S, Shuya H, Fangzhu X (2022) Progress of Uranium-Contaminated Soil Bioremediation Technology. *Journal of Environmental Radioactivity* 241:106773. <https://doi.org/10.1016/j.jenvrad.2021.106773>

Coelho E, Reis TA, Cotrim M, Mullan TK (2020a) Resistant Fungi Isolated from Contaminated Uranium Mine in Brazil Shows a High Capacity to Uptake Uranium from Water. *Chemosphere*. 248: 126068. <https://doi.org/10.1016/j.chemosphere.2020.126068>

Coelho E, Reis TA, Cotrim M, Rizzutto M, Corrêa B (2020b) Bioremediation of water contaminated with uranium using *Penicillium piscarium*. *Biotechnology Progress*. 36(5):e30322. <https://doi.org/10.1002/btpr.3032>

Dhevagi P, Ramya A, Priyatharshini S, Thanuja KG, Ambreetha S, Nivetha A (2021) Industrially important fungal enzymes: productions and applications. Chapter 11. In: Yadav A.N. (ed.), *Recent trends in mycological research*. *Fungal Biology*. Springer. 265–309. https://doi.org/10.1007/978-3-030-68260-6_11

Dusengemungu L, Cousins G, Grant S, Benjamin M (2022) Potential of bioaugmentation of heavy metal contaminated soils in the Zambian Copperbelt using autochthonous filamentous fungi. *Frontiers in Microbiology*. 13:1-18. <https://www.frontiersin.org/journals/microbiology/articles/10.3389/fmicb.2022.1045671/full#:~:text=https%3A//doi.org/10.3389/fmicb.2022.1045671>

Gadd GM (2007) *Geomycology : Biogeochemical Transformations of Rocks , Minerals , Metals and Radionuclides by Fungi*. *Mycological Research*. 111(1):3–49. <https://doi.org/10.1016/j.mycres.2006.12.001>

Gargarello R, Cavalitto S, Di Gregorio D, Niello JF, Huck H, Pardo A, Somacal H, Curutchet G (2008) Characterisation of Uranium(VI) Sorption by Two Environmental Fungal Species Using Gamma Spectrometry. *Environmental Technology*. 29(12):1341–48. <https://doi.org/10.1080/09593330802327069>

Günther A, Raff J, Merroun ML, Rossberg A, Kothe E, Bernhard G. (2014) Interaction of U(VI) with *Schizophyllum commune* studied by microscopic and spectroscopic methods. *Biometals*. 27(4):775-85. <https://doi.org/10.1007/s10534-014-9772-1>

Hall TA (1999). *BioEdit: a user-friendly biological sequence alignment editor and analysis* 330

program for Windows 95/98/NT. Nucleic Acids Symposium Series, 41(41):95-98. Date of access: February 11, 2024. Retrieved from https://www.academia.edu/2034992/BioEdit_a_user_friendly_biological_sequence_alignment_editor_and_analysis_program_for_Windows_95_98_NT

Harrington TC and Mcnew DL (2023) Phylogenetic analysis places the Phialophora-like anamorph genus *Cadophora* in the Helotiales. Mycotaxon. 87: 141-151. Retrieved from https://www.researchgate.net/publication/297325725_Phylogenetic_analysis_places_the_Phialophora-like_anamorph_genus_Cadophora_in_the_Helotiales

Hilpmann S, Rossberg A, Steudtner R, Drobot B, Hübner R, Bok F, Prieur D, Bauters S, Kvashnina KO, Stumpf T, Cherkouk, A (2023) Presence of Uranium(V) during Uranium(VI) Reduction by *Desulfosporosinus Hippei* DSM 8344T. Science of the Total Environment. 875:162593. <https://doi.org/10.1016/j.scitotenv.2023.162593>

Joo JH and Hussein KA (2012) Heavy Metal Tolerance of Fungi Isolated from Contaminated Soil. Korean Journal of Soil Science and Fertilizer. 45(4): 565–571. <http://dx.doi.org/10.7745/KJSSF.2012.45.4.565>

Kirk TK, Croan S, Tien M, Murtagh KE, Farrel RL (1986). Production of multiple ligninases by *Phanerochaete chrysosporium*: effect of selected growth conditions and use of a mutant strain. Enzyme and Microbial Technology. 8:27-32. [https://doi.org/10.1016/0141-0229\(86\)90006-2](https://doi.org/10.1016/0141-0229(86)90006-2)

Krause K, Jung EM, Lindner J, Hardiman I, Poetschner J, Madhavan S, Matthäus C, Kai M, Menezes RC, Popp J, Svatoš A, Kothe E. (2020) Response of the wood-decay fungus *Schizophyllum commune* to co-occurring microorganisms. PLoS One. 15(4):e0232145. <https://doi.org/10.1371/journal.pone.0232145>

Kumar A, Yadav AN, Mondal R, Kour D, Subrahmanyam G, Shabnam AA, Khan SA, Yadav KK, Sharma GK, Cabral-Pinto M, Fagodiya RK, Gupta DK, Hota S, Malyan SK (2021) Myco-remediation: A mechanistic understanding of contaminants alleviation from natural environment and future prospect. Chemosphere. 284: 131325. <https://doi.org/10.1016/j.chemosphere.2021.131325>

Lee J, Ko Y, Kim S, Hur H (2023) Highly Effective Biosorption Capacity of *Cladosporium* Sp. Strain F1 to Lead Phosphate Mineral and Perovskite Solar Cell PbI₂. Journal of Hazardous Materials 442:130106. <https://doi.org/10.1016/j.jhazmat.2022.130106>

Lee J, Lee SJ, Kim S, Lee JU, Shin KS, Hur HG (2021) Layers of Uranium Phosphate

Nanorods and Nanoplates Encrusted on Fungus *Cladosporium* sp. Strain F1 Hyphae. *Microbes and Environments*. 36(4):ME21036. <https://doi.org/10.1264%2Fjsme2.ME21036>

Li Q, Xian L, Yuan L, Lin Z, Chen X, Wang J, Li T (2023) The Use of Selenium for Controlling Plant Fungal Diseases and Insect Pests. *Frontiers in Plant Science*. 14:1–7. <https://doi.org/10.3389/fpls.2023.1102594>

Liang X, Hillier S, Pendlowski H, Gray N, Ceci A, Gadd GM (2015) Uranium phosphate biomineralization by fungi. *Environmental Microbiology*. 17(6):2064-2075. <https://doi.org/10.1111/1462-2920.12771>

Liang X, Perez MAMJ, Nwoko KC, Egbers P, Feldmann J, Csetenyi L, Gadd GM (2019) Fungal formation of selenium and tellurium nanoparticles. *Applied Microbiology and Biotechnology*. 103:7241–7259. <https://doi.org/10.1007/s00253-019-09995-6>

Liaquat F, Munis MFH, Haroon U, Arif S, Saqib S, Zaman W, Khan AR, Shi J, Che S, Liu Q (2020) Evaluation of Metal Tolerance of Fungal Strains Isolated from Contaminated Mining Soil of Nanjing, China. *Biology (Basel)*. 9(12):469. <https://doi.org/10.3390%2Fbiology9120469>

Lovley DR, Phillips EJP, Gorby YA, Landa ER (1991) Microbial reduction of uranium. *Nature*. 350:413–416. <https://doi.org/10.1038/350413a0>

Lusa M, Bomberg M (2021) Microbial Community Composition Correlates with Metal Sorption in an Ombrotrophic Boreal Bog: Implications for Radionuclide Retention. *Soil Systems*. 5(1):19. <https://doi.org/10.3390/soilsystems5010019>

Ma XK, Ling Wu L, Fam H (2014) Heavy metal ions affecting the removal of polycyclic aromatic hydrocarbons by fungi with heavy-metal resistance. *Applied Microbiology and Biotechnology*. 98(23):9817-27. <https://doi.org/10.1007/s00253-014-5905-2>

Maher K, Bargar JR, Brown GE Jr (2013) Environmental speciation of actinides. *Inorganic Chemistry*. 52(7):3510-3532. <https://doi.org/10.1021/ic301686d>

Martín-Platero AM, Valdivia E, Maqueda M, Martínez-Bueno M (2007) Fast, convenient, and economical method for isolating genomic DNA from lactic acid bacteria using a modification of the protein “salting-out” procedure. *Analytical Biochemistry*. 366(1):102-4. <https://doi.org/10.1016/j.ab.2007.03.010>

Martínez-Rodríguez P, Sánchez-Castro I, Ojeda JJ, Abad MM, Descostes M, Merroun

- ML (2023) Effect of different phosphate sources on uranium biomineralization by the *Microbacterium* sp. Be9 strain: A multidisciplinary approach study. *Frontiers in Microbiology*. 13:1092184. <https://doi.org/10.3389/fmicb.2022.1092184>
- Merroun ML, Raff J, Rossberg A, Hennig C, Reich T, Selenska-Pobell S (2005) Complexation of uranium by cells and S-layer sheets of *Bacillus sphaericus* JG-A12. *Applied and Environmental Microbiology*. 71(9):5532-43. <https://doi.org/10.1128/AEM.71.9.5532-5543.2005>
- Mohammadian E, Ahari AB, Arzanlou M, Oustan S, Khazaei SH (2017) Tolerance to Heavy Metals in Filamentous Fungi Isolated from Contaminated Mining Soils in the Zanzan Province, Iran. *Chemosphere*. 185:290–96. <https://doi.org/10.1016/j.chemosphere.2017.07.022>
- Mumtaz S, Streten-joyce C, Parry DL, McGuinness KA, Lu P, Gibb KS (2013) Fungi Outcompete Bacteria under Increased Uranium Concentration in Culture Media. *Journal of Environmental Radioactivity*. 120:39–44. <https://doi.org/10.1016/j.jenvrad.2013.01.007>
- Nandini B, Hariprasad P, Prakash HS, Shetty HS, Geetha N. (2017) Trichogenic-selenium nanoparticles enhance disease suppressive ability of *Trichoderma* against downy mildew disease caused by *Sclerospora graminicola* in pearl millet. *Scientific Reports*. 7(1):2612. <https://doi.org/10.1038/s41598-017-02737-6>
- Newman-Portela AM, Krawczyk-Bärsch E, Lopez-Fernandez M, Bok F, Kassahun A, Drobot B, Steudtner R, Stumpf T, Raff J, Merroun ML (2024) Biostimulation of indigenous microbes for uranium bioremediation in former U mine water: multidisciplinary approach assessment. *Environmental Science and Pollution Research*. 31(5):7227-7245. <https://doi.org/10.1007/s11356-023-31530-4>
- Newsome L, Morris K, Lloyd JR (2014) The biogeochemistry and bioremediation of uranium and other priority radionuclides. *Chemical Geology*. 363:164–184. <https://doi.org/10.1016/j.chemgeo.2013.10.034>
- Oladipo OG, Awotoye OO, Olayinka A, Bezuidenhout CC, Maboeta MS (2018) Heavy metal tolerance traits of filamentous fungi isolated from gold and gemstone mining sites. *Brazilian Journal of Microbiology*. 49(1):29-37. <https://doi.org/10.1016/j.bjm.2017.06.003>
- Pethkar AV, Kulkarni SK, Paknikar KM (2001) Comparative Studies on Metal Biosorption

by Two Strains of *Cladosporium Cladosporioides*. *Bioresource Technology*. 80(3):211–15. [https://doi.org/10.1016/S0960-8524\(01\)00080-3](https://doi.org/10.1016/S0960-8524(01)00080-3)

Phillips, EJP, Landa ER, Lovley DR (1995) Remediation of Uranium Contaminated Soils with Bicarbonate Extraction and Microbial U(VI) Reduction. *Journal of Industrial Microbiology*. 14(3–4):203–207. <https://doi.org/10.1007/BF01569928>

Povedano-Priego C, Fadwa J, Morales-Hidalgo M, Pinel-Cabello M (2024) Unveiling Fungal Diversity in Uranium and Glycerol-2-Phosphate-Amended Bentonite Microcosms: Implications for Radionuclide Immobilization within the Deep Geological Repository System. *Science of the Total Environment*. 908: 168284. <https://doi.org/10.1016/j.scitotenv.2023.168284>

Rosenfeld CE, Kenyon JA, James BR, Santelli CM (2017) Selenium (IV, VI) reduction and tolerance by fungi in an oxic environment. *Geobiology*. 15(3):441-452. <https://doi.org/10.1111/gbi.12224>

Ruiz-Fresneda MA, Martín JD, Bolívar JG, Cantos MVF, Bosch-Estévez G, Moreno MFM, Merroun ML (2018) Green synthesis and biotransformation of amorphous Se nanospheres to trigonal 1D Se nanostructures: impact on Se mobility within the concept of radioactive waste disposal. *Environmental Science Nano*. 5:2103-2116. <https://doi.org/10.1039/C8EN00221E>

Ruiz-Fresneda MA, Morales-Hidalgo M, Povedano-Priego C, Jroundi F, Hidalgo-Iruela J, Cano-Cano M, Pérez-Muelas E, Merroun ML, Martín-Sanchez I (2024) Unlocking the key role of bentonite fungal isolates in tellurium and selenium bioremediation and biorecovery: Implications in the safety of radioactive waste disposal. *Science of The Total Environment*. 912:169242. <https://doi.org/10.1016/j.scitotenv.2023.169242>

Ruiz-Fresneda MA, Staicu LC, Lazúen-López G, Merroun ML (2023) Allotropy of selenium nanoparticles: Colourful transition, synthesis, and biotechnological applications. *Microbial Biotechnology*. 16(5):877-892. <https://doi.org/10.1111/1751-7915.14209>

Sabuda MC, Rosenfeld CE, Dejournett TD, Schroeder K, Wuolo-Journey K, Santelli CM (2020) Fungal Bioremediation of Selenium-Contaminated Industrial and Municipal Wastewaters. 11:1-22. <https://doi.org/10.3389/fmicb.2020.02105>

Sana S, Roostaazad R, Yaghmaei S (2015) Biosorption of Uranium (VI) from Aqueous Solution by Pretreated *Aspergillus niger* Using Sodium Hydroxide. *Iranian Journal of Chemistry and Chemical Engineering*. 34(1):65-74. <https://doi.org/10.30492/>

- Sánchez C (2009) Lignocellulosic residues: biodegradation and bioconversion by fungi. *Biotechnology Advances*. 27(2):185-94. <https://doi.org/10.1016/j.biotechadv.2008.11.001>
- Sánchez-Castro I, Martínez-Rodríguez P, Abad MM, Descostes M, Merroun ML (2021) Uranium removal from complex mining waters by alginate beads doped with cells of *Stenotrophomonas* sp. Br8: Novel perspectives for metal bioremediation. *Journal of Environmental Management*. 296:113411. <https://doi.org/10.1016/j.jenvman.2021.113411>
- Schaefer S, Steudtner R, Hübner R, Krawczyk-Bärsch E, Merroun ML (2021) Effect of Temperature and Cell Viability on Uranium Biomineralization by the Uranium Mine Isolate *Penicillium simplicissimum*. *Frontiers in Microbiology*. 12(802926). <https://doi.org/10.3389/fmicb.2021.802926>
- Schulz WW (2023) Uranium processing. *Encyclopedia Britannica*. <https://www.britannica.com/technology/uranium-processing>
- Siddharthan S, Thangaraj S, Paulraj S, RajaMohmed B, Rakkamuthu K, Dharmaraj V, Renganathan M, Umadevi P (2023) Myco-remediation of selenium contaminated environment and future prospects: An overview. *Environmental Quality Management*. 1-9. <https://doi.org/10.1002/tqem.22159>
- Singh N, Saha P, Rajkumar K (2015) Biogenic Strain of Silver and Selenium Nanoparticles by *Pseudomonas fluorescens* and *Cladosporium* Sp. JAPSK3 Isolated from Coal Mine Samples and Their Antimicrobial Activity. 14:1–9. <https://doi.org/10.1142/S0219581X15500179>
- Staudenrausch S, Kaldorf M, Renker C, Luis P, Buscot F (2005) Diversity of the Ectomycorrhiza Community at a Uranium Mining Heap. *Biology and Fertility of Soils*. 41:439–46. <https://doi.org/10.1007/s00374-005-0849-4>
- Tomah AA, Zhang Z, Alamer ISA, Khattak AA, Ahmed T, Hu M, Wang D, Xu L, Li B, Wang Y (2023) The Potential of Trichoderma-Mediated Nanotechnology Application in Sustainable Development Scopes. *Nanomaterials*. 13(17):2475. <https://doi.org/10.3390/nano13172475>
- Ullah H, Chen B, Rashid A, Zhao R, Shahab A, Yu G, Wong MH, Khan S (2023) A Critical Review on Selenium Removal Capacity from Water Using Emerging

Non-Conventional Biosorbents. *Environmental Pollution*. 339:122644. <https://doi.org/10.1016/j.envpol.2023.122644>

Văcar CL, Covaci E, Chakraborty S, Li B, Weindorf DC, Frențiu T, Pârvu M, Podar D (2021) Heavy Metal-resistant Filamentous Fungi as Potential Mercury Bioremediators. *Journal of Fungi*. 7(5):386. <https://doi.org/10.3390/jof7050386>

Xu X, Hao R, Xu H, Lu A (2020) Removal mechanism of Pb(II) by *Penicillium polonicum*: immobilization, adsorption, and bioaccumulation. *Scientific Reports*. 10:9079. <https://doi.org/10.1038/s41598-020-66025-6>

Yaashikaa PR, Kumar PS, Jeevanantham S, Saravanan R (2022) A review on bioremediation approach for heavy metal detoxification and accumulation in plants. *Environmental Pollution*. 301:119035. <https://doi.org/10.1016/j.envpol.2022.119035>

Yang HB, Tan N, Wu FJ, Liu HJ, Sun M, She ZG, Lin YC (2012) Biosorption of uranium(VI) by a mangrove endophytic fungus *Fusarium* sp. #ZZF51 from the South China Sea. *Journal of Radioanalytical and Nuclear Chemistry*. 292(3):1011-1016. <https://doi.org/10.1007/s10967-011-1552-6>

Zhang D, Yin C, Abbas N, Mao Z, Zhang Y (2020) Multiple heavy metal tolerance and removal by an earthworm gut fungus *Trichoderma brevicompactum* QYCD-6. *Scientific Reports*. 10:6940. <https://doi.org/10.1038/s41598-020-63813-y>

Zhu YG, Chen BD (2009) Chapter 8. In: Elsevier, Principles and Technologies for Remediation of Uranium-Contaminated Environments. Radioactivity in the Environment. 14:357-374. [https://doi.org/10.1016/S1569-4860\(08\)00208-8](https://doi.org/10.1016/S1569-4860(08)00208-8)

Supplementary Material

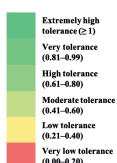
Table 1S. Minimum inhibitory concentration (MIC) determination of the fungal isolates on Se(IV).

Code	Isolate	Se (mM)										MIC
		0	0.25	0.5	1	2	4	8	16	32		
H1	<i>C. malorum</i>	+	+	+	+	+	+	+	+	+	+	> 32
H2	<i>C. cladosporioides</i>	+	+	+	+	+	+	+	-	-		16
H3	<i>P. magnielliptisporum</i>	+	+	+	+	-	-	-	-	-		2
H4	<i>Penicillium</i> sp.	+	+	+	+	+	+	+	+	+		> 32
H5	<i>A. sydowii</i>	+	+	+	+	+	+	+	+	+		> 32
H6	<i>P. mexicanum</i>	+	+	+	+	+	+	-	-	-		8
H7	<i>T. harzianum</i>	+	+	+	+	+	+	+	+	+		> 32
H8	<i>Acremonium</i> sp.	+	+	+	+	+	+	+	+	+		> 32
H9	<i>Cladosporium</i> sp.	+	+	+	+	+	-	-	-	-		4
H10	<i>S. commune</i>	+	+	+	+	+	-	-	-	-		8
H12	<i>Penicillium</i> sp.	+	+	+	+	+	+	+	+	+		> 32
H15	<i>C. limoniforme</i>	+	+	+	+	+	-	-	-	-		4
H16	<i>P. polonicum</i>	+	+	+	-	-	-	-	-	-		1
H17	<i>A. niger</i>	+	+	+	+	+	+	-	-	-		8

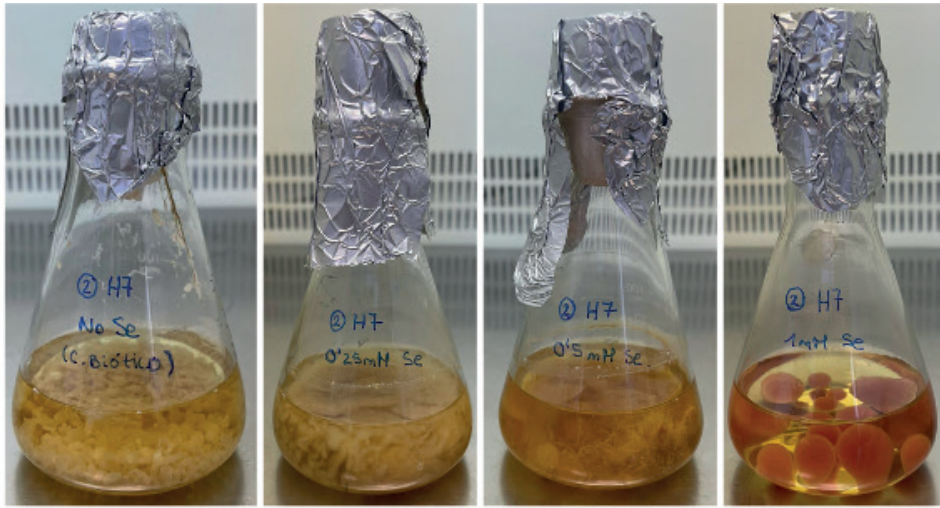
“+” (in green): growth, “-” (in red): no growth.

Table 2S. Tolerance Index (TI) determination of the fungal isolates on Se(IV).

Code	Isolate	Se (mM)								
		0	0.25	0.5	1	2	4	8	16	32
H1	<i>C. malorum</i>	1 ± 0.01	0.61 ± 0.03	0.46 ± 0.02	0.31 ± 0.02	0.19 ± 0.01	0.18 ± 0.01	0.18 ± 0.01	0.18 ± 0.01	0.18 ± 0.01
H2	<i>C. cladosporioides</i>	1 ± 0.04	1 ± 0.03	0.49 ± 0.03	0.33 ± 0.01	0.20 ± 0.01	0.20 ± 0.02	0.20 ± 0.02	0	0
H3	<i>P. magniliptisporum</i>	1 ± 0.05	0.93 ± 0.01	0.68 ± 0.02	0.60 ± 0.01	0	0	0	0	0
H4	<i>Penicillium sp.</i>	1 ± 0.01	0.55 ± 0.02	0.27 ± 0.02	0.27 ± 0.01	0.11 ± 0.01	0.11 ± 0.01	0.11 ± 0.01	0.11 ± 0.01	0.05 ± 0.01
H5	<i>A. sydowii</i>	1 ± 0.03	0.90 ± 0.01	0.60 ± 0.05	0.40 ± 0.01	0.40 ± 0.01	0.40 ± 0.01	0.40 ± 0.01	0.20 ± 0.02	0.10 ± 0.01
H6	<i>P. mexicanum</i>	1 ± 0.01	0.51 ± 0.03	0.60 ± 0.02	0.40 ± 0.01	0.32 ± 0.02	0.28 ± 0.01	0	0	0
H7	<i>T. harzianum</i>	1 ± 0.01	1 ± 0.03	1 ± 0.02	1 ± 0.01	1 ± 0.01	1 ± 0.01	0.89 ± 0.001	0.35 ± 0.01	0.12 ± 0.01
H8	<i>Acremonium sp.</i>	1 ± 0.01	0.66 ± 0.01	0.45 ± 0.02	0.42 ± 0.03	0.26 ± 0.01	0.26 ± 0.01	0.25 ± 0.01	0.25 ± 0.01	0.26 ± 0.01
H9	<i>Cladosporium sp.</i>	1 ± 0.02	0.76 ± 0.03	0.65 ± 0.01	0.47 ± 0.01	0.48 ± 0.02	0	0	0	0
H10	<i>S. commune</i>	1 ± 0.01	0.12 ± 0.02	0.07 ± 0.01	0.07 ± 0.01	0.07 ± 0.01	0.07 ± 0.01	0	0	0
H12	<i>Penicillium sp.</i>	1 ± 0.03	1 ± 0.02	1 ± 0.02	0.88 ± 0.01	0.31 ± 0.01	0.22 ± 0.01	0.13 ± 0.01	0.13 ± 0.01	0.13 ± 0.01
H15	<i>C. limoniforme</i>	1 ± 0.01	1 ± 0.01	0.74 ± 0.01	0.50 ± 0.01	0.40 ± 0.01	0.30 ± 0.01	0	0	0
H16	<i>P. polonicum</i>	1 ± 0.01	0.45 ± 0.02	0.79 ± 0.02	0	0	0	0	0	0
H17	<i>A. niger</i>	1 ± 0.02	0.75 ± 0.02	0.75 ± 0.01	0.17 ± 0.02	0.16 ± 0.01	0.16 ± 0.01	0	0	0



Very low tolerance: 0.00 – 0.20; Low tolerance: 0.21 – 0.40; Moderate tolerance: 0.41 – 0.60; High tolerance: 0.61 – 0.80; Very high tolerance: 0.81; – 0.99; Extremely high tolerance: ≥ 1.

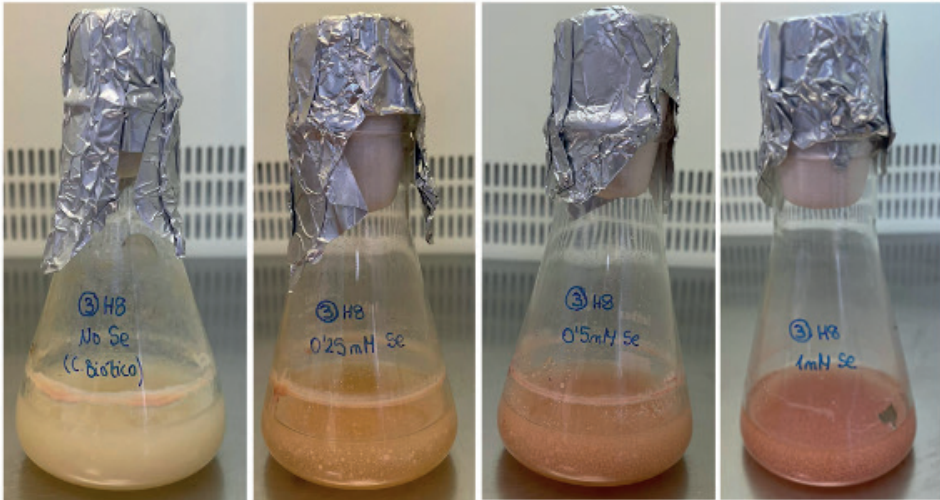


H7_B

H7_J

H7_K

H7_L



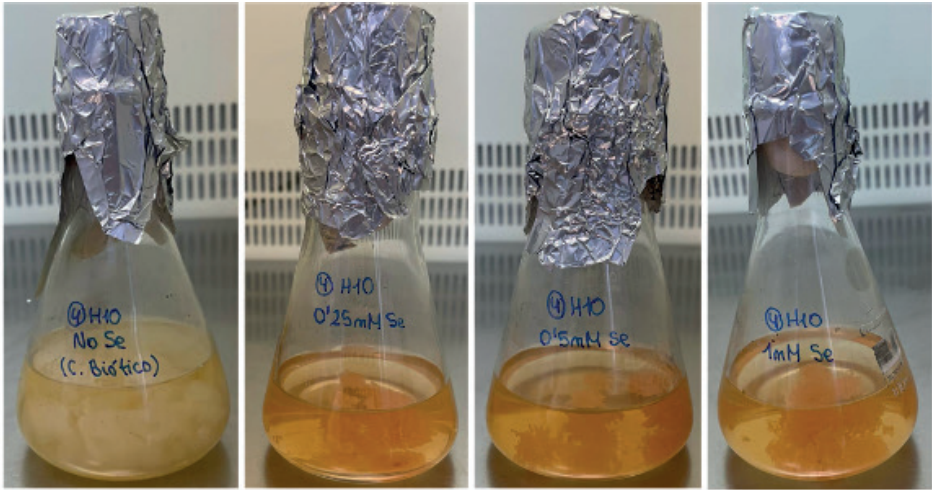
H8_B

H8_J

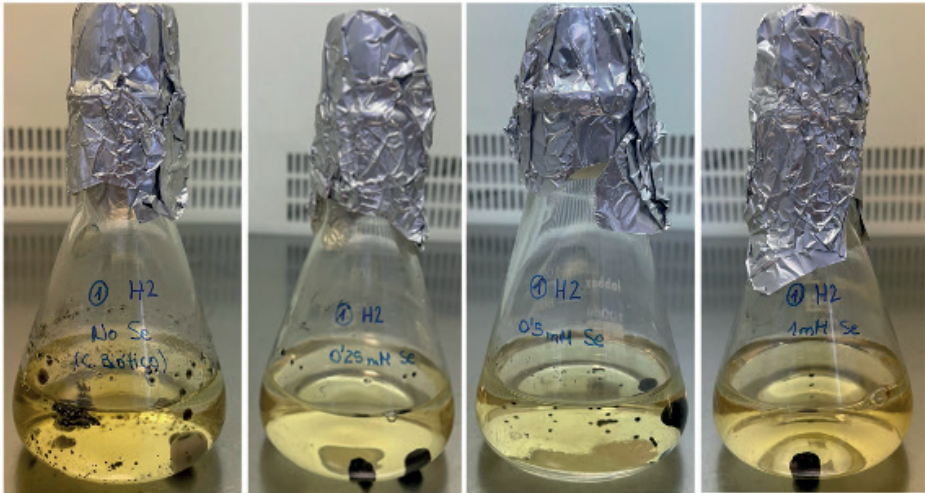
H8_K

H8_L

Fig. 2S. *T. harzianum* (H7) (B: Biotic control (without Se), J: 0.25 mM, K: 0.5 mM, L: 1 mM) and *Acremonium* sp. (H8) (B: Biotic control (without Se), J: 0.25 mM, K: 0.5 mM, L: 1 mM) mycelium after one month of incubation.



H10_B H10_J H10_K H10_L



H9_B H9_J H9_K H9_L

Fig. 3S. *S. commune* (H10) (B: Biotic control (without Se), J: 0.25 mM, K: 0.5 mM, L: 1 mM) and *C. cladosporioides* (H9) (B: Biotic control (without Se), J: 0.25 mM, K: 0.5 mM, L: 1 mM) mycelium after one month of incubation.

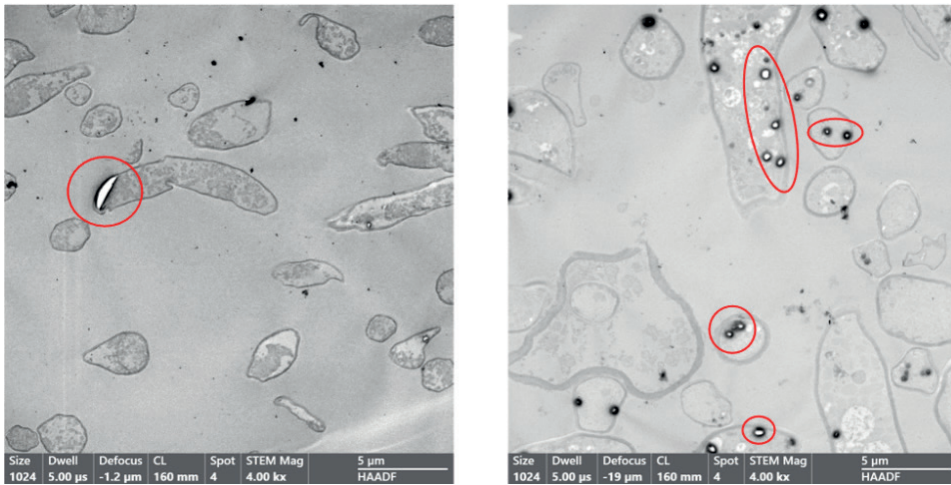


Fig. 4S. Micrograph showing empty spaces in *T. harzianum* (left) and *Acremonium* sp. (right) cells.

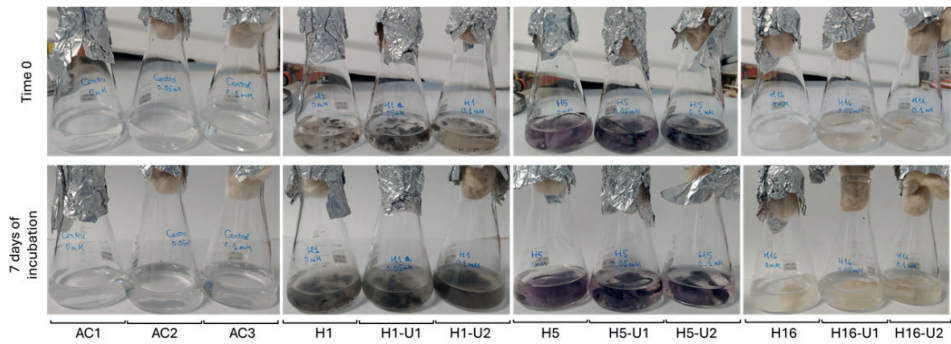


Fig. 5S. *C. malorum* (H1), *A. sydowii* (H5) and *P. polonicum* (H16) mycelium after 7 days of incubation. AC: Abiotic control; U1: 0.05 mM uranyl acetate treatment; U2: 0.1 mM uranyl acetate treatment.

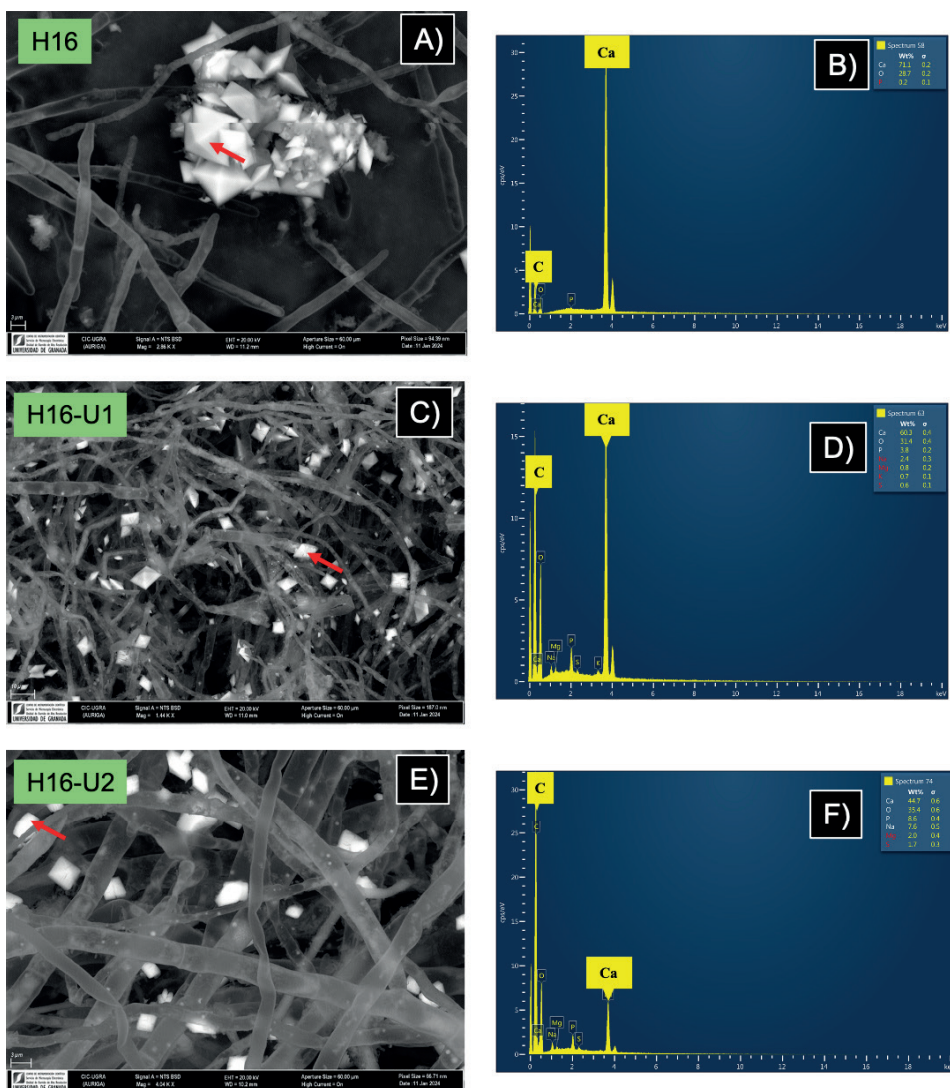
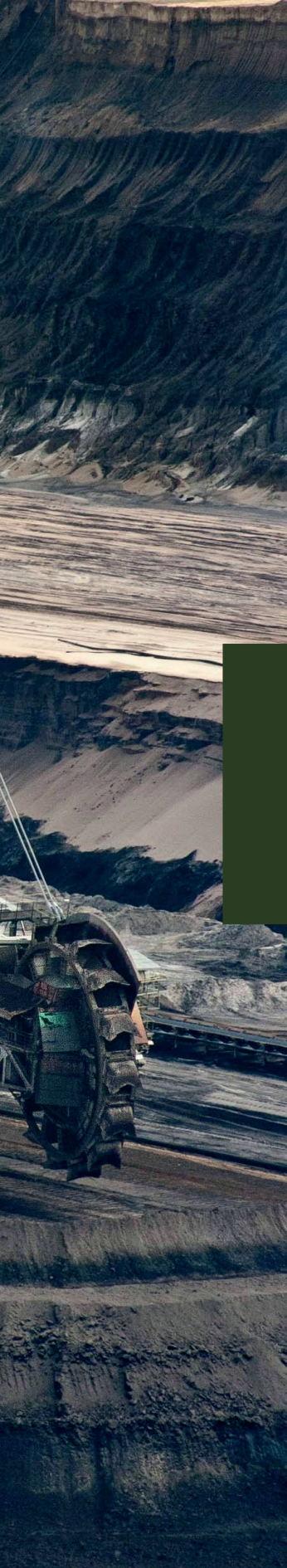


Fig. 6S. HRSEM image showing extracellular accumulations in fungal mycelium after 7 days of incubation in the no-amended Schlemma-Alberroda mine water (H16; A), 0.05 mM uranium acetate (H16-U1; C), and 0.1 mM (H16-U1; E) treatments. EDXS spectra confirm the composition of Ca and C in the electro-dense accumulations (B, D, and F).



Photo by Pixabay



General Discussion

GENERAL DISCUSSION

Since the last decade, the concentration of uranium (U) in the environment has increased due to human activities, such as nuclear industry, U mining, agronomic practices, and military conflicts (Smedleya and Kinniburgh 2023; Kumar et al. 2023). The infiltration of water contaminated with U and other heavy metals is a persistent environmental issue in many abandoned mines, continuing to impact the quality of the natural environment, affecting surface and groundwater, and posing a threat to human health. Some of the risks associated with U toxicity to human health include kidney damage, neurasthenia, infertility, among others (Smedleya and Kinniburgh 2023; Kumar et al. 2023). Recognizing these potential risks, U contamination has become an issue of significant global concern and has promoted a prosperous career in the progress of technologies for the remediation of U-contaminated environments. Moreover, the removal of U from contaminated environments presents a significant challenge as U often coexists with other contaminants such as As, Zn, ^{226}Ra and Pb, which also need to be addressed. The primary remediation technologies, known as conventional technologies, include chemical, physical, or a combination of both, but in recent years, bioremediation has emerged as a promising method to prospectively support or outperform chemical treatment due to its reduced costs, easy implementation, and effectiveness in remediating low concentrations of U. Research on the use of organisms (such as plants, fungi, bacteria, and archaea) for U removal has been extensively studied in recent years, and micro-organisms such as bacteria and fungi showed great potential in the bioremediation of this radionuclide. (Gadd and Fomina 2011; Banala et al. 2021; You et al. 2021). U contaminated environment exhibits high microbial diversity and activity. Many of these micro-organisms can interact with U through different mechanisms (bioreduction, biomineralization, biosorption, and bioaccumulation), but among them, the bioreduction and biomineralization of U by bacteria and fungi are the main mechanisms playing a key role in the design of efficient U bioremediation strategy (You et al. 2021). Therefore, this PhD thesis addresses the comprehensive investigation of two former German U mines (Schlema-

Alberoda and Pöhla, Wismut GmbH) with the aim of understanding the biogeochemical behaviour of U and subsequently designing an efficient U bioremediation technology.

In the **first chapter**, a geochemical and microbiological characterization of both mine waters collected in 2020 was conducted using a multidisciplinary approach combining spectroscopic, microscopic and microbial diversity-based techniques. The chemistry of the two mine waters was analysed by inductively coupled plasma mass spectrometry (ICP-MS) and high-performance ionic chromatography (HPIC). The U speciation of the two water samples was characterized by cryo-time-resolved laser fluorescence spectroscopy (cryo-TRFLS). The obtained data are needed for assessing the potential risk of contaminated water infiltration into uncontaminated water and the mobility of soluble U species. Both mine waters (Schlema-Alberoda and Pöhla) showed a circumneutral pH and considerable differences in the E_H , with higher reducing conditions identified in the Pöhla mine water sample (-91 mV) than in the Schlema-Alberoda sample ($+139$ mV). Additionally, a higher electrical conductivity (EC) was determined in Schlema-Alberoda (1.52 mS/cm) compared to the Pöhla sample (0.56 mS/cm), likely due to the higher concentration of dissolved ions.

Our analyses revealed significant differences between the Schlema-Alberoda and Pöhla samples in parameters such as U concentration (1.05 mg/l and 0.01 mg/l) and SO_4^{2-} (335 mg/l and 0.5 mg/l), respectively. Furthermore, U can exist as various chemical species in natural waters, including free metal ions and forming complexes with inorganic and organic ligands. Initially, our thermodynamic calculations predicted a calcium uranyl carbonate complex $[Ca_2UO_2(CO_3)_3(aq)]$ as the dominant U species in the Schlema-Alberoda mine water, which was also detected through cryo-TRLFS combined with PARAFAC analysis, in addition to a second species as $[UO_2(CO_3)_3^{4-}]$ according to (Wang et al. 2004). The first species, $Ca_2UO_2(CO_3)_3(aq)$, was also reported by other authors as the main species in Schlema-Alberoda water (Bernhard et al. 1996, 1998, 2001). Because of extremely low U concentrations in the Pöhla samples (0.01 mg/l), no detectable U signal was obtained by cryo-TRLFS measurements.

Understanding the impact of indigenous microbial community in the biogeochemical cycle of U and other relevant elements (e.g., Fe and S) in the mine water is crucial to design efficient bioremediation strategy of this radionuclide. Therefore, the characterization of the microbial community, both bacterial and fungal, was conducted using next-generation sequencing of the 16S ribosomal RNA (rRNA) gene and fungal internal transcribed spacer (ITS). The microbial community composition shared groups identified in other studies (Rastogi et al. 2010a, b; Zeng et al. 2019; Lusa et al. 2019). In both mine water samples, Campylobacterota, Proteobacteria, and Patescibacteria were the most represented bacterial phyla. These microorganisms have developed resistance to heavy metals and radionuclides, playing a crucial role in the biogeochemical cycles of S, N, and Fe, thus affecting U speciation. For example, the genera *Sulfuricurvum*, *Sulfurovum*, and *Sulfurimonas* (nitrate reducers and sulphur oxidizers) play a key role in maintaining reduced U species by coupling nitrate reduction to sulphur compound oxidation and subsequently promoting the growth of metal-reducing micro-organisms (e.g., SRB). The consequent increase in SO_4^{2-} concentration could favour the grow of SRB. For instance, the Desulfobacterota phylum, which is more abundant in Schlema-Alberoda water possibly due to higher SO_4^{2-} concentrations, harbour several SRB genera, including the genus *Desulfurivibrio* (Waite et al. 2020). Additionally, an unidentified genus of the *Rhodocyclaceae* family, which includes FeRB that are able to reduce U, was found.

The fungal community composition in U mine waters was dominated by Ascomycota and Basidiomycota. Interestingly, *Cadophora* is strongly dominating the Schlema-Alberoda mine water. Regarding U removal through U phosphate biomineralization, *Penicillium* and *Aspergillus* (Ascomycota) are traditionally the most reported genera, however their relative abundance was very low in both samples (Schaefer et al. 2021; Zhang et al. 2022). Nevertheless, fungal genera that could play a key role in lignocellulosic biomass decomposition and degradation were identified as mine walls are lined with wood. Decomposition of wood, both naturally and fungi-mediated, releases various compounds such as cellulose, lignin,

and low molecular weight molecules (such as vanillin, vanillic acid, and gluconic acid). These compounds can serve as electron donors for U-reducing bacteria. Based on these findings, bio-stimulation experiments were performed in this study on the native U-reducing microbial community in Schlema-Alberoda mine water to reduce the U concentration. With a U concentration of 1 mg/l, the mine water exceeds the U concentration limits established by the World Health Organization (WHO 2022), being 0.03 mg/l generally and the specific site discharge limit of 0.5 mg/l (Wismut GmbH Umweltbericht 2021). To evaluate the microbial community capacity to reduce U, microcosms with three different electron donors - gluconic acid, vanillic acid, and glycerol - were used. It was observed that only those treated with glycerol and vanillic acid eliminated U, while gluconic acid was ineffective. Glycerol-treated microcosms showed a notable reduction in U (99%), Fe (95%), and SO_4^{2-} (58%), suggesting that glycerol biostimulation is more effective and could promote key U-reducing bacteria.

The analysis of the 16S rRNA gene is useful for identifying micro-organisms in an environment and can provide key insights for the design of radionuclide remediation technologies. However, for a deeper understanding of the microbial role in biogeochemical processes, metatranscriptomic studies are needed. Therefore, in the **second chapter**, an analysis of functional genes was conducted through RNA sequencing to investigate key metabolic pathways and activities related to C, N, and S biogeochemical cycles in the mine waters of Schlema-Alberoda and Pöhla. This study, conducted in 2021, includes the investigation of the microbial community through 16S rRNA gene amplification and the analysis of the geochemistry of both mines using ICP-MS and HPIC.

Our results neither reveal significant changes between the 2020 and 2021 collected samples in the structure of the bacterial community nor in the concentration of parameters of interest such as U, Fe, As, and SO_4^{2-} .

The results revealed the utilization of carbon in the metabolic dynamics of the bacterial community in both mine waters. The presence of the Calvin-Benson-Bassham (CBB) cycle pathway was observed in bacteria such as *Sulfuritaela*, indicating the possibility of autotrophic carbon assimilation.

Additionally, the reverse tricarboxylic acid cycle (rTCA) pathway was identified in micro-organisms such as *Sulfurimonas* and *Sulfuricurvum*, suggesting another potential mechanism of carbon assimilation.

Nitrate is a common co-contaminant in environments contaminated with U and may inhibit microbial reduction of U(VI) (Finneran et al. 2002). The nitrate concentration in the mine waters of Schlema-Alberoda and Pöhla is low, possibly due to the activity of nitrate-reducing bacteria (NRB). However, in Pöhla, only *Dechloromonas* is positive related to nitrate reduction. Conversely, in Schlema-Alberoda, a bacterial community (e.g., *Sulfurimonas* and *Sulfuricurvum*) capable of reducing/oxidizing nitrates/nitrites and fixing N was identified. Both bacteria can oxidize reduced sulphur compounds and use nitrate as a terminal electron acceptor. Therefore, it is essential to consider the interaction between both cycles/metabolisms (N and S), as it may influence the stability of reduced U species by coupling nitrate reduction with sulphur compound oxidation, thereby promoting the growth of metal-reducing micro-organisms.

Genes responsible for encoding enzymes involved in two crucial pathways, DSR (Dissimilatory Sulphate Reduction) and ASR (Assimilatory Sulphate Reduction), for S transformation where SRB are closely involved (Kushkevych et al. 2020), were identified. In both mine waters, higher expression of the DSR pathway was observed compared to the ASR pathway. However, Pöhla mine water showed a higher activity in the DSR pathway compared to Schlema-Alberoda mine water. This disparity could be linked to the anoxic conditions present in the Pöhla mine water, as SRB show a preference for the DSR pathway under these circumstances (Dar et al. 2007). These results provide evidence of the participation of a microbial community in sulphate respiration, and from the perspective of U bioremediation, the active population of SRB could play a role in U reduction in the Pöhla mine water. Furthermore, we should consider a possible abiotic U reduction caused by hydrogen sulphides produced during the reduction of sulphates by SRB.

We were also able to identify different genes related to Fe biogeochemical processes, such as oxidation, storage, and regulation of this element in the

studied mine waters. However, the higher regulation of these processes was identified in the Pöhla mine water sample. Additionally, and exclusively, *OmcS* was identified as a gene involved in Fe reduction in the Pöhla sample. *OmcS* is closely related to U(VI) reduction (Qian et al. 2011). These findings could explain the lower concentration of U found in the Pöhla mine, where, due to its more hermetic nature, reducing conditions, and a more active community of SRB (e.g., *Desulfobacca*) and FeRB (e.g., *Geobacter*), a lower concentration of U (0.01 mg/l) was detected. Furthermore, bacterial communities exhibit various strategies to cope with heavy metal stress, including the regulation of metal and phosphate transporters for U phosphate biomineralization. The expression of functions related to flagellum biosynthesis and hydrogenase activity suggests mechanisms for bacterial relocation and metal reduction, respectively, contributing to reducing metal toxicity (Woolfolk and Whiteley, 1962; Zadvorny et al. 2006; Marshall et al. 2008; Gao and Francis 2013; Teng et al. 2019; Li et al. 2022). It is also important to note that both mine waters show expression of As resistance pathways, suggesting microbial adaptation to metal stress conditions. Furthermore, future work should focus on the detailed identification of genes directly involved in U reduction.

Based on the results obtained in the previous chapters, the main aim of the **third chapter** of this PhD thesis was to elaborate anoxic microcosms using Schlema-Alberoda mine water, amended with glycerol (10 mM) as an electron donor, for the biostimulation of the native U-reducing bacterial community as basis for the design of an efficient U bioremediation strategy. Glycerol biostimulation led to reducing conditions where the E_H dropped from +398 mV to -114 mV, with the formation of a black precipitate at the bottom of the microcosm. Over the course of the 130-day experiment, changes in physicochemical parameters were observed using ICP-MS and HPIC. At the end of the experiment, the concentration of soluble U decreased by 96% compared to the initial concentration. Similarly, there was a decrease of 98% and 68% in Fe and SO_4^{2-} concentrations, respectively. Therefore, glycerol clearly effectively stimulated the native bacterial community. Glycerol, through an oxidative pathway, may transform into

phosphoenolpyruvate, which in turn generates propionate and pyruvate. The latter can produce various compounds, including ethanol, lactate, and acetate, among others, depending on micro-organisms and environmental conditions (Zhou et al. 2022). SRB and FeRB can use these compounds as electron donors and simultaneously precipitate heavy metals and radionuclides (Petrie et al. 2003; Santos et al. 2018; Zhou et al. 2022).

Thermodynamic modelling predicted the theoretical chemical speciation of U at the end of the experiment, revealing the possible formation of uraninite as result of microbial U(VI) reduction. Furthermore, Ultraviolet-Visible Spectroscopy (UV/Vis) and Extended X-Ray Absorption Fine Structure (EXAFS) data corroborated the formation of this U(IV) phase in the black precipitates obtained in each sample with a different decrease in U concentration in the supernatant (20%, 60%, and 90%). Additionally, High-Energy-Resolution Fluorescence-Detected X-ray Absorption Near-Edge Structure (HERFD/XANES) and iterative target factor analysis (ITFA) estimated the approximate proportion of different U oxidation states in the black precipitates based on the decrease in U in the supernatant. U(IV) was clearly the dominant oxidation state compared to U(VI) and U(V). As expected, as the U concentration in the supernatant decreased, the fractions of U(VI) in the black precipitates decreased. Compared to other authors, we agree that U(IV) is the dominant oxidation state during microbial reduction (Schofield et al. 2008; Newsome et al. 2014; Hilpmann et al. 2023). Interestingly, U(V) species was identified at different ratios ranging between 21% and 32%, depending on the decrease in U concentration in the supernatant. Additionally, EXAFS spectra and the isolation of pure U species from spectral mixtures through ITFA clearly revealed not only colloidal uraninite but also U(VI)/U(V) carbonates could be present. The calculated structural parameters (bond distances) of U species in the samples favour the existence of a U(V)-carbonate complex than those of U(VI) carbonates species. However, we cannot exclude the presence of U(VI)-carbonate complex, especially in samples with a low decrease in U concentration in the supernatant. Furthermore, we used a combination of High-Angle Annular Dark-Field Scanning Transmission Electron

Microscopy (HAADF-STEM) and Energy-Dispersive X-Ray Spectroscopy (EDXS) to characterize at molecular and atomic scale the structure of the reduced U products, showing electron-dense clusters mainly rich in U. Also, dispersed Fe and S were identified around the cell wall. Inside the clusters, using High-Resolution Transmission Electron Microscopy (HRTEM), characteristic lattice spacings corresponding to uraninite NPs were identified. Additionally, other lattice spacings correlated with FeUO_4 , with possible predominance of U(V). Pyrite NPs were also found in smaller proportions. The results clearly show that glycerol based biostimulation of U reducers in Schlemma-Alberoda mine water is an excellent strategy for U bioremediation and removal of co-contaminants such as Fe, As, and SO_4^{2-} . However, the long-term stability of the biogenic U reduction products should be taken in account for the risk assessment of the bioremediation process. It is well known that U(IV) could be mobilized through reoxidation processes in presence of different oxidants like O_2 , nitrates, Fe(III), etc. In our work, clear evidence of U(IV) reoxidation to U(VI) was observed in a U(IV)-containing black precipitate exposed to O_2 for 4 weeks. This is not surprising since biogenic uraninite tends to re-oxidize easily in the presence of O_2 . However, what was genuinely surprising is that values of approximately 53% of U(V) were identified in the precipitate exposed to O_2 . This suggests that despite the reported instability of U(V) in presence of O_2 , the biogenic U(V) phase detected in the present study shows high stability, being the first documented example of prolonged stability of U(V) in environmental samples influenced by micro-organisms.

Bacterial U reduction is an excellent approach for U bioremediation. However, fungi have a greater adaptation capacity than bacteria to environments contaminated with heavy metals and/or radionuclides (Mumtaz et al. 2013).

In the **fourth chapter**, the isolation, molecular identification, and enzymatic characterization of fungi from both mine waters is described. Additionally, the potential of the native fungal community for U and Se remediation was evaluated. A total of fourteen fungal strains were isolated, identified through ITS sequencing and morphological characterization

techniques. Isolated genera include *Cadophora*, *Acremonium*, *Aspergillus*, *Penicillium*, *Cladosporium*, *Trichoderma*, and *Schizophyllum*. These taxonomic data are in agreement with those obtained previously through Next-generation sequencing-based ITS gene sequencing, according to the first chapter (Newman-Portela et al. 2024). Other authors have reported that some of these genera showed notable tolerance and interaction capabilities with heavy metals and U, suggesting their potential for remediation in contaminated environments (Gadd and Fomina 2011; Ma et al. 2014; Schaefer et al. 2021). In the context of U bioremediation, it is crucial to assess the metabolic versatility of fungi through characterization of their enzymatic activities, such as cellulase, amylase, laccase, and LiP. These activities can impact the fungus's survival capacity, and during the decomposition process of lignocellulosic biomass, such as wood present in the walls of former mines, releasing low weight organic molecules that can be used by U reducers, such as SRB (Krause et al. 2020). Most of the fungi studied showed activity in starch degradation, indicating an efficient enzymatic system for lignocellulose breakdown, thanks to enzymes such as laccase, LiP, and cellulase. Basidiomycetes like *Schizophyllum* sp. are the main lignocellulosic biomass decomposers, but Ascomycetes like *Aspergillus* sp. or *Trichoderma* sp. also stand out (Sánchez 2009; Krause et al. 2020). Our results indicate that *C. malorum*, *S. commune*, and *A. niger* could be possible candidates as bioremediation agents, as they showed positive activity for all the aforementioned enzymes. Consequently, these micro-organisms likely have a greater capacity to survive in oligotrophic environments contaminated with U compared to other isolates. On the other hand, other enzymatic activities with potential relevance for U bioremediation were identified, including alkaline phosphatase, acid phosphatase, and naphthol-AS-BI-phosphohydrolase. Phosphatase leads to the degradation of organic phosphates, releasing inorganic phosphates for U phosphate biomineralization (Martínez-Rodríguez et al. 2023). Additionally, the role of fungal phosphatase in U biomineralization was explored. It was observed that all analysed fungi showed acid phosphatase and naphthol-AS-BI-phosphohydrolase activity, suggesting their potential

for U phosphate biomineralization. This enzymatic activity could help transform U into less soluble and less toxic forms, thus contributing to the bioremediation of U-contaminated environments.

Based on the above described taxonomic and biochemical data, we investigated the U phosphate biomineralization potential of *C. malorum*, *A. sydowii*, and *P. polonicum* using Schlema-Alberoda mine water amended with 10 mM glycerol 2-phosphate (G2P) as an organic phosphate source. Using a combination of High-Resolution Scanning Electron Microscopy (HRSEM) and Energy-Dispersive X-ray Spectroscopy (EDXS), electron-dense accumulations containing U and phosphorus have been identified. These findings suggest the possible formation of a U phosphate association, possibly mediated by phosphatase activity. The formation of localized intracellular precipitates could be the result of active uptake of U(VI) and its subsequent precipitation with intracellular orthophosphates (Yang et al. 2012). Therefore, we have demonstrated that the fungal isolates *C. malorum*, *A. sydowii*, and *P. polonicum* have the ability to precipitate U phosphate biominerals when amended with an organic phosphorus source. Over time, the extraction and processing of U have generated residues that can be risky to the environment and public health. Additionally, during U fission, selenium 79 (^{79}Se), a relevant radionuclide in nuclear activities, is produced (Aguerre and Frechou 2006). Therefore, in this work, we used Se(IV) as an inactive but toxic analogue of ^{79}Se to study the interaction of the isolated fungi with Se. Our results demonstrate the toxicity of Se in fungi through Minimum Inhibitory Concentration (MIC) and Tolerance Index (TI) tests. There is notable variability in Se tolerance among different fungal strains, even within the same genus. Some strains, like *Acremonium* sp., show high MIC to Se, while others exhibit much lower tolerance. It was found that some strains, like *S. commune*, *T. harzianum*, and *Acremonium* sp., are capable of reducing soluble and mobile Se(IV) to a less toxic form, Se(0) (Nandini et al. 2017; Liang et al. 2019; Tomah et al. 2023). Furthermore, the fungal potential to produce Se(0) nanostructures with high stability was explored through SAED and HRTEM, observing crystalline Se(0) nanostructures with lattice spacings of 0.29 and 0.37 nm corresponding

to m-Se and t-Se (Ruiz-Fresneda et al. 2023). These results could have applications in the bioremediation of environments contaminated with Se. To summarise, this study shed light in the impact of microbial processes on the biogeochemical cycling of U in mine waters for designing a U bioremediation strategy in the Schlema-Alberoda mine water, as well as in other mine waters worldwide. Bio-stimulation of the native microbial community with glycerol proved to be a potential alternative to conventional technologies for the removal of low U concentrations. This not only reduced soluble U(VI) but also decreased the concentration of co-contaminants such as Fe, As, and SO_4^{2-} . Additionally, this study provides new insights into U(V), traditionally considered unstable, but in our case demonstrated long-term stability under oxidative and environmental conditions, making this methodology even more effective. To improve this strategy, it is necessary to investigate in a future work the involved bacterial community, enzymatic reduction mechanisms, and U(V) speciation in the glycerol-amended microcosms.

References

- Aguerre S and Frechou C (2006) Development of a Radiochemical Separation for Selenium with the Aim of Measuring Its Isotope 79 in Low and Intermediate Nuclear Wastes by ICP-MS. *Talanta*. 69(3): 565–571. <https://doi.org/10.1016/j.talanta.2005.10.028>
- Banala UK, Indradyumna Das NPI, Toleti SR (2021) Microbial interactions with uranium: towards an effective bioremediation approach. *Environmental Technology And Innovation*. 21:101254. <https://doi.org/10.1016/j.eti.2020.101254>
- Bernhard G, Geipel G, Brendler V, Nitsche H (1996) Speciation of Uranium in Seepage Waters of a Mine Tailing Pile Studied by Time-Resolved Laser-Induced Fluorescence Spectroscopy (TRLFS). *Radiochimica Acta*. 74:87–91. <https://doi.org/10.1524/ract.1996.74.special-issue.87>
- Bernhard G, Geipel G, Brendler V, Nitsche H (1998) Uranium speciation in waters of different uranium mining areas. *Journal of Alloys and Compounds*. 271–273: 201–205. [https://doi.org/10.1016/S0925-8388\(98\)00054-1](https://doi.org/10.1016/S0925-8388(98)00054-1)
- Bernhard G, Geipel G, Reich T, Brendler V, Amayri S, Nitsche H (2001) Uranyl(VI) carbonate complex formation: Validation of the $\text{Ca}_2\text{UO}_2(\text{CO}_3)_3(\text{aq.})$ species. *Radiochimica Acta*. 89(8): 511-518. <https://doi.org/10.1524/ract.2001.89.8.511>
- Dar SA, Yao L, van Dongen U, Kuenen JG, Muyzer G. Analysis of diversity and activity of sulfate-reducing bacterial communities in sulfidogenic bioreactors using 16S rRNA and *dsrB* genes as molecular markers (2007) *Applied and Environmental Microbiology*. 73(2):594-604. <https://doi.org/10.1128/aem.01875-06>
- Finneran KT, Housewright ME, Lovley DR (2002) Multiple influences of nitrate on uranium solubility during bioremediation of uranium-contaminated subsurface sediments. *Environmental Microbiology*. 4(9):510-516. <https://doi.org/10.1046/j.1462-2920.2002.00317.x>
- Gadd GM and Fomina M (2011) Uranium and Fungi. *Geomicrobiology Journal*. 28(5-6):471-482. <https://doi.org/10.1080/01490451.2010.508019>
- Gao W and Francis AJ (2013) Fermentation and hydrogen metabolism affect uranium reduction by *Clostridia*. *ISRN Biotechnology*. 2013:657160. <https://doi.org/10.5402%2F2013%2F657160>
- Hilpmann S, Rossberg A, Steudtner R, Drobot B, Hübner R, Bok F, Prieur D, Bauters

- S, Kvashnina KO, Stumpf T, Cherkouk, A (2023) Presence of Uranium(V) during Uranium(VI) Reduction by *Desulfosporosinus Hippei* DSM 8344T. *Science of the Total Environment*. 875:162593. <https://doi.org/10.1016/j.scitotenv.2023.162593>.
- Krause K, Jung EM, Lindner J, Hardiman I, Poetschner J, Madhavan S, Matthäus C, Kai M, Menezes RC, Popp J, Svatoš A, Kothe E. (2020) Response of the wood-decay fungus *Schizophyllum commune* to co-occurring microorganisms. *PLoS One*. 15(4):e0232145. <https://doi.org/10.1371/journal.pone.0232145>
- Kumar A, Kumar V, Saroop S, Arsenov D, Bali S, Radziemska M, Bhardwaj R (2023) A comprehensive review of Uranium in the terrestrial and aquatic environment: bioavailability, immobilization, tolerance and remediation approaches. *Plant Soil*. 490:31–65. <https://doi.org/10.1007/s11104-023-06101-8>
- Kushkevych I, Cejnar J, Treml J, Dordević D, Kollar P, Vítězová M (2020) Recent Advances in Metabolic Pathways of Sulfate Reduction in Intestinal Bacteria. *Cells*. 9(3):698. <https://doi.org/10.3390/cells9030698>
- Li X, Sun M, Zhang L, Finlay RD, Liu R, Lian B (2022) Widespread bacterial responses and their mechanism of bacterial metallogenic detoxification under high concentrations of heavy metals. *Ecotoxicology and Environmental Safety*. 246:114193. <https://doi.org/10.1016/j.ecoenv.2022.114193>
- Liang X, Perez MAMJ, Nwoko KC, Egbers P, Feldmann J, Csetenyi L, Gadd GM (2019) Fungal formation of selenium and tellurium nanoparticles. *Applied Microbiology and Biotechnology*. 103:7241–7259. <https://doi.org/10.1007/s00253-019-09995-6>
- Lusa M, Knuutinen J, Lindgren M, Virkanen J, Bomberg M (2019) Microbial communities in a former pilot-scale uranium mine in Eastern Finland - Association with radium immobilization. *Science of the Total Environment*. 686:619-640. <https://doi.org/10.1016/j.scitotenv.2019.05.432>
- Ma XK, Ling Wu L, Fam H (2014) Heavy metal ions affecting the removal of polycyclic aromatic hydrocarbons by fungi with heavy-metal resistance. *Applied Microbiology and Biotechnology*. 98(23):9817-27. <https://doi.org/10.1007/s00253-014-5905-2>
- Marshall MJ, Plymale AE, Kennedy DW, Shi L, Wang Z, Reed SB, Dohnalkova AC, Simonson CJ, Liu C, Saffarini DA, Romine MF, Zachara JM, Beliaev AS, Fredrickson JK (2008) Hydrogenase- and outer membrane c-type cytochrome-facilitated reduction of technetium(VII) by *Shewanella oneidensis* MR-1. *Environmental*

Microbiology. 10(1):125-136. <https://doi.org/10.1111/j.1462-2920.2007.01438.x>

- Martínez-Rodríguez P, Sánchez-Castro I, Ojeda JJ, Abad MM, Descostes M, Merroun ML (2023) Effect of different phosphate sources on uranium biomineralization by the *Microbacterium* sp. Be9 strain: A multidisciplinary approach study. *Frontiers in Microbiology*. 13:1092184. <https://doi.org/10.3389/fmicb.2022.1092184>
- Mumtaz S, Streten-Joyce C, Parry DL, McGuinness KA, Lu P, Gibb KS (2013) Fungi outcompete bacteria under increased uranium concentration in culture media. *Journal of Environmental Radioactivity*. 120:39-44. <https://doi.org/10.1016/j.jenvrad.2013.01.007>
- Nandini B, Hariprasad P, Prakash HS, Shetty HS, Geetha N. (2017) Trichogenic-selenium nanoparticles enhance disease suppressive ability of *Trichoderma* against downy mildew disease caused by *Sclerospora graminicola* in pearl millet. *Scientific Reports*. 7(1):2612. <https://doi.org/10.1038/s41598-017-02737-6>
- Newman-Portela AM, Krawczyk-Bärsch E, Lopez-Fernandez M, Bok F, Kassahun A, Drobot B, Steudtner R, Stumpf T, Raff J, Merroun ML (2024) Biostimulation of indigenous microbes for uranium bioremediation in former U mine water: multidisciplinary approach assessment. *Environmental Science and Pollution Research*. 31(5):7227-7245. <https://doi.org/10.1007/s11356-023-31530-4>
- Newsome L, Morris K, Lloyd JR (2014) The biogeochemistry and bioremediation of uranium and other priority radionuclides. *Chemical Geology*. 363:164–184. <https://doi.org/10.1016/j.chemgeo.2013.10.034>
- Petrie L, North NN, Dollhopf SL, Balkwill DL, Kostka JE (2003) Enumeration and characterization of iron(III)-reducing microbial communities from acidic subsurface sediments contaminated with uranium(VI). *Applied and Environmental Microbiology*. 69(12):7467-7479. <https://doi.org/10.1128/AEM.69.12.7467-7479.2003>
- Qian X, Mester T, Morgado L, Arakawa T, Sharma ML, Inoue K, Joseph C, Salgueiro CA, Maroney MJ, Lovley DR (2011) Biochemical characterization of purified OmcS, a c-type cytochrome required for insoluble Fe(III) reduction in *Geobacter sulfurreducens*. *Biochimica et Biophysica Acta*. 1807(4):404-412. <https://doi.org/10.1016/j.bbabi.2011.01.003>
- Rastogi G, Osman S, Kukkadapu R, Engelhard M, Vaishampayan PA, Andersen GL, and Sani RK (2010a) Microbial and Mineralogical Characterizations of Soils Collected

- from the Deep Biosphere of the Former Homestake Gold Mine, South Dakota. *Microbial Ecology*. 60(3):539–550. <https://doi.org/10.1007/s00248-010-9657-y>
- Rastogi G, Osman S, Vaishampayan PA, Andersen GL, Stetler LD, Sani RK (2010b) Microbial diversity in uranium mining-impacted soils as revealed by high-density 16S microarray and clone library. *Microbial Ecology*. 59(1):94–108. <https://doi.org/10.1007/s00248-009-9598-5>
- Ruiz-Fresneda MA, Staicu LC, Lazuén-López G, Merroun ML (2023) Allotropy of selenium nanoparticles: Colourful transition, synthesis, and biotechnological applications. *Microbial Biotechnology*. 16(5):877-892. <https://doi.org/10.1111/1751-7915.14209>
- Sánchez C (2009) Lignocellulosic residues: biodegradation and bioconversion by fungi. *Biotechnology Advances*. 27(2):185-94. <https://doi.org/10.1016/j.biotechadv.2008.11.001>
- Santos SC, Liebensteiner MG, van Gelder AH, Dimitrov MR, Almeida PF, Quintella CM, Stams AJM, Sánchez-Andrea I (2018) Bacterial glycerol oxidation coupled to sulfate reduction at neutral and acidic pH. *The Journal of General and Applied Microbiology*. 64(1):1-8. <https://doi.org/10.2323/jgam.2017.02.009>
- Schaefer S, Steudtner R, Hübner R, Krawczyk-Bärsch E, Merroun ML (2021) Effect of Temperature and Cell Viability on Uranium Biomineralization by the Uranium Mine Isolate *Penicillium simplicissimum*. *Frontiers in Microbiology*. 12(802926). <https://doi.org/10.3389/fmicb.2021.802926>
- Schofield EJ, Veeramani H, Sharp JO, Suvorova E, Bernier-Latmani R, Mehta A, Stahlman J, Webb S, Clark D, Conradson S, Ilton ES, Bargar JR (2008) Structure of Biogenic Uraninite Produced by *Shewanella Oneidensis* Strain MR-1. *Environmental Science and Technology*. 42(21):7898–7904. <https://doi.org/10.1021/es800579g>.
- Smedley PL and Kinniburgh DG (2023) Uranium in natural waters and the environment: Distribution, speciation and impact. *Applied Geochemistry*. 148:105534. <https://doi.org/10.1016/j.apgeochem.2022.105534>
- Teng Y, Xu Y, Wang X, Christie P (2019) Function of Biohydrogen Metabolism and Related Microbial Communities in Environmental Bioremediation. *Frontiers in Microbiology*. 10:106. <https://doi.org/10.3389/fmicb.2019.00106>
- Tomah AA, Zhang Z, Alamer ISA, Khattak AA, Ahmed T, Hu M, Wang D, Xu L, Li B, Wang Y (2023) The Potential of Trichoderma-Mediated Nanotechnology

- Application in Sustainable Development Scopes. *Nanomaterials*. 13(17):2475. <https://doi.org/10.3390/nano13172475>
- Waite DW, Chuvochina M, Pelikan C, Parks DH, Yilmaz P, Wagner M, Loy A, Naganuma T, Nakai R, Whitman WB, Hahn MW, Kuever J, Hugenholtz P (2021) Proposal to reclassify the proteobacterial classes Deltaproteobacteria and Oligoflexia, and the phylum Thermodesulfobacteria into four phyla reflecting major functional capabilities. *International Journal of Systematic and Evolutionary Microbiology*. 70(11):5972-6016. <https://doi.org/10.1099/ijsem.0.004213>
- Wang Z, Zachara JM, Yantasee W, Gassman PL, Liu C, Joly AG (2004) Cryogenic laser induced fluorescence characterization of U(VI) in Hanford vadose zone pore waters. *Environmental Science and Technology*. 38(21):5591–5597. <https://doi.org/10.1021/es049512u>
- WHO (2022) Guidelines for drinking-water quality: fourth edition incorporating the first and second addenda, Geneva: World Health Organization. 478-480. Date of access: February 20, 2023. Retrieved from <https://www.who.int/publications/item/9789240045064>
- WISMUT GmbH Umweltbericht (2021) Date of access: October 3, 2023. Retrieved from <https://www.wismut.de/de/>
- Woolfolk CA and Whiteley HR (1962) Reduction of inorganic compounds with molecular hydrogen by *Micrococcus lactilyticus*. I. Stoichiometry with compounds of arsenic, selenium, tellurium, transition and other elements. *Journal of Bacteriology*. 84(4):647-658. <https://doi.org/10.1128%2Fjb.84.4.647-658.1962>
- Yang HB, Tan N, Wu FJ, Liu HJ, Sun M, She ZG, Lin YC (2012) Biosorption of uranium(VI) by a mangrove endophytic fungus *Fusarium* sp. #ZZF51 from the South China Sea. *Journal of Radioanalytical and Nuclear Chemistry*. 292(3):1011-1016. <https://doi.org/10.1007/s10967-011-1552-6>
- You W, Peng W, Tian Z, Zheng M (2021) Uranium bioremediation with U(VI)-reducing bacteria. *Science of the Total Environment*. 798:149107. <https://doi.org/10.1016/j.scitotenv.2021.149107>
- Zadvorny OA, Zorin NA, Gogotov IN (2006) Transformation of metals and metal ions by hydrogenases from phototrophic bacteria. *Archives of Microbiology*. 184(5):279-85. <https://doi.org/10.1007/s00203-005-0040-1>

Zeng T, Li L, Mo G, Wang G, Liu H, Xie S (2019) Analysis of uranium removal capacity of anaerobic granular sludge bacterial communities under different initial pH conditions. *Environmental Science and Pollution Research*. 26(6):5613-5622. <https://doi.org/10.1007/s11356-018-4017-4>

Zhang L, Li J, Lai JL, Yang X, Zhang Y, Luo XG (2022) Non-targeted metabolomics reveals the stress response of a cellulase-containing *penicillium* to uranium. *Journal of Environmental Sciences*. 120:9–17. <https://doi.org/10.1016/j.jes.2021.12.043>

Zhou X, Fernández-Palacios E, Dorado AD, Gamisans X, Gabriel D (2022) Assessing main process mechanism and rates of sulfate reduction by granular biomass fed with glycerol under sulfidogenic conditions. *Chemosphere*. 286(1):131649. <https://doi.org/10.1016/j.chemosphere.2021.131649>



GLÜCK AUF

Besucherbe



Conclusiones

Conclusiones

Después de los resultados obtenidos en esta tesis doctoral, se establecen las siguientes conclusiones:

1. La caracterización fisicoquímica reveló concentraciones más altas de U y SO_4^{2-} en el agua de la mina de Schlema-Alberoda en comparación con la de Pöhla. Además, se observaron condiciones reductoras más fuertes en el agua de la mina de Pöhla que en la de Schlema-Alberoda.
2. La concentración de U en el agua de Schlema-Alberoda supera los límites permisibles para aguas potables y ambientales, habiéndose detectado dos especies diferentes de U(VI) solubles, siendo el complejo carbonato cálcico de U $[\text{Ca}_2\text{UO}_2(\text{CO}_3)_3(\text{aq})]$ el predominante, seguido de un complejo carbonato de U $[\text{UO}_2(\text{CO}_3)_3^{4-}]$.
3. La caracterización de la comunidad microbiana en ambas minas reveló una comunidad bacteriana relevante para el ciclo biogeoquímico de Fe, N y S. Además, los géneros bacterianos identificados son tolerantes a la toxicidad ambiental de metales pesados y radionucleidos como el U.
4. La comunidad fúngica en el agua de la mina mostró una alta diversidad estando compuesta por hongos con capacidad para la degradación de compuestos lignocelulósicos y alto potencial en la inmovilización de metales pesados y radionucleidos como el U.
5. El análisis funcional de la comunidad microbiana presente en el agua de ambas minas reveló la presencia de diversas rutas metabólicas relacionadas con la degradación de carbohidratos y con el metabolismo del azufre y nitrógeno, entre otras.
6. Las condiciones reductoras y la actividad enzimática asociada con la vía de reducción desasimilatoria de sulfato de bacterias sulfato

reductoras en el agua de mina de Pöhla sugiere la presencia de una comunidad microbiana involucrada en la respiración de SO_4^{2-} .

7. Los cambios en las concentraciones de U entre la mina de Schlema-Alberoda (1 mg/L) y Pöhla (0.01 mg/L) podrían ser atribuidas a factores como condiciones reductoras, la existencia de bacterias reductoras de metales, como por ejemplo *Geobacter*, y la reducción abiótica de U por sulfuros de hidrógeno, y presentes en el agua de la mina de Pöhla.
8. La bioestimulación de la comunidad bacteriana nativa reductora de U en el agua de la mina de Schlema-Alberoda parece ser más efectiva cuando se utiliza glicerol como donador de electrones que si se utilizan, con esta misma finalidad, el ácido vanílico o el ácido glucónico.
9. Se observó la reducción de U(VI) a U(IV) por bacterias reductoras de U a través de la oxidación de glicerol. El análisis espectroscópico y microscópico confirmó la formación de productos reducidos de U y de fases minerales como calcita y piritita.
10. Se identificaron productos de U reducidos en los estados de oxidación IV y V. El U(IV) estaba asociado con uraninita biogénica, mientras que U(V) se encontró como complejos de carbonato y como nanopartículas de FeUO_4 . Además, se observó estabilidad a largo plazo de U(V) bajo condiciones óxicas (en concreto, durante cuatro semanas), un fenómeno no descrito previamente en muestras ambientales biogénicas.
11. Se aislaron catorce cepas fúngicas, con actividad enzimática lignocelulolítica y fosfatasa, de aguas de ambas minas, con potencial para la biorremediación de U y Se. La actividad fúngica inmovilizó el U formando acúmulos de fosfato de U y el Se en forma de nanoestructuras de Se(0).



GLÜCK AUF

Besucherbe



Conclusions

Conclusions

After the results obtained in this PhD Thesis, the following conclusions are established:

1. Physicochemical characterization revealed higher concentrations of U and SO_4^{2-} in the mine water from Schlema-Alberoda compared to that from Pöhla. Furthermore, stronger reducing conditions were observed in Pöhla mine water than in Schlema-Alberoda.
2. The concentration of U in the water from Schlema-Alberoda exceeds permissible limits for drinking and environmental waters. Additionally, two different soluble U(VI) species were detected, with the calcium uranyl carbonate complex $[\text{Ca}_2\text{UO}_2(\text{CO}_3)_3(\text{aq})]$ being the most predominant, followed by an uranyl carbonate complex $[\text{UO}_2(\text{CO}_3)_3^{4-}]$.
3. Microbial community characterization in both mines revealed a bacterial community relevant for the biogeochemical cycling of Fe, N, and S. In addition, the identified bacterial genera are tolerant to environmental toxicity of heavy metals and radionuclides such as U.
4. The fungal community in the mine water showed a high diversity and was composed of fungi with a potential lignocellulosic compound degradation capacity and for immobilization of heavy metals and radionuclides such as U.
5. A functional profile of the active microbial community in both mine waters was identified, revealing the presence of diverse metabolic pathways (e.g., carbohydrate degradation, and sulphur and nitrogen metabolism).
6. Reducing conditions and enzymatic activity associated with dissimilatory sulphate reduction pathways of sulphate-reducing bacteria (SRB) in the Pöhla mine water suggest the presence of a bacterial SO_4^{2-} respiration process.

7. Changes in U concentrations between the Schlema-Alberoda mine (1 mg/L) and Pöhla (0.01 mg/L) could be attributed to factors such as reducing conditions, the presence of metal-reducing bacteria, such as *Geobacter*, and the abiotic indirect reduction of U by biogenic hydrogen sulphide, in the Pöhla mine water.
8. Biostimulation of the native U-reducing bacterial community in Schlema-Alberoda mine water seems to be more effective when glycerol is used as the electron donor, compared to vanillic acid or gluconic acid.
9. The reduction of U(VI) to U(IV) by U-reducing bacteria through glycerol oxidation was observed. Spectroscopic and microscopic analysis confirmed the formation of reduced U products and mineral phases such as calcite and pyrite.
10. Reduced U products were identified in oxidation states IV and V. U(IV) was associated with biogenic uraninite, while U(V) was found as carbonate complexes and as FeUO_4 nanoparticles. Additionally, a long-term stability of U(V) was observed for four weeks under oxic conditions, a phenomenon not previously documented in biogenic environmental samples.
11. Fourteen fungal strains with lignocellulolytic and phosphatase activities were isolated from both mine waters, with potential for U and Se bioremediation. Fungal activity immobilized U forming the U-phosphate phases and Se in the form of Se(0) nanostructures.



Photo by Philip Ackermann